

1972

Effects of weldments on the fatigue strength of steel beams-transverse stiffness and attachments, September 1972

J. W. Fisher

P. A. Albrecht

B. T. Yen

D. J. Klingerman

Follow this and additional works at: <http://preserve.lehigh.edu/engr-civil-environmental-fritz-lab-reports>

Recommended Citation

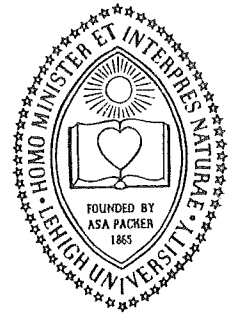
Fisher, J. W.; Albrecht, P. A.; Yen, B. T.; and Klingerman, D. J., "Effects of weldments on the fatigue strength of steel beams-transverse stiffness and attachments, September 1972" (1972). *Fritz Laboratory Reports*. Paper 326.
<http://preserve.lehigh.edu/engr-civil-environmental-fritz-lab-reports/326>

This Technical Report is brought to you for free and open access by the Civil and Environmental Engineering at Lehigh Preserve. It has been accepted for inclusion in Fritz Laboratory Reports by an authorized administrator of Lehigh Preserve. For more information, please contact preserve@lehigh.edu.

334.10

**OFFICE
OF
RESEARCH**

LEHIGH UNIVERSITY



EFFECT OF WELDMENTS ON THE FATIGUE STRENGTH OF STEEL BEAMS - TRANSVERSE STIFFENERS AND ATTACHMENTS

FRITZ ENGINEERING
LABORATORY LIBRARY

BY
JOHN W. FISHER
PEDRO A. ALBRECHT
BEN T. YEN
DAVID J. KLINGEMAN
BERNARD M. McNAMEE

SEPTEMBER 1972

FRITZ ENGINEERING LABORATORY REPORT 334.10

ERRATA SHEET

Page 20 Line One change carck to crack

Page 46 Line Sixteen change Fig. 24 to Fig. 26

Page 61 Line Twenty-two change 1/4 in. to 9/32 in.

Page 62 Line Seven change 1/4 in. to 9/32 in.

Page 108 Third sentence

change: It is proposed to undertake these studies on plate girder type specimens that have a single beveled groove weld with back-up strip in place.

To: These studies should be made on plate girder type specimens that have a single beveled groove weld with back-up strip in place.

Page 110 Line Eight

change: crack growth at the toe of the stiffener-to-web fillet welds when

To: crack growth at the toe of the stiffener-to-web fillet welds. When

Page 119 Line Sixteen - eliminate completely - was repeated in typing

Page 308

Add Reference

54. Natrella, M. G.
EXPERIMENTAL STATISTICS, Handbook 91,
U. S. Department of Commerce, 1963

12-7(1)

EFFECT OF WELDMENTS ON THE FATIGUE STRENGTH
OF STEEL BEAMS - TRANSVERSE STIFFENERS AND ATTACHMENTS

FINAL REPORT

Prepared for
Highway Research Board
National Cooperative Highway Research Program
National Academy of Sciences

John W. Fisher, Pedro A. Albrecht, Ben T. Yen
David J. Klingerman and Bernard M. McNamee

Fritz Engineering Laboratory
Department of Civil Engineering
Lehigh University
Bethlehem, Pennsylvania

September 1972

Fritz Engineering Laboratory Report 334.10

Acknowledgment

This work was sponsored by the American Association of State Highway Officials, in cooperation with the Federal Highway Administration, and was conducted in the National Cooperative Highway Research Program which is administered by the Highway Research Board of the National Academy of Sciences - National Research Council.

Disclaimer

This copy is an uncorrected draft as submitted by the research agency. A decision concerning acceptance by the Highway Research Board and publication in the regular NCHRP series will not be made until a complete technical review has been made and discussed with the researchers. The opinions and conclusions expressed or implied in the report are those of the research agency. They are not necessarily those of the Highway Research Board, the National Academy of Sciences, the Federal Highway Administration, the American Association of State Highway Officials, or of the individual states participating in the National Cooperative Highway Research Program.

TABLE OF CONTENTS

Part I

	<u>Page</u>
1. List of Figures	vi
2. List of Tables	xiii
3. Acknowledgements	xvi
4. Summary of Findings	xviii
5. Chapter 1 INTRODUCTION AND RESEARCH APPROACH	1
1.1 OBJECTIVE AND SCOPE	2
1.2 DESIGN VARIABLES AND SPECIMENS	4
1.3 EXPERIMENT DESIGN	8
1.4 FABRICATION	9
1.5 EXPERIMENTAL PROCEDURES	10
6. Chapter 2 FINDINGS	13
2.1 LITERATURE SURVEY	13
2.2 GENERAL RESULTS OF STUDY	14
2.3 RESULTS OF STIFFENER DETAILS	16
2.4 RESULTS OF FLANGE ATTACHMENT DETAILS	18
2.5 DESIGN	20

TABLE OF CONTENTS (Continued)

Part I

	<u>Page</u>
7. Chapter 3 RESULTS AND EVALUATION OF FATIGUE STRENGTH	23
3.1 FATIGUE STRENGTH OF A514 STEEL ROLLED BEAMS	23
3.1.1 Crack Initiation and Growth	24
3.1.2 Effect of Stress Variables and Type of Steel	25
3.2 FATIGUE STRENGTH OF BEAMS AND GIRDERS WITH TRANSVERSE STIFFENERS	30
3.2.1 Crack Initiation and Growth	31
3.2.2 Analysis of Data for Stiffeners Welded to the Web Alone	41
3.2.2.1 Effect of Type of Steel	44
3.2.2.2 Effect of Stress Variables	45
3.2.2.3 Effect of Out-of-Plane Deformation from Transverse Bracing	46
3.2.2.4 Effect of Specimen Size	47
3.2.2.5 Effect of Alternating Shear	48
3.2.2.6 Bending Versus Principal Stress	49
3.2.3 Analysis of Data for Stiffeners Welded to the Web and Flanges	51
3.2.3.1 Effect of Type of Steel	51
3.2.3.2 Effect of Stress Variables	51
3.2.3.3 Effect of Out-of-Plane Deformations from Transverse Bracing	52
3.2.3.4 Effect of Specimen Size	52
3.2.4 Comparison of Stiffeners Welded to Web Alone with Stiffeners Welded to the Web and Flange	53

TABLE OF CONTENTS (Continued)

Part I

	<u>Page</u>
3.2.5 Comparison with Previous Results	54
3.3 FATIGUE STRENGTH OF PLAIN WELDED BEAMS AND GIRDERS	57
3.3.1 Crack Initiation and Growth	58
3.3.2 Correlation with Previous Studies	59
3.4 FATIGUE STRENGTH OF BEAMS WITH WELDED FLANGE ATTACHMENTS	60
3.4.1 Crack Initiation and Growth	61
3.4.2 Analysis of Data for Welded Flange Attachments	67
3.4.2.1 Effect of Stress Variables	67
3.4.2.2 Effect of Attachment Length	70
3.4.3 Comparison with Previous Results	72
3.5 STRESS ANALYSIS OF CRACK PROPAGATION	75
3.5.1 Crack-Growth Rates	77
3.5.2 Stress Intensity Factors for Fillet Weld Toes	80
3.5.3 Analysis of Crack Growth at Stiffeners	85
3.5.4 Analysis of Crack Growth at Attachments	87
8. Chapter 4 RECOMMENDATIONS AND APPLICATION	90
9. Chapter 5 CONCLUSIONS	95

TABLE OF CONTENTS (Continued)

Part I

	<u>Page</u>
5.1 TRANSVERSE STIFFENER DETAILS	97
5.2 WELDED BEAM ATTACHMENTS	99
5.3 A514 STEEL ROLLED BEAMS	100
10. Chapter 6 RECOMMENDATIONS FOR FURTHER WORK	102
6.1 SUGGESTED STUDIES	103

Part II

11. Appendix A LITERATURE SURVEY	108
A1 Beams and Girders with Stiffeners	108
A2 Beams with Fillet Welded Flange Attachments	118
12. Appendix B EXPERIMENT DESIGN	121
13. Appendix C MATERIAL PROPERTIES AND BEAM CHARACTERISTICS	123
14. Appendix D A514 ROLLED STEEL BEAMS	126
15. Appendix E FATIGUE STRENGTH OF BEAMS AND GIRDERS WITH STIFFENERS	130
16. Appendix F FATIGUE STRENGTH OF WELDED ATTACHMENTS	149
17. Appendix G NOMENCLATURE	161

LIST OF FIGURES

Part I

Figure

- 1a Details of SC Beams
- 1b Details of SG and SB Girders
- 2 Details of SA Beams
- 3 Details of Beams with Flange Attachments
- 4 Test Set-up for SG Girders
- 5 Experiment Design, SC Beams
- 6 Tension Flange Splice to Arrest Crack Growth
- 7 Crack Initiation from a Flaw in the Rolled Surface of a Plain-Rolled Beam
- 8 Example of Crack Initiation from the Flange Tip
- 9 Comparison of Rolled-Beam Test Data with Previous Results of Beams that Developed Cracks from the Rolled Surface
- 10 Comparison of Plain-Rolled and Plain-Welded Beams with Cracks Originating at the Flange Tip
- 11 Summary of Rolled-Beam Data from this Study and other Investigations
- 12 Typical Failure at Type 1 Stiffener
- 13 Typical Fatigue Crack Surface at Type 1 Stiffener at Failure
- 14 Fatigue Crack at the Toe of Type 1 Stiffener-to-Web Weld
 - (a) 0.035 In. Deep Crack (SCB243)
 - (b) Multiple Fatigue Cracks
 - (c) Multiple Fatigue Cracks through the Web

LIST OF FIGURES (Continued)

Figure

- | | |
|----|---|
| 15 | Stages of Crack Growth at Type 1 Stiffener |
| 16 | Typical Failure at Type 2 Stiffener |
| 17 | Typical Fatigue Crack Surface at Type 2 Stiffener at Failure |
| 18 | Stages of Crack Growth at Type 2 Stiffener |
| 19 | Typical Failure at Type 3 Stiffener |
| 20 | Stages of Crack Growth at Type 3 Stiffener |
| 21 | 0.028 in. Deep Crack at the Toe of Type 3 Stiffener-to-Tension Flange Weld (SGC333) |
| 22 | Multiple Fatigue Crack Growth at the Toe of Type 3 Stiffener-to-Tension Flange Weld |
| 23 | Typical Fatigue Crack Surface at Type 3 Stiffener at Failure |
| 24 | S-N Plot for Type 1 Stiffeners, SG Girders & SC Beams |
| 25 | S-N Plot for Type 2 Stiffeners, SG Girders |
| 26 | S-N Plot for Type 1 Stiffeners, SB Girders with Transverse Bracing |
| 27 | S-N Plot for Type 1 Stiffeners, SA Beams with Alternation Direction of Principal Stress |
| 28 | Effect of Bending and Principal Stress Range on the Fatigue Strength of Type 1 Stiffeners |
| 29 | S-N Plot for Type 3 Stiffeners |
| 30 | Summary S-N Plot for Type 1, 2, and 3 Stiffeners |

LIST OF FIGURES (Continued)

<u>Figure</u>	
31	Comparison of Present Study with Previous Work, All Stiffeners
32	Typical Plain-Welded Beam Failure
33	S-N Plot for Plain-Welded Girders
34a,b	Typical Failure at Flange Attachment with no Transverse Weld
34c,d	Typical Failure at Flange Attachment with Welds All Around
35	Typical Fatigue Crack Surface at Flange Attachment with Transverse Weld
36	Fatigue Crack at Short (1/4 in.) Attachment to Flange
37a,b	Typical Fatigue Crack Surface at Flange Attachment with Longitudinal Weld
38	Simultaneous Crack Growth from Weld Toe Terminations
39	S-N Plot for 4 in. Attachments Welded All Around
40	S-N Plot for 1/4 in. Attachments
41	S-N Plot for 2 in. Attachments
42	S-N Plot for 4 in. Attachments Welded Longitudinally
43	S-N Plot for 8 in. Attachments
44	Summary of S-N Plots for Flange Attachments and Transverse Stiffeners

LIST OF FIGURES (Continued)

Figure

- 45 Strain Distribution in Beam Flange near the Toe of Transverse Weldment of Attachment
- 46 Comparison of Present Study with Previous Work, 4 in. Attachments
- 47 Comparison of Present Study with Previous Work, 8 in. Attachments
- 48 Comparison of Previous Test Data of 6 in. Attachments with Results of 4 in. Attachments
- 49 Comparison of Previous 10 in. Groove-Welded Attachments with 8 in. Attachments and Cover Plated Beams
- 50 Comparison of Previous Non-Load Carrying Fillet-Welded Joints with Stiffeners and 1/4 in. Attachments
- 51 Crack Growth Rates in Fatigue
- 52a Part-Through Crack in a Flat Plate
- 52b Part-Through Crack at the Toe of a Non-Load Carrying Fillet Weld
- 53 Stress Concentration Correction for the Applied Stress Field
- 54 Propagation of a Part-Through Crack at Type 1 Stiffeners
- 55 Propagation of a Part-Through Crack at Type 3 Stiffeners
- 56 Comparison of Predicted Fatigue Life with Type 3 Stiffener Test Data

LIST OF FIGURES (Continued)

Figure

- 57 Effect of Plate Thickness on the Propagation of a Part-Through Crack
- 58 Effect of Attachment Length on Stress Concentration Factor K_t
- 59 Predicted Mean Fatigue Strength Compared with Mean Regression Lines, Flange Attachments
- 60 95% Confidence Limits for 95% Survival

Part II

- A1 S-N Plot for Type 1 Stiffeners Welded to the Web Alone, Summary of Previous Fatigue Test Data
- A2 S-N Plot for Type 2 Stiffeners Welded to the Web Alone, Summary of Previous Fatigue Test Data
- A3 S-N Plot for Type 3 Stiffeners Welded to the Web and Flange, Summary of Previous Fatigue Test Data
- A4 Ratio of Shear-to-Bending Stresses at the End of Type 1 Stiffener-to-Web Weld
- A5 Types of Fatigue Cracks
- E1 Details of Pilot Test Beams
- E2 Finite Element Mesh for Stress Analysis of 38-in. Girders

LIST OF FIGURES (Continued)

Figure

- | | |
|-----|---|
| E3 | Stresses in the Beam Web by Beam Theory and a Finite Element Analysis |
| E4 | Stresses in the Girder Web by Beam Theory and a Finite Element Analysis |
| E5 | Cumulative Frequency Distribution for Type 1 Failure |
| E6 | Cumulative Frequency Distribution for Type 2 Failure |
| E7 | Cumulative Frequency Distribution for Type 3 Failure |
| E8 | Mohr Circles for Stresses at the End of Stiffener-to-Web Weld |
| E9 | Bar Diagram for Crack Growth at Type 1 Stiffeners |
| E10 | Bar Diagram for Crack Growth at Type 2 Stiffeners |
| E11 | Bar Diagram for Crack Growth at Type 3 Stiffeners |
| E12 | Size of Part-Through Cracks at Fillet Weld Toe |
| E13 | Typical Finite Element Mesh for the Computation of the Stress Concentration at the Weld Toe |
| E14 | Stress-Intensity Factor at the Weld Toe of Type 3 Girder Stiffeners |
| F1 | Measured Strain in Beam Flange at the End of Flange Attachment |

LIST OF FIGURES (Continued)

Figure

- | | |
|----|--|
| F2 | Finite Element Mesh for the Computation of Stress Distribution at Flange Attachment |
| F3 | Finite Element Mesh for the Computation of Stress Concentration at the Weld Toe of Flange Attachment |
| F4 | Stress-Intensity Factor at the Weld Toe of 4 in. Attachment |
| F5 | Stress Distribution Diagram, Flange Attachment |
| F6 | Effect of Flange Attachment Length on Fatigue Strength |

LIST OF TABLES

Part I

Table

- | | |
|---|----------------------|
| 1 | Fatigue Stresses |
| 2 | Joint Classification |

Part II

- | | |
|----|---|
| A1 | Discussion of Stiffened Beams Tested in Previous Studies |
| A2 | Stiffeners and Weld Details for Beams Listed in Table A1 |
| A3 | Results of Previous Fatigue Tests on Type 1 Stiffeners |
| A4 | Results of Previous Fatigue Tests on Type 2 Stiffeners |
| A5 | Results of Previous Fatigue Tests on Type 3 Stiffeners |
| A6 | Modes of Failure in Previous Stiffened Beam Tests |
| B1 | Specimen Designation |
| B2 | Experiment Design for Plain Rolled Beams (PRC) |
| B3 | Experiment Design for SC Beams |
| B4 | Experiment Design for SA Beams |
| B5 | Experiment Design for SG Girders |
| B6 | Experiment Design for SB Girders |
| B7 | Experiment Design for Welded Beams with Attachments, 9/32" long (AOB) |

LIST OF TABLES (Continued)

Table

B8	Experiment Design for Welded Beams with Attachments, 2" long (A2B)
B9	Experiment Design for Welded Beams with Attachments, 4" long (A4B)
B10	Experiment Design for Welded Beams with Attachments, 8" long (A8B)
C1A	Typical Cross-Sectional Properties of Test Specimens
C1B	Stiffener Dimensions
C2A	Tensile Properties of Plain-Rolled Beams (PRC)
C2B	Tensile Properties of Beam and Girder Plates
C3	Mill Test Report of Beam and Girder Plates
D1	Summary of Data for Rolled A514 Steel Beams
E1	Summary of Fatigue Test Data of Type 1 Stiffeners
E2	Summary of Fatigue Test Data of Type 2 Stiffeners
E3	Summary of Fatigue Test Data of Type 3 Stiffeners
E4	Summary of Data for Pilot Tests
E5	Summary of Fatigue Test Data of Plain Welded Beams
E6	Analysis of Variance of Type 1 Stiffeners
E7	Analysis of Variance of Type 2 Stiffeners
E8	Analysis of Variance of Type 3 Stiffeners

LIST OF TABLES (Continued)

Table

E9	Stress Range Versus Steel Quality Factorial
E10	Stress Range Versus Transverse Bracing Factorial
E11	Size of Part-Through Cracks at Fillet Weld Toes
E12	Data for Analysis of Propagation of Part-Through Cracks
F1	Summary of Finite Element Analysis
F2	Summary of Test Data: 1/4 in. Attachments
F3	Summary of Test Data: 2 in. Attachments
F4	Summary of Test Data: 4 in. Attachments
F5	Summary of Test Data: 8 in. Attachments
F6	Summary of Secondary Crack Data: 1/4 in. Attachments
F7	Summary of Secondary Crack Data: 2 in. Attachments
F8	Summary of Secondary Crack Data: 4 in. Attachments
F9	Summary of Secondary Crack Data: 8 in. Attachments
F10	Comparison of 4 in. Attachment Failures

ACKNOWLEDGEMENTS

The research reported herein was performed under NCHRP Project 12-7(1) by the Fritz Engineering Laboratory, Department of Civil Engineering, Lehigh University, and the Department of Mechanics and Civil Engineering, Drexel University. Lehigh University was the contractor for this study. The work undertaken at Drexel University was under a subcontract with Lehigh University.

John W. Fisher, Professor of Civil Engineering, Lehigh University, was the principal investigator. The other authors' of this report are: Pedro A. Albrecht, former Research Assistant at Fritz Engineering Laboratory, now Assistant Professor of Civil Engineering, University of Maryland, Ben T. Yen, Associate Professor of Civil Engineering, Lehigh University, David J. Klingerman, Research Assistant, Fritz Engineering Laboratory, and Bernard M. McNamee, Professor of Civil Engineering, Drexel University.

The work was done under the general supervision of Professor Fisher, the principal investigator. The work at Drexel was done under the supervision of Professor McNamee with the assistance of Richard Gray and Robert Baldasanno, Research Assistants and Allen Yerger, technician. The work at Lehigh was under the supervision of Professors Fisher and Yen, with the assistance of Research Assistants Pedro A. Albrecht and David J. Klingerman.

Both Lehigh University and Drexel University financially supported a portion of this work as a public service by permitting the project to be undertaken at a less-than-audited rate.

Sincere thanks are due Fritz Laboratory staff members Charlotte Yost, Mary Ann Yost, and Phyllis Raudenbush who typed the manuscript; Richard Sopko for outstanding photographic work; John M. Gera and Sharon Balogh for the line drawings and Dorothy Fielding for assistance with reproduction of the manuscript. Kenneth L. Harpel, Laboratory Superintendent, Robert Dales and Charles Hittinger, Laboratory Foremen and their staff were invaluable in their assistance during fabrication and testing.

Appreciation is also due Joseph Krulikowski, graduate student at Drexel University for the computer work on flange attachment which was done on the UNIVAC 1108 computer in the Structural Branch Division of the Philadelphia Naval Shipyard. Invaluable assistance was also provided by Suresh Desai, Post-Doctoral Research Associate and John H. Struik, Research Assistant at Fritz Engineering Laboratory for providing the computer program and finite element analysis of the stress concentration factors for fillet weld toes.

SUMMARY OF FINDINGS

Stress range was observed to account for nearly all the variation in cycle life for all stiffener and attachment details examined in this study. Use of this finding should be made in appropriate provisions of the AASHTO Standard Specifications for Highway Bridges.

For purposes of design the fatigue strength of ASTM A514 steel rolled beams was found to be about the same as A36 and A441 steel rolled beams. The same stress range cycle life relationship described the fatigue strength for all three grades of steel.

The beam bending stress range at the weld toe termination was found to dominate the fatigue strength of full depth stiffener details welded to the web alone. The bending stress range at the stiffener-to-flange weld defined the strength for stiffeners welded to the web and flanges.

For design purposes the same fatigue strength values are applicable to transverse stiffeners welded to the web alone or welded to the web and tension flange. The allowable bending stress range at the termination of the flange weld toe is the same as for stiffeners welded to the web alone. The magnitude of shear need not be considered when determining the allowable

bending stress range for fatigue of full depth stiffeners welded to the web alone.

Welding transverse stiffeners to the tension flange should be permitted when desired. The fatigue strength provided by such details is much greater than that provided by attachments with lengths equal or greater than their width. The AASHO Specifications should be modified to permit the transverse welded stiffener.

New design categories should be added to the AASHO Specifications to provide for the effect of attachment length on allowable fatigue stresses. The same fatigue strength values are applicable to transverse stiffeners and very short attachments (less than 1 1/2 in.). A category should be provided for attachments welded to the flange or web with lengths between 1 1/2 in. and 12 times the attachment thickness but not more than 4 in. When the attachment length exceeds 12 times the attachment thickness or is greater than 4 in., the fatigue strength decreases to that of the cover plated beams.

All welded details were observed to experience fatigue crack growth from an initial micro-flaw at the toe of fillet welds. The fatigue crack grew as a semi-elliptical part-through crack

during most of the fatigue life. From 80 to 95% of the life was consumed propagating the crack through the plate thickness, depending on the detail.

Attaching diagonal bracing to the transverse stiffeners had no effect on their fatigue strength. Within the range of estimated lateral forces and displacements at the stiffeners on highway bridges, the out-of-plane deflection had no influence on fatigue strength.

The empirical exponential model relating stress range to cycle life provided the best fit to the test data.

A theoretical stress analysis based on the fracture mechanics of crack growth confirmed the suitability of the empirical regression models. The theoretical analysis also provided a means of rationally explaining the observed behavior and permitted the effect of other variables such as plate thickness and initial crack size to be examined in a rational way.

CHAPTER ONE

INTRODUCTION AND RESEARCH APPROACH

Fatigue studies on rolled, welded, cover plated, and groove welded beams fabricated from A36, A441, and A514 steels were reported in NCHRP Report 102⁽¹⁾ and revealed that the primary variables influencing the fatigue strength were the type of detail and the stress range to which it was subjected. These conclusions were based on a comprehensive experimental program that included 374 beam specimens each with one or more details.

However, large gaps in the state of knowledge of welded details exist because studies of many details are incomplete and not sufficiently extensive for the evaluation of the significant variables that effect the fatigue strength. Additional research was desirable to extend the applicability of the findings into regions not adequately covered. This would permit the development of comprehensive design and specification provisions.

Fatigue has been observed to be a process of initiation of microscopic cracks (flaws or discontinuities) and their propagation into macroscopic cracks during repeated application of load. The rate of growth of the cracks increases exponentially as the crack

size increases. Eventually, the applied stresses on the uncracked area are large enough to cause yielding of the net section and static failure. In some cases rapid crack growth or complete fracture is observed at failure.

The fatigue fractures observed in the cover-plated steel beam bridges included in the AASHO Road Test, as well as those obtained in other similar structures, emphasize the importance of the detail on the life expectancy of highway beam or girder bridges. Overall, the history of welded highway bridges has been satisfactory. Most field failures have been due to negligence in either design or fabrication. These failures also have pointed out the importance of properly considering in design and fabrication the factors that influence the fatigue strength of steel highway bridge structures.

1.1 OBJECTIVES AND SCOPE

The principal objective of this project was to develop mathematical design relationships that would define in general terms the fatigue strength of stiffeners and of lateral and transverse connections under constant amplitude fatigue loading. This would permit extending the basic knowledge obtained during the first phase of the study (see NCHRP Report 102). In addition rolled steel beams of ASTM A514 material were examined

so that direct correlation with the previous work on A36 and A441 steel rolled beams could be made and the full range of structural steels examined for base metal conditions.

Existing fatigue data for beams and girders with transverse stiffeners were reviewed and used to assist with the development of statistically controlled experiments that would permit formulation of suitable mathematical design relationships for the welded beam with stiffeners or with lateral and transverse connections.

One hundred and fifty-seven steel beams and girders were fabricated and tested during this phase of the research program. Of these there were 29 plain rolled A514 steel beams tested to determine the fatigue strength of these high strength basic members and to provide correlation with the earlier studies.

One hundred and six plain welded beams, identical in size to the beams of Phase I were fabricated and used as the basic structural member for transverse stiffeners attached to the web alone or to the web and flanges and for flange attachments. Of this total 47 were fabricated with transverse one sided stiffeners and 59 were fabricated with the flange attachments.

The remaining 22 members were larger welded build-up girders with transverse stiffeners on one side. They provided

the basis for assessing the influence of size and stress gradient on fatigue crack growth from the transverse stiffener details.

The testing of beams and girders was limited to constant magnitude cyclic loading. This was identical to the earlier studies of the project (NCHRP Project 12-7). Research now underway on NCHRP Project 12-12 is examining variable cycle loading, and unpublished preliminary results indicate that it can be related to constant cycle conditions.

1.2 DESIGN VARIABLES AND SPECIMENS

The principal design variables for this study were the type of detail and the stress conditions. Since the study reported in NCHRP Report 102 had indicated that type of steel was not a significant variable for either the upper bound (plain welded beam) or lower bound (cover-plated beam) welded details, it was assumed that this condition existed for the welded details of this study. Nevertheless four A514 girders were fabricated to provide additional data on this variable. All of the remaining welded built-up members were fabricated from A441 steel. It was anticipated that the results would fall between the upper and lower bound welded details.

Basic tests on A514 plain rolled beams without any details were made to complete an evaluation of the base metal condition and to correlate with the previous studies on A36 and A441 rolled steel beams. Two sizes of beams were studied. They included nine W14x30 beams 10 ft. 6 in. long which were tested on a 10-ft. span. These were identical in size to the previous tests on A36 and A441 rolled beams and were tested under identical loading conditions. The remaining 20 rolled beams were W10x25, 8 ft. long and tested on a 7 ft. 6 in. span.

The welded built-up beams and girders with transverse stiffeners had two basic types of one-sided stiffeners as illustrated in Fig. 1. Stiffeners attached to the web alone were classified as Type 1 or Type 2 depending on whether they were in the moment gradient or constant moment regions. These stiffeners were not fitted between flanges and the weld terminated on the beam web 1/2 in. to 4 in. above the tension flange surface. The second basic type of stiffener was classified as Type 3 and was welded to the beam flanges as well as the web.

The stiffeners welded to the web alone provided basic data on fatigue crack growth originating in the web under the combined effects of bending and shear. Earlier studies had indicated that the combined effect of bending and shear was significant.⁽⁷⁾⁽³³⁾

Stiffeners welded to the web and flanges provided data on fatigue crack growth from either the flange or web, or both. These stiffeners stiffened the web and provided restraint to out-of-plane lateral forces.

All three stiffener types were placed on both beam and girder specimens. The stiffeners were placed in such a position as to ensure failure at the stiffener detail prior to failure as a plain welded beam. The 14 in. deep beams for the basic experiment were classified as SC series. The experiment design was directly related to the plain welded beams (PW) reported in NCHRP Report 102⁽¹⁾.

The SA series beams had only Type 1 stiffeners and were subjected to an alternating shear condition as illustrated in Fig. 2. This changed the direction and the magnitude of the principal stress during each stress cycle. These beams were designed to evaluate the effect of oscillating the principal stress between two limits as opposed to the constant direction of principal stress range experienced by the other test series and earlier studies. This loading provided a simulation of the actual service condition of bridge structures where comparable oscillations occur.

The SG and SB series specimens were 38 in. deep welded girders, 20 ft. long and tested on a 19 ft. span. Each girder had all

three types of stiffeners. The SG series was composed of ten A441 steel girders and four A514 steel girders. The SB series had eight A441 steel girders which were identical to the SG girders but

Type 1 and Type 3 stiffeners adjacent to the load points as illustrated in Fig. 1b. The lateral bracing introduced an out-of-plane displacement that was proportional to the vertical displacement of the girder.

The remaining 14 in. deep welded beams had attachments of different lengths welded to both flanges as illustrated in Fig. 3. These beams were grouped into four different series corresponding to the attachment length. The A8, A4, and A2 series had 8 in., 4 in., and 2 in. plates 3 inches wide and $9/32$ inches thick welded flat on the outside of the flanges. The AQ series had $9/32$ in. x 2 in. x 3 in. plates welded outstanding on the flanges. All attachment plates extended beyond the flange edge by 1 in. All beams with attachments were 10 ft. 6 in. long and were tested on a 10-ft. span as shown in Fig. 3. The attachments were all positioned in the moment gradient region 6 to 10 inches from the load points. The distance was selected to ensure fatigue failure at the attachment prior to failure as a plain welded beam.

Minimum stress and stress range were selected as the controlled stress variables in all tests except for the SA series.

This permitted variation in one variable while the other was maintained at a constant level. The nominal flexural stresses in the base metal of the tension flange or web at the welded detail were used as design variables. The flexural stresses for the plain welded beam were also related to those of the earlier studies. Because the stiffeners were all full depth to simulate those used on bridge members, it was not possible to generate extreme values of shear to bending stress ratios and their corresponding high principal stress conditions that would lead to crack growth. Earlier studies had accomplished this by terminating the stiffeners several inches above the tension flange.

1.3 EXPERIMENT DESIGN

Each beam series was arranged into factorial experiments defined by the stress variables. The factorial used for the stiffened beam series is shown in Appendix B with the minimum stress and stress range being the variables. Similar factorials were used for the other test series but most were incomplete with some empty cells because of yielding, equipment capacity, and extreme long life.

Each cell of the factorial which had test specimens contained at least two details for a given beam series. Most contained three or four details. Because the study reported in NCHRP Report 102 had indicated that minimum stress was not a significant factor, the total specimens for each level of stress range was made as nearly equal as possible so that the distribution was not

biased. This was necessary since few of the factorials were complete.

1.4 FABRICATION

All welded beams and girders were fabricated by a typical bridge fabrication shop. The fabricator was instructed to use normal fabrication techniques, workmanship, and inspection procedures. Each beam and girder were fabricated using the same technique and procedure. All attachments or stiffeners were added after the beam fabrication.

For each thickness of material, most beam and girder component plates were produced from the same heat. The rolled W14x30 beams meeting the physical and chemical requirements of A514 steel were furnished from one heat and the W10x25 beams from two heats.

Components of the welded beams and girders were flame cut to size and the weld areas blast cleaned. All longitudinal fillet welds joining the flanges and web of the steel beams and girders were made by the automatic submerged arc process. Tack welds required to hold the plates in alignment were manually placed. The 3/16 inch web-to-flange fillets for the 14 in. deep A441 steel beams were made with AWS F72-EL12 electrodes of 5/64 in. diameter. The 38 in. deep A441 steel girders had 1/4 in. web-to-

flange fillets made with 3/32 in. F71-EL12 electrodes and the corresponding A514 steel girders had 1/4 in. fillet made with 3/32 in. F72-EM12K electrodes. No preheating was used prior to the welding of any of the steels.

The longitudinal fillet welds were kept continuous although several stop-start positions were unavoidable. Any defects that were visually apparent were gouged out and rewelded and the repair identified.

The stiffeners for the SG and SB girders were welded manually in the fabricating shop. All other stiffeners and attachments were placed at Fritz Engineering Laboratory using manual welding.

1.5 EXPERIMENTAL PROCEDURES

All 14 in. deep specimens were tested initially on a 10-ft. span with two point loading as illustrated in Figs. 1a, 2 and 3. The distance between the loading points was 2 ft. for the W14x30 rolled beams, 5 ft. 6 in. for SA series beams and 3 ft. 6 in. for all other beams with stiffeners and attachments. The W10x25 beams were tested on a 7 ft. 6 in. span with two load points 1 ft. 6 in. apart. The 38 in. deep girders were tested on a 19 ft. span with two-point loading 5 ft. apart as shown in Figs. 1b and 4.

Since the stiffeners and attachments were located in the moment gradient region, testing could be continued on a shorter span when failure occurred at only one end of the 10 ft. long specimens. A single concentrated load was applied at the load point of the other end such that the same stress condition existed at the weld detail (Fig. 5).

In a number of 14 in. beams and all of the 38 in. girders testing was continued after a failure at a detail by splicing the cracked region. The splicing was accomplished by placing lap plates on both sides of the tension flange and fastening into place with C-clamps as illustrated in Fig. 6. When substantial portions of the web had cracked in the shear span of girders with stiffeners, it was also necessary to add a doubler plate to the beam web. This plate was attached by fillet welds.

The order of testing of the specimens for each test series was randomized so that uncontrolled variables would be randomly distributed. This prevented any systematic bias from being introduced into the experimental data.

The testing equipment used at both Lehigh and Drexel Universities was manufactured by Amsler. The pulsators activating the jacks operated at between 200 and 800 cycles of load applications per minute. When reversal of loading was required and the

tests on alternating direction of principal stress (SA) were conducted, a constant upward load was applied by a hydraulic accumulator - load system.

All reversal loading of rolled and welded beams was done at Lehigh. All 38 in. girders were also tested at Lehigh.

The deflection criterion used to define failure was the same as used for the studies reported in NCHRP Report 102. An increase of deflection by 0.020 in. terminated the loading automatically by activating a micro switch. This usually occurred when the crack had propagated through enough of the flange for net section yielding to occur. The cracks at flange attachments and at Type 3 stiffeners were larger than the cracks in the flange at Type 1 stiffeners when failure occurred. However, much more of the web was cracked in the latter cases which caused yielding of the flange.

CHAPTER TWO

FINDINGS

The findings of the continued work on the effect of weldments on the fatigue strength are summarized in this chapter. Included are the results from previous studies which can be found in the published literature, and the results of analysis and evaluation of the data obtained in this study. Justification for these findings is given in Chapters three and four. Detailed documentation of the test results and statistical analyses appear in the Appendices. Appendix A summarized the status of knowledge from earlier published literature.

2.1 LITERATURE SURVEY

1. Fatigue studies on beams and girders with transverse stiffeners indicated that the principal stress range provided reasonable correlation with the fatigue life of stiffeners attached to the web alone. An increase in the shear-to-bending ratio appeared to decrease the fatigue strength for extreme values of shear-to-bending.

2. Most of the tests on stiffeners welded to the web were carried out on special test specimens with unrealistically high shear-to-bending stress ratios in the web at the stiffener weld end. This resulted in a principal stress at the stiffener weld end which equaled or exceeded the maximum bending stress in the beam to which the stiffener was attached. This condition cannot occur in a structural member with normal proportions and full depth stiffeners.
3. No evidence was available to ascertain the significance of a change in the direction of principal stress. All tests were carried out with a change of magnitude of principal stress which retained a constant direction. In actual structures both the magnitude and direction change as vehicles traverse the span.
4. Very little data was available on welded beam attachments. Most of the available information on attachments was obtained from small plate specimens. These did not simulate the residual stress conditions and the enforced beam curvature that exist in welded built-up members.

2.2 GENERAL RESULTS OF STUDY

1. Stress range was the dominant stress variable for all stiffener and attachment details and A514 steel rolled beams. This results in part from the presence of a residual tensile stress field near the crack in most details.

2. The type of steel did not significantly effect the fatigue strength.
3. There was no apparent difference in the results of beams tested at the two laboratories. Also rest periods, interruptions of the tests, rate of loading, and laboratory environmental effects had no observable influence.
4. The empirical exponential model relating stress range to cycle life was observed to provide the best fit to the test data for every detail. This resulted in a log-log linear relationship between the stress range and cycle life for each detail.
5. Allowable stress ranges can be computed for any desired life from the mathematical regression models and the standard error of estimate.
6. The fatigue behavior was defined in this study between 100,000 and 10 million cycles of loading.
7. A theoretical stress analysis based on the fracture mechanics of crack growth confirmed the suitability of the mathematical regression models. The analysis showed that the primary factor causing variation in the fatigue test data was the size of the initial micro-flaw.

8. The theoretical stress analysis permitted the effect of other variables, such as plate thickness and flaw size, to be examined and evaluated in a rational way.
9. All details were observed to experience fatigue crack growth from an initial micro-flaw at the toe of fillet welds. The initial micro-flaw grew in the form of a semi-elliptical, part-through crack which propagated through the thickness of the web or flange. From 80 to 95% of the fatigue life was consumed propagating the crack through the plate thickness, depending on the detail.
10. Cracks also formed at the fillet weld toes connecting the stiffeners and attachments to the flange and web in the compression regions of the specimens. These cracks arrested or grew very slowly after they propagated out of the residual tensile stress zone. None of the beams failed at a detail subjected to a nominal compression - compression stress cycle.
11. No brittle or sudden fracture occurred during the testing of any specimen. Failure was by yielding of the flange when most of its area was destroyed by the fatigue crack.

2.3 EFFECT OF STIFFENER DETAILS

1. The beam bending stress range at the weld toe termination was found to dominate the fatigue strength of full-depth stiffener details welded to the web alone. The bending stress range at the stiffener-to-flange weld was dominant for stiffeners welded to the web and flanges.

2. Minimum stress was not a significant design factor for any stiffener detail. The presence of residual tensile stresses at the toe of transverse stiffener welds made the full stress range effective.
3. The principal stress and its direction are not significant for purposes of design in stiffened bridge members even though principal stress provides the best theoretical correlation.
4. The type of steel was not a significant design factor for any stiffener detail.
5. The crack causing failure at all stiffeners welded to the web alone initiated at the end of the stiffener-to-web weld. When stiffeners were welded to the web and flange the crack initiated at the toe of the stiffener-to-flange weld.
6. Failure of beams occurred after the crack had destroyed most of the tension flange of all beams. Cracks originating in the web propagated into the flange and eventually terminated the test.
7. The same stress range-life relationship is equally applicable to stiffeners welded to the web alone or stiffeners welded to the web and flange when the stress is determined in terms of the beam bending stress range at the weld toe termination where cracks first occur.
8. Attaching diagonal bracing to the stiffeners of beams and girders had no effect on their fatigue strength. Within the

range of estimated lateral forces and displacements on highway bridges, the out-of-plane deflection at the stiffeners had no influence on crack growth.

9. No fatigue (endurance) limit was observed for the bending stress ranges that were examined for the stiffener details (13.7 to 28.7 ksi). The 9/32 in. attachments which were analogous to stiffeners welded to the flange sustained 10.8 to 15.5 million cycles without failure or visible crack growth at a stress range of 12 ksi.
10. A fracture mechanics analysis of crack growth indicated that the behavior of stiffener details was not significantly affected by the thickness of the flange or web plate.

2.4 EFFECT OF FLANGE ATTACHMENT DETAILS

1. The failure lives of the different attachment details differed. The life decreased as the attachment length increased.
2. The crack causing failure of all attachment details originated at the most highly stressed weld toes of the welds connecting the attachment to the beam flange. At ends of transversely welded attachments the crack originated at several sites along the weld toe but was more severe near the center of the weld. At attachments without transverse welds the cracks

initiated at the weld toe at the termination of the longitudinal fillet weld.

3. End-welded short attachments gave shorter lives than those with unwelded ends. The difference was apparent but not statistically significant.
4. Failure occurred in the tension flange of all beams with flange attachments. Many cracks were also observed in the compression flange at the weld toe terminations. When the flange was subjected to nominal compression stress these cracks were arrested after they grew out of the local residual tensile stress zone. When subjected to stress reversal some additional crack growth was apparent.
5. Minimum stress was not a significant variable for any of the attachments examined. The presence of residual tensile stresses at weld toes made the full stress range effective.
6. Although slight differences in the slope of the mean regression lines existed, these differences were not significant. The difference reflected the small number of test specimens evaluated for each attachment length. Overall, the slope of all attachments were about the same as the plain welded and cover plated beams.

7. A fracture mechanics analysis of ^{crack} crack growth accounted for the fatigue behavior of the flange attachments. The primary cause of the differences in fatigue life among various attachment lengths was found to be the differences in the stress concentration at the terminating weld toes.
8. No fatigue limit was observed for the 4 in. and 8 in. attachments for the stress ranges that were examined (8 to 24 ksi). The 9/32 in. and 2 in. attachments were tested with the stress ranges of 12 and 28 ksi. No fatigue limit was observed for the 2 in. attachment. The 9/32 in. attachments exhibited no failures at the 12 ksi stress range level.

2.5 DESIGN

1. Stress range should be used for the fatigue design of the details which are evaluated in this study. The results of this study coupled with the work reported in NCHRP Report 102 suggest that a comprehensive fatigue specification based on stress range is appropriate.
2. For purposes of design, the type of steel does not significantly influence the fatigue strength. Although most of the specimens were fabricated from A441 steel, the few tests undertaken on A514 steel girders and rolled beams during this study continued to confirm the earlier findings.

3. The same stress range values are applicable to transverse stiffeners and very short attachments (less than 2 inches) when defined in terms of the beam bending stress range at the weld toe termination. The stress range values are 10 ksi for more than 2 million cycles, 13 ksi for 2 million cycles, 19 ksi for 500,000 cycles, and 32 ksi for 100,000 cycles.
4. The magnitude of shear need not be considered when determining the allowable bending stress range for fatigue of full-depth stiffener details welded to the web alone.
5. Welding transverse stiffeners to the tension flange should be permitted where desired. The allowable bending stress range at the termination of the flange weld toe is the same as for stiffeners welded to the web alone. The fatigue strength is directly comparable to the behavior observed for 9/32 in. attachments and much greater than for attachments with length equal to or greater than their width.
6. Diagonal bracing for beam and girder bridges can be attached to stiffeners without influencing their fatigue resistance.
7. New design categories should be added to the AASHTO specifications to provide for the effect of attachment length on the fatigue strength.

8. When the attachment length L is greater than 2 in. but less than twice the attachment width (the width is defined by the part overlapping the flange surface) and is connected by welds parallel to the line of stress, the stress range values are 7.0 ksi for more than 2 million cycles, 10 ksi for 2 million cycles, 16 ksi for 500,000 cycles, and 27 ksi for 100,000 cycles.
9. When the attachment length L is greater than twice the attachment width, the stress range values should be the same as those used for cover plated beams.
10. The provisions for A36 and A441 rolled beams (base metal) are applicable to A514 steel rolled beams.
11. Design criteria are recommended on the basis of fatigue life and stress range. During most of the fatigue life the cracks were very small and not visible. When the cracks that grew at the stiffener or attachment weld toe penetrated the web or flange plate thickness, most of the fatigue life was exhausted.

CHAPTER THREE

RESULTS AND EVALUATION OF FATIGUE STRENGTH

The results of the experimental and theoretical work undertaken on this project are summarized in this chapter for the rolled beams, welded beams and girders with stiffeners, and the welded beams with attachments that were studied. Each detail is examined in terms of crack initiation and growth, an evaluation of the stress variables and special test conditions, and finally a comparison with the results available from previous studies. A complete documentation of the test data and details of the analysis are given in the appendices.

3.1 FATIGUE STRENGTH OF A514 STEEL ROLLED BEAMS

Twenty-two rolled W14x30 beams of the ASTM A36 and A441 grade steels were tested in the original test program⁽¹⁾. The experiment was not as extensive as that for the welded beam study and reflected the limitations in stresses because of yield strength or excessive cycle life. A514 steel rolled beams were tested during the continuation of the test program. Nine W14x30 and twenty W10x25 beams were tested.

3.1.1 Crack Initiation and Growth

From the original program, many cracks in the A36 and A441 steel rolled beams originated at locations of high local stresses at the load points⁽¹⁾. Fretting contributed to the initiation of these cracks⁽²⁾. It was difficult to judge the influence of fretting and local stresses. This was also true for cracks that originated underneath the wooden stiffeners that were inserted at the load points.

The test on the A514 steel rolled beams used improved set-up arrangements which made it possible to eliminate most of the local influences. Lateral braces in the shear span were used in place of the wooden stiffeners. Cracks usually developed from the flange-tip or from the flange surface.

The cracks in the plain-rolled A514 steel beams originated from the rolled surface of the tension flange. Cracks generally initiated from small discontinuities in the flange surface that were apparently introduced by the normal rolling operation or by locally adhered mill-scale. These discontinuities were much smaller than the porosity observed in the plain-welded beams. A typical crack starting from a surface discontinuity is shown in Fig. 7. The region where slow growth had prevailed over a large portion of the life is apparent from the smooth fracture appearance.

Cracks that initiated from the flange-tip developed from both the inside and outside corners of the flange tip. This location probably was an exposed part in the rolling process. A few laminations in the flange edge were observed to cause crack initiation and growth as illustrated in Fig. 8.

Cracks also started on the inside flange surface as well as from the extreme fiber. Five run-outs (10 million cycles) were observed for the A514 steel rolled beams at stress ranges between 34 and 36 ksi.

3.1.2 Effect of Stress Variables and Type of Steel

Part of the test data from A36, A441, and A514 steel beams are compared with data from previous investigators^(3,4,5,6) in Fig. 9. Only cracks that originated from the rolled flange surface away from possible load influence are shown in Fig. 9. The solid points identify the grades of steel beams tested at Lehigh. Previous studies are also categorized according to the yield strengths reported. Most of these data from previous studies are for the high strength T-1 steel rolled beams. No failure occurred for a number of beams at 4 to 7 million cycles of loading even with stress ranges as high as 55 ksi⁽⁴⁾. Run-out of the beams was then assumed in these studies. Runouts are indicated by arrows attached to the data points in this report. The number of beams

surviving a large number of cycles increased with decreasing stress range. All data fall above the mean of the plain welded beams and a small increase in life is found at the lower stress ranges.

Gurney⁽⁷⁾ reported that four plain-welded beams failed from the extreme fiber and approached the life of rolled beams. A small reduction in life is apparent in Fig. 9 when these data are compared to the rolled-beam data. This might be due to higher residual tensile stresses at the flange-web junction in the welded beams and difference in beam geometry.

Rolled beams with cracks originating from the flange-tip were distinguished from beams with surface flaws in the study, and are plotted with solid symbols in Fig. 10. The scatter is relatively large at each level of stress range. The plain-welded beams with flange-tip cracks from Ref. 1 are also replotted in Fig. 10 by open symbols. The comparison reveals a reduction in fatigue life for cracks that started at the flame-cut flange-tip of welded beams as compared to those that started at the flange-tip of rolled beams. This was expected for the following reasons:

- (1) Only the most severe flange-tip notches in welded beams became critical because the discontinuities in the longitudinal fillet-weld generally provided the critical flaw-condition and terminated the test before failure was possible from the flange tip.

- (2) The notches introduced by good quality flame-cutting (equivalent ASA smoothness of 1000 or less) that caused failure were more severe and sharper than the notches introduced by the rolling operation.
- (3) The notches in the flame-cut edge were in zones of high residual tensile stresses. The residual stresses at the tips of rolled beams are usually compressive.

A summary of all rolled beam data, including the beams failing from the possible influence of load, is shown in Fig. 11. The test data are classified according to the failure mode regardless of grade of steel. All data from other investigators^(3,4,5,6) are from beams that failed from the rolled surface (Fig. 9). Also indicated in Fig. 11 are test data from machined tension specimens of T-1 steel.⁽⁸⁾

The following conclusions can be drawn from Figs. 9, 10 and 11:

- (1) The longest lives observed for rolled beams approach the life of plain plate specimens.
- (2) A run-out level (assumed to be 10^7 cycles or more) may exist in the vicinity of 30 ksi stress range.

This run-out level appeared to be higher for A514 steel beams. Three achieved 10 million cycles at a 34 ksi stress range without visible cracking.

- (3) At higher stress ranges, the number of beams that sustained a large number of cycles without failure decreased.
- (4) Severe notches in a flange surface or at a flange tip can initiate cracks in a rolled beam and cause failure at much lower levels of stress range, as was illustrated by the failure of an A514 steel beam at the 20.5 ksi stress range level.

Rolled beams provide the least severe flaw condition for a structural element and can yield extremely long lives at high stress range levels. However, a large discontinuity in the surface or at the flange-tip can reduce the fatigue life of the beam substantially. This was observed in a few beams in the high stress range region, and in one beam failing in the shear span from a large notch in the flange-tip. These beams yielded fatigue lives equivalent to the mean life for welded beams.

Flaw size estimates for rolled beams were derived from the fatigue test data using fracture mechanics concepts. A depth of discontinuity between 0.004 and 0.006 in. was estimated for cracks that originated from the rolled surface. This crack size is an order of magnitude smaller than the equivalent penny-shaped crack ($a_e = 0.04$ in.) in welded beams⁽⁹⁾. The discontinuities in the rolled beams are believed to be introduced during the rolling operation or result from mill scale which adhered locally to the flange surface.

The analysis also indicated that flange-tip flaws in the rolled beams were somewhat larger than the surface flaws. The radius of a quarter-circular crack with origin at the flange-corner was estimated to be 0.010 in. to 0.014 in. This larger defect was reflected by the fatigue data which indicated shorter lives for rolled beams failing from flange-tip flaws. Large or sharp notches at the flange-tip should be repaired by grinding to avoid a reduction in the fatigue life of the beam.

Run-out data ($N > 10$ million cycles) were observed in Figs. 9 to 11 at the 30 ksi stress range level for A36 steel rolled beams and at 34 to 36 ksi for A514 steel rolled beams. These run-out levels were confirmed by comparison with other rolled beam data. The run-out levels appear related to the fracture mechanics stress intensity range threshold values of 3.3 ksi $\sqrt{\text{in.}}$ and 4.6 ksi $\sqrt{\text{in.}}$ for mild steel and low-alloy steel, respectively suggested in Ref. 10.

3.2 FATIGUE STRENGTH OF BEAMS AND GIRDERS WITH TRANSVERSE STIFFENERS

Sixty-nine welded beams and girders with transverse stiffeners were tested during this study and provided data on 118 stiffener details. The stiffeners were either welded to the web alone or welded to both the web and flanges. Depending on their location on the test specimens, they were defined as

Type 1: welded to web alone, in a region of bending and shear

Type 2: welded to web alone, in a region of pure bending

Type 3: welded to web and flanges, in a region of bending and shear

With the exception of the beams subjected to alternating direction of principal stress (SA series), all specimens had these three types of stiffeners as illustrated in Fig. 1.

The 14 in. beams (SC series) were designed to fail first at the Type 3 stiffener at the tension flange. The test was then continued on a shorter span by applying a single concentrated load as illustrated in Fig. 5. During this retest the shear and bending moment in the moment gradient region were identical to those previously applied to the Type 1 stiffener. The stress condition for the Type 2 stiffeners changed and prevented

data from being acquired at this detail. Data on the Type 1 stiffeners were acquired when the beams were further tested after the completion of all initial tests at the Type 3 stiffener. The rest period between tests had no detectable effect on the fatigue life.

The first failure of the girder specimens could occur at any one of the three stiffener details or along the web-to-flange fillet welds. The details had been designed for comparable behavior. Splicing the tension with lap plates and high strength C-clamps after failure at a detail permitted data acquisition from other details.

Beams with stiffeners subjected to alternating direction of principal stress (SA beams) had only one type of test stiffener. They were not retested and cracks were only detected at the most severely stressed stiffener.

3.2.1 Crack Initiation and Growth

Fatigue crack propagation at all three types of stiffeners had one major feature in common: the cracks initiated and grew from the toe of non-load carrying stiffener fillet welds. The extent of crack propagation during testing was determined by visual inspection with a magnifying glass and by magnetic particle inspection with the Parker Contour Probe.

In general, initiation and growth of fatigue cracks are most likely to occur in areas subjected to a high tensile stress range and where initial flaws exist. The higher the stress range and the larger the initial flaw, the faster fatigue cracks will propagate. Stress concentrations and initial flaws exist along the toe of the fillet welds connecting the stiffeners to the web or flanges and provide a condition favorable for crack growth.

The initial micro flaw condition is provided by discontinuities at the weld toe, such as weld cracking, slag inclusions and undercut. Imperfections of this nature are common to all welding procedures.^(11,12) These flaws cannot be avoided although their sizes and frequency of occurrence may be controlled by good welding techniques.

The high tensile stress range is brought about by a combination of two effects. One is the geometrical stress concentration produced by the weld and the stiffener which magnify the nominal stresses due to loading. Further, a residual tensile stress field exists as the result of the welding process. The net effect of having residual tensile stresses and the stresses due to applied repeated loads is a tension-tension stress range at the weld toe, even in cases of nominal stress reversal. In fact, fatigue cracks were observed at stiffener weld toes which were subjected to a nominal compression-compression stress cycle. These

cracks, however, were arrested as they outgrew the residual tension field and did not impair the load carrying capability of the beam. Only when reversal of load occurred was there continued growth of these cracks.

Type 1 Stiffeners

The cracks causing failure at Type 1 stiffeners, welded to the web alone, initiated at one or more points along the toe of the stiffener-to-web weld. They propagated in a direction perpendicular to the principal tensile stress. Similar behavior was observed in the past^(33,34).

The overall appearance of the crack seemed to indicate two growth patterns, one diagonally off the end of the stiffener, the other following the weld toe before branching off diagonally into the web as illustrated in Fig. 12. The fatigue crack surfaces at Type 1 stiffeners were exposed by saw cutting most of the remaining net section of the beams and prying the remaining ligaments open. This fractographic examination revealed the reasons for the two observed patterns. Cracks initiating at the weld toe at the end of the stiffener grew in a direction perpendicular to the direction of the principal stress diagonally upward into the web and downward towards the web-to-flange junction,

as illustrated in Fig. 13. Cracks following the weld toe had multiple initiation points from which individual cracks grew in separate planes, each one perpendicular to the direction of the principal stress at that point. As the individual cracks overlapped, they broke through and joined each other, forming a longer crack with an irregular contour along the weld toe as illustrated in Fig. 14. This phenomena gave the appearance of a crack growing along the toe of the weld. Once this pattern had developed, it was sustained by the stress concentration effect of the weld which created a more severe path for propagation along the toe than for growing diagonally into the web away from the weld toe. Eventually the crack branched off when the principal stress became comparatively more severe.

Typically, the crack advanced through three stages of growth as depicted by Fig. 15. In the first stage, one or more semi-elliptical cracks were driven through the thickness of the web plate, as shown in Fig. 14. Each crack retained the approximate shape of a semi-ellipse as long as it did not join and interact with adjacent cracks.

Once the crack front had penetrated the web plate, the crack changed into a two-ended through crack. This transition from stage 1 into stage 2 after web plate penetration occurred

within a small number of cycles. Figure 14c shows one part-through crack at the beginning of the transition and one at the end.

In the third stage, after the lower front of the two-ended crack had broken through the extreme fiber of the tension flange, it grew as a three-ended crack (see Fig. 13) across the flange and extended further up into the web. Eventually, the ever decreasing net cross section of the flange yielded, and the test was terminated before the flange fractured. No "brittle" fracture was observed in these specimens.

Of the total number of cycles to failure at Type 1 stiffeners, about 80% were consumed growing the crack through the thickness of the web plate during stage 1. The second and third stages amounted to approximately 16% and 4% respectively as indicated schematically in Fig. 15. A more detailed discussion is given in Appendix E.

Figures 13 and 14 show small ellipses inside the fatigue crack surface. They correspond to the crack size at the time the beam had failed at Type 3 stiffeners and reflect the oxidation of the crack area.

The 14-in. SC beams had a shear-to-bending stress ratio of 0.31 at the end of the Type 1 stiffener. Six of the 22 detected cracks were ob-

served to have grown for some length along the weld toe of the stiffener under these stress conditions. In previous fatigue tests where the shear-to-bending stress ratios varied between 0.72 and 5.16 (see Appendix A), all cracks at Type 1 stiffeners grew diagonally off the stiffener-to-web weld.

Good agreement was found between the plane of the cracks, 71° to 74° , and the plane of the principal stress, 74° , at the tension (bottom) end of the Type 1 stiffener. At the compression (upper) end of Type 1 stiffeners, the direction in which the crack grew varied from -51° to -63° . There the direction of the principal stress cannot be defined precisely because it varies with the magnitude of the residual tensile stresses. It was also affected by the nearby loading point.

The 38 in. girders had a less steep bending stress gradient over the depth. This condition combined with the lower shear-to-bending stress ratio of 0.22 at the end of the Type 1 stiffener enhanced the likelihood for multiple crack initiation and growth along the toe of the stiffener-to-web weld. Indeed, of all 22 girders tested, only one specimen (SGB 211) exhibited crack propagation diagonally off the end of the stiffener, at an angle of 81° . The plane direction of the principal tensile stress had an inclination of 78° and 81° according to beam theory and a finite element analysis respectively.

Two SG girders developed cracks at the toe of the stiffener-to-web weld facing the support. In three specimens, cracks developed simultaneously along weld toes at both sides of the stiffener. These cracks were at different elevations on the girder web and grew on separate vertical planes at each side of the stiffener. When the approaching fronts of two small cracks overlapped each other, their growth was arrested. Growth then continued at other locations along the weld toe. In contrast to the beams, no cracks were observed at the stiffener end in the compression region of the girder web.

The four SG girders fabricated from A514 high strength steel appeared to be more susceptible to multiple crack initiation along the weld toe of the stiffeners. This indicated that there was greater likelihood of comparable defects all along the weld toe.

Crack initiation and propagation at the transversely braced Type 1 stiffeners of the SB girders followed the same characteristic pattern. Three of the eight specimens had cracks at the weld toes on both sides of Type 1 stiffeners. In the remaining five, the cracks leading to failure propagated along the toe nearer to the support.

Type 2 Stiffeners

Crack initiation and propagation at Type 2 stiffeners, welded to the girder web in a constant bending moment region, was identical to cracks at Type 1 stiffeners except that, in the absence of shear stresses, the plane of crack propagation remained perpendicular to the longitudinal axis of the girder. A Type 2 stiffener at failure is shown in Fig. 16 and an exposed fracture surface in Fig. 17.

Approximately 80%, 16%, and 4% of the total number of cycles to failure were spent in propagating a crack at a Type 2 stiffener through the three stages of growth illustrated in Fig. 18. This is comparable to the behavior of Type 1 stiffeners.

The initial flaw condition along the web weld toes of Type 2 stiffeners in girders fabricated from A514 steel was observed to be more severe than that in the A441 steel girders. The crack front spread over several inches along the weld toe early in stage 1 of growth, forming a tunnel-like shallow crack with one free surface, rather than the single or multiple semi-elliptical cracks characteristic of the A441 steel specimens. No visual difference in the A441 and A514 steel girder welds was apparent. As the front of the half-tunnel crack approached the far side of the web plate, the plane of the crack changed direction, a pheno-

mena indicative of the transition from a plane strain to a plane stress condition of crack growth. The exposed fracture surfaces of the cracks along Type 2 stiffeners in A514 steel specimens revealed the existence of a shear lip on the far side of the web plate.

From fracture mechanics, the larger the ratio of major to minor half-axis of a part-through crack, the higher the stress-intensity-factor and the faster the fatigue crack will grow in the direction of the minor axis. This is believed to explain why crack propagation during Stage 1 was more rapid and hence the fatigue lives shorter for A514 steel than for A441 steel specimens of this study.

Several reasons could have caused the severe initial crack condition in A514 steel beams. The fabrication process may have produced more severe micro defects along the weld toe, such as slag inclusions and weld cracking. The A514 steel specimens had not been preheated before the A36 steel stiffeners were welded on with E70 electrodes. This may have resulted in a more severe initial flaw condition. The combined effect of the residual tensile stresses and applied loads may also have influenced crack growth.

Type 3 Stiffeners

Type 3 stiffeners were welded to the web and the flanges. A typical fatigue crack causing failure at a Type 3 stiffener is shown in Fig. 19. The crack initiated at several points along the toe of the fillet weld connecting the stiffener to the tension flange. Crack growth was characterized by the two stages illustrated in Fig. 20. During the first stage, each individual crack propagated in a semi-elliptical shape as shown in Fig. 21. As the small cracks grew larger they joined each other and eventually assumed the shape of a larger semi-elliptical crack as illustrated in Fig. 22. Before the crack front reached the extreme fiber of the tension flange, the crack width had spread over most of the weld length. After breaking through the extreme fiber, it grew in the second stage as a through crack across the tension flange and up into the web. Approximately 96% of the number of cycles to failure were consumed growing the crack through the thickness of the flange as illustrated in Fig. 20. This was confirmed by visual observations of a number of beams. The remaining 4% of the life was spent in propagating the crack across the flange width and into the web. A more detailed discussion of this behavior is given in Appendix E.

Figure 23 shows a fatigue crack surface at a Type 3 stiffener after failure. The crack is seen to have initiated at the stiffener-to-flange weld. As it eventually advanced up into the web, it joined with a series of semi-elliptical cracks growing from the toe of the stiffener-to-web weld.

Three out of four SG girders that were tested at a stress range of 18 ksi had no detectable cracks at Type 3 stiffeners after 4 to 6 million cycles of load application. Eight SG and SB girder specimens had part-through cracks in the flange. Testing was discontinued because of extensive cracking elsewhere.

The behavior of crack initiation and propagation at Type 3 stiffeners with transverse bracing (Series SB) was identical to the behavior observed in SC beams and SG girders.

3.2.2 Analysis of Data for Stiffeners Welded to the Web Alone

The effects of the primary variables were analyzed using the statistical techniques of analysis of variance and multiple regression analysis. An explanation of these analysis are given in Ref. 1 and the results are given in detail in Appendix E.

Prior to examining the stress variables and their effect, the influence of locating the stiffeners near the load

points was evaluated. As was noted earlier, the stiffeners were located in a position that would insure fatigue crack growth at the weld toe termination prior to developing a failure crack from the web-to-flange fillet welds. Pilot studies had shown that the location finally adopted was necessary to achieve this condition.

To gain insight into the local effects of load point on the stress distribution at the stiffener a plane stress finite element analysis of the test specimens was carried out and the results compared with stress distribution by the conventional beam theory. Details are given in Appendix E.

The stress analysis indicated that at the stiffeners, the load had a negligible effect on the stress distribution in the beam and girder specimens. Hence the stresses predicted by beam theory could be applied to the evaluation without biasing the results.

Stiffeners subjected to bending and shear (Type 1) and stiffeners subjected to bending alone (Type 2) are examined individually to determine whether or not combined stresses needed to be considered in design. When stiffeners were located in a region of moment gradient, crack growth at stiffeners was observed at the weld toe termination. The crack grew approximately perpendicular to the principal stress.

In evaluating the test data it was desirable to ascertain the significance of all the controlled variables. However, particular emphasis was given to the relative effects of the principle stress as compared with the bending stress.

Type 2 stiffeners were located in a region of pure bending moment and therefore subjected to a stress condition not often encountered in structures. These stiffeners were provided to prevent buckling of the web between the loading points. They were cut 4 in. short of the tension flange, so that the weld detail at the end of the stiffener would provide about the same degree of severity as the other types of stiffener details.

Plain welded girder failures limited the acquisition of complete fatigue test data for the Type 2 stiffeners. Whenever a girder failed due to a crack growing from a defect in the web-to-tension flange weld and was 12 in. or less away from a Type 2 stiffener, it was not possible to acquire data at Type 2 stiffeners. The repair (see Fig. 6) influenced the stress distribution and subsequent crack growth at the nearby stiffener.

There were two Type 2 stiffener details thus two observations for each of the 22 SG and SB girders. Six of these 44 stiffeners developed three-ended cracks and constituted complete failure; at 21 details a two-ended through crack in the web

was found; and 17 Type 2 stiffeners exhibited only the first stage crack growth without penetrating the web.

3.2.2.1 Effect of Type of Steel

To determine the effect of steel quality, the fatigue test data for the 6 SG girder specimens at the 2 ksi minimum stress level were evaluated. Three of these girders were made of A441 steel; the other three of A514 steel. The results indicated that the stress range is the dominant variable and that the effect of steel on the fatigue strength of Type 1 and Type 2 stiffeners was not significant.

From this small size sample no general conclusion can be drawn, although the data points corresponding to the A514 high strength specimens tend to fall along the lower half of the confidence band for all SG specimens with Type 1 stiffeners as illustrated in Fig. 24.

The data points corresponding to the four A514 girders with Type 2 stiffeners are plotted in Fig. 25 with solid symbols. At each stress range level they are seen to give slightly shorter lives than obtained from the A441 specimens. The difference is however not significant when measured against the variance of the test data at a given stress range level. Since varying amounts of crack growth was experienced at the Type 2 stiffener, the three categories shown in Fig. 18 are indicated in Fig. 25 for each of the 44 details.

3.2.2.2 Effect of Stress Variables

In the analysis of the stress factorials for Series SC and SG specimens the stress range was found to be the dominant variable while the effect of the minimum stress on the fatigue life was insignificant for both Type 1 and Type 2 stiffeners. As a result of this finding, the minimum stress was deleted from further consideration and a regression of the number of cycles to failure was performed on the principal stress range at the end of the stiffener. The fatigue test data for the Type 1 stiffeners of the SC and SG series are plotted in Fig. 24 together with the mean regression line and the limits of dispersion provided by two standard errors of estimate from the mean. As a visual check on the effect of the minimum stress, different symbols were used to plot the data at each level. That the effect of minimum stress was insignificant is also visually apparent for the Type 2 stiffeners from the test data summarized in Fig. 25. The existence of residual tensile stresses in the regions adjacent to the stiffener weld toes is believed to be the major factor making the full stress range effective at all minimum stress levels.

Only two of the five SC beams tested at the lowest stress range level exhibited visible cracking at the Type 1 stiffener. All five points were excluded from the analysis of variance and the regression analysis to avoid any bias. At this stress range level (principal stress range = 14.8 ksi), the threshold of fatigue crack growth is being approached. However,

the fatigue limit was not defined by this study since failures were observed at this lower level.

3.2.2.3 Effect of Out-of-Plane Deformation from Transverse Bracing

The analysis of variance for SB girders with transverse bracing revealed that the variation of the ratio between horizontal and vertical deflections at Type 1 stiffener had no significant effect on the number of cycles to failure. Stress range accounted for the variation of fatigue life and was not affected by the out-of-plane deformation. These results were compared to those from the SG girders with no out-of-plane deformation. A significant difference between the two girder series was observed when all girders were considered. The A514 steel specimens were then deleted from the SG series since none were included in the SB series and the factorial reanalyzed. The results confirmed that the transverse bracing did not affect the fatigue life at the 5% significance level. The results are summarized in Fig. ~~24~~²⁶ for the Type 1 stiffeners. It is visually apparent that the bracing provided a lower bound to the test data since the SB data points fall near or above the mean line for the 28 SG and SC specimens.

The results regarding the effect of steel type on bracing appears to contradict those at other details. This simply suggests that the A514 steel girder sample was too small to permit

a conclusive analysis. The effect of type of steel appears to be marginal for the welding procedure used. Even if the observed trend were to be confirmed by testing a larger sample of A514 steel girders, the slight difference in fatigue life is probably not sufficient to treat type of steel as a variable in design.

Transverse bracing members were only attached to Type 1 and Type 3 stiffeners. Hence the bracing was not expected to influence the fatigue life of Type 2 stiffeners. The results of the analysis of variance confirmed this.

The mean line given in Fig. 25 represents a low estimate of the fatigue life, because both samples include data points from all three stages of growth were included in the regression analysis. It is apparent that most of the specimens had only exhibited fatigue cracking in the web and that additional increments of life would have been possible had the test not been terminated.

3.2.2.4 Effect of Specimen Size

The effect of specimen size was checked with a "t-test" in which the significance of the difference between the corresponding coefficients of the mean regression lines for Type 1 stiffener of the SC beams and SG girders was determined. The results indi-

cated that welding a Type 1 stiffener to a 14 in. or 38 in. specimen did not significantly affect the fatigue life of the detail at the 5% significance level.

Although statistically insignificant, the fatigue strength of stiffeners welded to the web alone appears to be slightly higher for the 14 in. deep beams as can be seen in Fig. 24. It is believed that this results from the stress gradient across the specimen depth. The stresses along the toe of the stiffener-to-web weld decrease more rapidly in the 14 in. beams than in the 38 in. girders and this logically will increase the fatigue life. The 38 in. deep specimens are more representative of the large-size welded plate girders used in highway bridge construction.

3.2.2.5 Effect of Alternating Shear

The SA beams were subjected to alternating loads which caused the direction of the principal stress at the end of Type 1 stiffener to change about the horizontal axis from -9.5° to 6.7° . The corresponding shear-to-bending stress ratio varied from 0.17 to 0.12. Since the difference between the principal and the bending stress at the maximum load amounted to less than 2%, the fatigue lives were plotted in Fig. 27 against the bending stress range at the stiffener end. Good agreement was observed between

the fatigue strength of Type 1 stiffeners in Series SA and SC. The data points fall just below the mean regression line for plain welded (PW) beams. The results suggest that details subjected to variable principal stress conditions are more dependent on bending stress than principal stress.

3.2.2.6 Bending Versus Principal Stresses

The AASHO specifications⁽¹³⁾ set limits of $0.55F_y$ and $0.33F_y$ on the allowable bending and shear stresses for structural steels. If both were to occur at the same point, the shear-to-bending stress ratio would be 0.6, and the principal stress 28% higher than the bending stress.

Stress ranges are induced by live loads. Single truck loads contribute most to the fatigue damage of short and intermediate span highway bridges because they produce the largest stress ranges. Typically, the load position that generates maximum bending moment at midspan or over an intermediate support of continuous bridges is not the same as the load position that would cause maximum shear force at those points. The highest principal stress range is obtained by maximizing the bending stress range. This will lead to shear-to-bending stress ratios substantially lower than 0.6 and hence to only a slight difference between principal and bending stresses.

Conversely, a loading position that maximizes the shear forces leads to high shear-to-bending stress ratios. However, the principal stress will be smaller than the bending stress obtained from the loads positioned for maximum bending moment. No crack growth was observed at stiffener details where this situation occurred.

The beams and the girders of this study had a shear-to-bending stress ratio of 0.31 and 0.22 at the stiffener. At those ratios the bending stress is only 8% and 4% smaller than the principal stress. This difference is not significant as shown in Fig. 28 where the fatigue lives of Type 1 stiffeners welded to the web alone are plotted against the principal and the bending stress range at the stiffener end. It should also be noted that stiffeners placed further away from the maximum bending moment resulted in high shear-to-bending stress ratio but a decreased principal stress. No fatigue crack growth was observed at those stiffener details.

Actual bridge girders have longer spans than the specimens in this study and an even smaller difference between bending and principal stresses at the critical stiffener details can be anticipated. This results from a number of factors.

- (1) In actual bridges the principal stress is not acting in a constant direction and the experimental indication is that bending alone is more dominant under those conditions.

- (2) The shear stress in the web at the end of transverse stiffeners is between 70-80% of the value estimated on the basis of the gross web area.
- (3) Specifications do not permit the distance between the stiffener-to-web connection and the face of the tension flange to exceed four times the web thickness.
- (4) As the span length increases, the live load shear stress decreases since large members are required.

Hence, principal stresses that occur in regions where the shear-to-bending stress ratio are high will not be large enough to result in crack propagation. Only those stiffeners located in regions of high bending stress range can have principal stresses high enough to result in crack propagation.

Several pilot specimens were tested at higher shear-to-bending ratios (0.5). None of these specimens exhibited crack growth at the stiffener detail prior to failure at some other location (i.e., a plain welded beam or under a loading stiffener). It does not appear possible to generate data on stiffeners at higher shear-to-bending ratios unless special test specimens are used that are not comparable to stiffened bridge members. This was also apparent in earlier tests when full depth stiffeners were used.

3.2.3 Analysis of Data for Stiffeners Welded to the Web and Flanges (Type 3)

3.2.3.1 Effect of Type of Steel

In contrast to results from both Type 1 and Type 2 stiffeners, the data for A514 steel girders with Type 3 stiffeners fall along the mean regression line, as can be seen in Fig. 29. The F-ratio for steel type was much lower than the critical F-ratio at the 5% significance level (see Appendix E). Hence, the effect of the type of steel was not significant for stiffeners welded to the tension flange.

3.2.3.2 Effect of Stress Variables

Since three of the four SG girders tested at the lowest stress range level did not exhibit any visible cracking at the Type 3 stiffener, all four were excluded from the analysis of variance and the regression analysis.

The results of the analysis of variance showed that the effect of the minimum stress was insignificant. The stress range continued to account for most of the variation in fatigue life. This conclusion is visually reflected in the plots of the test data given in Fig. 29 for both the welded beams and girders. The existence of tensile residual stress in the beam flange makes the full stress range effective at all levels of minimum stress.

3.2.3.3 Effect of Out-of-Plane Deformation from Transverse Bracing

Neither the variation of the bracing angle nor the absence or presence of transverse bracing had any effect on the fatigue strength of Type 3 stiffeners. The data for transversely braced girders is plotted in Fig. 29 and visually confirms the results of the statistical analysis.

3.2.3.4 Effect of Specimen Size

Once the stress range was singled out to be the only significant variable, comparisons were made of the mean regression lines of the two samples corresponding to the 22 beams and the 18 girders. The four SG girders tested at the lowest stress range level were again excluded. The results of the t-test showed that welding a Type 3 stiffener to a 14-in. or 38-in. specimen did not significantly affect the fatigue life of the detail. The results from both sizes of specimens are summarized in Fig. 29 together with the mean regression line and the limits of dispersion. It is visually apparent that no significant difference exists.

3.2.4 Comparison of Stiffeners Welded to Web Alone with Stiffeners Welded to the Web and Flange

The test results yielded comparable findings on the

variables examined. Stress range was the dominant variable that defined the fatigue strength for each stiffener detail. The variation attributed to other variables such as minimum stress, specimen size, transverse bracing, and type of steel were not significant.

Since all three stiffener details provided data that were distributed just below the mean regression line for plain welded beams, the results for the three types were examined to determine whether or not they differed significantly. The comparison was made on the basis of principal stress for the Type 1 stiffeners and on the basis of bending stress for the Type 2 and 3 stiffeners. No significant difference was observed between the Type 1, Type 2, and Type 3 stiffeners. The differences were even less when bending stress alone was used for the Type 1 stiffener detail.

The test data are compared in Fig. 30. Only the bending stress range was used for the Type 1 stiffener. For purposes of design the difference between the bending and principal stress range in the critical crack growth region was not significant. The difference is even less in bridge structures where the direction of principal stress changes and shear stresses are likely to be much less than the allowable shear values. Other factors are discussed in Art. 3.2.2.

The mean regression line for 131 data points and defining

the fatigue strength of all three stiffener details is given by the equation

$$\log N = 10.0852 - 3.10 \log S_r \quad (1)$$

The standard error of estimate was equal to 0.1581. The 95% confidence limit for 95% survival shown in Fig. 30 can be used to define the allowable bending stress range at the weld toe of a transverse stiffener. This relationship is applicable to stiffeners welded to the web alone or to the web and flanges.

3.2.5 Comparison with Previous Results

The results of earlier tests are summarized in Appendix A. The data were acquired from a variety of specimens, some were subjected to a stress condition which cannot occur in actual structures. Other specimens exhibited web slenderness ratios and stiffener cut-offs in excess of the values imposed by current specifications. This resulted in severe out-of-plane deformations of the web and fatigue crack growth from secondary deformations that are not permitted.

To permit a meaningful comparison with previous work, the data acquired from specimens which fall into one of the following categories were excluded:

- (1) Girders with a web slenderness ratio exceeding 192.

- (2) Beams and girders with a gap that exceeds 4 times the web thickness between the stiffener end and the face of the tension flange.
- (3) Specimens subjected to shear-to-bending stress ratios at the stiffener end which exceeded 0.6.
- (4) All tests discontinued prior to visible cracking, or because of failure elsewhere.
- (5) Specimens subjected to shear stresses at the stiffener end which exceeded $0.33 \sigma_y$.

Ignoring test data generated under shear-to-bending stress ratios greater than 0.6 appears reasonable as noted earlier when discussing the difference between bending and principal stress conditions. In actual bridge members, crack growth does not occur at locations where the ratio is high because the principal stress generated is not large enough to cause crack growth. The tests on beams subjected to alternating shear further confirmed this observation. When the direction of principal stress changes during cyclic load, the bending stress becomes even more dominant and the principal stress less critical. Actual bridges are subjected to loads which result in a changing principal stress as vehicles cross the structure. Hence bending stress is the appropriate stress condition to consider.

The earlier work on stiffened beams could only provide the high shear-to-bending stress conditions by fabricating special

beams with large flange thickness and thin webs. These beams do not represent actual structural members. Cracks were formed under high shear-low bending stress conditions only when the stiffeners were not full depth. When stiffeners were terminated 1/2 in. short of the flange no cracks were observed to form at locations where nearly comparable stress conditions existed. Further discussion of these conditions are given in Appendices A and E.

The data points retained for the comparison were plotted in Fig. 31 together with the two confidence limits given in Fig. 30.

In general the agreement was found to be good for all stiffener details. The points below the 95% confidence limit for 95% survival correspond to the three early failures attributed by Gurney⁽¹⁴⁾ to undercut at the weld toe of Type 3 stiffeners, and to two failures at load bearing stiffeners of 37 in. girders with a web slenderness ratio of 192⁽¹⁵⁾.

The poor quality welds which resulted in the lower fatigue strength had a more serrated toe and a slight amount of undercutting. The beams failing at load bearing stiffeners had secondary stresses at the terminating weld toe caused by directly loading the stiffener with an extreme load range which was required to generate the stress condition. In addition, lateral deflection of the web aggravated the situation.

There appears to be no rational reason to consider the magnitude of shear when determining the allowable bending stress range at stiffener details welded to the web alone. When full depth stiffeners are used it is not possible to generate a principal stress range that is significantly larger than the bending stress range which will cause fatigue crack growth. This condition can only occur in regions of small bending stress where no crack growth will occur. Hence, the detail is not fatigue critical when this condition exists.

3.3 FATIGUE STRENGTH OF PLAIN WELDED BEAMS AND GIRDERS

Since the stiffener detail was observed to have high fatigue strength, a number of beams and girders developed failures from the flange-to-web fillet welds. This was expected, since the stress range at the stiffener detail could not be increased without a corresponding increase in the stress at the flange-to-web connection. The pilot studies had shown that it was necessary to move the stiffeners as close to the load point as possible without introducing the local load influence in order to cause failure at the stiffener details.

The results of the failures as plain welded specimens provided additional data on the plain welded beam for different beam sizes and increased the available data.

3.3.1 Crack Initiation and Growth

The studies reported in NCHRP Report 102 showed that plain welded beam failures are caused by cracks initiating at a porosity, weld repair, tack weld, or at a stop-start position in the longitudinal flange-to-web fillet weld. Growth from flange tip defects were also reported.

Hirt and Fisher⁽⁹⁾ found that these cracks grow approximately in a circular or penny-shape, with the initial defect at its center, until the crack front reaches the extreme fiber of the tension flange. After penetrating the tension flange, the crack changes into a three-ended crack with two fronts propagating across flange and one front advancing upward into the web as shown in Fig. 32.

Crack growth observations recorded in detail for six girder specimens indicated that the lower front of the penny-shape crack breaks through the extreme fiber of the tension flange at approximately 96% of the total number of cycles to failure. This is comparable to the 94% reported in Ref. 9 for 14 in. deep beams.

3.3.2 Correlation with Previous Studies

Fatigue cracks originating at defects in the longitudinal web-to-flange fillet welds led to failure in 19 of the 22

girders, whereas only a few beams exhibited plain welded beam (PW) failures. This is mainly due to the retesting procedures. The SC beams were retested on a 6 ft. 6in. span, in which the constant bending moment region was eliminated and the probability for PW failures greatly reduced⁽¹⁾. The last 5 SC beams were retested on a 10 ft. span by repairing the initial failure at Type 3 stiffeners. They also exhibited plain welded beam failures.

Since all PW cracks initiated from defects in the longitudinal weld, it would be appropriate to relate the fatigue life to the bending stress range at the center of the weld. For simplicity, the bending stress range at the interface of weld and flange was selected as the independent variable for the regression analysis.

The results of the analysis of variance of the SG girders indicated that the secondary variables, that is, steel type and minimum stress, had no effect on the fatigue life of plain welded girders at the 5% significance level. Transverse bracing was not expected to exert any effect either, since the additional bending stress range induced at the weld by weak axis bending was negligible. The analysis of the factorial for transversely braced SB girders and the comparison of both girder series confirmed this.

The data from both girder series were combined into one sample and a regression analysis performed. The results are shown in Fig. 33. The three data points with an added arrow represent tests that were discontinued or tests for which further acquisition of data was invalidated by substantial repairs at the Type 2 stiffeners. The results are directly comparable to the results reported in Ref. 1. It is readily apparent from Fig. 33 that the test results fall within the confidence limits for the plain welded beam detail reported in Ref. 1.

3.4 FATIGUE STRENGTH OF BEAMS WITH WELDED FLANGE ATTACHMENTS

Fifty-six welded beams were tested with attachment plates welded to the tension and compression flanges. Each beam provided data on crack growth at two cross-sections. The attachments were all welded to the outer surfaces of the flange as shown in Fig. 3.

The attachment length and the stress at the terminating fillet weld toes were the major variables in this study. Generally crack growth was greater at one cross-section and resulted in failure of the test beam. The test was continued on a shorter span until the second cross-section also failed.

The AQ series had $\frac{9}{32}$ in. attachments welded transversely to the flange. This was analogous to the Type 3

stiffener detail. The A2 and A8 series had 2 in. and 8 in. attachment plates, respectively, and 1/4 in. fillet welds around the edges of the plate as illustrated in Fig. 3. The A4 series tests had half of the 4 in. long details attached in the same manner. The other half of this series were welded to the flange with longitudinal welds alone.

Since the ^{9/32}~~1/4~~ in., 2 in., and 8 in. attachment plates had only one weld configuration, each beam provided data on two identical details. This provided for replication of the test data. The 4 in. attachment plates had two different detail configurations as shown in Fig. 3 on each beam. Hence it was necessary to test more than one beam to provide replication.

3.4.1 Crack Initiation and Propagation

Fatigue cracks at all attachment details initiated and grew from the fillet weld toe as illustrated in Fig. 34. Cracks were observed at both ends of an attachment in many instances, even though the attachment was placed in a region of moment gradient. Failure always occurred at the end nearer to the load point because that was the higher stressed location. When no transverse end weld was used to attach a plate, the crack initiated at the weld toe termination of one or both of the longitudinal weldments, and grew through and

across the flange as illustrated in Fig. 34a and 34b. When welds were all around the plate, crack growth was primarily from the transverse weld toe as shown in Figs. 34c and 34d. In general crack growth occurred from a weld toe region that was perpendicular to the applied stress field.

All attachment failures occurred in the bottom flange of the beam except for the retest of member AQ 131 (see Table B1 for member designation system) which failed in the compression flange under one of the loading blocks. Of the tension flange failures, all occurred on the midspan side of the attachment. On the retest of member AQ 261, the failure surface propagated from the midspan side of one of the 1/4 in. attachments to the support side of the adjacent attachment on the opposite side of the web. Although cracks were observed to form in both the top and bottom flanges of the beams, only one beam (AQ 131) failed from the top flange. This beam was subjected to a reversal of stress (-6 ksi to 10 ksi). When the top flange was subjected to a compression stress cycle alone, the cracks were confined to the residual tension zones and were not detrimental to the beams behavior. Comparable behavior was observed in earlier studies on other details.

After a failure occurred in a test, a magnetic probe examination was made of the remaining attachment welds to locate secondary cracks or cracks not associated with the main failure

surface. The data from this examination are documented in Appendix F.

Upon completion of testing, 17 failure crack surfaces were cut out of the beams and examined to determine initiation sites and propagation directions. Failure surfaces of cracks were generally in two categories. These were associated with the type of weld detail.

The first category of failure surface is shown in Figs. 34c, d, and 35 for attachments which were welded all around. Fatigue crack initiation occurred in the main member at the toe of the transverse fillet weld. The magnetic probe examination of secondary cracks indicated that the initiation sites were distributed along the transverse weld. The 1/4 in. attachment weld detail had a significantly greater number of midlength initiation sites than the other three details because it did not have the edge condition caused by the longitudinal welds. One third of the cracks examined were too long to determine precisely their initial propagation sites. The multiple initiation of surface cracks at the terminating fillet weld toe was identical to the condition found at stiffeners welded to the tension flange. This was particularly true for the quarter inch attachments of the AW series.

Twelve failure surfaces of crack growth in the first category were sawed open and examined. Initial crack propagation sites were always at the toe of the transverse weld either where

it was intersected by the longitudinal weld or along the midlength of the transverse weld. The cracks propagating from the weld toe, progressed through the flange and then across the flange towards the web as illustrated in Fig. 35. Quite often, the cracks at the transverse weld toe merged with a crack propagating from the longitudinal fillet weld toe. Often these cracks were offset by as much as 1/4 of an inch and caused a change of plane of the fatigue fracture surface as they merged into single, large crack.

In all cases, the appearance of the failure surface adjacent to the attachment showed that the crack progressed very slowly and presented a plain strain condition. After the crack penetrated the flange a high rate of crack propagation was apparent as the crack front moved toward the web.

Figure 35 shows a typical fatigue failure surface with the primary crack growth along the midlength of the attachment. A second initiation site at the edge of the flange occurred at a later stage of growth. Merger of the two cracks occurred about 3/8 in. in from the edge of the flange. Rapid crack propagation is apparent after the crack penetrated the flange.

Figure 36 shows the fracture surface at a 1/4 in. flange attachment. The crack propagated through the flange thickness on the midspan side of the attachment and ran diagonally across the

flange under the web. A second crack, also apparent on the left of Fig. 36, had propagated on the support side of the attachment. The fracture surface shows that the rate of crack propagation increased after the flange thickness was penetrated.

Crack propagation at the weld toe termination of details with only longitudinal fillet welds constituted a second category of failure surface of crack growth, which is shown in Figs. 34, b, and 37. Crack growth occurred simultaneously from both weld toe terminations as is apparent in Fig. 37. This fact was confirmed by exposing the surface of several small cracks that had not penetrated the flange thickness. Figure 38 shows the small cracks at the weld toe terminations.

Since the 4 in. attachments had both weld configurations on a single beam, failure at the detail with welds all around resulted in an interruption of the test. Oxidation of the fatigue cracked surface at the other detail took place before retesting. This is visually apparent in Fig. 37a. The semi-elliptical surface cracks at the ends of the weldment adjacent to the web are apparent.

It is also obvious from this photograph that a greater amount of crack growth was experienced at the end of the weldment placed along the flange tip. This was expected because the pro-

pagation of an edge crack from the flange tip is more rapid than a semi-elliptical surface crack when both are subjected to the same nominal stress conditions. This is compatible with the theoretical concepts of fracture mechanics. A somewhat analogous condition existed for cover plated beams with the cover plate wider than the flange⁽¹⁾.

A 1/2 in. long crack at the edge of the flange (see Fig. 37b) was observed with the magnetic probe after the initial failure at the detail at the other end of this beam. Four hundred thousand cycles, or 82 percent of the fatigue life, was exhausted at that time. The magnetic probe did not detect the surface cracks which had propagated from the two inner longitudinal weld locations. The cracks had penetrated half the flange thickness, as evidenced by the darkened oxidized area, yet still could not be detected on the flange surface.

Figure 37b shows a similar surface for beam A4 262. There were no cracks detected on the flange surface after the initial test that resulted in failure at the end-welded detail after 143,000 cycles or 63 percent of final life.

3.4.2 Analysis of Data for Welded Flange Attachments

The variables in the study of fatigue life of the welded attachment details were length of attachment, stress and type of weld detail. The material in all cases was A441 steel. There were four attachment lengths: 1/4, 2, 4, and 8 in. There were 2 weld details for the 4 in. attachments: longitudinal welds only and welds all around as illustrated in Fig. 3. The weldment was placed all around the 1/4, 2, and 8 in. attachments.

The effects of the primary variables were evaluated using statistical analysis and theoretical considerations. Details of the results and a summary of the test data are given in Appendix F.

3.4.2.1 Effect of Stress Variables

The effects of the primary stress variables of minimum stress and stress range were examined in detail for each attachment. The results of the analysis indicated that the dominant stress variable was stress range for all the attachment configurations tested. Figure 39 illustrates this fact for the 4 in. attachment with welds all around. It is visually apparent that minimum stress was insignificant at all levels of stress range. Stress range alone accounted for the variation in cycle life.

The existence of residual tensile stresses in the beam flange made the full stress range effective at all levels of minimum stress including stress reversal. Since most of the fatigue life was consumed growing the crack through the flange thickness in the region of tensile residual stress, beams subjected to some reversal of stress provided the same fatigue life.

Similar results were obtained for the other attachment length as illustrated in Figs. 40 to 43. Stress range is seen to account for the variation in cycle life for each detail studied.

Mean regression lines and the standard error of estimate for the 2 in., 4 in., and 8 in. attachments were defined by the following equations:

2 in. attachment

$$\log N = 10.0384 - 3.25 \log S_r \quad (2)$$

standard error of estimate equals 0.0628

4 in. attachment (welded around)

$$\log N = 9.7461 - 3.23 \log S_r \quad (3)$$

standard error of estimate equals 0.0927

4 in. attachment (no end welds)

$$\log N = 9.3480 - 2.82 \log S_r \quad (4)$$

standard error of estimate equals 0.0801

8 in. attachment

$$\log N = 9.5610 - 3.18 \log S_r \quad (5)$$

standard error of estimate equals 0.1182

Because the 1/4 in. attachment series were similar to the stiffeners welded to the flange, a comparison was made. The mean regression line and the limits of dispersion for the Type 3 stiffener are shown in Fig. 40. It is visually apparent that the test data for the 1/4 in. attachments falls within the limits of dispersion and provide good agreement with the mean regression. The test data were distributed between the mean regression line and the upper confidence limit. The results were not significantly different than the stiffener details.

Although slight differences in the slopes of the mean regression lines are apparent, this is primarily attributed to the small sample size for each detail. The slopes were not significantly different when the regression coefficients were tested.

No fatigue limit (10,000,000 or more cycles) was apparent for any detail but the 1/4 in. attachment when subjected to stresses of the experiment design. The 1/4 in. attachments did not exhibit any visible fatigue crack growth at a stress range level of 12 ksi. Several stiffener details were subjected to a bending stress range of 13.7 ksi. Two beams did not fail at that level of stress range. The cycle life at the stiffener detail varied from 3 million up to 13 million when one test was discontinued. The threshold of fatigue crack growth might have been reached in the region of 12 to 13.7 ksi. One beam with four inch attachments was tested at a stress range of 5.9 ksi and did not experience any visible crack growth up to 10 million cycles of loading.

3.4.2.2 Effect of Attachment Length

The fatigue crack growth behavior of the 1/4 in., 2 in., 4 in., and 8 in. attachments was essentially the same. All experienced crack growth at the terminating weld toes of the fillet welds connecting the plates to the beam flanges. However, it is apparent from Figs. 39 to 43 that each detail length yielded a different stress range-life relationship.

The mean regression lines for each detail are compared in Fig. 44 together with the mean lines for the plain welded and cover plated beams. It is visually apparent that a

significant difference exists. The attachment length was a significant variable. The fatigue strengths provided by the attachment series are bounded by the plain welded and cover plated beam conditions. It was noted in Ref. 1 that these latter details provided an upper and lower bound to the fatigue behavior of welded details.

The fatigue strength is observed to decrease as the attachment length increases. Similar observations were made in earlier studies⁽⁵³⁾. The decrease is exponential and quickly approaches the lower bound provided by the cover plated beam. This fact was verified by a pilot test with 16 in. attachments. The test results fell just below the mean for the cover plated beam. At a stress range of 16 ksi, the 16 in. attachment yielded a life of 307,000 cycles.

The variation in fatigue strength appears to be directly related to the development length of the flange attachment. Studies by Ozell and Conyers⁽¹⁶⁾ showed that a cover plated section reached conformance with the theory of flexure at a distance from the end equal to approximately two times the cover plate width for beams with end welds across the cover plate end, and at a distance equal to approximately three times the cover plate width for beams with no weld across the end. The fatigue test results of the attachments appear compatible with the development length. As more force

is transferred into the attachment, the stress concentration at the terminating fillet weld toe is increased.

Experimental studies were conducted to examine the strain distribution in the flange near the toe of the transverse weldment. Strain gage readings were taken under static loading at distances $1/8$ in., $3/4$ in., $1-3/4$ in. from the terminating fillet weld toe. The results are plotted in Fig. 45 by symbols and confirm the strain increase with attachment length. It is also apparent that the development of force in the attachment distorts the bending strain some distance away from the weld toe. For the 8 in. attachments this effect was present up to $1-1/2$ in. from the toe.

A finite element analysis of the stress field and stress concentration condition confirmed the experimental observations. The solid lines in Fig. 45 show the predicted strain distribution. Details of the analysis are given in Appendix F. The stress concentration was observed to increase with attachment length. When the length was about four times the attachment width an upper bound appeared to be reached for attachments with welds all around, corresponding to the case of a cover plated beam. Subsequent increases in length did not effect the condition at the weld toe.

3.4.3 Comparison with Previous Results

A review of fatigue studies on attachments to beams and plates is given in Appendix A. Unfortunately little information is available on beams^(6, 14). Most of the data available is from short gussets fillet-welded to the surface of plates. The gusset length has generally varied between 3 and 6 in. These previous test series did not in general provide much if any replication, nor was an attempt made at randomization of the tests. Hence, uncontrolled variables such as the initial flaw size were not distributed uniformly or accounted for.

The results of these previous tests^(6,14,18,19,20,21) are compared with the appropriate attachment details in Figs. 46 to 50. Unfortunately, only a few tests are available for gusset lengths of 4 in. and 8 in. These are in good agreement with the beam attachments as illustrated in Figs. 46 and 47. It should also be noted that 8 in. groove welded gussets⁽⁴²⁾ are also shown in Fig. 47. These results are also comparable to the fillet welded details. Hence, the groove weld termination of an attachment to a flange or plate is directly comparable to the weld toe termination of a fillet-welded attachment.

A large number of tests have been made on 6 in. gusset attachments^(18,19,20) and these results are shown in Fig. 48 together with the mean regression line and lower confidence limit

for the 4 in. attachments. The results fall above the mean regression line. This results from the smaller stress concentration effect of the gusset type attachment. It should be noted that the gusset test data cover a range of steels and stress conditions⁽¹⁸⁾. The yield point varied from 35 to 112 ksi. The tests included both tension-to-tension stress cycles and reversal of stress. None of these factors appeared to significantly influence the results even with the plate specimens.

A few tests were also made on single groove welded 10 in. gussets attached to the plate edge⁽⁴²⁾. These are compared with the 8 in. attachments and cover plated beams in Fig. 49. Again the results are in good agreement. Crack growth from the end of the groove weld was about the same as for the fillet welded details. The test data are reasonably comparable to the 8 in. attachment.

The stiffeners and 1/4 in. attachments were compared in Fig. 40 for the tests conducted in this study. The results were directly comparable and indicated that the same basic condition existed at the termination weld toe of the stiffeners and short attachment. Earlier tests with stiffeners welded transversely to the flange were compared in Fig. 31. The results of a large number of studies on non-load carrying fillet-welded joints^(14,21,22) are compared with the mean regression curve for stiffeners and 2 in. attachments and limits of dispersion in Fig. 50. These tests included high strength steel specimens⁽²²⁾. It is readily apparent

that the results are in good agreement with the mean regression curve including the tests at high stress ranges in the 50,000 to 100,000 cycle region. Again the type of steel is seen to have a negligible effect on the fatigue strength.

Also shown in Fig. 50 are tests on plates with welded studs. The diameter of the stud and the stud weld toe do not greatly differ from the short attachment. Hence about the same strength should result from crack growth at the weld toe. This is verified by the data plotted in Fig. 50.

The regression lines developed from this study are seen to describe the current test results as well as previous studies.

3.5 STRESS ANALYSIS OF CRACK PROPAGATION

The fatigue life of a detail is defined by the sum of the number of cycles required for crack initiation and the number of cycles required for crack propagation to failure. Nearly all available information indicates that the fatigue life prediction of welded details can be based on crack propagation alone^(1,9,10,22).

Signes et al⁽¹¹⁾ showed that fatigue cracks initiate at the toes of fillet welds from discontinuities constituting a sharp notch when the applied stress is perpendicular to the weld toe. These crack-like discontinuities exist in welds made by all conventional welding processes⁽¹²⁾. These discontinuities are equivalent to initial cracks which propagate under repeated loading.

The fracture mechanics approach to crack propagation appears to be the most rational method currently available for predicting the fatigue life. It has been used to provide an explanation of the fatigue crack growth of a number of welded steel details^(1,9,22,23).

The semi-empirical differential equation of crack growth proposed by Paris^(25,29) has the form:

$$\frac{da}{dN} = C \Delta K^n \quad (6)$$

and relates measured rates of crack growth (da/dN) to ΔK , the range of the stress-intensity factor (K) proposed by Irwin⁽²⁶⁾. The constants C and n are material properties. Equation 6 can be integrated to obtain the number of cycles N required to propagate a crack from an initial size a_i to a final size a_f .

$$N = \frac{1}{C} \int_{a_i}^{a_f} \frac{1}{\Delta K^n} da = \frac{\sigma_r^{-n}}{C} \int_{a_i}^{a_f} \frac{da}{(\Delta K/\sigma_r)^n} \quad (7)$$

The solution of Eq. 7 requires a knowledge of the crack properties of the material and an adequate solution for the stress intensity factor for the detail being examined.

As was noted in Ref. 1, Eq. 7 suggests that the relationship between the life N , and the applied stress range σ_r is exponential in form. The linear regression equation $\log N = B_1 - B_2 \log \sigma_r$ that provided the best fit to the experimental data can also be expressed in exponential form as

$$N = G \sigma_r^{-B_2} \quad (8)$$

in which $G = \log B_1$.

The exponents B_2 and N are the same and reflect the exponential nature of crack growth.

3.5.1 Crack-Growth Rates

In order to solve Eq. 7, the crack growth rate relationship (Eq. 6) is required for the detail under examination. Crack growth rates are material properties that are determined empirically from tests of precracked "fracture mechanics" specimens for which an analytical expression for the stress intensity factor, K , is known. From measurements of crack size, the increases in size corresponding to increments of cyclic loading are related to the range of the stress-intensity factor, ΔK .

Several investigators have reported the growth rates for structural steels^(28,45,47). Barsom⁽²⁸⁾ found that the growth rates in four ferrite-pearlite steels fell into a band as illustrated in Fig. 51. He suggested that the slope of the logarithmically transformed data decreased slightly as the yield strength increased. The slope varied from 3.3 to 2.8 for steels with yield strengths between 36 and 69 ksi. Data have also been reported by Crooker and Lange⁽⁴⁷⁾. A relatively large scatterband was indicated for carbon and low-alloy steels with yield strengths between 34 ksi and 127 ksi. Maddox⁽⁴⁸⁾ determined the growth rates for four different weld metals and their scatterband is also shown in Fig. 51. Three of these four had yield strengths equal to about 67 ksi and the fourth to 90 ksi. It is apparent from Fig. 51 that all of the test data on crack growth is for ΔK values above 10 ksi $\sqrt{\text{in}}$. Only a limited amount of data is available below that level. Paris⁽⁴⁵⁾ reported on very slow growth on ASTM 9310 steel and suggested a threshold value at $\Delta K = 5$ ksi $\sqrt{\text{in}}$.

From a study of experimental results published in the literature, Harrison⁽¹⁰⁾ concluded that fatigue cracks will not propagate in mild steel if $\Delta K < 3.3$ ksi $\sqrt{\text{in}}$. The level of the threshold was observed to be also a function of the mean stress⁽⁴⁵⁾, the threshold being lower the higher the mean stress. Hence, a low threshold value can be expected for fatigue crack growth from

weld toes where the applied stresses are magnified by the discontinuities of the weld geometry and where high residual tensile stresses are known to exist.

The coefficients of the crack growth equation were also established by Hirt and Fisher⁽⁹⁾ using the equivalence between the crack growth equation and the stress range-cyclic life relationship for plain welded beams. A penny-shaped crack was assumed to describe the disc-like cracks that grew in the flange-to-web weldment of beams. This yielded the constants C and n of the crack growth relationship with the values $n \cong 3$ and $C = 2.05 \times 10^{-10}$.

In this study it was assumed that C and n remained constant for all values of ΔK . The relationship found by Hirt and Fisher was rounded and used. The crack growth rate was taken as

$$\frac{da}{dN} = 2 \times 10^{-10} \Delta K^3 \quad (9)$$

for all details. Equation 9 is plotted in Fig. 51 and compared with the data from crack-growth specimens. The relationship developed from beam test is in good agreement with the crack growth data from fracture mechanics specimens. The beam tests had indicated that crack initiation took place at values of ΔK equal to 4 or 5 ksi $\sqrt{\text{in}}$. This was at or below the threshold level suggested

by Paris. It was also observed that most of the beam life was spent at growth rates smaller than 10^{-6} inches/cycle⁽⁹⁾.

3.5.2 Stress Intensity Factors for Fillet Weld Toes

An analytical expression for the stress-intensity factor K for crack growth from the toe of a non-load carrying fillet weld is needed for the solution of stiffener details. A similar solution is required for crack growth from attachments which must reflect the influence of geometry and the force transfer at the attachments.

With an appropriate expression for K , the propagation of a crack through the thickness of the web or flange can be predicted. As noted in the discussion of crack growth at stiffener details, 80% and 96% of the total number of cycles to failure at Type 1 and Type 3 stiffeners were consumed by crack propagation of a flaw through the thickness of the web and flange. Crack propagation at the weld toe of attachment details also resulted in about 90% of the life being consumed during propagation through the flange thickness. Hence, an analysis of this stage of fatigue crack growth represents essentially a study of the fatigue life of beams with stiffeners and details.

Crack initiation and propagation was discussed in detail in Sections 3.2 and 3.3. It was shown that cracks at all three types of stiffener initiated from defects at the weld toe and propagated as a semi-elliptical crack through the thickness of the web or the flange plate during most of the specimens' life.

The change in shape of crack with increasing crack size was found empirically. Over 100 stiffeners were examined by exposing the plane through the weld toe perpendicular to the direction of applied stress⁽⁵⁰⁾. This examination of the fracture surfaces was made at stiffeners where visible cracking was evident, as well as at other stiffeners where no crack was detected.

An exponential relationship was developed between the two semi-axis, a and b, of the semi-ellipse.

$$b = 1.088a^{0.946} \quad (10)$$

Details of the crack measurements and the data evaluation are given in Appendix E.

The stress intensity factor for a part-through crack developed by Irwin^(27,51) can be used with the secant correction for a finite width plate⁽⁵²⁾ to describe the condition illustrated in Fig. 52a. This results in

$$K = \frac{1+0.12(1-a/b)}{\Phi_0} \sigma \sqrt{\pi a} \sqrt{\sec \pi a / 2t} \quad (11)$$

where Φ_0 is an elliptical integral that depends on the minor to major axis ratio, a/b , of the crack.

Equation 11 cannot be directly applied to part-through cracks at the toe of non-load carrying fillet welds connecting stiffeners and very short attachments to the flange and the web, unless the stress concentration effect of the weld is considered. If the part-through crack is removed from the uniformly stressed flat plate shown in Fig. 52a, then the stress field, σ , will remain constant throughout the plate. This is not the case for the detail shown in Fig. 52b which represents a plate strip of either the web or the flange with a portion of the stiffener welded on. In the absence of a crack, the stresses at the weld toe are magnified by the theoretical stress concentration factor K_t . This has been shown to be true for a micro-crack initiating from the surface of a hole in a plate⁽⁴⁹⁾. The effect of the stress concentration decays as the crack grows away from the hole.

The stress concentration effect at weld toes is well known^(3,16,24). An assumption of its influence was made in Ref. 1 when evaluating the behavior of cover plated beams. Gurney has assumed that the stress at fillet weld toes is amplified by a

stress concentration factor $K_t \approx 3.0$, but does not consider its decay. Frank applied a finite element technique and a compliance analysis to evaluate the stress intensity factor for tunnel-shaped cracks at the weld toe of cruciform joints⁽²²⁾. On the basis of this analysis he concluded that the stress concentration effect decreased as the crack propagated into the plate.

The geometry effect can be modeled by considering the stress variation across the thickness of the plate at the weld toe. The crack initiates at the weld toe in a region of stress concentration as illustrated in Fig. 53a. As the crack deepens, it quickly runs out of the area affected by the stress concentration.

The stress concentration factor for points through the thickness of a plate at fillet weld toes of stiffener details was assumed to decrease parabolically in Ref. 50 from a maximum value with no crack, to no effect at a depth equal to the weld size. This decay with increasing crack depth was used with the stress intensity factor for a part through crack. The decay in the stress concentration effect was similar to the decay polynomial developed for tunnel-shaped cracks at the weld toe of cruciform joints⁽²²⁾.

It was obvious from the examination of the fracture surfaces that the crack propagating from the weld toe of stiffener

and attachment details initially grew as semi-elliptical cracks. Much of the fatigue life was consumed as the cracks grew from their initial micro-crack size in the semi-elliptical form. This initial stage of growth requires a more accurate estimate of the stress intensity factor than the later stages of growth.

On the basis of the studies reported in Refs. 22 and 50, the stress intensity factor was defined in terms of the semi-elliptical crack corrected for the stress concentration effect and its decay with increasing crack depth. The decay polynomial developed by Frank from a finite element and compliance analysis was used to reflect this decay characteristic. This resulted in the following expression for the stress intensity factor for cracks at weld toe terminations.

$$K = K_T \left[1 - 3.215 \left(\frac{a}{t} \right) + 7.897 \left(\frac{a}{t} \right)^2 - 9.288 \left(\frac{a}{t} \right)^3 + 4.086 \left(\frac{a}{t} \right)^4 \right] \sigma \left[\frac{1 + 0.12(1-a/b)}{\Phi_0} \right] \quad (12)$$

$$\sqrt{\pi a} \sqrt{\sec \frac{\pi a}{2t}}$$

where K_T is the stress concentration factor at the fillet weld toe, a is the crack depth, and t is the thickness of the plate in which the crack is growing. The decay of the stress concentration factor in Eq. 12 as the crack grows into the plate and away from the weld toe is provided by the polynomial of a/t .

3.5.3 Analysis of Crack Growth at Stiffeners

Equations 7, 9, and 12 were used to evaluate the crack propagation through the web and flange of Type 1 and Type 3 stiffener details and the flange attachments. Before the analysis could be carried out, the theoretical stress concentration factor K_t had to be determined at the fillet weld toe. A finite element solution was used for this purpose. Details are given in Appendix E. The results indicated that the weld and stiffener geometry had only a local concentration effect on the stress field.

The nominal stress range at stiffeners welded to the web alone (Type 1) was taken as the principal stress range at the end of the stiffener-to-web weld. At Type 3 stiffeners the nominal bending stress range at the stiffener-to-flange weld was used.

Equations 7, 9, and 12 were used to construct a family of curves depicting the relationship between initial crack sizes and fatigue life for the stress range levels of this study. These curves are plotted in Figs. 54 and 55 for the Type 1 and Type 3 stiffeners. The points on the curves correspond to the observed fatigue lives of beams with stiffeners which experienced crack propagation through the web or flange thickness at weld toe. For Type 1 stiffeners this corresponded to about 80% of the total life. For Type 3 stiffeners the failure life was used.

The observed fatigue lives correspond to initial crack sizes which are within the range of weld flaws reported in the literature^(11,12). The average initial crack size is about 0.004 in.

The solution of Eq. 7 can be used to construct stress range-cycle life relationships for various initial crack sizes. This was done for the Type 3 stiffener details since nearly all the fatigue life was consumed when the crack propagated through the flange thickness. The results are shown in Fig. 56 for crack sizes of 0.001 in., 0.003 in., and 0.02 in. The predicted life is in good agreement with the experimental data for Type 3 stiffeners. The relationship derived for an initial crack size of 0.003 in. is directly comparable to the mean fatigue strength. The predicted relationship for an initial crack size of 0.02 in. provides good agreement with the lower bound of the test data, initial crack size of 0.001 in. agreed well with the upper scatterband of the test data. Only test data at the 13.8 ksi stress range level exceeded the predicted life. The corresponding ΔK values were below the threshold levels suggested in Refs. 10 and 45 at this lower stress range level.

The results obtained from the analysis indicate that the proposed mathematical model for propagation of a part-through

crack at the weld toe of stiffeners is in good agreement with the observed fatigue behavior.

To determine the effect of flange thickness the mathematical model was applied to 1/2 in. stiffeners connected with 1/4 in. fillet welds to 1 in., 1-1/2 in., and 2 in. thick flange plates. These dimensions simulate the welded stiffener-to-flange connections used in actual highway bridges. The stress concentration effect was assumed to decay out after the crack had penetrated into the flange a distance equal to the stiffener thickness. The results of the integration over the interval $0.001 \text{ in.} < a < a_f$ are shown in Fig. 57. It is readily apparent that flange thickness has an insignificant effect on the fatigue strength for the initial flaw conditions that exist at fillet weld toes. The increase in the stress concentration effect was offset by the increased flange thickness.

3.5.4 Analysis of Crack Growth at Attachments

Equations 7, 9, and 12 were also used to evaluate the crack propagation at the terminating weld toe of long attachments. As with the stiffeners it was necessary to provide solutions for the stress concentration factor K_t at the terminating fillet weld toe. The finite element solution considered the longitudinal fillets connecting the attachments to the beam flange. The attachment welds were simulated by connecting nodes along the plate edges. Details of the analysis are given in Appendix F.

The stress concentration factor K_t was observed to increase as the attachment length increased. The variation of K_t as a function of length is shown in Fig. 58. The 1/4 in. length corresponds to stiffeners and the AQ series attachments. The value of K_t for short attachments was not greatly influenced by the presence of the longitudinal fillet welds. The measurements of the strain field shown in Fig. 45 confirm the predicted trend given by the stress concentration factor K_t .

As the attachment length increased more force was transferred into the attachment and the stress concentration at the weld toe increased. The analysis indicated that after the attachments were about 4 times as long as they were wide, further increases in length did not increase the stress concentration at the terminating weld toe.

The mean value for the initial flaw size was assumed to equal 0.003 in., the mean flaw size for stiffener details. For attachments 2 in., 4 in., and 8 in. long, Eq. 7 yielded the cycles required to propagate the crack through the flange. The predicted mean fatigue strength curves are compared with the mean curves determined from the regression analysis of the test data in Fig. 59. Since the predicted life only considered propagation through the thickness of the flange the mean fatigue strength

would be underestimated by about 5%. The mathematical model used to predict crack propagation at the terminating weld toe of the attachments slightly underestimated the fatigue strength of the 2 in. attachments and overestimated the fatigue strength of the 4 in. and 8 in. attachments. Two factors account for this variation. One is the estimate of the stress concentration factor K_t and the second the assumption of the same initial crack size. The experiment design for the attachment series did not provide sufficient details to adequately distribute the flaw size at all stress levels.

This study has shown that life estimated from Eq. 7 results in an exponential relationship for all welded details of the form

$$N \propto G(K_t \sigma_r)^{-3} (a_i^{-1/2} - a_f^{-1/2}) \quad (15)$$

where a_i and a_f correspond to the initial and final crack sizes, G is the crack geometry correction factor for the detail, K_t is the stress concentration factor, and σ_r is the stress range. Since the final crack size is usually large, it has a negligible influence on the life. The most important parameters governing the fatigue strength are a_i , G , K_t , and σ_r .

CHAPTER FOUR

RECOMMENDATIONS AND APPLICATION

1. The current (1969) specifications of the American Association of State Highway Officials (AASHO) limit the maximum applied stress for fatigue⁽¹³⁾. The fatigue stress is considered a function of minimum stress and maximum stress, the type of steel, and the slope (k_2) of a maximum fatigue stress (F_r) equation. Interim specifications were adopted in 1971⁽³⁰⁾ and indirectly provided a stress range design for the several details that were reported in NCHRP Report 102.

This study has continued to confirm that stress range alone is the only significant factor for designing a given detail against fatigue. Minimum stress and type of steel did not significantly affect the fatigue strength of beams with transverse stiffeners or attachments.

The 95 percent confidence limits for 95% survival are shown in Fig. 60 for the stiffener details and attachments tested in this study as well as the cover plated and plain welded beams reported in NCHRP Report 102. It is apparent

that the stress range-cycle life relationships for these details are provided by a family of lines that are approximately parallel.

2. It is recommended that allowable stress range values for fatigue design be selected from the lower confidence limits. This provides a rational means of selecting design stress values and takes into consideration the variability of the test data and the size of the sample tested.

For the stiffener details, the sample size was large enough to ensure that twice the standard error of estimate was about equal to the 95 percent confidence limit for 95 percent survivals. The attachment test series were not as extensive and an increased multiplier was required⁽⁵⁴⁾.

3. For purposes of design, this study had confirmed the applicability of the design stress values developed for A36 and A441 steel rolled beams to A514 steel rolled beams.
4. Current (1969) AASHTO specifications do not provide sufficient latitude for base metal adjacent to or connected by fillet welds. Only one category (F) is provided and was derived from the cover plated beam. A second category (K) is applicable to base metal adjacent to transverse stiffeners in A514/A517 steel.

Provisions should be added to reflect the higher fatigue strength of very short length attachments as compared to the fatigue strength of cover plates on beams. The cover plated beam is a "lower bound" detail and provides the least fatigue strength. At least one category should be added intermediate to the cases of cover plated beam and beam with transverse stiffeners. In addition, recognition of the adverse effect of a groove weld termination at an abrupt change in geometry is needed. The same fatigue crack growth behavior and fatigue strength results when a groove weld or a fillet weld toe terminates in a region of stress concentration with the micro-crack in a plane perpendicular to the applied stresses.

5. The AASHTO specification provision for base metal adjacent to transverse stiffeners in A514/A517 steel should be applied to all steels. Only the stress range should control the design as the strength of the detail is independent of the type of steel.
6. None of the details or beams examined developed a fatigue limit at 2 million cycles. Only the 1/4 in. attachments and the A514 rolled steel beams experienced no visible crack growth up to 10 million or more cycles at the lowest stress range level. It appears desirable to specify a loading condition on high-

way bridges for over 2 million cycles so as to reduce the possibility of crack growth under extreme cyclic applications.

7. This study and the earlier work reported in Ref. 1 can provide the basis for a comprehensive change in the fatigue provisions of the AASHO specifications. The use of stress range for each design detail and loading condition will greatly simplify design computations. At the same time it will reflect the available experimental and theoretical findings on the significant design variables.

Although all design details have not been evaluated during this study, the basic framework has been developed and the critical design parameters defined. Hence, a review of published fatigue data with these findings in mind will permit a more rational interpretation of the results and the development of design values that are more rational than existing specification provisions.

Table 1 gives suggested allowable ranges of stress for a number of categories that are defined in detail in Table 2. The framework is directly comparable to the provisions given in the AISC specification. Similar provisions are now being prepared for the new British fatigue design rules⁽⁴⁶⁾.

Four categories of life are included rather than the three used in the current AASHO specifications. Since the fatigue strength at 2 million cycles does not correspond to the fatigue limit, a fourth category was added to account for extreme cyclic fatigue conditions.

The suggested values of stress range S_r are based on the 95 percent confidence limits for 95 percent survival. They provide a uniform estimate of survival and account for the variation in the available test observations. Only stress ranges which cause tensile or reversal stresses are included. This study and the study reported in Ref. 1 all showed that although cracks may form in the residual tension zones of details subjected to compression stresses, these cracks arrested when they grew out of the residual tensile zone. When subjected to stress reversal the tension component of the stress cycle is enough to continue driving the crack after it grows out of the residual tensile zone. The slight differences in life at this stage of fatigue crack growth is not significant for design purposes.

Several details described in Table 2 are not supported by data from the 12-7 study. The stress category assigned to these details was based on data available in the literature. Current specification provisions are based on these same sources. These details include: (1) built-up plates or shapes connected

by continuous full penetration groove welds parallel to the line of stress; (2) base metal and weld metal in or adjacent to full penetration groove welded splices at transitions in thickness, with the welds ground to provide slopes no steeper than 1 to 2-1/2, with grinding in the direction of applied stress, and the weld soundness established by non-destructive inspection; (3) base metal and weld metal in or adjacent to full penetration groove welded splices, with or without transitions having slopes no greater than 1 to 2-1/2 when the reinforcement is not removed and weld soundness is established by non-destructive inspection; and (4) base metal at details attached by groove welds subject to transverse or longitudinal loading.

CHAPTER FIVE

CONCLUSIONS

This study supplements the findings reported earlier in NCHRP Report 102⁽¹⁾. The conclusions in this chapter are based on the analysis and evaluation of the test data of this study and its relationship to earlier published work, and on theoretical studies based on the application of fracture mechanics to stable crack propagation.

The conclusions applicable to all beams and details are described first. Those applicable to specific beams and details are described under the various categories examined.

1. Stress range was the dominant stress variable influencing the behavior of the welded details and beams tested during this study. The existence of residual tensile stresses in the web or flange at the weld toe makes the full stress range effective.
2. Other stress variables such as minimum stress, stress ratio, and maximum stress were not significant for purposes of design.
3. The log-transformation of cycle life and stress range resulted in a normal distribution of the test data at all levels of stress range and a log-log linear relationship between the two variables.

4. Failures occurred due to destruction of the primary tension flange of all beams with weld details subjected to tension-tension and partial reversal of stress. Crack growth was also observed in the compression flange. However, the growth arrested after the cracks grew out of the tensile residual stress region unless there was a reversal of stress. There were no failures when the flange was subjected to a compression-compression stress-cycle.
5. There was no observable differences in the results of beams tested at the two laboratories. Also, rest periods, interruptions of the tests, and laboratory environmental differences had no influence on the test data.
6. A theoretical stress analysis based on the fracture mechanics of stable crack growth confirmed the suitability of the log-log linear regression models that related the test data stress range and cycle life. The analysis also permitted examination of other effects not tested in this study.
7. No fatigue limit was observed for the stiffener details and for flange attachments 2 in. or longer in length. Their fatigue behavior was defined in this study between 100,000 and 10 million cycles.

8. This study can be used as a basis for further modifications to the fatigue provisions of the AASHO Specifications.

5.1 TRANSVERSE STIFFENER DETAILS

1. The bending stress range at the toe of stiffener-to-web welds and at the toe of the stiffener-to-flange transverse welds can be used as the stress variable to define the fatigue strength of full-depth stiffener details.
2. The principal stress and its direction are not significant for purposes of design in bridge members with stiffeners. Hence the magnitude of shear stress need not be considered when determining the allowable bending stress range at full-depth stiffeners welded to the web.
3. The type of steel was not a significant design factor for any stiffener detail. However, the test data for ASTM-A514 steel girders with A36 steel stiffeners welded to the web alone was near the lower confidence limit.
4. The cracks causing failure of stiffeners welded to the web alone initiated at the terminating weld toe of the stiffener to web weld. When stiffeners were welded to the web and flanges, cracks originated at the toe of the transverse stiffener-to-flange weld. Cracks also formed at the stiffener

ends in the compression regions of the test beams. These cracks arrested after they grew out of the residual tensile stress zone.

5. Welding transverse stiffeners to the tension flange should be permitted when it is needed or desired. The condition of the detail can be considered to be the same as at the terminating weld toe of stiffeners welded to the web alone.
6. The same stress range-cycle life relationship is applicable to stiffeners welded to the web alone and to stiffeners welded to the web and flange.
7. Attaching diagonal lateral bracing to the transverse stiffeners had no effect on their fatigue strength. The resulting out-of-plane deformation did not adversely affect the rate of crack growth. This was true of stiffeners welded to the web alone as well as of stiffeners welded transversely to the flange as well.
8. No fatigue limit was reached within the limits of bending stress range (13.7 to 28.7 ksi) that was examined.

5.2 WELDED BEAM ATTACHMENTS

1. The crack causing failure at all welded flange attachments originated at the weld toe termination. At transversely welded attachments, the crack originating near the mid length of the weld was most severe although other initiation sites were also observed and eventually connected. At attachments without transverse welds the cracks originated at the termination of both longitudinal fillet weld toes.
2. The fatigue strength decreased as the attachment length increased. The observed behavior was directly related to the force development in the attachment plate.
3. Failure occurred in the tension flange of all beams with flange attachments. Cracks were also observed in the compression flange at the weld toe termination, but they seldom penetrated the flange thickness and mainly grew in a region of local residual tensile stress. These compression flange cracks did not adversely affect the beam behavior.
4. The stress range-cycle life relationships of the flange attachment series were essentially a family of parallel lines when the stress range and cycle life were logarithmically transformed. They were bounded by the parallel lines from the cover plated beam and the plain welded beam data.

5. No fatigue limit was observed for the 4 in. and 8 in. attachments with the magnitudes of stress range (8 to 24 ksi) that were examined. The 1/4 in. and 2 in. attachments were tested at stress ranges between 12 and 28 ksi and no fatigue limit was observed for the 2 in. attachment. The 1/4 in. attachments did not fail at the 12 ksi stress range level at 10 to 15 million cycles of load application. A fatigue limit and threshold of crack growth may have been reached.
6. The differences in fatigue strength of the attachment details as a result of their length were accounted for by a fracture mechanics analysis of stable crack growth. The primary cause of the reduced strength with increasing attachment length was found to be the change in the stress concentration at the terminating weld toe.

5.3 A514 STEEL ROLLED BEAMS

1. A fatigue limit appeared to be reached at a stress range level of 34 to 36 ksi for the A514 steel beams. A number of beams were subjected to 10 million cycles without visible crack growth.
2. The test data were in good agreement with the tests on A36 and A441 steel beams. Type of steel does not appear to have a significant effect on the fatigue strength except for a slight

difference in the fatigue limit. The fatigue limit and crack growth threshold was not clearly defined in this study.

3. Severe notches in a flange surface can initiate cracks and cause failure at much reduced levels of stress range. Obvious notches on flanges should be removed by grinding.
4. The 1971 interim AASHO Specifications for the fatigue strength of base metal can be used to define the fatigue strength of rolled beams for 100,000 and 500,000 cycles. A higher threshold of stress range appears appropriate for 2 million or more cycles of loads.

CHAPTER 6

RECOMMENDATIONS FOR FURTHER WORK

The initial work on welded beams indicated that the plain-welded beams possess the best fatigue behavior that can be expected of a welded built-up beam. The test results yielded information on a minimum notch condition and hence provided an upper bound for the fatigue strength of welded built-up beams. A maximum notch condition was provided by the beams with partial length cover plates. The cover plated beam represents one of the most severe conditions that can be expected and yields a lower bound condition. Unfortunately many details exhibit comparable behavior although they are not cover plates.

The experimental work reported herein and in NCHRP Report 102 has indicated that of all the controlled variables thought to have some influence on the fatigue strength, the primary ones are the range of stress and the type of detail. This was illustrated in Ref. 1 for the upper bound plain welded beam tests, and the lower bound beams with partial length cover plates. In the current study provisions were made to isolate the design factors that were thought to have some influence upon the fatigue behavior of rolled A514 steel beams, welded beams with stiffeners,

and welded beams with welded attachments. These studies have continued to confirm that the range of stress and the type of detail are the dominant variables controlling the fatigue strength.

The continuing studies have also confirmed that the initial flaw condition is a major contributing factor to the fatigue strength. In welded details it is not possible to control this variable. Hence, it must be considered as random and uncontrolled. Because of this factor, reasonable-sized experiment designs must be provided to ensure a satisfactory distribution of the uncontrolled flaw size. Only in this matter can rational fatigue data be generated.

6.1 SUGGESTED STUDIES

It is recommended that consideration be given to the following further studies so that appropriate design criteria can be developed for these conditions. A number of these studies were listed in NCHRP Report 102. They are repeated here for completeness.

1. Butt splices with and without reinforcement in place. The studies on beam splices with the reinforcement removed needs supplementing. That study indicated that the beam

splice at width transitions with reinforcement removed will approach the upper bound provided by the plain welded beam. Previous studies on simple butt welded plates have indicated substantially different strengths for welds with reinforcement in place compared to those with the reinforcement removed. Because the plain welded beam provides an upper bound to the fatigue strength, it is desirable to ascertain whether or not butt welds with part or all of the reinforcement in place cause a substantial reduction in fatigue strength from the upper bound. This will assist in determining whether or not excessive effort is being made to condition the splice even though it cannot exceed the upper bound behavior. Some removal of the reinforcement may be necessary to provide satisfactory non-destructive inspection. Also needed are studies on groove welded splices of flange plates with different thicknesses and with cope holes.

2. An evaluation of hybrid groove welded splices should also be undertaken. This would involve the evaluation of welded details connecting two different grades of steel together. The influence of dilution of the weldment and whether or not it influenced the fatigue behavior should be determined. In addition, other miscellaneous details should be studied including the basic behavior of the weldment. The studies on A514 steel girders with A36 steel stiffeners indicated a possible increase in initial micro-flaw condition. Additional work is needed to characterize this.

3. Studies are needed on groove welded attachments and cross beams. These are commonly used details today. The groove welded plate attached to a tension flange tip or web is commonly used in nearly all bridge construction to attach lateral bracing and diaphragms. Often nothing is done with the weld termination on the flange tip or web. Crack growth can be expected at these weld toes comparable to that observed at toes of fillet welds. Substantial reductions in fatigue strength can be expected from these groove welded plates. Further experimental studies are needed on this detail. It is suggested that studies be undertaken to determine the variation in fatigue strength with plate length and the condition of the weld termination, its transition and reinforcement condition.

4. Further studies are needed with stiffeners welded to the flange and web. The current study has shown clearly that significant improvements in fatigue strength are possible with stiffeners welded directly to the flange as compared to the fatigue strength provided by welded attachments with some length. It is apparent that there is a need to examine factors not covered extensively in the current program. Among factors needing consideration are the relationship of the stiffener thickness to flange thickness, the effect increase in flange thickness, the geometrical configuration of the stiffener welds and the sizes of copes, and whether or not the welds can be passed continuously over the longitudinal welds. Variations in the size of the

stiffener-flange weld should be considered as larger welds are needed to resist higher out-of-plane forces when used to connect intermediate diaphragms on curved girder bridges. The behavior of groove welded stiffeners should be examined. Further studies on hybrid steels and their influence on the initial flaw size are needed.

Other special stiffener details are in use. For example, a thicker plate is inserted into the web at the stiffener. These and other conditions should be examined to determine their merit and their relationship to simpler details. These studies should all be undertaken on girders at least as large as the SG series tests.

5. Further studies are needed on the behavior of attachments to beams and girders. Again it should be noted that in the review comments provided by the Panel, suggestions were made that attachments should also be placed on deeper girders. It is proposed that the 14-inch beam studies with welded attachments be extended to deeper girders. Actual bridge details in common use today should also be used and their behavior correlated to the small attachments that were placed on beams during the initial test program. The attachments should be located on both the flange and the web depending on the detail configuration.

6. It is common practice today to use longitudinal groove welds with the back-up strip in place in box girder sections. Studies are needed on this weld configuration to determine whether or not the flaw condition and its resulting fatigue strengths under these welding conditions are more severe than the plain-welded beam condition. It is proposed to undertake these studies on plate girder type specimens that have a ^{These studies should be made on} single beveled groove weld with back-up strip in place. ~~single beveled groove weld with back-up strip in place.~~

7. Studies are also needed on bolted beam splices. Existing studies have only involved tests on simple butt splices. As with welded details, the experiment designs have not permitted a rational evaluation of the design factors. Recent studies have indicated that type steel may only have a minor influence as is the case for welded beams. Since this class of joints form an important segment of practical fastening methods, it is desirable to extend the studies into this region.

APPENDIX A: LITERATURE SURVEY

A history and summary of previous work in rolled beams, welded beams without attachments, cover plated beams and beams with groove welded splices was given to NCHRP Report 102. This appendix extends the evaluation of further work to stiffened beams and girders and beams with flange attachments.

A1 Beams and Girders with Stiffeners

A review of the literature indicated that most of the studies on stiffened beams and girders were undertaken on 11 to 37 in. deep welded beams fabricated from steels with a yield strength between 32 and 100 ksi. The stiffeners of varying length were fabricated from mild steel and welded to the web alone or to the web and flanges.

The dimensions of stiffened beams tested in previous investigations are listed chronologically in Table A1. Information on the stiffeners and welds are given in Table A2. The applicable test results from these studies are listed individually in Tables A3 through A5 and the data are summarized in Figs. A1 through A3. Also shown are the mean regression lines for the plain welded and cover plated beams⁽¹⁾ which define the upper and lower bound of the fatigue strength of welded beams. Ratios

of shear-to-bending stresses at crack initiation points in the web are shown in Fig. A4. It is readily apparent that high shear-to-bending stress conditions were usually examined. Figure A5 illustrates the different types of fatigue cracks and Table A6 shows the number of fatigue failures in each series by type of crack.

Stiffeners Welded to the Web

Two distinct conditions in the web may induce fatigue crack growth at the toe of the stiffener-to-web fillet welds, ^Wwhen subjected to moment and shear the weld toe termination is subjected to a principal stress condition that is more severe than the bending stress alone. Generally fatigue cracks have always formed perpendicular to this principal stress or in plane stress condition.

A second condition can develop in very thin web girders. The thin webs are prone to instability before the maximum applied load is reached and deform out-of-plane and allow a redistribution of stresses. Such bulging of the web produces membrane stresses and secondary bending stresses.

Thin web flexural members with severe out-of-plane deformations have substantially reduced fatigue lives. For example, Hall⁽³¹⁾ reported fatigue lives of 20,000 and 250,000 cycles

at 20 ksi stress range for two stiffened beams with a web slenderness ratio of 244 and large initial out of flatness. In a later investigation on a similar type of specimen, Hall⁽³²⁾ actually recorded initial web deflections due to distortion during fabrication of up to three times the web thickness, and web deflections at maximum test load of up to six times the web thickness. Such test specimens are not compatible with bridge and building fabrication practice.

The first major investigation of the fatigue strength of stiffened steel beams dates back to 1948. Wilson⁽⁶⁾ tested nine beams with stiffeners located under the load points. Unfortunately, the lack of information on crack initiation and growth does not permit reliable plotting of the fatigue test data.

In 1959, Kouba and Stallmeyer⁽³³⁾ reported the results of 45 fatigue tests on manually welded, twelve-inch deep stiffened beams. The major variables considered were stress, one and two sided stiffeners, continuous and intermittent stiffener-to-web welds, and the stiffener cut off point. Fatigue failure of the beams with stiffeners welded to the web alone was caused by cracks which initiated at the lower end of the stiffener-to-web weld toe and grew diagonally upward into the web and downward towards the web-to-flange weld. Upon reaching the web-to-flange

weld, the crack proceeded horizontally along the weld toe. Only one of thirty-one such beam failures exhibited crack penetration into the tension flange. This crack propagation behavior is believed due to the high shear-to-bending stress ratio in the web. This ratio varied from 0.83 to 5.16 at the crack initiation points as shown in Fig. A4. The tests were generally stopped after two-inch long cracks formed. The results are plotted as open squares in Fig. A1. It should also be noted that cracks only formed at high shear-to-bending stress ratios when the stiffener welds terminated 2 or more inches above the flange.

Gurney⁽³⁴⁾ tested eleven-inch deep welded beams of high strength steel. The stiffeners were cut off at varying distances from the tension flange, resulting in shear-to-bending stress ratios at the lower end of the stiffener-to-web welds between 0.72 and 1.60 (see Fig. A4). In ten out of eleven beams, cracks initiated at the stiffener weld toe and propagated in a direction approximately perpendicular to the direction of the principal tensile stress. One crack originated at the upper end of the stiffener-to-web weld in the compression side of the web. The test points are plotted as open circles in Fig. A1 and fall below the scatter band observed by Kouba and Stallmeyer⁽³³⁾. Crack growth was also confined to the web.

In an attempt to verify the size effect, Braithwaite⁽³⁵⁾ carried out four tests on 25 in. welded girders. Only two failed

from cracks growing in a way that resembled the crack growth reported by previous investigators. The shear-to-bending stress ratio at the lower end of stiffener-to-web welds was 1.18, and the tests were stopped when the web cracks were four inches long. The results are plotted as solid dots in Fig. A1.

Hall, Goodpasture, and Stallmeyer^(36,32) studied the effect of flange rigidity, vertical stiffener rigidity and initial web deflection on the fatigue behavior of individual panels of thirty thin web girders with web slenderness ratios between 267 and 312. All thirty specimens failed from cracks growing at varying heights along the toe of the stiffener-to-web welds. The cracks were due to severe bulging of the web under applied loads. No correlation was found between the rigidity parameters of the members on the panel boundaries and the fatigue life. The specimens with smaller initial web deflections, however, appeared to have longer fatigue lives. These results were not considered in view of the unrealistic cross sectional dimensions and initial web deflections of the test specimens.

The same type of behavior, although less severe, was observed by Yen and Mueller⁽³⁷⁾, who tested nine 50-inch deep plate girders. The girders developed fatigue cracks along weld toes at any one of the four panel boundaries.

Fielding and Toprac^(15,38) investigated the fatigue strength of hybrid girders with A36 webs and A514 flanges. Test parameters included stress range, web slenderness ratio, web aspect ratio and transverse stiffener length. Cracks grew at the end of the load bearing stiffeners where the shear and bending moment diagrams are discontinuous, thus leaving some uncertainty about the magnitude of the principal stress at the crack initiation point. The results of a finite element stress analysis of the girders tested in the present investigation indicated that the principal stresses in the web at the lower end of the bearing stiffener are approximately equal to the bending stresses at midspan at the same distance from the neutral axis. Hence, this value was used to plot Fielding and Toprac's fatigue test data as open triangles in Fig. A1. Cracks were not observed in a number of specimens and the data points are indicated by arrows. The lower points correspond to stiffeners with an 8 in. cut off, the higher points to stiffeners with 2 in. cut off. It is probable that out-of-plane deformations occurred at the end of the load-bearing stiffeners with an 8 in. gap between the flange and stiffener end. This would introduce secondary stresses and decrease the fatigue strength.

The available tests on stiffeners welded to the web alone indicate that the principal stress at the terminating fillet

weld toe provides good correlation of the test data. Whether stiffeners were provided on one or both sides of the web, and whether the stiffener-web welds were continuous or intermittent did not seem to significantly affect the fatigue resistance, provided that it is plotted against the principal stress range at the crack initiation point. Increasing the shear-to-bending stress ratio appeared to decrease the fatigue life. This was especially true when extreme values of shear to bending stress were tested.

The fatigue tests carried out in the past on beams with Type 1 stiffeners have several drawbacks, among which are unrealistically high shear-to-bending stress ratios in the web which results from partial depth stiffeners. This resulted in principal stress values approaching and even exceeding the maximum bending stress at midspan, as indicated by the numbers in Fig. A4 which gives the principal stress of the stiffener as a percentage of the maximum bending stress. Crack growth was only experienced under these high shear-to-bending ratios when the stiffeners were cut short of the tension flange. Furthermore, variation of too many parameters in a series makes a rational evaluation of the significance of the individual parameters on the fatigue strength almost impossible. In most cases crack growth was limited to the web.

The fatigue behavior of the web to which stiffeners have been welded in a constant bending moment region is similar to the behavior in a moment gradient region. Crack initiation at these stiffeners occurs at the toe along the lower portion of the stiffener-to-web weld. After growing through the web plate, the crack propagates in the absence of shear stresses vertically upward along the weld toe and downward to the web-to-flange junction and eventually into the flange.

Gurney⁽³⁴⁾ reported five tests on 11 inch welded beams of high strength steel. They are plotted as circles in Fig. A2. Nee⁽⁴⁾ investigated the fatigue strength of 8 inch stiffened rolled I-beams of A514 steel. Applied bending stress ranges at midspan varied from approximately 18 to 65 ksi. The test data is plotted with open squares. Two failures were also observed by Yen and Mueller⁽³⁷⁾ on 50-inch deep girders, shown with solid dots in Fig. A2.

Of the 39 tests of hybrid girders with stiffeners in the constant moment region that were reported by Toprac, Natarajan, Fielding and Vinh^(38,39,40), only 11 failed from cracks initiating at the lower end of the stiffener-to-web weld. They are plotted as open triangles in Fig. A2. Six girders failed as plain welded beams, five had typical thin web cracks along the weld joining the web and the compression flange, and 15 tests were stopped after two to five million load cycles and prior to visible cracking. They are shown with arrows. Only girders with primary

cracks leading to failure are included in Fig. A2. Vinh⁽⁴⁰⁾ computed secondary bending stresses at the compression flange boundary of the web panel which exceeded the yield strength for one girder with a ten gage web and a slenderness ratio of 268. This girder had a 10 inch long crack at that boundary, but it failed as a plain welded beam from a crack originating in the web-to-flange fillet weld. The ratio of initial web deflection to web thickness was 1.9 for this specimen. Vinh and Toprac⁽⁴⁰⁾ observed that thin web cracks along the toe of the web-to-compression flange weld of hybrid girders did not occur when the web slenderness ratio was less than 192 and the ratio between initial web deflection and web thickness less than one. This is in agreement with the web slenderness ratio limit proposed by Yen⁽⁴¹⁾ for plate girders.

Figure A2 includes tests on 8, 11, and 37 inch deep, homogeneous and hybrid specimens, with welded or rolled sections, of mild and high strength steels. Stress range is seen to account for most of the variation in fatigue life. Only in Nee's⁽⁴⁾ tests were the cracks allowed to propagate into the tension flange.

Stiffeners Welded to the Web and Flanges

In most previous investigations^(14,33,35) stiffeners welded to the web and flange were situated in a constant bending moment region.

Kouba and Stallmeyer⁽³³⁾ tested beams with several stiffeners. The test data are plotted as open squares in Fig. A3. Three specimens exhibited crack growth from the toe of the stiffener-to-flange weld in the constant moment region. The remaining two failures occurred in the moment gradient region, with cracks developing simultaneously at the toes of the stiffener-to-web and the stiffener-to-flange welds. This is mainly due to the cross sectional dimensions of the 12-inch welded test beam. The critical stiffener in the moment gradient region had nominal principal stresses at the end of the stiffener-to-web weld which exceeded the bending stresses at the toe of the stiffener-to-flange weld by 32 percent. This does not correspond to conditions normally experienced in beams.

Gurney's tests were carried out on 7-inch deep rolled steel beams and are plotted as circles in Fig. A3. The three early failures reported by Gurney⁽¹⁴⁾ were attributed to undercut at the weld toe. Braithwaite's⁽³⁵⁾ tests on 25-inch welded steel girders are shown as open triangles. The stiffeners were located in a constant bending moment region.

Except for the three early failures reported by Gurney there is good agreement among the test data which lies just below the strength of the welded beams. The bending stress range is seen to define the fatigue strength.

A2 Beams with Fillet Welded Flange Attachments

As far as is known only two investigations have been carried out on beams with short attachments welded to the flange with longitudinal fillet welds^(6,14). Wilson tested six rolled beams with 4 in. long plates attached to the tension flange. Gurney tested beams with stiffeners that were welded to short 3 in. plates which were in turn welded to the flange by longitudinal fillet welds as shown in Fig. A6. No other tests are available on beams with fillet welded short flange attachments. Cover plated beams have had cover plates of varying lengths. However, in all these tests the length was always sufficient to develop the cover plate and provide the same stress condition at the terminating fillet weld toe of the cover plate end.

There are numerous tests available on flat plate specimens with short gussets attached to the surface of a plate and a few with the gussets attached to the surface of a plate and a few with the gussets attached to the edge of the plate as illustrated in Fig. A6^(14,18,19,20,21). These joints are classified as longitudinal non-load-carrying fillet welded joints⁽²⁴⁾. In general the gusset plates have been attached to 1/2 in. plate specimens with longitudinal fillet welds with no weld deposited at the end of the gusset.

These studies have in general also confirmed that stress range is the only significant stress variable and that the type

of steel is not a significant design factor⁽¹⁸⁾. Most of the specimens with 3/8 in. gussets welded on the plate surface had a gusset length in the direction of stress of 6 in.

A few tests were conducted on specimens with increased thickness⁽¹⁹⁾. These fell near the upper limit of dispersion of the test data and appeared to reflect the additional time needed to propagate the crack through the plate thickness.

A few tests with the gusset welded all around produced conflicting results^(10,21). It is probable this reflects the sample size and variability in the initial flaw condition more than any other factor.

Only a few tests were made with gussets attached to the plate edge⁽¹⁹⁾. The length of the gusset was varied. These tests indicated that a decrease in the size of the attachment improved the fatigue strength.

A number of tests have also been carried out on plates with welded pads attached as shown in Fig. A6. These specimens are similar to the fillet welded flange attachments reported in this study.

A large number of transverse non-load carrying welded joints have been tested in the past. Generally gusset plates

were welded transversely to the surfaces of the plate as illustrated in Fig. A6. These short attachments appear to be comparable in many respects to transverse stiffener details. A detailed discussion of these studies is given in Ref. 24.

APPENDIX B: EXPERIMENT DESIGN

The objective of the beam and girder test series reported in this study was to determine their stress life relationships and to ascertain whether or not the controlled variables were significant. Since type of detail and the stress range were shown to be the major factors which influence the fatigue strength in NCHRP Report 102 they were accorded primary attention in this study.

The experimental variables selected for the rolled beam series (designated PRC) were nominal stress in the outer beam fiber and the size of beam. The W14x30 was identical to the basic unit used in the previous studies on A36 and A441 rolled steel beams. The W10x25 permitted higher levels of minimum stress and stress range. Coupled with the earlier work⁽¹⁾ the proposed experiment design permitted an evaluation of the stress variables, type of steel, and beam size. The W14x30 A514 beams were furnished from one heat. The W10x25 beams were furnished from two heats.

The controlled variables selected for the welded beams and girders with stiffeners were nominal stress, type of stiffener, type of steel, and lateral bracing support for the stiffener. Each plate thickness for each type of steel was taken from the

same heat. The same fabrication procedures were used for each welded beam and girder.

The controlled variables selected for the welded attachment beam series were nominal stress at the welded attachment terminus, attachment length, and attachment weld detail. All attachments were welded to the outside flange surfaces of A441 steel welded built-up beams.

All 14 in. welded built-up beams for this study were fabricated from A441 steel. They had a yield point of 50 ksi. A441 steel was selected to permit higher maximum stress levels to be reached without difficulty. The study reported in Ref. 1 had indicated that type of steel was not a significant design variable. The 38 in. welded girders were fabricated from A441 and A514 steel. Only four of the 22 girders were fabricated from A514 steel.

To evaluate the systematic effect of the stress range, minimum stress, maximum stress, and type of detail, factorial experiments were constructed. This permitted the effects of the controlled variables to be determined statistically using analysis of variance and regression analysis techniques.

APPENDIX C: MATERIAL PROPERTIES AND BEAM CHARACTERISTICS

Details of the beams and girders are given in Figs. 1, 2, and 3 with nominal dimensions and weld details. The nominal dimensions of the welded 14 in. beams were identical to the plain welded (PW) series reported in Ref. 1. Plates with nominal thicknesses of $3/8$ in. were used for the flanges and the nominal web thickness was $9/32$ in. The girder flange was $1/2$ in. thick and the web was $1/4$ in.

All stiffeners and flange attachments welded beams were fabricated from $9/32$ in. A36 steel plate. Stiffeners attached to the 38 in. girders were fabricated from $1/4$ in. and $1/2$ in. A36 steel plate.

The thickness of the flanges and web was measured with a micrometer. Widths of the flanges and the depth of the beam was measured using a dial gage mounted on a fixed caliper. Average measurements were used to determine the cross-sectional properties.

Table C-1 summarizes typical measured dimensions and cross-sectional properties of typical rolled and welded beams. The cross-section properties were directly comparable to the rolled and welded beams used in Phase I of NCHRP project 12-7⁽¹⁾:

Mechanical Properties of Material

Tension specimens were fabricated from sections of the beam flanges and webs. The test sections were randomly selected from two typical beams for each heat and plate thickness. All test specimens conformed to ASTM A370. The width of the specimens was 1.50 in. All tests were conducted in a Tinius-Olsen 120-kip capacity screw-type mechanical testing machine. Specimen dimensions, yield load, static yield load, ultimate load, fracture load, failure dimensions, and location of break were recorded. Several complete stress strain curves were also determined.

Testing speed was 0.025 in./min. until the yield point was established. The speed was increased to 0.100 in./min. and maintained at that rate up to rupture after strain hardening was observed. The initial gauge length was 8 in. and was used to determine elongation characteristics.

Table C-2 summarizes the averages and standard deviation for the static yield stress and tensile strength of the various steel plates and shapes. Average values of elongation and reduction in area are also tabulated.

Mill Reports of Chemical and Physical Properties

The results of mill tests on specimens from plates and rolled beams are given in Table C-3. For a given beam flange and web the heat number, mechanical properties, and the result of the chemical analysis are given. The mechanical properties include dynamic yield point (usually provided at 0.100 in./min.), tensile strength, and elongation.

APPENDIX D: A514 STEEL ROLLED BEAMS

Details of the tests on A36 and A441 steel rolled beams and a summary of earlier work on rolled beams is given in NCHRP Report 102.

The controlled variables selected for the supplementary work on A514 steel beams were influenced by the earlier work. To provide direct correlation with the A36 and A441 steel beam tests 9 W14x30 beams were tested. Minimum stress and stress range provided the controlled test variables. The factorial design is shown in Table B2. The four specimens at $S_{\min} = 2$ and 14 ksi and $S_r = 36$ ksi permitted direct correlation with the earlier work.

Because it was desirable to extend the stress range coverage to higher stresses that were compatible with the static working load stresses, it was necessary to use a second profile in order to achieve the higher stress levels. A W10x25 section was used for this purpose. The minimum stress level was extended to -22 ksi and 26 ksi to better simulate possible working load conditions. The stress range level was extended to 45 ksi and 54 ksi.

All W14x30 rolled beams were furnished from the same heat. The beams were cut to 10 ft.-6 in. lengths in Fritz Laboratory from 40 ft. long members. The W10x24 beams were

furnished from 2 heats and were cut to 8 ft. lengths in Fritz Laboratory. The properties of these members are summarized in Tables C1, C2, and C3.

Test Results

Table D1 summarizes the test data from the beam tests. A detailed description of each column in Table D1 and a schematic of the crack size is given in Table D2. The crack location in Column 4 defines the point along the beam length at which the failure crack occurred.

Column 7 of Table D1 describes the initial flaw condition that precipitated crack growth and failure. When defined as arbitrary the crack generally initiated from the flange surface as shown in Fig. 7. The fracture surface provided this indication. A second major cause was an arbitrary flange tip flaw. These arbitrary flaws were all very small and in the micro-flaw range.

Sometimes the loading arrangement caused a stress-raising and fretting effect and resulted in crack growth. In most of these cases crack growth originated under the loading jacks, at bracing or a stiffener. In general these conditions were directly comparable to the data generated from the other crack growth conditions.

Many of the specimens were tested without using stiffeners in order to minimize these uncontrolled secondary factors. No doubt this contributed to the wide variation in the test data which reflected the sensitivity of the beams to variation in the initial micro-flaw condition.

Analysis

An analysis of variance of the data for A36, A441, and A514 steel beams at the common minimum stress level of 2 ksi and 35 ksi stress range indicated a significant difference in the life. This was expected since three A514 steel beams did not fail after 10 million cycles.

The test data summarized in Fig. 11 was evaluated by visual inspection and regression analysis. The A36 and A514 steel beams that did not exhibit any cracking were excluded from the analysis. The earlier studies had indicated no significant improvement in the correlation of the test data when minimum stress was included in the analysis.

A visual inspection of the data in Figs. 9, 10 and 11 shows that the type of steel did not significantly effect the results except near the run-out level. The A514 steel beams appeared to have a higher threshold of crack growth than the

A36 and A441 steel beams. This finding is consistent with the fracture mechanics of crack growth.⁽¹⁰⁾

The results of the regression analysis are summarized in Fig. 11. The coefficient of correlation was 0.76. The smallest standard error of estimate was obtained when the logarithmic transformation of both cycle life and stress range were used.

Figure D1 shows the cumulative frequency distribution of the test data on probability paper for the A514 steel beams. The results are compatible with the A36 and A441 steel beams reported in Ref. 1

The fatigue limit of rolled beams is sensitive to variation in the micro-flaw condition on the flange surface or tip. Assuming that the same conditions existed in all three grades of steel confirms that the A514 steel beams should have a higher threshold or run-out level. However, a severe mechanical notch can adversely effect this threshold level as was shown by specimen PRC-442. A severe edge notch in the shear span resulted in early failure.

APPENDIX E: FATIGUE STRENGTH OF BEAMS AND GIRDERS WITH STIFFENERS

A detailed review of previous work on stiffener details is given in Appendix A. These earlier studies indicated that fatigue crack growth initiated at the terminating weld toe of the stiffener-to-web fillet welds of stiffeners welded to the web alone. In general the fatigue crack formed perpendicular to the principal stress when the detail was situated in a region of moment gradient.

In order to achieve a high shear-to-bending stress ratio in the web and a high principal stress at the terminating fillet weld toe, special test beams were devised with thick flanges in previous studies. This limited the bending stress and prevented failure from the flange-to-web connection. In addition, many of the stiffener details were terminated several inches above the tension flange. With the profiles used, the shear stress distribution in the web was much more severe than normally encountered. The average shear stress V/A_w was nearly equal to the maximum shear stress given by VQ/It . These conditions do not represent the situation that exists in fabricated bridges.

In this study the stiffener details were attached to beams and girders with cross-sections more comparable to fabricated structural applications. The placement of the stiffeners was developed from pilot tests. Details of the experiment design are given in Tables B3 to B7. The SC beams were used to establish the critical location of the stiffener to insure failure at the stiffener detail prior to experiencing a failure from the flange-to-web fillet welds.

The basic stresses in the welded beam were directly comparable to the experiment design used for plain welded beams and reported in NCHRP Report 102. These are shown in Table B3. Also shown are the stress range conditions at the terminating weld toe of each stiffener detail.

The stress variables for the SA series beams with alternating direction of principal stress are given in Table B4. It was not possible to correlate the experiment design with the other beam series, since the loading system would not permit the minimum stress to be controlled independently.

The girder series SG and SB had the same nominal bending stresses as the SC series beams. However, the stresses at the critical weld toe terminations of all three details on girders differed slightly from those of the SC series beams. The Type 1 stiffeners were deliberately made more critical to insure failure and valid test data. The stress conditions at the Type 2 and Type 3 stiffeners were about the same so that either detail could develop fatigue cracks. When the test series were planned it was questionable that the girders could be repaired and testing continued. Hence if only one failure was possible the Type 1 stiffeners would provide the major source of test data. This problem was overcome with the C-clamp splices. Generally all three details

as well as the plain welded girder experienced fatigue crack growth.

Locating the SC beam stiffeners 9 in. from the loading points, as shown in Fig. E1, produced a stress condition for crack growth at the stiffeners which was less severe than the crack growth condition from mechanical defects in the web-to-flange fillet weld. The desired type of failure was only achieved by moving the stiffeners closer to the loading points, as shown in Fig. 1a, raising the nominal stresses at the stiffener end.

To ascertain whether or not the local load effect would alter the stress distribution predicted by beam theory, a plane stress finite element analysis⁽¹⁷⁾ of the test specimens was carried out and the results were compared with conventional beam theory.

Figure E2 shows the finite element mesh selected for the stress analysis of the girder specimens. Each flange was modeled by 32 bar elements placed along the center of gravity of the trapezoidal stress distribution through the flange thickness. The web of the girder was subdivided into 576 rectangular elements. Bar elements were also provided from the load point down to the center line of the girder to simulate the load bearing stiffeners shown in Fig. 1b. The load was applied at three adjacent nodal points, proportional to the bearing area of the jack ram on the

web and the bearing stiffeners. The total magnitude P was equal to the load required to produce a maximum bending stress of 100 units at midspan according to beam theory.

The beam specimen was modeled with a similar mesh, except that it did not have the bar elements simulating the bearing stiffeners since none were used.

Figure E3 shows the principal stress (σ_p) and shear (τ) stress distribution along two lines parallel to the beam center line at distances of 1/4 in. and 3/4 in. from the inside face of either flange. The web stiffener terminated 1/2 in. from the flange. The position of the Type 1 stiffener is shown by the vertical dashed line which lies just outside the local zone affected by the load introduction. Conventional beam theory and the finite element method yielded identical principal stresses at the lower end of the Type 1 stiffener. At the upper end of the stiffener where crack growth was also observed, the principal stresses computed by the finite element method were 3% higher. The directions of principal stresses at the stiffener end differed by less than one degree between the beam theory and the finite element analysis.

A similar comparison was carried out for the girder specimen. The principal and shear stress distribution along two

lines parallel to the girder center line $1/8$ and $7/8$ in. from the inside face of the tension flange are shown in Fig. E4. The difference in the results can be attributed mainly to the low span-to-depth ratio of 6:1. Beam theory does not give an accurate stress distribution for this geometric condition. The actual test was conducted with loads that produced the desired extreme fiber strain readings at midspan. This procedure corresponds to matching the midspan stress levels of the two sets of curves in Fig. E4. After this adjustment was made, the principal stress in the girder web at the lower end of the Type 1 stiffener as computed by the finite element method was less than three percent smaller than the value predicted by beam theory.

The stress analysis indicated that the load had a negligible effect on the stress distribution in the beam and girder specimens at the stiffeners which were 5 to 8 in. from the loading points. The testing procedure automatically compensated for any error due to the low span-to-depth ratio of the girders. For these reasons, the stresses predicted by beam theory were retained for the regression analysis of the fatigue test data.

Results and Analysis

The results of the tests for each type of stiffener detail are summarized in Tables E1 to E3. The stress conditions in the extreme beam fiber in the constant moment region and at the stiffener weld toe termination are listed together with the cycles to failure for each detail. For the Type 1 stiffeners the observed direction of crack propagation is also listed. Also shown are the crack sizes at test termination in the flange and web of the member at the test detail.

Results of the pilot tests shown in Fig. E1 are summarized in Table E4. Only beams D and E exhibited crack growth at the stiffener details. The principal stress range at the Type 1 and Type 3 stiffeners was 80% of the bending stress range at mid-span. Because the Type 1 stiffener was on the borderline it was moved to 5 in. from the load point to increase the failure probability.

Several girders and beams failed at defects in the flange-to-web fillet welds. These plain welded beam failures are summarized in Table E5. The test data are documented in the same manner reported in NCHRP Report 102.

Analysis of Results

The statistical analysis of the effects of the controlled variables was done using analysis of variance and regression analysis techniques.

The analysis of variance of two-way classified experiments permits the determination of whether certain chosen values of each of the two variables affect the fatigue life of the detail. The replication within a cell makes it possible to estimate the interaction between the variables. For reasons of economy, time, and equipment limitations some of the cells were not tested and the number of replicates was not equal for all cells. In addition, complete data could not be gathered, whenever tests had to be discontinued because of failure elsewhere or by extreme cycle life.

In spite of the unequal number of observations, an analysis of variance over the entire experiment design can still be carried out. There are several ways of dealing with such data. The iterative method used is described by Pearce⁽⁵¹⁾. It consists of filling the gaps with estimated values so that the number of observations in each cell are equal. From these initial guesses, new estimates are obtained, and the iterative process is continued until the residuals of the missing values are reduced to zero.

Thus, they do not contribute to the residual error. The analysis of variance of the two-way classified data, with equal numbers of observations per cell can then proceed normally apart from subtracting the number of missing values from the degrees of freedom in the total and residual error lines. Iteration on all guessed values was terminated after the logarithms of the fictitious fatigue lives differed by less than 0.000005 between two consecutive iteration steps.

The mean sum of squares of the residual error was used to form the F-ratios for the variables and their interaction, which were then compared with the tabulated F-ratios for a level of significance of $\alpha = 0.05$.

The regression analysis model used to relate the number of cycles to failure to the stress range at the crack initiation point had the form:

$$\log N = B_1 + B_2 \log \sigma_r \quad (E1)$$

The coefficients B_1 and B_2 were obtained through a least square fit. As a measure of the goodness of the fit, the squares of the regression coefficient and of the standard deviation were computed. The first measure indicates the fraction of the fatigue life variance accounted for by the regression, and the second is an estimate of that part of the variance left unexplained by the

regression of the fatigue life on the stress range.

In all stress range versus life (S-N) plots the data points are shown together with the mean regression line and the confidence limits at two standard deviations from the mean. The results of the analysis of variance are summarized in Tables E6, E7 and E8 for the three stiffener details.

Type 1 Stiffeners

The determination of the significance of the effects of the stress variables (minimum stress and stress range), type steel, bracing, and type of beams was evaluated and the results of the analysis are summarized in Table E6. The mean sum of squares of each variable considered and their interaction was divided by the residual error to form the calculated F-ratios.

To determine the effect of steel, the 6 SG girder specimens at the 2 ksi minimum stress level were arranged into the factorial shown in Table E9. The results of the analysis show that stress range accounts for the variation.

The analysis of the stress factorials for series SA, SC, and SG all confirmed that stress range was the dominant variable and minimum stress was not a significant factor. The F-ratios calculated for stress range are nearly an order of

magnitude greater than the tabulated values. The calculated F-ratios for minimum stress are in every instance less than the tabulated values.

A cumulative frequency diagram was constructed for each principal stress range level and is shown in Fig. E5. The predicted line was determined from the regression model. It can be seen that the regression model predicts the distribution reasonably well. Hence, the logarithmic transformation and its assumed normal distribution appear reasonable.

The effect of bracing and the resulting out-of-plane deformation were examined with the aid of the factorial shown in Table E10. An analysis of the SB series had indicated that changing the ratio of horizontal and vertical deflection had no effect. However, when compared with the SG girders a slightly significant difference was observed at the 5% level. This difference was attributed to the A514 steel specimens which fall near the lower confidence limit in Fig. 24. The reanalysis confirmed this observation as is apparent in Table E6.

The disparity of the results suggests that the A514 steel sample is too small to provide a conclusive analysis. The difference does not appear to be sufficient to treat type of steel as a significant factor in design.

Type 2 Stiffeners

The results of the analysis of variance of Type 2 stiffeners are summarized in Table E7. The A514 steel girders tended to provide slightly shorter lives than the A441 steel girders, however, the difference was not significant at the 5% level as is apparent in Table E7. Stress range was the dominant variable at a given stress range level. Comparable results were obtained for minimum stress and bracing. Stress range clearly accounted for the variance of the test data even with the few observed failures.

The cumulative frequency distribution of the Type 2 stiffener is plotted in Fig. E6.

Type 3 Stiffeners

The results of the analysis of variance of the Type 3 stiffeners test data are summarized in Table E8. As is readily apparent from the comparison of the calculated and tabulated F-ratios only stress range was a significant variable. No other variable or interaction between variables exceeded or even approached the critical F-ratio for the 5% significance level.

The cumulative frequency distribution shown in Fig. E7 also confirmed the normality of the logarithmic transformation of stress range and cycle life.

Bending versus Principal Stresses

In the tests reported by Kouba and Stallmeyer⁽³³⁾ and Gurney⁽³⁴⁾ the beam geometry was purposely selected to generate principal stress conditions at the stiffener details that were comparable or in excess of the maximum flange bending stress. This resulted in extreme shear-to-bending stress ratios in the web at the weld toe termination as illustrated in Fig. A4. Figure E8 shows the Mohr circle diagrams for these earlier studies and compares them with the girders tested during this study. It is readily apparent that the weld toe termination was subjected to stress conditions in the earlier studies that differed substantially from the test girders reported herein.

As discussed earlier actual structures with full depth stiffeners cannot be subjected to such stress conditions. The stiffened beams and girders reported in this study are more representative of the state of stress than can be expected at details which may experience fatigue crack growth. Details placed on these beams that were located in regions that resulted in higher shear-to-bending stress ratios did not experience fatigue crack growth. In fact efforts to test beams with higher shear-to-bending stress ratios always resulted in failure as a plain welded beam or at a load point.

The alternating shear specimens also showed that

bending stress tends to become more dominant as the direction of principal stress changes. In bridge structures the cyclic load will be caused by vehicles crossing the span and will also result in a changing direction and magnitude of the principal stress at stiffener details.

The overall behavior strongly suggests that shear should not be considered in the design of stiffener details located in regions of bending and shear. Bending stress alone provides a satisfactory measure of the stresses that will cause fatigue crack growth.

Crack Growth at Stiffener Details

In all the stiffener details it was observed that most of the fatigue life was consumed initiating and propagating the crack through the thickness of the web or flange. This was illustrated schematically in Figs. 15, 18 and 20.

Random visual observations on a large number of beams and girders provided information on the first observation of a crack and its subsequent growth. The results of these observations are summarized in Figs. E9 to E11. The bar graph represents the observed fatigue life of each detail. The triangular marker notes the interval of life at which a visible fatigue crack was noted.

The cracks were detected on the surface while the test was being conducted with either a magnifying glass or by magnetic particle inspection with the Parker Contour Probe. It is apparent that these cracks could only be detected by either method towards the end of the first stage of crack propagation as a part-through crack.

For stiffeners welded to the web alone about 80% of the fatigue life was consumed propagating the fatigue crack through the web plate. Sixteen more percent of the life was consumed growing the crack into the flange and through its thickness. The short interval of life remaining was exhausted as a three ended crack propagated in the flanges and web.

For stiffeners welded to the flange and web 96% of the fatigue life was consumed propagating the crack through the flange thickness. Hence both types of stiffeners had about the same life interval remaining once the crack penetrated the bottom surface of the flange.

A detailed examination of the crack propagation through the thickness of the web and flange plate was made for all three stiffener details. Over 100 stiffener details were examined visually by exposing the region at the weld toe and searching the area with a 50X travelling microscope. Table E11 summarizes the

location and dimensions of all single cracks with a semi-elliptical shape that were detected at the weld toe termination. The smallest crack depth found was 0.009 in. The location T refers to the tension flange area and C references the compression flange area.

The semi-elliptical shapes were plotted to determine the relationship between the minor and major axis of the crack surface. Figure E12 shows the results for a wide range of crack sizes. The mean relationship for single cracks at the stiffener weld toes was

$$b = 1.088a^{0.946} \quad (E2)$$

Equation E2 is plotted in Fig. E12 and approached the circular crack with increasing crack size ($a/b = 1$).

Part-through cracks which initiated at more than one point (see Fig. 22) are also plotted in Fig. E11 as open triangles. They were not included in the regression of b on a . Their formation is a random process which depends on the distance between the weld defects and their severity. Cracks were observed to have joined at depths $a > 0.050$ in. in a number of details. This corresponds to at least 2/3 of the number of cycles spent in Stage 1 of growth. Thus, Eq. E2 provides only an approximate definition of the crack shape for the remaining interval of life.

Three part-through cracks that were observed at the end of longitudinally welded cover plates⁽¹⁾ are plotted as circles and fall within the band of crack size data.

Stress Analysis of Crack Propagation

Since the first stage of crack propagation dominated the fatigue life for all details (see Figs. 15, 19 and 20) the stress analysis of crack propagation concentrated on that aspect of crack growth.

Before the analysis of propagation of the part-through crack could be carried out the theoretical stress concentration factor K_t had to be determined. The finite element method was used for this purpose. A typical mesh modeling a strip of the girder flange with a portion of the stiffener welded on is shown in Fig. E13. The mesh size around the weld toe was kept the same for all four geometries corresponding to Type 1 and Type 3 stiffeners on beams and girders (Fig. 1a and 1b). To simulate the assumed zero weld penetration at the weld root, non-connected double nodes were provided all along the interface of the stiffener end with the main plate. The analysis was restricted to one-half of the symmetric joint, the second half being accounted for by restraining the x-displacements of the nodes along the center line of the stiffener. A uniform stress was applied at the end of the main plate in all

geometries. The maximum stress at the weld toe was obtained by passing a surface through the principal stress at the centroid of six elements situated in the area adjacent to the weld toe in Fig. E13.

The weld and stiffener geometry appeared to have only a local concentration effect on the stress field. At 0.1 in. from the weld toe, the maximum element stresses were reduced to the applied stresses, as shown by the stress distribution along sections A-A and B-B in Fig. E13.

The numerical solution of the finite element analysis was carried out with the aid of a program written at Fritz Engineering Laboratory by S. Desai and J. Struik⁽¹⁷⁾. The stress concentration factors K_t for the beam and girder stiffener details are summarized in Table E12.

The K value for a crack embedded at the stiffener fillet weld toe was estimated at each stage of crack growth from Eq. 12. The equation is plotted in Fig. E14 for a girder with a 1/2 in. flange and a 1/4 in. fillet weld. Also shown in Fig. E14 with dashed lines are the factors accounting for the shape of the crack front, the geometrical stress concentration, and the finite thickness of the plate. The product of all three factors is equal to K non-dimensionalized by the value of $\sigma\sqrt{\pi a}$.

Stage 2 of growth at Type 1 stiffener began after the part-through crack in the web broke through the far side of the web plate. It ended when the lower front of the two-ended through crack reaches the extreme fiber of the tension flange.

The stress-intensity factor for such a crack is difficult to define, because the two crack fronts propagate under different conditions. In many cases the upper front was observed to follow the stiffener-to-web weld toe, before branching off diagonally into the web. Several specimens exhibited crack growth directly off the end of the stiffener-to-web weld. The point where the crack path deviated from the toe line depended on the number of initiation points, the relative distance between them, and also on the shear-to-bending stress ratio.

The lower crack front extended quickly past the weld toe and grew in the plain web plate and then entered the web-to-flange junction. While growing through the junction, the front appeared to assume a circular shape, as shown schematically in Fig. 15 until it reached the extreme fiber of the tension flange. The stress gradient across the depth of the specimen, combined with the stress concentration effect of the stiffener-to-web weld on the upper crack front, further complicates the problem of estimating a stress-intensity factor for the overall crack.

Stage 2 of growth only accounted for 16% of the total number of cycles to failure at Type 1 stiffener, as shown in Fig. 15. To approximate the observed behavior during this stage of growth, the lower crack front was assumed to grow as a circular crack in an infinite solid under a constant stress applied away from the crack tip. The interaction between the two crack fronts was neglected.

The stress-intensity factor for a circular crack and a finite thickness correction yields

$$K = \frac{2}{\pi} \sigma \sqrt{\pi a} \sqrt{\sec \pi a / 2t} \quad (E3)$$

APPENDIX F: FATIGUE STRENGTH OF WELDED ATTACHMENTS

Appendix A contains a discussion of the previous work done on the fatigue strength of attachment weld details. For the most part, little has been reported in the literature. There is a significant amount of work available on attachment plates welded perpendicular to main plates with the longitudinal axis of the attachment plate parallel to the direction of the applied stress. The attachment plates in the present study are considered as being transverse to the direction of stress in the flange of the beam to which they are welded.

The amount of load carried by the attachment plates varies with their length along the beam. It has been shown and is shown in this study that the attachment plate will develop its full capacity in a length along the beam equal to 3 to 4 times its width. The width of all attachment plates on the beam flange in the study is 2 in. with an additional 1 in. extending outside the flange tips. The shortest detail was the AQ attachment. This detail had a length of $9/32$ in. and can be considered as non-load carrying. The A8 attachments are nearly full load carrying and approach a cover plated beam in their behavior.

The attachments were welded to the flange of the beam in a region of constant shearing stress and varying bending moment. The nominal stresses controlling the experimental studies were

calculated using beam theory and were applicable to the face of the attachment closest to the midspan of the beam. The controlling stresses for the tests are shown in Tables B7 to B10.

All of the failure surfaces, except for the one noted in Section 3.3 for member AQB 261, were through the flange material at the toe of the transverse weld on the midspan side of the attachment. For the 4 in. attachments with the longitudinal weld detail, the crack surfaces propagated into the flange material at the ends of the longitudinal weld on the midspan side of the attachment. Thus, the failure surface always coincided with the location of maximum nominal stress on the beam at the attachment weld detail.

Seventeen failure surfaces were sawed open and examined under a 30 power microscope. Observations of the cracked surfaces indicated that the fatigue cracks originated in the flange material on the surface closest to the attachment. In all cases, there appeared to be multiple crack surfaces being propagated.

Surfaces relatively close to each other merged early in the fatigue life of the specimen forming a ridge between the two surfaces. These two surfaces gradually merged within a depth of 1/16 of an inch of penetration into the flange thickness eliminating the ridge. They then propagated as one surface across the remaining thickness of the flange.

In the longitudinal weld detail failures, there was usually 2 or 3 of these surfaces joining at the end of each longitudinal weld. The joined areas at the end of one of the longitudinal welds propagated across the thickness of the flange and along the width. Usually, it met with a similar failure surface that was propagating from the end of the adjacent longitudinal weld. These two surfaces most often did not coincide. A tearing of the flange material, transverse to the two propagating surfaces, took place. This resulted in a combined crack surface with a step or ridge that extended across the flange thickness.

A similar joining of propagating failure surfaces was observed in the cracks with the transverse weld detail. Generally, there were many initiation sites in the beam flange at the toe of the transverse weld. The resulting surfaces tended to conform to the irregularity in the life of the weld detail. The length of the tapered ridge, which formed, was small, usually 1/16 in. The farther apart that the merging areas were initially, the longer was the ridge line. When the merging areas were joined, they propagated as one surface across the thickness and along the width of the flanges. When two such larger propagating surfaces approached each other, they tried to merge without a ridge forming.

However, ridges across the flanges thickness, as described above for the longitudinal weld detail, were often formed.

As was described in Section 3.4.2, the length of the attachment had a significant effect on the fatigue strength of the weld detail. Experimental studies using 1/8 in. long foil strain gages were used to determine the localized stress distribution throughout the attachment length under static loading.

These studies gave a very clear indication of the attachment behavior under static load. Stress distributions were obtainable for gages at a distance of 0.125 in. from the toe of the weld. These studies indicated that the magnitude of the stress near the attachment increased with an increase in the attachment length. When plotted on a log-log scale (Fig. F1), the relationship between the maximum measured strain and the attachment length is relatively linear.

As the length of the attachment plate increased, the length of the local stress concentration zone increased toward the midspan of the beam as illustrated in Fig. 45. Hence, the stress concentration effects were increased as the attachment plate increased in length.

In order to further determine the effect of the geometry of the attachment weld detail on the fatigue strength, a finite element analysis was made. Since it was determined experimentally that the local stress concentration was the controlling factor in the variation of the fatigue life with the attachment length, the weld detail containing the attachment plate and flange plate was modeled.

Figure F2 shows the finite element mesh selected for the stress analyses. The area being studied was divided at its mid-length because of symmetry. The resulting half model was divided into 200 plate elements. The basic size of the element adjacent to the transverse weld was 0.25 by 0.25 in. in horizontal area. The thickness of the element for the attachment plate was 0.25 in. and the thickness for the flange plate was 0.375 in. Each nodal point had 5 degrees of freedom. The rotation about the z axis or vertical axes was not considered. Together, there were over one thousand unknown displacements for each attachment plate study. In addition, the effect of the flexibility of the weld was modeled into the program. Stiffness coefficients were developed for both the longitudinal and the transverse weld from experimental studies of similarly welded tensile strap specimens.

The boundary condition assumed for the web side of the finite element model proved to be significant in correlating the data from the finite element analysis and that for the experiments on the static loading of the test specimens. This boundary was assumed to be fixed against rotation and translation in the y and z directions, and free for translation in the x direction. The surface of contact between the attachment plate and the flange plate was assumed to be frictionless.

The values of the strain distribution obtained in the computer analysis are compared with the measured strains in Fig. 45 and were in general agreement. The maximum error for the maximum strain that was calculated was within 5 percent of the maximum measured in the experimental study. The maximum capacity for the attachment was determined on the basis of the ratio of the area of the attachment to the area of the attachment and flange plate. The maximum capacity of the attachment is 31.5 percent of load applied across the detail. Table F1 shows that an attachment plate length of 4 in. ($1 \frac{1}{3} w$) develops 90 percent of its maximum capacity.

Results and Analysis

The results of the tests for each type of attachment detail are summarized in Tables F2 to F6. The nominal stress

conditions that existed at the crack or face of the attachment are listed together with the cycles to failure for each detail. The symbols I and R indicate whether the failure was the initial or second detail that failed. In a few cases, the cracks at each end were of a sufficient length that further testing was not undertaken. In these cases, two equal values of cycle life are reported.

After the initial test period, a magnetic probe was used to determine small cracks, if any, that existed in the remaining attachment weld details. The number of cycles at which the cracks were first observed in the failure surface are listed. A stage 1 crack is one that had not propagated through the thickness of the flange when first observed. A stage 2 crack is one that has propagated through the flange thickness.

The cracks reported in Table F7 to F10 are for the cracks that were not a part of the failure surface. Generally, cracks could not be observed during testing until after they had penetrated through the flange. This corresponded to approximately 90 percent of the fatigue life of the attachment.

Analysis of Results

The statistical analysis of the effects of the controlled variables was done using analysis of variance and regression analysis techniques.

The regression analysis model used to relate the number of cycles to failure to the stress range at the crack initiation point was

$$\text{Log } N = B_1 + B_2 \text{ Log } S_R \quad (\text{Fl})$$

The coefficients B_1 and B_2 were obtained through a least square fit. Figures 39 to 43 show the mean regression curves for each of the attachment weld details. In all of the stress range versus life (S-N) plots the data points are shown together with the mean regression line and the confidence limits at two standard deviations from the mean.

The 1/4 in. attachment weld detail's upper bound confidence limit (Fig. 40) falls very close to the mean regression curve for the plain welded beam. This shows that the latter is an upper bound for the fatigue strength of the attachment weld detail series.

The mean regression curve for the 4 in. longitudinal weld detail (Fig. 42) gives a slightly greater fatigue strength than that for the A4B around weld detail. Figures 39 and 42 show that the initial failures in the test of the beams with the 4 in. attachments tended to fail in the longitudinal detail at the lower values of stress range and in the around detail at the higher values of stress range. These variations, while significant, have only

a slight effect on the fatigue strength of the 4 in. attachment. From a design viewpoint, there would be no difference.

The regression analysis curves are relatively parallel as shown in Fig. 44. The numerical values of the coefficient B_2 fall in the range of 2.82 to 3.24. These values are relatively close to -3.098 and -3.372, which are the values of the coefficients reported in NCHRB Report 102 for the cover plated beams and plain welded beams respectively.

The lower bound confidence limit (2σ) curve for the 8 in. attachment almost coincides with the mean regression curve for the cover plated beam (Fig. 43). The latter acts as a lower bound for the attachment weld details. It was noted in Table F1 that the 8 in. attachment developed 99 percent of its capacity and was rapidly approaching the cover plated beam condition.

Stress Analysis of Crack Propagation

Before the analysis of the part through crack at the weld toe, perpendicular to the stress field in the beam flanges, could be made it was necessary to establish the stress concentration factor. The finite element method was used for this purpose. A model of the flange and attachment was utilized to estimate the stress field near the weld toe. A typical mesh layout is

shown in Fig. F2. To simulate the weldment connecting the attachments to the flange, double nodes were provided all along the interface of the attachment and plate. Shear stiffness reported by Kulak was used to connect the nodes.⁽⁵²⁾ The analysis was restricted to one-half of the symmetric joint with no displacements permitted along the centerline of the attachments. Displacements were also restricted along the flange surface to simulate the web restraint. A uniform stress was applied to the end of the flange plate.

After the stress field was defined the stress concentration was determined from a second finite element solution (see Fig. E14). The maximum stress at the weld toe was determined by passing a plane through the principal stress at the centroid of each element. The results of this extrapolation are summarized in Fig. 58. The stress concentration at the weld toe is plotted as a function of attachment length. It is readily apparent that the stress concentration factor K_t approaches an asymptote with increasing length.

Summary and Conclusions

It has been shown that as the length of the attachment increases the fatigue strength decreases. The decrease is a function of the increase of bending or prying action that takes place in the flange plate immediately in front of the attachment

plate on the midspan side of the beam (Fig. 45). Figure F1 shows that the strain measured 0.125 in. from the toe of the transverse weld varies linearly with attachment length when plotted on a log log basis. Also, the finite element solution indicates that the amount of load transferred through the attachment increases as the length of the attachment increases. The A4B attachment plate has a length along the flange equal to twice its width across the flange and is carrying 90 percent of its rated development capacity.

When the length of the attachment is less than one-half an inch, the amount of force that is being transmitted through the attachment plate is relatively small. The weld detail approaches a non-loaded attachment as the attachment length gets smaller. Unfortunately, even at a length of one-half inch, there is a significant reduction in fatigue strength at a given cycle life (Fig. 44) from the plain welded beam.

APPENDIX G: NOMENCLATURESymbols

a	= crack size (depth of semi-elliptical crack)
a_i	= initial crack size
a_f	= crack size at failure
α	= level of significance
b	= half crack width
B_1, B_2	= constants determined from regression analysis
F	= ratio of the measured variation of the yield of a treatment to that of the unassigned or error variation, a tabulated value of the F-statistic
G	= constant in regression equation ($= 10^{B_1}$)
i	= order number for cumulative frequency distribution
ΔK	= elastic stress intensity factor for the leading edge of a crack
K	= range of K
K_t	= stress concentration factor
ΔN	= number of applied cycles
N	= number of cycles required for a crack to grow from initial size to size at failure or specified depth
n	= sample size; = exponent
P_i	= plotting position on cumulative frequency diagram for observation i
S, σ	= stress
S_{\max}	= maximum stress

S_{\min}	= minimum stress
S_r, σ_r	= stress range
t	= thickness
Φ_0	= elliptical integral of the second kind

Glossary

For beam specimen designation see Table B1

AASHO	= American Association of State Highway Officials
ASA	= American Standards Association
ASTM	= American Society for Testing and Materials
A2	= beams - 2 in. attachments welded to flanges
A4	= beams - 4 in. attachments welded to flanges
A8	= beams - 8 in. attachments welded to flanges
AQ	= beams - 9/32 in. thick plates welded to flanges
Cycle life	= number of load cycles to failure
Empirical exponential model	= mathematical equation in exponential form relating stress range and cycle life. Values of coefficient and exponent are determined empirically
Factorial experiment	= experimental plan where observations are taken at all possible combinations that can be formed for the different levels of factors
Failure	= significant increase in midspan deflection due to fatigue cracking of the test specimen
Fatigue	= initiation and propagation of microscopic cracks into macroscopic cracks by repeated application of stress
Fatigue life	= number of load cycles to failure

- Fatigue limit = stress range below which no crack occurs.
Threshold of crack growth
- Fatigue strength = relationship between fatigue life and applied stress
- Flaw = any discontinuity in the material
- Fretting = rubbing or chafing between plates
- Lateral connection = connection or bracing normal to beam or girder
- Limits of dispersion = limits of the test data from the mean regression line determined from the standard error of estimate
- Lower bound welded detail = detail of welded beam which exhibited relatively lowest fatigue strength.
Cover-plated beams
- Maximum stress = highest algebraic stress per cycle
- Minimum stress = lowest algebraic stress per cycle
- Porosity = pores in welds
- PRC = plain rolled beams, the third letter designates grade of steel (A for A36, B for A441, C for A514)
- Regression analysis = the use of least square curve fitting to statistically evaluate the significance of the independent stress variables
- Stress intensity range = range of stress intensity factor K
- Stress range = algebraic difference between maximum and minimum stress

Stress ratio	= algebraic ratio of minimum stress to maximum stress
SA	= beams with transverse stiffeners and alternating direction of principal stress
SB	= girders with transverse stiffeners with bracing attached
SC	= beams with transverse stiffeners and constant direction of principal stress
SG	= girders with transverse stiffeners and constant direction of principal stress
Threshold value	= lowest value of stress intensity range above which fatigue crack growth occurs
Transverse connection	= connection transverse to the longitudinal direction of beam or girder web
Upper bound welded detail	= detail of welded beams which exhibited relatively highest fatigue strength. Plain welded beam
95% confidence limit	= statistical limits that define interval of cycle life within which fatigue test data occur 95% of the time
95% survival	= an estimate of the number of stress cycles that 95% of the beams would survive at a given stress range

TABLE 1
Fatigue Stresses

Category See Table 2	Allowable Range of Stress, F_{sr} (ksi)			
	For 100,000 Cycles	For 500,000 Cycles	For 2,000,000 Cycles	Over 2,000,000 Cycles
A	60	36	24	24
B	45	27.5	18	16
C	32	19	13	10
D	27	16	10	7
E	21	12.5	8	5

TABLE 2

DESCRIPTION OF DESIGN CONDITIONS
Joint Classifications

General Condition	Situation	Kind of Stress ⁽¹⁾	Stress Category (See Table 1)
Plain Material	Base metal with rolled or cleaned surfaces. Flame cut edges with ASA smoothness of 1000 or less	T or Rev.	A
Built-up Members	Base metal and weld metal in members without attachments, built-up of plates or shapes connected by continuous full penetration groove welds or by continuous fillet welds parallel to the direction of applied stress	T or Rev.	B
	Calculated flexural stress at toe of transverse stiffener welds on girder webs or flanges	T or Rev.	C
	Base metal at end of partial length welded cover plates having square or tapered ends, with or without welds across the ends	T or Rev.	E

TABLE 2 (Continued)

General Condition	Situation	Kind of Stress ⁽¹⁾	Stress Category (See Table 1)
Groove Welds	Base metal and weld metal at full penetration groove welded splices of rolled, and welded sections having similar profiles when welds are ground flush and weld soundness established by non-destructive inspection	T or Rev.	B
	Base metal and weld metal in or adjacent to full penetration groove welded splices at transitions in width or thickness, with welds ground to provide slopes no steeper than 1 to 2 1/2, with grinding in the direction of applied stress, and weld soundness established by non-destructive inspection	T or Rev.	B
	Base metal and weld metal in or adjacent to full penetration groove welded splices, with or without transitions having slopes no greater than 1 to 2 1/2 when reinforcement is not removed and weld soundness is established by non-destructive inspection	T or Rev.	C

TABLE 2 (Continued)

General Conditions	Situation	Kind of Stress ⁽¹⁾	Stress Category (See Table 1)
Groove Welds	Base metal at details attached by groove welds subject to transverse and/or longitudinal loading when the detail length, L, parallel to the line of stress is between 2 in. and 12 times the plate thickness, but less than 4 in.	T or Rev.	D
	Base metal at details attached by groove welds subject to transverse and/or longitudinal loading when the detail length L is greater than 12 times the plate thickness or greater than 4 in. long	T or Rev.	E
Fillet Welded Connections	Base metal at intermittent fillet welds	T or Rev.	E
	Base metal adjacent to fillet welded attachments with length L in direction of stress less than 2 in. and stud-type shear connectors	T or Rev.	C
	Base metal at details attached by fillet welds with detail length L in direction of stress between 2 in. and 12 times the plate thickness but less than 4 in.	T or Rev.	D

TABLE 2 (Continued)

General Conditions	Situation	Kind of Stress ⁽¹⁾	Stress Category (See Table 1)
Fillet Welded Connections	Base metal at attachment-details with detail length L in direction of stress (length of fillet weld) greater than 12 times the plate thickness or greater than 4 in.	T or Rev.	E

- (1) "T" signifies range in tensile stress only; "Rev." signifies a range of stress involving both tension and compression during the stress cycle.

TABLE A1

DIMENSIONS OF STIFFENED BEAMS TESTED IN PREVIOUS STUDIES

Ref.	Series	Depth (in.)	Weight (lb./ft.)	Span ¹ (ft.-in.)	Constant Moment ₂ Region (ft.-in.)	Flange		Web		Steel ⁴	Welding Procedure
						Thick- ness (in.)	Width (in.)	Thick- ness (in.)	Slender- ness ³		
6	H	15-7/8	36	8-6	1-0	7/16	7	5/16	48	--	(rolled)
33	All A	12	41	8-6	1-0	1	5	3/16	53	A373	man.
		16	43	8-6	1-0	1	5	3/16	75	A373	man.
14	BT	7	34	6-8	1-8	0.55	7	0.35	17	B.S.15	(rolled)
31	-	16	16	8-6	1-0	3/8	5	1/16	244	A373	man.
34	BM BS	11	24	5-2	1-10	1/2	4	5/16	32	B.S.968	aut.subm.
		11	24-31	5-2	varies	1/2	4-6	5/16	32	B.S.968	aut.subm.
32	FT	~21	14-39	10-0	-	1/4-1	5	0.075	267	A373/A366	
	FTSB	~18	10-11	10-3	-	1/4-1	4-3/8to1	1/16	267	A373/A245	
	VSTB	21	11-20	11-0	-	1/2	2to4-1/2	1/16	320	A373/A245	
35	2 3	25-1/2	92	12-9	2-9	3/4	12	3/8	64	B.S.15	aut.subm.
		25-1/4	61	12-10	2-9	5/8	9-1/2	1/4	96	B.S.15	aut.subm.
4	W	8	18	6-6	2-0	7/16	4	5/16	23	A514	(rolled)
37	F	~52	varies	varies	varies	varies	12	3/16to3/8	133-267	A373,A36	varies

(Continued on the next page)

TABLE A1 (continued)

DIMENSIONS OF STIFFENED BEAMS TESTED IN PREVIOUS STUDIES

Ref.	Series	Depth (in.)	Weight (lb./ft.)	Span ¹ (ft.-in.)	Constant Moment ₂ Region ² (ft.-in.)	Flange		Web		Steel ⁴	Welding Procedure
						Thick- ness (in.)	Width (in.)	Thick- ness (in.)	Slender- ness ³		
36	FT-A	21	14,39	10-0	-	1/4,1	5	0.075	267	A441/A415	
	FTSB-A	21	15	10-3	-	3/8,1	4,1-1/2	0.075	267	A7/A415	semi-aut.
	VST-A	20	17	11-1	-	1/2	4-1/2	0.06	312	A441	metallic-
	HSB	21	15,18	10-3	-	3/8,3/4	4,2-1/2	0.075	267	A441/A415	inert gas
	HVSB	20	17	11-1	-	1/2	4-1/2	0.06	312	A441	
38	A	37	43-73	36-0	16-0	1/2	8	1/8 - 3/8	96-288	A514/A36	man.arc
	B	37	43-73	23-0	16-0	1/2	8	1/8 - 3/8	96-288	A514/A36	man.arc
15	C	37	43,58	22-8,19-2	4-8	1/2	8	3/16,1/4	144,192	A514/A36	aut.subm.
40	D	37	44,51	24-0	8-0	1/2	8	.135,3/16	192,268	A514/A36	aut.subm.
38	F	37	43	22-8	1-8	1/2	8	3/16	192	A514/A36	aut.subm.
39	H	37	43,58	24-0	9-0	1/2	8	3/16,1/4	144,192	A441/A36	aut.subm.

- Notes:
1. Series A specimens of Ref. 38 and all specimens of Refs. 36 and 32 were panel specimens. All others were full length specimens.
 2. Specimens for which there is an entry in this column were simple beams with two equal concentrated loads symmetrically placed.
 3. Depth-to-thickness ratio of web plate.
 4. Specimens of Refs. 15, 36, 32, 39 and 38 were hybrid girders. All others were homogeneous specimens.

TABLE A2

STIFFENER AND WELD DETAILS FOR BEAMS LISTED IN TABLE A1

Reference Series		Stiffener				Stiffener-to-web weld ¹			
		Thickness (in.)	Width (in.)	Arrangement	Steel	Electrode Welded to ²	Weld cut off ³ (in.)	Weld Size (in.)	
6	Ha	3/8	3	Pair		TWC			
	Hb	3/8	3	Pair		WC			
	Hc	3/8	3	Pair		WC	3		
33	A	1/4	2	Single	A7	E7016	WC	1/2	3/16
	B	1/4	2	Single	A7	E7016	TWC	1/2	3/16
	C	1/4	2	Single	A7	E7016	W	1-1/2	3/16
	D	1/4	2	Pair	A7	E7016	WC	1/2	3/16
	E	1/4	2-1/4	Single	A7	E7016	WC	2	3/16
	F	1/4	2-1/4	Single	A7	E7016	WC	2,5	3/16
	CX	1/4	2	Single	A7	E7016	TWC	1-1/2	3/16
14	BT	1/2	3	Pair	B.S.15	E217	TWC	1/2	5/16
31				Pair		E6013	WC		1/8
34	BM	1/2	1-1/2	Pair	B.S.15	E217	W	3/4,1	5/16
	BS	1/2	Varies	Pair	B.S.15	E217	W	Varies	5/16
32	FT	1/8	2	Pair		E6013	W		
	FTSB					E6013	W		
	VSTB	1/16-1/8	1/2-2	Pair		E6013	W		
35	2	5/16	5-1/2	Pair	B.S.15		TWC	3/4	
	3	5/16	5-1/2	Pair	B.S.15		WC	Varies	1/4
4	W	1/4	1-7/8	Pair	Carbon	E7018	W	~1/2	

(Continued on the next page)

TABLE A2 (continued)

STIFFENER AND WELD DETAILS FOR BEAMS LISTED IN TABLE A1

Reference Series		Stiffener				Stiffener-web weld ¹			
		Thickness (in.)	Width (in.)	Arrangement	Steel	Electrode	Welded to ²	Weld cut off ³ (in.)	Weld Size (in.)
37	F	1/4	3	Pair	A373,A36	E60	W	1	1/8,3/16
36	FT	1/8	2	Pair			W		
	FTSB-A			Pair			W		
	VST	1/8	1/2,2	Pair			W		
	HSB	1/4	1-1/4	Single			W		
	HVSB	1/8,1/4	1-1/4,2-1/2	Single			W		
38	A	3/16	3	Pair	A36	E7010	W	2	3/16
38	B	3/16	3	Pair	A36	E7010	W	2	3/16
15	C	3/16	3	Pair	A514,A36	E7018	WC	2,8	1/4
40	D	3/16	3	Pair	A36	E6018	W	2	3/16
38	F	1/2	3-1/2		A514,A36		W	2	
39	H			Pair		E7018	WC	2	3/16

- Notes: 1. Series C specimens of Ref. 33 had stiffeners welded intermittently (1-3) to web. All others were welded continuously.
2. Abbreviations denote T = tension flange, W = web, C = compression flange. See also nomenclature.
3. Distance between the end of the stiffener-to-web weld and the inside flange face.

TABLE A3

RESULTS OF PREVIOUS FATIGUE TESTS ON TYPE 1 STIFFENERS

Speci- men	Bending Stress at Midspan Extreme Fiber		Stress Range at Stiffener End		Direction of Crack (Degr.)	Cycles to Failure x10 ³	Notes
	Min. (ksi)	Range (ksi)	Princ. Range (ksi)	Shear to Bending			
<u>Ref. 33 (Kouba and Stallmeyer)</u>							
	(9)						
27 A+SA	1.0	29.9	30.4	.80	60	294	3
28 A+SA	1.0	29.4	30.9	1.17	50	696	3
37 A+SA	1.0	28.4	23.9	1.23	50	575	4
12 A+SA	1.0	29.7	23.9	1.30	52	631	4
11 A+SA	1.0	29.6	28.6	.85	58	713	
10 A+SA	1.0	29.6	28.6	.85	55	566	4
18 A+SA	1.0	29.0	23.3	1.30	52	630	4
38 B+SA	0.7	23.6	23.1	.83	55	1183	4
40 B+SA	0.7	23.0	19.7	1.10	50	1412	4
39 B+SA	0.7	22.9	19.6	1.10	48	1350	4
53 B+SA	0.4	19.9	19.5	.83	55	2733	4
54 B+SA	0.4	18.1	17.7	.83	--	4956	2
14 A+SC	1.0	29.0	22.8	1.60	51	649	45
15 A+SC	1.0	28.9	21.8	1.71	50	864	4
13 A+SC	1.0	28.5	21.5	1.71	47	911	4
46 B+SC	0.7	24.6	17.5	2.19	49	1049	4
45 B+SC	0.7	24.2	16.4	3.12	46	1753	45
44 B+SC	0.7	23.8	16.9	2.19	46	1903	4
57 B+SC	0.4	19.6	17.3	1.09	52	2832	4
58 B+SC	0.4	19.3	17.0	1.09	52	4608	4
34 B+SD	1.0	30.6	29.9	0.83	57	587	4
33 B+SD	1.0	30.3	29.6	0.83	56	670	4
32 B+SD	1.0	30.0	29.3	0.83	52	511	4
49 B+SD	0.7	24.2	18.0	1.66	43	1932	4
47 B+SD	0.7	24.2	23.7	0.83	49	1129	4
48 B+SD	0.7	24.0	20.5	1.10	Toe(10)	815	4 6
16 A+SE	1.0	30.0	20.0	2.65	45	887	4
17 A+SE	1.0	28.9	21.2	2.02	43	606	4
35 B+SE	1.0	28.8	20.0	2.58	44	1071	4
52 B+SE	0.7	24.1	15.2	5.16	46	1774	4
51 B+SE	0.7	23.9	20.0	1.29	48	1265	4
50 B+SE	0.7	23.8	18.2	1.72	45	1009	4
60 B+SE	0.4	22.4	14.1	5.16	44	3497	4
59 B+SE	0.4	19.3	16.2	1.29	--	5769	2
36 B+SF1	1.0	28.8	--	--	--	830	1 3
61 B+SF2	1.0	30.0	18.9	5.16	40	1138	4

(Continued on the next page)

TABLE A3 (continued)

RESULTS OF PREVIOUS FATIGUE TESTS ON TYPE 1 STIFFENERS

Speci- men	Bending		Stress Range		Direction of Crack (Degr.)	Cycles to Failure $\times 10^3$	Notes
	Stress at Midspan		at				
	Extreme Fiber		Stiffener	End			
	Min.	Range	Princ. Range	Shear to Bending			
(ksi)	(ksi)	(ksi)	(ksi)	(Degr.)	$\times 10^3$		
<u>Ref. 34 (Gurney)</u>							
BS 7	~ 1.1	39.6	25.6	1.19	53	227	4
BS 9	~ 1.1	36.6	23.4	0.80	60	394	4
BS 5	~ 1.1	30.9	21.0	0.90	50	388	4
BS 6	~ 1.1	29.8	19.8	0.89	60	559	4
BS 3	~ 1.1	28.3	17.7	0.91	49	957	4
BS 4	~ 1.1	28.0	16.4	1.22	45	903	4
BS 1	~ 1.1	27.3	15.2	0.72	56	974	4
BS 2	~ 1.1	27.9	14.0	1.60	48	1212	4
BS 11	~ 1.1	23.5	12.1	1.40	47	2028	4
BS 12	~ 1.1	21.5	11.7	1.05	47	2795	4 7
BS 10	~ 1.1	21.4	11.7	0.72	58	4010	4
<u>Ref. 35 (Braithwaite)</u>							
3 A	1.8	23.3	15.6	1.18	51	1020	4
3 B	1.8	26.9	18.0	1.18	51	290	4
3 C	1.8	20.6	13.8	--	--	719	3 8
3 D	1.8	18.6	12.5	--	--	3850	1
<u>Ref. 15 (Fielding)</u>							
32550C2	25.0	25.0	21.6	--	90	567	8
32550C2R	25.0	25.0	21.6	--	90	656	4 8
32550C2RR	25.0	25.0	21.6	--	--	803	1
33550C2	35.0	15.0	13.0	--	90	2158	4 8
33550C2R	35.0	15.0	13.0	--	--	2539	2
32150C2	21.0	29.0	25.1	--	--	622	1
32150C2R	21.0	29.0	25.1	--	--	500	1
32550C8	25.0	25.0	13.5	--	90	742	4 8
32550C8R	25.0	25.0	13.5	--	90	668	4 8
33550C8	35.0	15.0	8.1	--	--	1229	2
42550C2	25.0	25.0	21.6	--	90	870	4 8
42550C2R	25.0	25.0	21.6	--	--	723	1
42550C2RR	25.0	25.0	21.6	--	--	1896	1
<u>Ref. 38 (Toprac and Natarajan)</u>							
32540F05	25.0	15.0	13.0	--	--	2124	2
32540F15	25.0	15.0	13.0	--	--	2146	2
32550F05	25.0	25.0	21.6	--	--	671	1
32550F15	25.0	25.0	21.6	--	--	329	4 8

(Continued on the next page)

TABLE A3 (continued)

RESULTS OF PREVIOUS FATIGUE TESTS ON TYPE 1 STIFFENERS

Notes

1. Plain welded beam failure.
2. Test discontinued.
3. Test result not comparable.
4. Two-ended through crack in web plate at stiffener end, no crack extension into flange.
5. Crack growth from top of lowest intermittent fillet weld.
6. Multiple crack initiation at toe of stiffener-to-web weld.
7. Crack growth at toe of stiffener-to-web weld in compression region of web.
8. Failed at load bearing stiffener.
9. Estimated minimum stress.
10. Crack growth along weld toe before branching off diagonally into the web.

TABLE A4

RESULTS OF PREVIOUS FATIGUE TESTS ON TYPE 2 STIFFENERS

Specimen	Bending Stress at Midspan Extreme Fiber		Bending Stress at Stiffener	Cycles to Failure x10 ³	Notes
	Min. (ksi)	Range (ksi)	Range (ksi)		
<u>Ref. 34 (Gurney)</u>					
BM 1	~ 1.1	32.7	25.5	563	
BM 2		30.0	22.2	685	
BM 5		26.2	19.5	1,440	
BM 3		24.4	18.1	2,028	
BM 4		21.5	15.7	3,909	
<u>Ref. 4 (Nee)</u>					
W 19	4.9	65.1	48.8	101	
W 18	4.9	65.1	48.8	125	
W 29	3.5	46.5	34.9	331	
W 27	2.8	37.2	27.9	290	
W 28	2.8	37.2	27.9	579	
W 33	2.1	27.9	20.9	1,716	
W 30	2.1	27.9	20.9	1,828	
W 26	1.8	23.2	17.4	3,418	
W 38	1.6	21.4	16.0	4,856	
W 37	1.4	18.6	13.9	7,503	
W 32	1.0	14.0	10.5	10,000	2
<u>Ref. 38 (Toprac and Natarajan)</u>					
21020A	10.0	10.0	8.6	2,927	2
21530A	15.0	15.0	13.0	2,000	2
21540A	15.0	25.0	21.6	294	6
22540A	25.0	15.0	13.0	1,722	6
22550A	25.0	25.0	21.6	618	4
41020A	10.0	10.0	8.6	2,311	2
41530A	15.0	15.0	13.0	2,000	2
41540A	15.0	25.0	21.6	630	1
42540A	25.0	15.0	13.0	947	1
42550A	25.0	25.0	21.6	640	1
61530A	15.0	15.0	13.0	2,000	2
61540A	15.0	25.0	21.6	1,395	4
62540A	25.0	15.0	13.0	2,530	2
62550A	25.0	25.0	21.6	479	1
21020B	10.0	10.0	8.6	2,233	2
21530B	15.0	15.0	13.0	2,137	2
21540B	15.0	25.0	21.6	277	23
22540B	25.0	15.0	13.0	1,588	6

(Continued on the next page)

TABLE A4 (continued)
RESULTS OF PREVIOUS FATIGUE TESTS ON TYPE 2 STIFFENERS

Specimen	Bending Stress at Midspan Extreme Fiber		Bending Stress at Stiffener End	Cycles to Failure $\times 10^3$	Notes
	Min. (ksi)	Range (ksi)	Range (ksi)		
<u>Ref. 38 (continued)</u>					
22550B	25.0	25.0	21.6	672	6
31020B	10.0	10.0	8.6	4,771	2
31530B	15.0	15.0	13.0	2,104	2
31540B	15.0	25.0	21.6	890	4
32540B	25.0	15.0	13.0	2,440	2
32550B	25.0	25.0	21.6	815	6
41530B	15.0	15.0	13.0	2,053	2
41540B	15.0	25.0	21.6	974	4
42540B	25.0	15.0	13.0	3,643	2
42550B	25.0	25.0	21.6	421	4
<u>Ref. 40 (Toprac and Vinh)</u>					
22050D	20.0	30.0	26.0	544	1
22050DR	20.0	30.0	26.0	615	5
32050D	20.0	30.0	26.0	571	1
32050DR	20.0	30.0	26.0	657	4
<u>Ref. 39 (Toprac and Fielding)</u>					
31030H	10.0	20.0	17.3	2,015	5
31530H	15.0	15.0	13.0	2,941	2
31530HR	15.0	15.0	13.0	2,360	2
41030H	10.0	20.0	17.3	2,041	5
40530H	5.0	25.0	21.6	888	5
40530HR	5.0	25.0	21.6	934	5

Notes

1. Plain welded beam failure, initiating either at web-to-flange fillet weld or at the flange tip.
2. Test discontinued.
3. Test result not comparable.
4. Two-ended through crack in web plate at stiffener end, no crack extension into flange.
5. Part-through crack in web plate at stiffener end.
6. Web crack along toe of fillet weld connecting the web to the compression flange (thin web failure).

TABLE A5

RESULTS OF PREVIOUS FATIGUE TESTS ON TYPE 3 STIFFENERS

Specimen	Bending Stress at Midspan		Bending Stress at	Cycles to Failure	Notes
	Extreme Fiber	Range	Stiffener-to-flange weld		
	Min.		Range		
	(ksi)	(ksi)	(ksi)	$\times 10^3$	
<u>Ref. 33 (Kouba and Stallmeyer)</u>					
	(8)				
29 B+SB	1.0	30.4	22.5	628	5
30 B+SB	1.0	30.1	25.1	447	4
31 B+SB	1.0	30.0	25.0	524	4
43 B+SB	0.7	25.1	18.6	1272	6
41 B+SB	0.7	24.6	18.2	1110	5
42 B+SB	0.7	24.3	--	4031	3
56 B+SB	0.4	20.7	15.3	5078	1
55 B+SB	0.4	19.8	14.7	4115	1
44 B+SCX	0.7	24.4	20.3	1187	4
<u>Ref. 14 (Gurney)</u>					
BT 1	~ 1.1	37.3	31.4	264	4
BT 2		32.7	27.6	352	4
BT 3		27.9	23.5	254	4 7
BT 4		27.1	22.8	293	4 7
BT 5		26.8	22.6	687	4
BT 6		22.6	19.1	1105	4
BT 7		21.8	18.4	509	4
BT 8		19.7	16.6	1600	4 7
BT 9		18.9	15.9	3370	2
BT 10		17.3	14.6	2121	2
<u>Ref. 35 (Braithwaite)</u>					
2 B	~ 1.8	23.1	21.7	984	4
2 C		20.9	19.7	1410	4
2 D		19.3	18.2	1530	4
2 A		16.7	15.7	4290	4

- Notes:
1. Plain welded beam failure.
 2. Test discontinued.
 3. Test result not comparable.
 4. Failure at stiffener in constant bending moment region.
 5. Crack growth at toes of stiffener-to-web weld and stiffener-to-tension flange weld simultaneously.
 6. Crack growth at toe of stiffener-to-web weld alone.
 7. Rough weld, slight amount of undercut.
 8. Estimated minimum stress.

TABLE A6

MODES OF FAILURE IN PREVIOUS STIFFENED BEAM TESTS

Ref.	Series	Specimens tested	<u>Typical modes of failure¹</u>				Thin web fail.	Test discontinued	Not comparable	Notes
			1	2	3	PW				
6	Ha	3	-	-	2	-	-	1	-	2
	Hb	3	3	-	-	-	-	-	-	2
	Hc	3	2	-	-	-	-	1	-	2
33	A	12	9	-	-	-	-	1	2	
	B	8	-	-	4	2	-	1	1	
	C	8	8	-	-	-	-	-	-	
	D	6	6	-	-	-	-	-	-	
	E	8	7	-	-	-	-	1	-	
	CX	1	-	-	1	-	-	-	-	3
	F1	1	-	-	-	-	-	-	1	
	F2	1	1	-	-	-	-	-	-	
14	BT	10	-	-	8	-	-	2	-	3
31	-	2	-	-	-	-	2	-	-	
34	BM	5	-	5	-	-	-	-	-	
	BS	11	11	-	-	-	-	-	-	
32	All	20	-	-	-	-	20	-	-	
35	2	4	-	-	4	-	-	-	-	3
	3	4	2	-	-	1	-	-	1	

(Continued on the next page)

TABLE A6 (continued)

MODES OF FAILURE IN PREVIOUS STIFFENED BEAM TESTS

Ref.	Series	Specimens tested	Typical modes of failure ¹				Thin web fail.	Test discontinued	Not comparable	Notes
			1	2	3	PW				
4	W	11	-	10	-	-	-	1	-	
37	F	9	-	2	-	-	7	-	-	
36	All	10	-	-	-	-	10	-	-	
15	C	13	6	-	-	5	-	2	-	2
40	D	4	-	2	-	2	-	-	-	
39	H	6	-	4	-	-	-	2	-	
38	A	14	-	2	-	4	2	6	-	
38	B	14	-	3	-	-	3	7	1	
38	F	4	1	-	-	1	-	2	-	2
Total		195	56	28	19	15	44	27	6	

Notes

- (1) See Fig. A5 for types of cracks
- (2) Load bearing stiffeners
- (3) Stiffener located in a constant bending moment region

TABLE B1
SPECIMEN DESIGNATION

Example: PRC 342

PR	C	3	4	2
Beam Type	Steel	S_{min}	S_r	Specimen No.

Plain rolled beam of A514 Steel.
Third minimum stress S_{min} (14 ksi).
Fourth stress range S_r (36 ksi).

Specimen No. 2

Beam Type: PR - Plain rolled beam

Welded beam with stiffeners

SC, constant direction of principal stress

SA, alternating direction of principal stress

SG, girders

SB, girders with lateral bracing

Welded beam with attachments

A8, 8" long

A4, 4" long

A2, 2" long

AQ, 9/32" long

Steel: A - A36

B - A441

C - A514

S_{min} : 0, 1, 2 etc. indicate magnitude of S_{min} .

S_r : 1, 2, 3 etc. indicate magnitude of S_r .

TABLE B2
 EXPERIMENT DESIGN FOR PLAIN ROLLED BEAMS
 (PRC)

Section	S _{min} ksi	S _r , ksi		
		36	45	54
W14x30	-22	PRC 041	PRC 061	
	2	PRC 241 PRC 242	PRC 261 PRC 262	
	14	PRC 341 PRC 342		
	26	PRC 441		
W10x25	-22	PRC 042	PRC 062	PRC 081 PRC 082 PRC 083
	2	PRC 243 PRC 244	PRC 263 PRC 264	PRC 281 PRC 282 PRC 283
	14	PRC 343 PRC 344		PRC 381 PRC 382 PRC 383
	26	PRC 442	PRC 461 PRC 462	

TABLE B3

EXPERIMENT DESIGN FOR SC BEAMS

(a) Nominal stresses at midspan, extreme fiber

σ_{min} ksi	σ_r , ksi			
	18	24	30	36
-10			SCB 131 SCB 132	SCB 141 SCB 142
2	SCB 211* SCB 212 SCB 213*	SCB 221 SCB 222 SCB 223*	SCB 231 SCB 232 SCB 233	SCB 241* SCB 242 SCB 243
14	SCB 311 SCB 312*	SCB 321 SCB 322*	SCB 331 SCB 332	

* Modified beams

(b) Stress ranges at critical weld toe termination (ksi)

Type 1 stiffener:

Bending	13.7	18.2	22.8	27.4
Shear	4.2	5.6	7.0	8.4
Principal	14.8	19.8	24.7	29.7

Type 2 stiffener:

Bending	16.2	21.6	26.9	32.3
---------	------	------	------	------

Type 3 stiffener:

Bending	14.4	19.2	23.9	28.7
---------	------	------	------	------

TABLE B4

EXPERIMENT DESIGN FOR SA BEAMS

(a) Nominal stresses at load P_1 , extreme fiber (see Fig. 2)

σ_{min} ksi	σ_r , ksi	
	22.2	30.1
5.5	SAB 111 SAB 112 SAB 113 SAB 114	
8.7		SAB 221 SAB 222 SAB 223 SAB 224

(b) Stresses at end of Type 1 stiffener

Cell	Net loads (Fig. 2)			State of Stress			
		P_1 kip	P_2 kip	σ_b ksi	τ ksi	σ_p ksi	ϕ deg.
1	Min.	5	20.2	5.2	-0.8	5.3	8.3
	Range	50	-20.2	17.6	3.6	-	15.2
	Max.	55	0	22.8	2.8	23.2	6.9
2	Min.	7	35	8.2	-1.4	8.5	-9.5
	Range	70	-35	23.8	5.2	-	16.2
	Max.	77	0	32.0	3.8	32.5	6.7

TABLE B5

EXPERIMENT DESIGN FOR SG GIRDERS

(a) Nominal stresses at midspan, extreme fiber

σ_{min} ksi	σ_r , ksi		
	18	24	30
2	SGB 211 SGC 212	SGB 221 SGC 222	SGB 231 SGC 232
14	SGB 311 SGB 312	SGB 321 SGB 322 SGB 323	SGB 331 SGB 332 SGC 333

(b) Stress ranges at critical weld toe termination (ksi)

Type 1 stiffener

Bending	15.4	20.5	25.7
Shear	3.4	4.5	5.6
Principal	16.1	21.5	26.9

Type 2 stiffener

Bending	13.7	18.3	22.9
---------	------	------	------

Type 3 stiffener

Bending	13.8	18.4	22.9
---------	------	------	------

TABLE B6
EXPERIMENT DESIGN FOR SB GIRDERS

($\sigma_{\min} = 2$ ksi)

$\frac{\Delta_h}{\Delta_v}$	σ_r , ksi	
	24	30
1/6	SBB 221 SBB 222	SBB 231 SBB 232
1/3	SBB 321 SBB 322	SBB 331 SBB 332

TABLE B7

EXPERIMENT DESIGN FOR WELDED BEAMS WITH ATTACHMENTS

9/32" LONG (AQB)

S _{min} ksi	S _r , ksi					
	8	12	16	20	24	28
-6			AQB 131	AQB 141		AQB 161
2		AQB 221	AQB 231	AQB 241		AQB 261
10		AQB 321	AQB 331	AQB 341		

Each beam has two identical details.

TABLE B8

EXPERIMENT DESIGN FOR WELDED BEAMS WITH ATTACHMENTS

2" LONG (A2B)

S _{min} ksi	S _r , ksi					
	8	12	16	20	24	28
-6			A2B 131	A2B 141		A2B 161
2		A2B 221	A2B 231	A2B 241		A2B 261
10		A2B 321	A2B 331	A2B 341		

Each beam has two identical details.

Stresses are at nominal edge of attachment.

TABLE B9

EXPERIMENT DESIGN FOR WELDED BEAMS WITH ATTACHMENTS

4" LONG (A4B)

S_{min} ksi	S_r , ksi					
	8	12	16	20	24	28
-6			A4B 131 A4B 132	A4B 141 A4B 142		A4B 161 A4B 162
2	A4B 211 A4B 212	A4B 221 A4B 222	A4B 231 A4B 232	A4B 241 A4B 242		A4B 261 A4B 262
10	A4B 311 A4B 312	A4B 321 A4B 322	A4B 331 A4B 332	A4B 341 A4B 342		

Each beam has two different details. The attachments in the left shear span of the beam are welded longitudinally, the attachments in the right shear span are welded all around.

TABLE B10

EXPERIMENT DESIGN FOR WELDED BEAMS WITH ATTACHMENTS
8" LONG (A8B)

S _{min} ksi	S _r , ksi					
	8	12	16	20	24	28
-6			A8B 131	A8B 141	A8B 151	
2	A8B 211	A8B 221	A8B 231	A8B 241	A8B 251	
10	A8B 311	A8B 321	A8B 331	A8B 341		

Each beam has two identical details.

S_r = at attachment

TABLE C-1A

TYPICAL CROSS-SECTIONAL PROPERTIES OF TEST SPECIMENS

Rolled Beams and Welded Beams and Girders								
Beam Type	Steel	Section	Flange		Web		Moment of Inertia	Section Modulus
			Width	Thickness	Thickness	Depth		
			(in.)	(in.)	(in.)	(in.)	(in. ⁴)	(in. ³)
Plain Rolled (PRC)	A514	W10x25	5.74	0.429	0.255	10.08	132	26.2
	A514	W14x30	6.79	0.408	0.281	13.86	304	43.9
Welded Beams with Stiffeners (SA)	A441	W14x30	6.73	0.384	0.290	13.81	287	41.6
	A441	W14x30	6.76	0.381	0.289	13.81	286	41.3
Welded Girders with Stiffeners (SG,SB)	A441	W38x50	7.73	0.486	0.259	38.0	3737	196.7
	A514	W38x50	7.72	0.524	0.262	38.0	3958	208.3

TABLE C-1B

STIFFENER AND WELD DETAILS FOR SPECIMENS IN TABLE C-1A

Series	Stiffener				Stiffener-Web Weld ¹			
	Thickness (in.)	Width (in.)	Arrangement	Steel	Electrode	Welded to ²	Weld cut off ³ (in.)	Weld Size (in.)
SC	9/32	2-3/4	Single	A36	E7028	TWC,W	1/2, 3/4	3/16
SS	9/32	2-3/4	Single	A36	E7028	TWC,W	1/2	3/16
SA	9/32	2-3/4	Single	A36	E7028	W	1/2	3/16
SG	1/4	3-1/2	Single	A36	E7028	TWC,W	1/2, 2	3/16
SB	1/4	3-1/2	Single	A36	E7028	TWC,W	1/2, 2	3/16

- Notes:
1. Automatic Submerged Arc
 2. Abbreviations denote T = tension flange, W = web, C = compression flange. See also nomenclature.
 3. Distance between the end of the stiffener-to-web weld and the inside flange face.

TABLE C-2A

TENSILE PROPERTIES OF PLAIN ROLLED BEAMS
(PRC)

Component	Thickness	Steel	Heat No.	No. of Tension Specimens	Static Yield Stress		Tensile Strength		Elongation	Reduction in Area
					Mean (ksi)	St. Dev. (ksi)	Mean (ksi)	St. Dev. (ksi)	Mean (%)	Mean (%)
W10x25 web	1/4	A514	66E448	4	110.8	2.6	119.0	3.1	8	48
W10x25 flange	7/16	A514	66E448	4	117.8	1.3	127.2	1.4	11	44
W10x25 web	1/4	A514	69E253	4	105.0	3.8	113.7	3.6	9	51
W10x25 flange	7/16	A514	69E253	4	110.6	2.1	120.3	2.0	12	48
W14x30 web	5/16	A514	67D685	4	117.1	2.3	127.4	2.4	10	46
W14x30 flange	3/8	A514	67D685	4	119.8	0.9	129.5	1.3	11	43

TABLE C-2B

TENSILE PROPERTIES OF BEAM AND GIRDER PLATES

Component	Thickness	Steel	Heat No.	No. of Tension Specimens	Upper Yield Point		Static Yield Stress		Tensile Strength		Elong. Mean (%)	Reduction in Area Mean (%)
					Mean (ksi)	St. Dev. (ksi)	Mean (ksi)	St. Dev. (ksi)	Mean (ksi)	St. Dev. (ksi)		
Beam web	9/32	A441	477B0421	3	55.8	1.3	52.3	1.1	72.8	1.3	24	51
Beam flange	3/8	A441	655B155	3	55.4	1.4	52.0	0.6	74.4	0.7	24	55
Girder web	1/4	A441	485B1022	3	59.5	5.0	56.5	2.5	78.2	0.8	24	53
Girder flange	1/2	A441	654B163	3	44.2	2.0	40.7	2.0	64.9	1.2	28	57
Girder web	1/4	A514	485B1022	3	121.4	0.7	115.3	1.6	121.3	0.8	10	55
Girder flange	1/2	A514	802B2530	3	120.0	0.8	113.9	0.6	121.7	0.8	13	49

TABLE C-3

MILL TEST REPORT OF BEAM AND GIRDER PLATES

Component	Plate No.	Steel thickness	Steel	Heat No.	Yield Point	Tensile Strength	Elong. (8" Gage)	Chemical Analysis								
								C	Mn	P	S	Si	Cu	Va	Mo	B
					(ksi)	(ksi)	(%)									
Beam web	92	9/32	A441	485B1022	62.8	81.4	26	.18	1.06	.008	.022	.21	.24	.056	-	-
	12	9/32	A441	477B0421	56.6	78.9	24	.19	1.05	.008	.023	.04	.24	.052	-	-
	6	9/32	A441	479A1501	57.4	78.8	26	.19	1.08	.008	.029	.02	.24	.062	-	-
	3	9/32	A441	432A0891	54.7	76.4	26	.20	1.05	.017	.023	.04	.21	.055	-	-
Beam flange	226	3/8	A441	655B155	56.2	77.6	28	.17	1.05	.017	.023	.17	.29	.040	-	-
Girder web	15	1/4	A441	485B1022	62.9	81.6	23	.18	1.06	.008	.022	.21	.24	.056	-	-
	3	1/4	A441	485B1272	64.3	77.2	18	.15	1.07	.012	.022	.21	.25	.034	-	-
Girder flange	36	1/2	A441	654B163	50.1	71.0	26	.18	.98	.021	.026	.01	.33	.030	-	-
Girder web	2	1/4	A514	802B02530	118.5	122.0	24*	.13	.70	.009	.017	.25	-	-	.55	.0034
	1	1/4	A514	802A10090	126.8	130.8	20*	.19	.64	.015	.020	.30	-	-	.56	.0040
	1	1/4	A514	518B1097	121.3	126.3	23*	.19	.56	.016	.020	.27	-	-	.61	.0050
Girder flange	8	1/2	A514	802B2530	121.8	125.4	24*	.13	.70	.009	.017	.25	-	-	.55	.0034
Stiffener	9/32	A36	411B2252	45.0	71.3	25	.19	.92	.020	.023	.05	-	-	-	-	
	1/4	A36	411B2252	47.2	73.0	23	.19	.92	.020	.023	.05	-	-	-	-	
	1/2	A36	411B2252	44.4	68.6	26	.19	.92	.020	.023	.05	-	-	-	-	

* 2 inch gage length

TABLE D-1

SUMMARY OF DATA FOR ROLLED A514 STEEL BEAMS - INITIAL TEST

BEAM NO. (1)	S_r (ksi) (2)	S_{min} (ksi) (3)	CRACK LOCATION (4)	CYCLES TO FAILURE ($\times 10^3$) (5)	CRACK-SIZE FLANGE, WEB (6)	DESCRIPTION OF CRACK LOCATION AND CRACK INITIATION (7)
<u>W14x30</u>						
PRC-041	36.0	-22.0	57.0 C	3,113	6.75 ₍₂₎ 8.50	Arbitrary
PRC-061	45.0	-22.0	53.0 T	759	4.87 ₍₁₎ 2.00	Arbitrary, From Flange Tip
PRC-241	34.3	1.9	No Crack	10,000	No Crack	Runout
PRC-242	34.3	1.9	No Crack	10,000	No Crack	Runout
PRC-261	45.7	1.9	53.0 T	702	3.91 ₍₁₎ 0.57	Arbitrary, From Flange Tip
PRC-262	45.0	2.0	60.0 T	338	3.82 ₍₁₎ 0.30	At Flaw in Flange Tip
PRC-342	34.3	13.3	No Crack	10,000	No Crack	Runout
PRC-441	34.3	24.8	71.5 T	5,194	3.25 0.20	Under Stiffener
<u>W10x25</u>						
PRC-042	36.0	-22.0	40.25 C	1,983	2.63 ₍₁₎ 0.75	Near Top Load, From Extreme Fiber
PRC-062	45.0	-22.0	41.0 C	1,789	5.75 ₍₂₎ 6.50	At Bracing
PRC-081	54.0	-22.0	36.5 C	247	3.85 ₍₁₎ 1.00	Under Top Jack, From Extreme Fiber
PRC-082	54.0	-22.0	36.0 T	1,164	3.85 ₍₁₎ 1.25	Under Top Jack, From Flange Tip
PRC-083	54.0	-22.0	35.75 C	1,067	3.95 ₍₁₎ 0.38	Under Top Jack, From Notch in Flange Tip

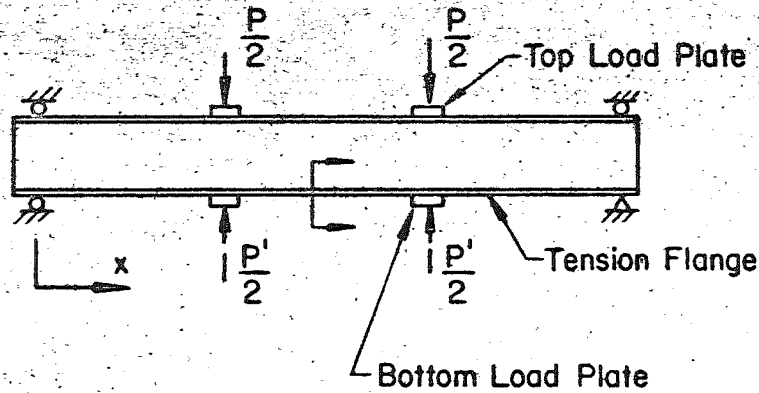
TABLE D-1

SUMMARY OF DATA FOR ROLLED A514 STEEL BEAMS - INITIAL TEST (continued)

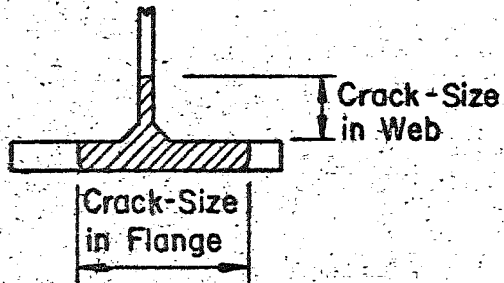
BEAM NO. (1)	S_r (ksi) (2)	S_{min} (ksi) (3)	CRACK LOCATION (4)	CYCLES TO FAILURE ($\times 10^3$) (5)	CRACK-SIZE FLANGE, WEB (6)	DESCRIPTION OF CRACK LOCATION AND CRACK INITIATION (7)
<u>W10x25 (con't)</u>						
PRC-243	36.0	2.0	No Crack	10,000	No Crack	Runout
PRC-244	36.0	2.0	27.0 T	3,090	3.37 ₍₁₎ 0.79	At Bracing
PRC-263	45.0	2.0	37.75 T	2,284	3.75 ₍₁₎ 1.00	At Edge of Stiffener, From Extreme Fiber
PRC-264	45.0	2.0	54.0 T	1,242	3.54 ₍₁₎ 0.93	Under Stiffener, From Flange Tip
PRC-281	54.0	2.0	35.0 T	440	2.25 ₍₁₎ 0.0	Under Stiffener, From Extreme Fiber
PRC-282	54.0	2.0	26.5 T	238	5.75 ₍₂₎ 3.80	At Bracing, From Flange Tip
PRC-283	54.0	2.0	64.0 T	645	3.20 ₍₁₎ 0.34	At Bracing
PRC-343	36.0	14.0	39.0 T	2,396	2.93 0.30	Near Load, From Extreme Fiber
PRC-344	36.0	14.0	No Crack	10,000	No Crack	Runout
PRC-381	54.0	14.0	38.63 T	211	2.87 ₍₁₎ 0.0	Arbitrary, From Notch in Flange Tip
PRC-382	51.4	13.3	52.5 T	615	2.69 0.38	Near Load, From Extreme Fiber
PRC-383	54.0	14.0	54.5 T	1,196	2.70 0.95	At Load, Flange-to-Web Transition
PRC-442	20.5	26.0	20.5 T	2,846	4.25 ₍₁₎ 1.50	In Shear Span
PRC-461	45.0	26.0	51.0 T	558	2.20 ₍₁₎ 0.0	Arbitrary, From Flange Tip
PRC-462	42.8	24.8	49.0 T	2,717	2.47 ₍₁₎ 0.0	Arbitrary, From Flange Tip

TABLE D2

DOCUMENTATION OF ROLLED BEAMS



ELEVATION



CROSS-SECTION

(EXPLANATION FOR TABLE D1)

- (1) Beam Number
- (2) Stress-Range (ksi) See Appendix B, Tables B1 & B2
- (3) Minimum-Stress (ksi)
- (4) Crack Location x measured in inches from the support. Loads applied at $x = 39"$ and $81"$.
T denotes crack in Tension Flange
C denotes crack in Compression flange
- (5) Cycles to Failure in kilo-cycles
(usually for an increase in deflection of 0.020 inches)
See Section 1.5
- (6) Crack Size Measurements (see sketch)
 - Crack in Flange
 - Index (1): Crack out to one edge
 - Index (2): Crack across width of flange
 - Crack in Web
- (7) Description of Crack Location with respect to Load Plates or Wooden Stiffeners.

Crack Initiation from observation of Fracture Surface of the Crack

TABLE E-1

SUMMARY OF FATIGUE TEST DATA OF TYPE 1 STIFFENERS

Specimen	Bending Stress at Midspan Extreme Fiber		Stress Ranges at end of Stiffener			Cycles to Failure N ($\times 10^3$)	Direction of Crack ⁹ ϕ (Deg.)	Crack Size ⁸		Notes
	Min. (ksi)	Range (ksi)	Bend. (ksi)	Shear (ksi)	Princ. (ksi)			a_{f1} (in.)	a_w (in.)	
<u>SC beams</u>										
SCB 211*	2	18	13.7	4.2	14.8	2893	74	3.7	4.1	
SCB 212	2	18	13.7	4.2	14.8	9743	--	-	-	
SCB 213*	2	18	13.7	4.2	14.8	7037	--	-	-	3
SCB 311	14	18	13.7	4.2	14.8	13080	--	-	-	2
SCB 312*	14	18	13.7	4.2	14.8	3197	73	3.5	3.2	
SCB 221	2	24	18.2	5.6	19.8	2907	Toe ⁷	3.0	3.6	
SCB 222	2	24	18.2	5.6	19.8	3165	-51	3.4	3.5	1 4
SCB 223*	2	24	18.2	5.6	19.8	2320	--	-	-	1
SCB 321	14	24	18.2	5.6	19.8	1828	--	-	-	1
SCB 322*	14	24	18.2	5.6	19.8	1481	Toe	0.0	3.0	
SCB 131	-10	30	22.8	7.0	24.7	1119	-62	6.4	4.0	4
SCB 132	-10	30	22.8	7.0	24.7	1210	-50	4.4	3.5	4
SCB 231	2	30	22.8	7.0	24.7	774	71	4.0	3.4	
SCB 232	2	30	22.8	7.0	24.7	860	73	5.9	2.6	
SCB 233	2	30	22.8	7.0	24.7	1030	--	-	-	2
SCB 331	14	30	22.8	7.0	24.7	1150	Toe	0.0	2.8	1
SCB 332	14	30	22.8	7.0	24.7	819	Toe	2.0	3.5	

(Continued on the next page)

TABLE E-1 (Continued)

SUMMARY OF FATIGUE TEST DATA OF TYPE 1 STIFFENERS

Specimen	Bending Stress at Midspan Extreme Fiber		Stress Ranges at end of Stiffener			Cycles to Failure N (x10 ³)	Direction of Crack ⁹ ∅ (Deg.)	Crack Size ⁸		Notes
	Min.	Range	Bend.	Shear	Princ.			a _{fl}	a _w	
	(ksi)	(ksi)	(ksi)	(ksi)	(ksi)			(in.)	(in.)	
<u>SC beams (continued)</u>										
SCB 141	-10	36	27.4	8.4	29.7	867	-55	3.3	2.3	4
SCB 142	-10	36	27.4	8.4	29.7	574	Toe	3.8	4.7	
SCB 241*	2	36	27.4	8.4	29.7	521	Toe	4.0	4.0	6
SCB 242	2	36	27.4	8.4	29.7	676	Toe	4.3	4.0	
SCB 243	2	36	27.4	8.4	29.7	669	-63	0.0	1.2	34
<u>SA beams with alternating shear</u>										
SAB 111	5.5	22.2	17.6	3.6		4770	Toe	6.6	5.1	
SAB 112	5.5	22.2	17.6	3.6		3190	Toe	4.6	3.4	
SAB 113	5.5	22.2	17.6	3.6		3425	Toe	0.0	0.9	1
SAB 114	5.5	22.2	17.6	3.6		6227	Toe	1.2	4.1	6
SAB 221	8.7	30.1	23.8	5.2		883	Toe	1.3	4.4	5
SAB 222	8.7	30.1	23.8	5.2		1017	Toe	0.0	3.6	1
SAB 223	8.7	30.1	23.8	5.2		1161	Toe	1.8	4.0	
SAB 224	8.7	30.1	23.8	5.2		1064	Toe	2.4	2.8	
<u>SG girders</u>										
SGB 211	2	18	15.4	3.4	16.1	4433	81	4.0	7.8	
SGC 212	2	18	15.4	3.4	16.1	3016	Toe	6.1	2.8	

(Continued on the next page)

TABLE E-1 (Continued)

SUMMARY OF FATIGUE TEST DATA OF TYPE 1 STIFFENERS

Specimen	Bending		Stress Ranges at			Cycles to Failure	Direction of Crack ⁹	Crack Size ⁸		Notes		
	Stress at Midspan Extreme Fiber		End of Stiffener					N	∅		a _{f1}	a _w
	Min. (ksi)	Range (ksi)	Bend. (ksi)	Shear (ksi)	Princ. (ksi)							
<u>SG girders (continued)</u>												
SGB 311	14	18	15.4	3.4	16.1	4869	--	0.0	0.7			
SGB 312	14	18	15.4	3.4	16.1	2293	Toe	4.9	7.0			
SGB 221	2	24	20.5	4.5	21.5	1939	Toe	5.5	8.0			
SGC 222	2	24	20.5	4.5	21.5	838	Toe	0.0	9.7	5		
SGB 321	14	24	20.5	4.5	21.5	769	Toe	2.2	7.4	6		
SGB 322	14	24	20.5	4.5	21.5	1210	Toe	2.3	7.9			
SGB 323	14	24	20.5	4.5	21.5	774	Toe	2.8	9.7	6		
SGB 231	2	30	25.7	5.6	26.9	643	Toe	2.7	9.2			
SGC 232	2	30	25.7	5.6	26.9	452	Toe	2.6	10.7	5		
SGB 331	14	30	25.7	5.6	26.9	413	Toe	2.1	6.0			
SGB 332	14	30	25.7	5.6	26.9	500	Toe	3.0	4.8			
SGC 333	14	30	25.7	5.6	26.9	401	Toe	5.4	11.4	5		
<u>SB girders with transverse bracing</u>												
SBB 221	2	24	20.5	4.5	21.5	1264	Toe	5.2	7.9	6		
SBB 222	2	24	20.5	4.5	21.5	1409	Toe	1.8	9.0	5		
SBB 321	2	24	20.5	4.5	21.5	1388	Toe	6.8	9.0	6		
SBB 322	2	24	20.5	4.5	21.5	1401	Toe	3.4	8.5	6		

(Continued on the next page)

TABLE E-1 (Continued)

SUMMARY OF FATIGUE TEST DATA OF TYPE 1 STIFFENERS

Specimen	Bending Stress at Midspan Extreme Fiber		Stress Ranges at End of Stiffener			Cycles to Failure N (x10 ³)	Direction of Crack ⁹ ∅ (Deg.)	Crack Size ⁸		Notes
	Min.	Range	Bend.	Shear	Princ.			a _{fl}	a _w	
	(ksi)	(ksi)	(ksi)	(ksi)	(ksi)			(in.)	(in.)	
<u>SB girders with transverse bracing (continued)</u>										
SBB 231	2	30	25.7	5.6	26.9	1037	Toe	0.0	8.9	5
SBB 232	2	30	25.7	5.6	26.9	561	Toe	6.0	8.5	6
SBB 331	2	30	25.7	5.6	26.9	577	Toe	4.2	7.7	6
SBB 332	2	30	25.7	5.6	26.9	555	Toe	4.2	7.7	5

- Notes:
1. Plain welded beam failure.
 2. Test discontinued.
 3. Failure at Type 2 stiffener.
 4. Crack at Type 1 stiffener in compression (top) region of web.
 5. Crack at weld toes on both sides of Type 1 stiffener.
 6. Crack at Type 1 stiffener-to-web weld toe closer to the support.
 7. Crack growth along weld toe before bracing off diagonally into the web.
 8. For crack sizes see Fig. 15.
 9. Plane perpendicular to the direction of the principal stress:
 - 74° for Series SC
 - 78° for Series SG and SB.

TABLE E-2

SUMMARY OF FATIGUE TEST DATA OF TYPE 2 STIFFENERS

Specimen	Bending Stress at Midspan		Bending Stress at End of	Cycles to Failure	Crack - Size			Notes
	Extreme Fiber	Fiber	Stiffener		5			
	Min. (ksi)	Range (ksi)	Range (ksi)	N (x10 ³)	a _{f1} (in)	a _w (in)	e (in)	
<u>SG Girders</u>								
SGB 211	2	18	13.7	4433	-	-	-	1
				4433	-	-	-	1
SGC 212	2	18	13.7	1790	-	7.0	3.2	2
				1790	-	10.7	2.8	2
SGB 311	14	18	13.7	3230	-	-	-	1
				5229	-	-	-	1
SGB 312	14	18	13.7	2204	2.2	13.0	-	3
				2012	-	3.5	3.1	2
SGB 221	2	24	18.3	1408	-	-	-	1
				1165	-	5.2	3.0	2
SGC 222	2	24	18.3	838	-	7.5	3.2	2
				838	-	11.2	2.4	2
SGB 321	14	24	18.3	1316	-	-	-	1
				1063	-	4.5	2.7	2
SGB 322	14	24	18.3	1452	-	-	-	1
				1553	-	-	-	1
SGB 323	14	24	18.3	1261	-	-	-	1
				1131	-	-	-	1
SGB 231	2	30	22.9	520	-	-	-	1
				552	-	-	-	1
SGC 232	2	30	22.9	452	-	12.5	1.6	2
				452	-	6.7	3.0	2
SGB 331	14	30	22.9	786	-	3.4	3.1	2
				746	-	-	-	1
SGB 332	14	30	22.9	539	-	-	-	1
				481	-	7.1	0.3	2
SGC 333	14	30	22.9	537	-	14.0	-	2
				537	4.4	16.0	-	3

(Continued on the next page)

TABLE E-2 (Continued)

SUMMARY OF FATIGUE TEST DATA OF TYPE 2 STIFFENERS

Speci- men	Bending Stress at Midspan		Bending Stress at End of Stiffener	Cycles to Failure N (x10 ³)	Crack - Size			Notes
	Min. (ksi)	Range (ksi)	Range (ksi)		a _{fl} (in)	a _w (in)	e (in)	
<u>SB Girders with transverse bracing</u>								
SBB 221	2	24	18.3	1264	-	7.8	2.2	2
				1197	-	-	-	1
SBB 222	2	24	18.3	1061	-	-	-	1
				1234	-	3.2	3.6	2
SBB 321	2	24	18.3	1388	-	4.0	3.7	2
				1388	-	2.6	4.7	2
SBB 322	2	24	18.3	1329	2.0	14.8	-	3
				1401	-	9.6	1.8	2
SBB 231	2	30	22.9	718	2.3	14.4	-	3
				718	-	-	-	1
SBB 232	2	30	22.9	533	2.1	14.1	-	3
				533	-	12.2	0.4	2
SBB 331	2	30	22.9	684	-	4.5	2.8	2
				684	-	9.2	1.5	2
SBB 332	2	30	22.9	499	2.0	14.2	-	3
				725	-	3.9	2.9	2

- Notes:
1. Part-through crack.
 2. Two-ended crack.
 3. Three-ended crack.
 4. Cycles to failure correspond to either failure at Type 2 stiffener or number of cycles applied until repair of a plain welded girder failure at less than 12 inches from Type 2 stiffener.
 5. For size of two-ended and three-ended cracks see Fig. 18

TABLE E-3

SUMMARY OF FATIGUE TEST DATA OF TYPE 3 STIFFENERS

Specimen	Bending Stress at Midspan Extreme Fiber		Bending Stress at Stiffener-to-Flange Weld	Cycles to Failure	Crack Size ⁶			Notes
	Min (ksi)	Range (ksi)	Range (ksi)	N (x10 ³)	a (in)	a _{fl} (in)	a _w (in)	
<u>SC beams</u>								
SCB 211*	2	18	14.4	2616	-	5.0	3.3	
SCB 212	2	18	14.4	3787	-	2.0	0.0	
SCB 213*	2	18	14.4	4512	-	5.5	5.0	
SCB 311	14	18	14.4	4741	-	4.5	1.2	5
SCB 312	14	18	14.4	3197	-	3.4	0.0	
SCB 221	2	24	19.2	1691	-	5.2	2.2	
SCB 222	2	24	19.2	1329	-	5.0	2.2	
SCB 223*	2	24	19.2	807	-	3.5	0.2	
SCB 321	14	24	19.2	1438	-	4.0	0.5	
SCB 322*	14	24	19.2	1092	-	3.8	0.9	
SCB 131	-10	30	23.9	584	-	5.5	3.4	
SCB 132	-10	30	23.9	579	-	5.6	3.0	
SCB 231	2	30	23.9	492	-	4.2	1.0	
SCB 232	2	30	23.9	527	-	5.3	2.5	
SCB 233	2	30	23.9	421	-	4.8	1.5	
SCB 331	14	30	23.9	322	-	3.6	0.3	
SCB 332	14	30	23.9	428	-	3.8	0.3	

(Continued on the next page)

TABLE E-3 (Continued)

SUMMARY OF FATIGUE TEST DATA OF TYPE 3 STIFFENERS

Specimen	Bending Stress at Midspan Extreme Fiber		Bending Stress at Stiffener-to-Flange Weld	Cycles to Failure	Crack Size ⁶			Notes
	Min (ksi)	Range (ksi)	Range (ksi)	N ($\times 10^3$)	a (in)	a _{fl} (in)	a _w (in)	
<u>SC beams (continued)</u>								
SCB 141	-10	36	28.7	355	-	4.8	1.5	
SCB 142	-10	36	28.7	302	-	5.2	2.8	
SCB 241*	2	36	28.7	214	-	3.7	1.0	
SCB 242	2	36	28.7	361	-	3.8	0.2	
SCB 243	2	36	28.7	495	-	4.5	1.3	
<u>SG girders</u>								
SGB 211	2	18	13.8	6617	-	-	-	4
SGC 212	2	18	13.8	3854	-	-	-	4
SGB 311	14	18	13.8	6060	-	-	-	4
SGB 312	14	18	13.8	2012	-	4.6	0.7	
SGB 221	2	24	18.4	1742	-	7.1	7.0	3 5
SGC 222	2	24	18.4	1366	-	6.1	11.7	3 5
SGB 321	14	24	18.4	1316	0.29	2.1	-	1
SGB 322	14	24	18.4	1553	0.25	1.8	-	12
SGB 323	14	24	18.4	1261	-	5.8	3.3	
SGB 231	2	30	22.9	676	0.16	1.8	-	1
SGC 232	2	30	22.9	737	-	5.1	4.9	2
SGB 331	14	30	22.9	786	0.38	2.3	-	1
SGB 332	14	30	22.9	700	-	3.2	0.0	
SGC 333	14	30	22.9	627	0.30	2.4	-	1

(Continued on the next page)

TABLE E-3 (Continued)

SUMMARY OF FATIGUE TEST DATA OF TYPE 3 STIFFENERS

Specimen	Bending Stress at Midspan Extreme Fiber		Bending Stress at Stiffener-to-Flange Weld	to Failure N ($\times 10^3$)	Crack Size ⁶			Notes
	Min. (ksi)	Range (ksi)	Range (ksi)		a (in)	a _{fl} (in)	a _w (in)	
<u>SB girders with transverse bracing</u>								
SBB 221	2	24	18.4	1264	-	2.7	0.0	
SBB 222	2	24	18.4	1641	0.14	0.38	-	1
SBB 321	2	24	18.4	1206	-	3.5	0.0	
SBB 322	2	24	18.4	1329	-	2.2	0.0	
SBB 231	2	30	22.9	1037	0.14	0.39	1.6	1
SBB 232	2	30	22.9	561	-	5.8	10.6	3 5
SBB 331	2	30	22.9	804	-	3.9	0.3	
SBB 332	2	30	22.9	950	0.13	0.56	-	1

- Notes:
1. Part-through cracks in flange.
 2. Crack growth at weld toes in flange and web.
 3. Crack leading to failure at Type 3 stiffener initiated at weld toe in web.
 4. No visible cracking.
 5. Crack at stiffener-to-flange weld toe closer to the support.
 6. For crack sizes see Fig. 20.

TABLE E-4

SUMMARY OF DATA FOR PILOT TESTS

Specimen	Bending Stress at Midspan Extreme Fiber		First Failure		Second Failure	
	Min. (ksi)	Range (ksi)	Type	Life ($\times 10^3$)	Type	Life ($\times 10^3$)
A	2	24	PW	1702	-	--
B	14	24	PW	1597	-	--
C	2	30	PW	1114	-	--
D	2	36	3	181	2	445
E	14	18	PW	2532	1	5724

TABLE E-5

SUMMARY OF FATIGUE TEST DATA OF PLAIN WELDED GIRDERS

Specimen	Bending Stress at Midspan		Bending Stress at Crack	Cycles to Failure	Crack Location	Crack-Size		Notes
	Extreme Fiber	Inner Fiber	Inner Fiber of Flange	N		a _{fl}	a _w	
	Min.	Range	Range	(x10 ³)	(ft-in)	(in)	(in)	
	(ksi)	(ksi)	(ksi)					
<u>SG girders</u>								
SGB 211	2	18	17.5	4433	11-10	7.0	3.7	
SGC 212	2	18	17.5	2194	7- 0	-	-	4
SGB 311	14	18	17.5	3230	8- 4	4.7	2.4	
SGB 312	14	18	17.5	2012	11- 2	1.7	1.3	
SGB 221	2	24	23.4	1046	10- 0	6.7	3.5	
SGC 222	2	24	23.4	838	-	-	-	2
SGB 321	14	24	23.4	1063	10- 7	1.6	0.9	
SGB 322	14	24	23.4	1052	12- 0	2.8	1.8	
SGB 323	14	24	23.4	1131	11- 2	4.0	2.0	
SGB 231	2	30	29.2	520	8- 2	5.7	2.2	
SGC 232	2	30	29.2	452	-	-	-	2
SGB 331	14	30	29.2	746	11- 0	-	-	4
SGB 332	14	30	29.2	539	12- 0	1.6	0.9	
SGC 333	14	30	29.2	627	9- 0	5.5	-	
<u>SB girders with transverse bracing</u>								
SBB 221	2	24	23.4	1197	10-11	7.0	4.5	
SBB 222	2	24	23.4	1061	8- 5	1.8	1.2	
SBB 321	2	24	23.4	1388	10- 1	-	-	3
SBB 322	2	24	23.4	1401	-	-	-	1

(Continued on the next page)

TABLE E-5 (Continued)

SUMMARY OF FATIGUE TEST DATA OF PLAIN WELDED GIRDERS

Specimen	Bending Stress at Midspan Extreme Fiber		Bending Stress at Crack Inner Fiber of Flange	Cycles to Failure	Crack ⁶ Location	Crack-Size ⁷		Notes
	Min.	Range	Range	N		a _{fl}	a _w	
	(ksi)	(ksi)	(ksi)	(x10 ³)	(ft-in)	(in)	(in)	

SB girders with transverse bracing (continued)

SBB 231	2	30	29.2	718	11- 1	-	-	3
SBB 232	2	30	29.2	533	11- 6	-	-	3
SBB 331	2	30	29.2	684	11- 2	3.8	1.9	
SBB 332	2	30	29.2	725	10- 8	3.0	1.4	

- Notes:
1. Test discontinued.
 2. Number of cycles applied when failures at both Type 2 stiffeners required extensive repairs.
 3. Crack in web-to-tension flange weld, did not reach extreme fiber of tension flange.
 4. Crack size not recorded.

5. Distance between left support and crack.
6. Crack size:

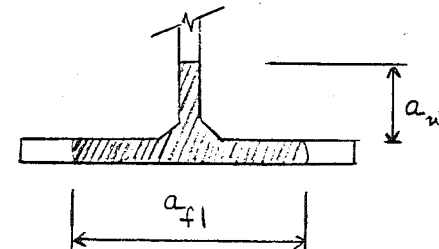


TABLE E-6

ANALYSIS OF VARIANCE OF TYPE 1 STIFFENERS

Series	Specimens Included	Specimens Excluded	Source of Variation	Calculated F-ratio	F-ratio @ $\alpha=0.05$	Variation Significant
SC	17	5 spec. @ $\sigma_r=18$ ksi	Stress range	101.4	4.5	Yes
			Min. stress	6.7	4.5	Yes
			Interaction	1.1	3.8	No
SA	8	None	Stress range	96.2	7.7	Yes
			Min. stress	0.0	7.7	No
SG	6	8 spec. @ $\sigma_{min}=14$ ksi	Stress range	49.7	19.0	Yes
			A441 vs A514	11.2	18.5	No
SG	14	None	Stress range	50.2	4.5	Yes
			Min. stress	1.9	5.3	No
			Interaction	0.1	4.5	No
SB	8	None	Stress range	21.9	7.7	Yes
			Bracing angle	0.7	7.7	No
			Interaction	1.2	7.7	No
SG, SB	22	None	Stress range	112.2	3.6	Yes
			SG vs SB	7.7	4.5	Yes
			Interaction	0.0	3.6	No
SG, SB	18	4-A514	Stress range	72.6	3.9	Yes
			SG vs SB	3.2	4.7	No
			Interaction	0.0	3.9	No

TABLE E-7

ANALYSIS OF VARIANCE OF TYPE 2 STIFFENERS

Series	Specimens ¹ Included	Specimens Excluded	Source of Variation	Calculated F-ratio	F-ratio @ $\alpha=0.05$	Variation Significant
SG	6	8 spec. @ $\sigma_{\min}=14$ ksi	Stress range A441 vs A514	19.7 4.0	19.0 18.5	Yes No
SG	14	None	Stress range Min. stress Interaction	95.1 2.5 0.2	3.4 4.3 3.4	Yes No No
SB	8	None	Stress range Bracing angle Interaction	123.2 2.1 0.8	4.8 4.8 4.8	Yes No No
SG,SB	22	None	Stress range SG vs SB Interaction	216.9 2.8 0.1	3.3 4.1 3.3	Yes No No

Notes: 1. One data point per specimen in test for effect of steel quality;
two data points per specimen in all other tests.

TABLE E-8

ANALYSIS OF VARIANCE OF TYPE 3 STIFFENER

Series	Specimens Included	Specimens Excluded	Source of Variation	Calculated F-ratio	F-ratio @ $\alpha=0.05$	Variation Significant
SC	22	None	Stress range	108.4	3.7	Yes
			Min. stress	1.2	4.1	No
			Interaction	0.2	3.2	No
SG	6	8 spec. @ $\sigma_{\min}=14$ ksi	Stress range	39.9	19.0	Yes
			A441 vs A514	1.7	18.5	No
SG	10	4 spec. @ $\sigma_r=18$ ksi	Stress range	108.8	6.0	Yes
			Min. stress	0.8	6.0	No
			Interaction	0.4	6.0	No
SB	8	None	Stress range	9.9	7.7	Yes
			Bracing angle	0.0	7.7	No
			Interaction	0.5	7.7	No
SG,SB	18	4 spec. @ $\sigma_r=18$ ksi	Stress range	82.6	4.6	Yes
			SG vs SB	0.7	4.6	No
			Interaction	2.5	4.6	No

TABLE E-9

STRESS RANGE VERSUS STEEL QUALITY FACTORIAL

FOR SG GIRDERS

($\sigma_{\min} = 2$ ksi)

Steel quality	σ_r (ksi)		
	18	24	30
A441	SGB 211	SGB 221	SGB 231
A514	SGC 212	SGC 222	SGC 232

TABLE E-10

STRESS RANGE VERSUS TRANSVERSE BRACING

FACTORIAL FOR SG AND SB GIRDERS

Series	σ_r (ksi)		
	18	24	30
SG without bracing	SGB 211	SGB 221	SGB 231
	SGC 212	SGC 222	SGC 232
	SGB 311	SGB 321	SGB 331
	SGB 312	SGB 322	SGB 332
		SGB 323	SGC 333
SB with bracing		SBB 221	SBB 231
		SBB 222	SBB 232
		SBB 321	SBB 331
		SBB 322	SBB 332

TABLE E-11
 SIZE OF PART-THROUGH CRACKS
 AT FILLET WELD TOES

Specimen	Crack depth a (in)	Crack width 2b (in)	Location
<u>Single crack (continued)</u>			
SCB 232	.025	.072	2 T
	.057	.139	2 T
SCB 331	.075	.170	1 C
SCB 332	.025	.070	2 T
	.009	.028	2 T
	.022	.051	2 T
SCB 142	.250	.550	1 C
SCB 243	.028	.078	1 T
	.070	.156	1 T
	.220	.560	1 C
	.041	.110	3 C
<u>Multiple cracks</u>			
Pilot C	.109	.366	3 T
	.171	.530	3 T
SCB 221	.320	2.200	3 C
SCB 222	.136	.455	3 C
SCB 242	.250	1.790	3 C
SCB 243	.063	.234	3 C
	.055	.427	3 C
SGC 222	.237	.881	3 T
SGB 321	.176	.528	3 T
	.261	1.130	3 T
	.069	.401	3 T
SGB 322	.074	.271	3 T
SGB 231	.076	.208	3 T
	.135	1.157	3 T
SGB 331	.367	2.370	3 T
SGC 333	.044	.126	3 T

TABLE E-11 (Continued)
 SIZE OF PART-THROUGH CRACKS
 AT FILLET WELD TOES

Specimen	Crack depth a (in)	Crack width 2b (in)	Location
<u>Single crack</u>			
Pilot D	.051	.120	1 T
	.038	.084	1 T
	.134	.278	1 T
	.035	.079	1 T
	.029	.081	1 T
SGB 221	.143	.407	3 T
	.082	.202	3 T
SGB 321	.014	.031	3 T
SGB 322	.029	.078	3 T
SGB 323	.035	.100	2 T
	.044	.135	2 T
	.115	.286	2 T
	.013	.051	2 T
SGC 333	.051	.107	3 T
	.028	.061	3 T
	.016	.052	3 T
	.235	.875	3 T
SCG 311	.023	.065	1 T
	.026	.061	1 T
	.060	.140	2 T
SCB 222	.042	.088	2 T
	.067	.169	2 T
	.102	.237	1 T
	.127	.339	1 T
SCB 322	.281	.569	1 T
SCB 131	.089	.250	1 T
	.290	.700	1 T
SCB 132	.190	.440	1 T
	.033	.092	2 T
	.021	.059	2 T
	.034	.085	2 T

(Continued on the next page)

TABLE E-12

DATA FOR ANALYSIS OF PROPAGATION OF PART-THROUGH CRACKS

Specimen	Plate thickness (in) t	Stiffener thickness (in)	Weld ¹ Size (in) w	Stress concentration factor K_t	Crack growth rates		Stress range at detail (ksi)			
					C	n	(18) ²	(24)	(30)	(36)
<u>Type 1 stiffeners</u>										
Beam	9/32	9/32	1/4	2.20	2.0×10^{-10}	3.0	14.8	19.8	24.7	29.7
Girder	1/4	1/4	1/4	2.12			16.1	21.5	26.9	
<u>Type 3 stiffeners</u>										
Beam	3/8	9/32	1/4	2.42	2.0×10^{-10}	3.0	14.4	19.2	23.9	28.7
Girder	1/2	1/4	1/4	2.64			13.8	18.4	22.9	

- Notes: 1. 3/16" fillet welds were specified, but actual weld sizes were almost 1/4".
 2. Stress range at midspan, extreme fiber.

TABLE F1

SUMMARY OF FINITE ELEMENT ANALYSIS

Attachment Length Inches	Percent of Load Att.	Flange	Attachment Percent Capacity	Stress Concentration Factor K_t
0.25	5.6	94.4	19	2.42
2	23.0	77.0	73	2.97
4	28.5	74.1	90	3.05
8	31.2	68.8	99	3.15

TABLE F2

SUMMARY OF TEST DATA BEAMS WITH 9/32 IN. ATTACHMENTS, AQB

Member No.	Stress at Crack (ksi)		Test	Cycles to First Observed Crack ($\times 10^3$)	Stage	Cycles to Failure ($\times 10^3$)
	S_r	$S_{min.}$				
221	12	2	I,R	-	-	10,762 ⁺
321	12	2	I,R	-	-	15,607 ⁺
131	16	-6	I	-	-	3,095
			R	3,095	2	3,619
231	16	2	I	-	-	3,113*
			R	-	-	5,143*
331	16	10	I	-	-	3,703
141	20	-6	I,R	-	-	1,096
241	20	2	I	-	-	1,616
			R	1,616	1	1,861
341	20	10	I	1,585	2	1,593
			R	1,593	1	1,821
161	28	-6	I	-	-	353
			R	353	1	440
261	28	2	I	-	-	506
			R	506	1	521

* Failed as plain welded beam

+ Did not exhibit any visible crack

TABLE F3

SUMMARY OF TEST DATA BEAMS WITH 2 IN. ATTACHMENTS, A2B

Member No.	Stress at Crack (ksi)		Test	Cycles to First Observed Crack ($\times 10^3$)	Stage	Cycles to Failure ($\times 10^3$)
	S_r	S_{min}				
221	12	2	I	-	-	3,812
			R	3,812	2	3,911
321	12	10	I	-	-	2,881
			R	2,881	1	4,368
231	16	2	I	-	-	1,121
			R	-	-	1,258
331	16	10	I	-	-	1,168
			R	1,168	-	1,476
241	20	2	I	-	-	658
			R	658	-	685
341	20	10	I	-	-	543
			R	543	-	627
261	28	2	I	-	-	242
			R	242	1	250

TABLE F4

SUMMARY OF TEST DATA BEAMS WITH 4 IN. ATTACHMENTS, A4B

Member No.	Stress at Crack (ksi)		Test	Cycles to First Observed Crack ($\times 10^3$)	Stage	Cycles to Failure ($\times 10^3$)
	S_r	S_{min}				
211	8	2	I-L	-	-	6,023
212	8	2	I-L	5,104	2	5,621
			R	-	-	11,072
(311)	5.9	7.4	I-L	10,000	2	13,597 Runout
312	8	10	I-L	8,815	2	9,057
221	12	2	I-A	1,741	2	1,858
			R-L	1,858	2	2,439
(222)	8.9	1.5	I-L	-	-	4,844
			R-A	-	-	7,177
222	12	2	I-A	-	-	1,124
			A			
321	12	10	I-L	-	-	1,208
			R-A	1,208	1	1,509
322	12	10	I-A	-	-	1,743
			R-L	-	-	2,154
131	16	-6	I-A	740	2	793
			R-L	740	1	850
132	16	-6	I-A	-	-	801
			R-L	801	1	931
231	16	2	I-L	704	2	785
			R-A	785	1	819
232	16	2	I-A	-	-	652
			R-L	652	2	760
331	16	10	I-L	-	-	732
			R-A	732	1/1	882
(332)	11.9	7.4	I-L&A	-	-	2,205

TABLE F4 (Continued)

SUMMARY OF TEST DATA BEAMS WITH 4 IN. ATTACHMENTS, A4B

Member No.	Stress at Crack (ksi)		Test	Cycles to First Observed Crack ($\times 10^3$)	Stage	Cycles to Failure ($\times 10^3$)
	S_r	S_{min}				
332	16	10	I-A	-	-	499
			R-A	499	2	536
141	20	-6	I-A	-	-	310
			R-L	310	1	589
142	20	-6	I-A	-	-	378
			R-L	378	1	491
241	20	2	I-A	-	-	305
			R-L	305	1	593
242	20	2	I-A	-	-	400
			R-L	400	2	486
341	20	10	I-A	-	-	401
			R-L	401	2	526
342	20	10	I-A	-	-	368
			R-L	368	1/2	440
161	28	-6	I-A	-	-	116
			R-L	116	1	181
162	28	-6	I-A	-	-	123
			R-L	123	2	161
261	28	2	I-A	-	-	101
			R-L	101	1	175
262	28	2	I-A	-	-	143
			R-L	-	-	227

() Tested with modified stress values

TABLE F5

SUMMARY OF DATA BEAMS WITH 8 IN. ATTACHMENTS, A8B

Member No.	Stress at Crack (ksi)		Test	Cycles to First Observed Crack (x 10 ³)	Stage	Cycles to Failure (x 10 ³)
	S _r	S _{min}				
211	8	2	I	5,959	2	6,111
	8	(10) ?	R	6,111	1	6,317
311	8	10	I	-	-	2,866
			R	-	-	7,004
(221)	8.9	1.5	I	-	-	2,960
			R	-	-	3,681
221	12	2	I	-	-	808
321	12	10	I	-	-	1,147
			R	-	-	1,225
131	16	-6	I	-	-	595
			R	-	-	714
231	16	2	I	-	-	491
			R	-	-	885
331	16	10	I	-	-	518
			R	-	-	714
141	20	-6	I	-	-	279
			R	-	-	279
241	20	2	I	-	-	192
			R	192	2	213
(341)	14.9	7.4	I	-	-	786
			R	-	-	855
341	20	10	I	-	-	175
			R	175	2	190
151	24	-6	I	-	-	165
			R	-	-	165
251	24	2	I-R	-	-	167

TABLE F6

SUMMARY OF SECONDARY CRACK DATA FOR 9/32 IN. ATTACHMENTS

BEAM NO.	CRACK LENGTH	CRACK LOCATION	CRACK TYPE	FLANGE POSITION	SIDE OF ATTACHMENT	DETERMINED AFTER TEST	COMMENT
221	1/8	3/4 ⁽¹⁾	1 ⁽²⁾	B ⁽³⁾	S ⁽⁴⁾	E ⁽⁵⁾	
	1/4	1-3/4	1	B	M	E	Web Side
	3/16	1/2	1	T	M	E	
	3/16	1	1	T	M	E	
	3/16	1-1/4	1	T	S	E	
321	3/8	3/4	1	B	M	E	
131	-	-					
231	3/8	1-1/2	1	B	M	I	NR(6)
331	1-1/4	1-1/2	1	B	M	I	NP-Failed as PW
	1/4	3/4	1	B	M	I	NP
	1-1/2	1-1/4	1	B	M	I	2-1/8" @ 1-1/4"
141	-	-					
241	1/2	1-1/2	1	B	M	I	NR
	1/2	1-1/4	1	B	M	R	
	3/4	1-3/4	1	T	M	R	
341	1-1/4	1-1/8	1	B	S	I	NR
	3/4	1-3/4	1	B	M	I	NR
	1/8	3/4	1	T	M	I	NR
161	-	-					
261	1	1-1/2	1	B	S	I	NR
	3/4	1	1	B	M	I	NR

(1) From Edge of Flange

(2) 1=Weld Side, 2=Through Flange

(3) B=Bottom, T=Top

(4) S=Support, M=Midspan

(5) R=Retest, I=Initial, E=Runout

(6) NP=No Propagation, NR=Occurred at Failed End, No Retest

TABLE F7

SUMMARY OF SECONDARY CRACK DATA FOR 2 IN. ATTACHMENT

BEAM NO.	CRACK LENGTH	CRACK* LOCATION	CRACK TYPE	FLANGE POSITION	SIDE OF ATTACHMENT	DETERMINED AFTER TEST	COMMENT
221	3/8	1-1/ 4	1	B	S	I	NR
	1	1-1/ 2	2	B	S	I	NR
321	1-3/4	1-1/ 2	1	B	M	I	NR
	1/8	1/16	1	T	M	R	
	1/8	1/16	1	T	S	R	
131	-	-					
231	1/2	1-3/ 4	1	B	M	I	NR
	1/4	1	1	B	M	I	NR
	1/8	1-3/ 4	1	B	M	R	
	1/8	1/16	1	B	S	R	
331	1	1-1/ 2	1	B	M	I	NR
141	-	-					
241	1-1/2	1-1/ 4	1	B	M	I	NR
341	3/4	3/ 4	1	B	S	I	NR
	1-1/4	1-1/ 2	1	B	S	I	1-3/4"@ 1-1/4"
161	-	-					
261	3/4	1-3/ 4	1	B	M	I	NR
	1/4	1-1/ 2	1	B	S	I	NR

TABLE F8

SUMMARY OF SECONDARY CRACK DATA FOR 4 IN. ATTACHMENT

BEAM NO.	CRACK LENGTH	CRACK LOCATION	CRACK TYPE	FLANGE POSITION	SIDE OF ATTACHMENT	DETERMINED AFTER TEST	COMMENT
211	0.25	1.25	1,A ⁽¹⁾	B	M	I	NR
212	0.25	0.12	1,L	B	S	I	NR
	0.12	0.06	1,A	T	S	R	RUNOUT
311	—	—					
312	1.0	2.0	1,A	B	S	I	RUNOUT
	0.12	0.06	1,A	B	M	R	
221	0.25	1.5	1,L	B	S	I	NP
	0.25	0.12	1,L	B	S	I	0.5@0.25
	0.5	0.25	1,L	T	M	I	NP
	2.0	1.0	1,L	T	S	I	NP
	2.0	1.0	1,L	T	M	I	NP
	0.2	1.0	1,A	T	M	I	NP
	0.2	1.5	1,A	T	M	I	NP
	0.2	0.8	1,A	T	S	I	NP
222	1.0	0.5	1,L	T	M	I	NR
322	0.12	1.75	1,A	B	M	I	NR
	0.25	0.12	1,A	B	S	I	NR
	0.12	1.25	1,A	T	S	I	NR
	0.12	0.75	1,A	T	M	I	0.25 @0.75
	0.25	0.12	1,L	T	S	R	
231	1.0	2.0	1,L	B	M	I	NR
	0.75	1.75	1,A	B	M	I	1.8 1.5

TABLE F8 (Continued)

SUMMARY OF SECONDARY CRACK DATA FOR 4 IN. ATTACHMENT

BEAM NO.	CRACK LENGTH	CRACK LOCATION	CRACK TYPE	FLANGE POSITION	SIDE OF ATTACHMENT	DETERMINED AFTER TEST	COMMENT
231	0.12	0.06	1,A	T	M	I	0.4
							@0.2
232	0.25	0.12	1,L	T	M	I	NR
	2.0	1.0	1,L	B	M	I	NR
	0.75	0.37	1,L	T	M	I	NP
331	0.25	0.12	2,L	T	S	R	
	1.0	1.5	1,L	B	M	I	NR
	1.75	1.5	1,L	B	S	I	NR
332	0.12	1.5	1,A	T	S	I	NP
	-	-					
242	2.0	1.5	1,A	B	M	I	NR
	0.12	0.06	1,L	T	S	R	
341	1.0	1.5	1,A	B	M	I	NR
	0.12	1.75	1,A	B	S	I	NR
342	0.12	1.75	1,L	B	M	I	NR
	1.0	1.75	1,A	B	M	I	NR
262	0.25	0.12	1,A	B	S	I	NR
	2.12	1.06	1,A	B	M	I	NR
	0.12	1.75	1,L	B	S	I	NP
	0.25	0.12	1,L	B	S	R	
	0.37	0.18	1,L	T	M	R	

TABLE F9

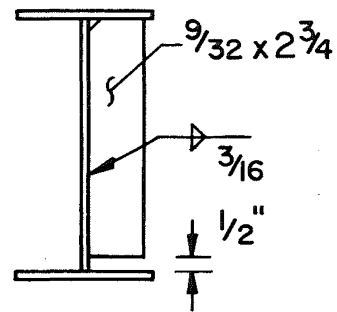
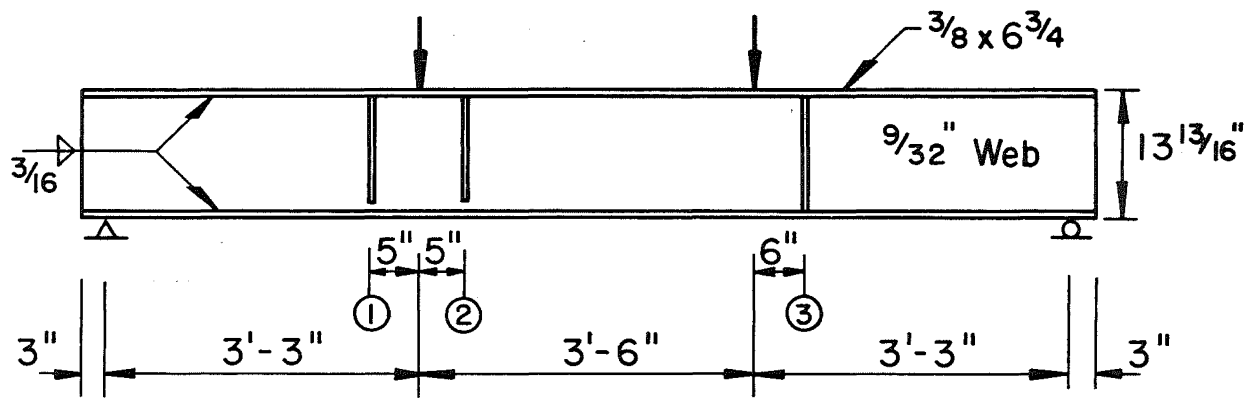
SUMMARY OF SECONDARY CRACK DATA FOR 8 IN. ATTACHMENT

BEAM NO.	CRACK LENGTH	CRACK LOCATION	CRACK TYPE	FLANGE POSITION	SIDE OF ATTACHMENT	DETERMINED AFTER TEST	COMMENT
211	0.25	1.87	1	T	S	I	NR
311	0.12	0.5	1	T	M	I	NR
	0.12	0.75	1	T	M	I	NR
221	0.25	2.0	1	B	M	R	
231	1.12	1.5	1	B	M	R	
	0.25	0.12	1	T	M	R	
	0.5	0.25	1	T	M	R	
331	1.12	1.5	1	B	M	I	NR
341	0.75	1.75	1	B	M	I	NR
251	1.75	1.12	1	B	M	I	NR

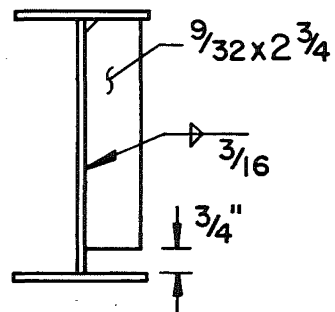
TABLE F10

COMPARISON OF LONGITUDINAL AND ALL AROUND WELD DETAILS -
4 INCH ATTACHMENT, INITIAL TEST FAILURES

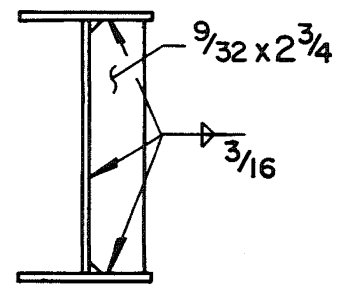
Weld Detail	STRESS RANGE, (ksi)				
	8	12	16	20	28
Longitudinal	4	2	3	0	0
All Around	0	2	5	6	4



STIFFENER ①

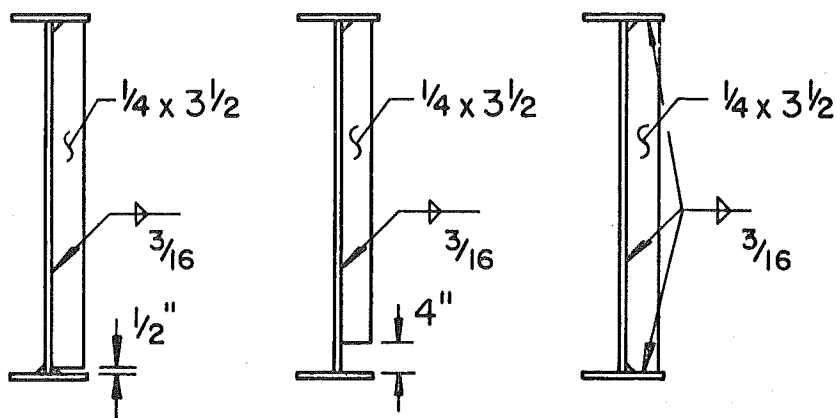
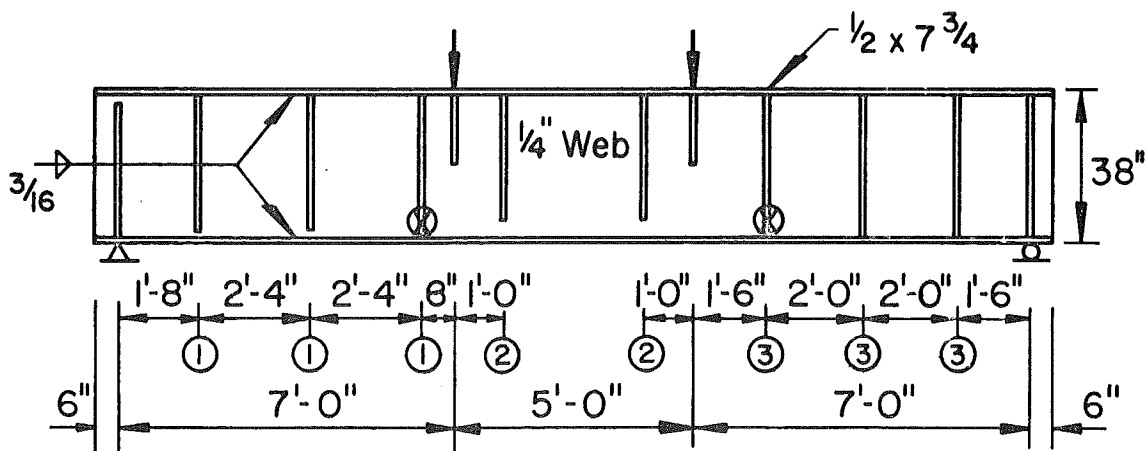


STIFFENER ②

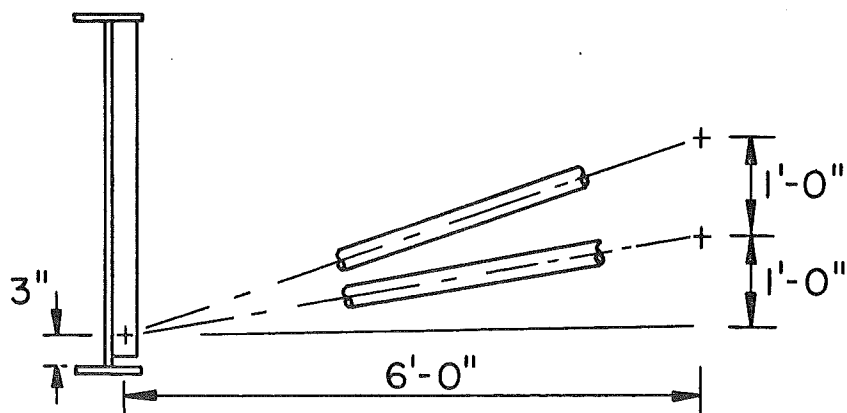


STIFFENER ③

Fig. 1a Details of SC Beams



STIFFENER ① STIFFENER ② STIFFENER ③



DIAGONAL BRACING DESIGNATED ABOVE BY ⊗

Fig. 1b Details of SG and SB Girders

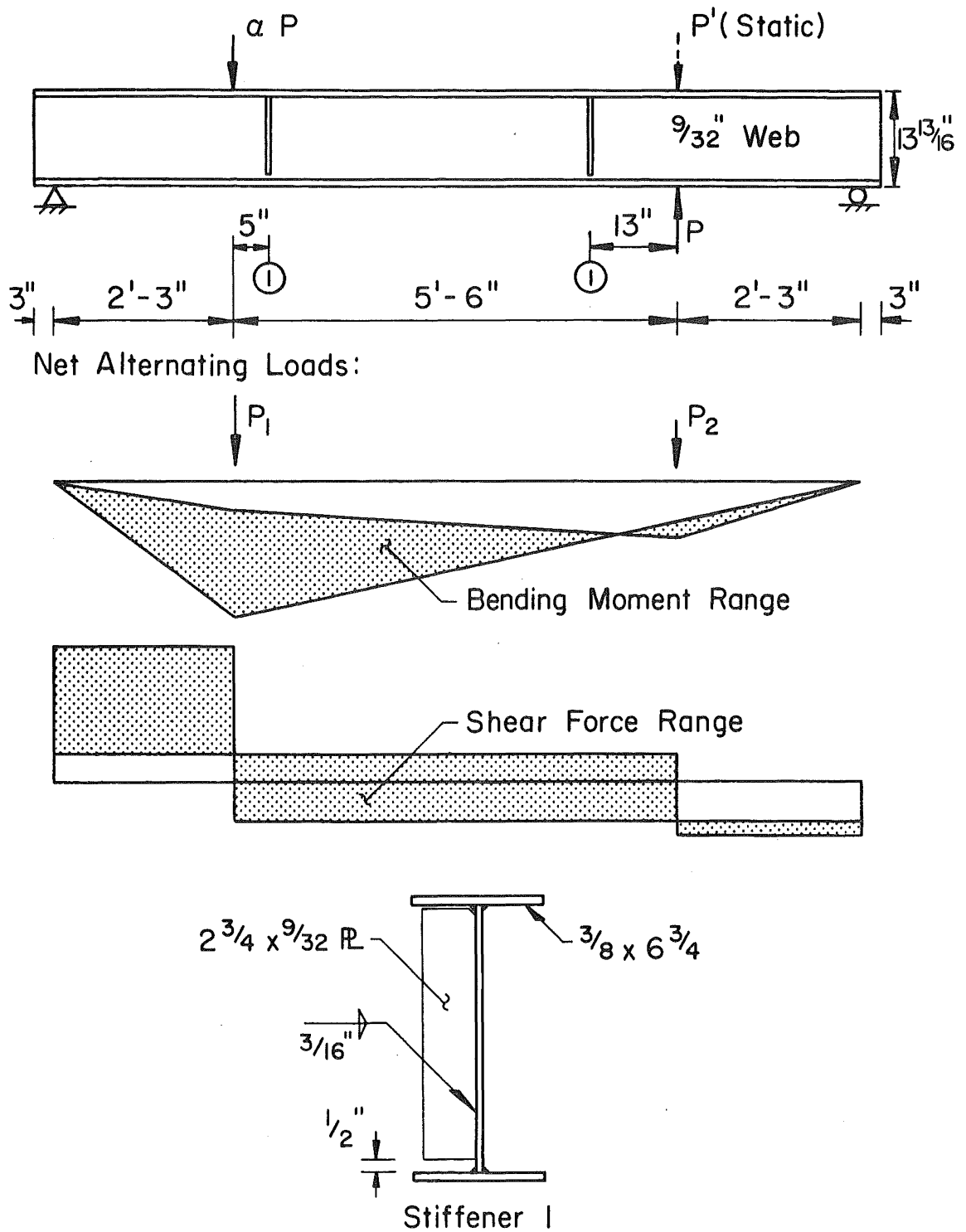


Fig. 2 Details of SA beams with alternating shear

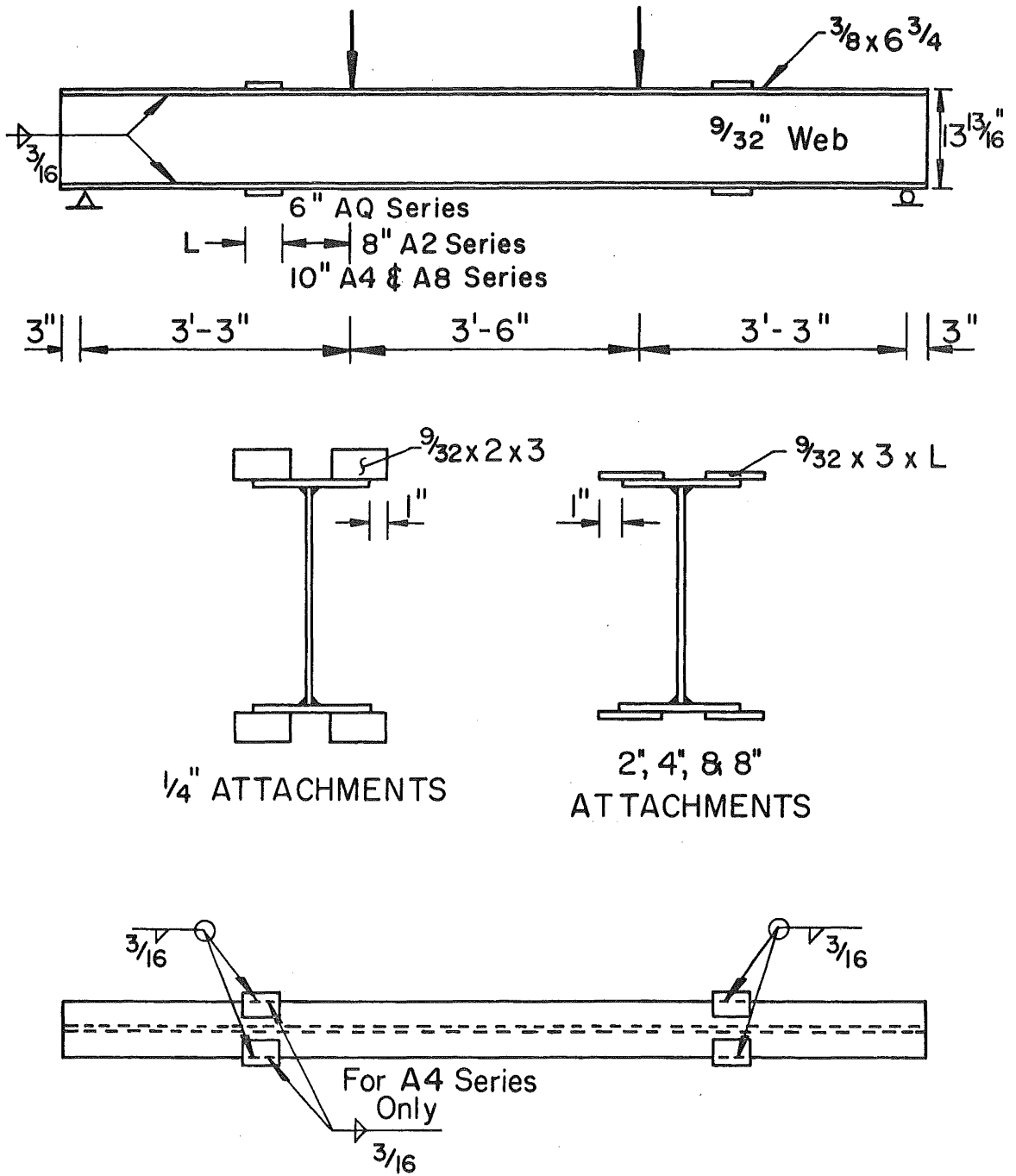


Fig. 3 Details of Beams with Flange Attachments

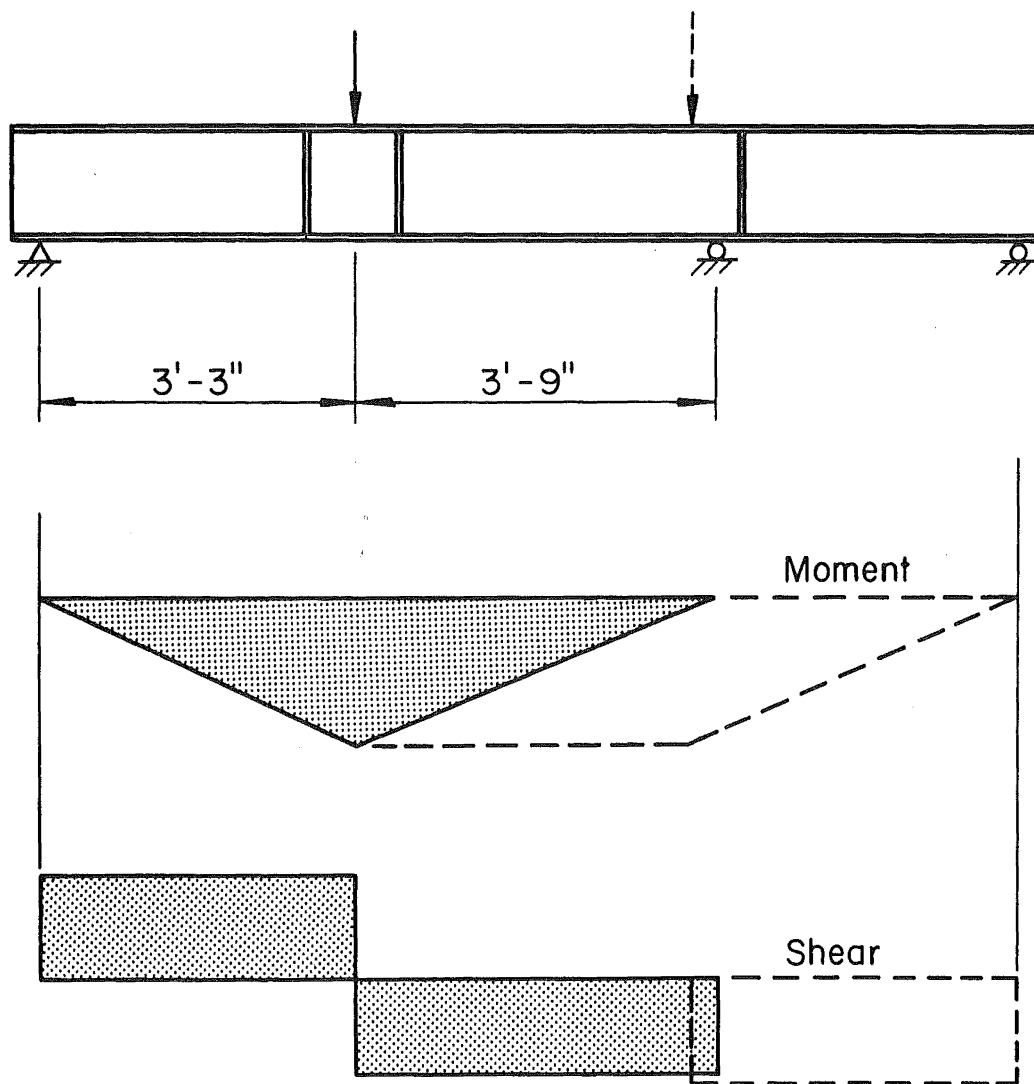


Fig. 5 Moment and Shear Diagram for Continuation of Beam Testing

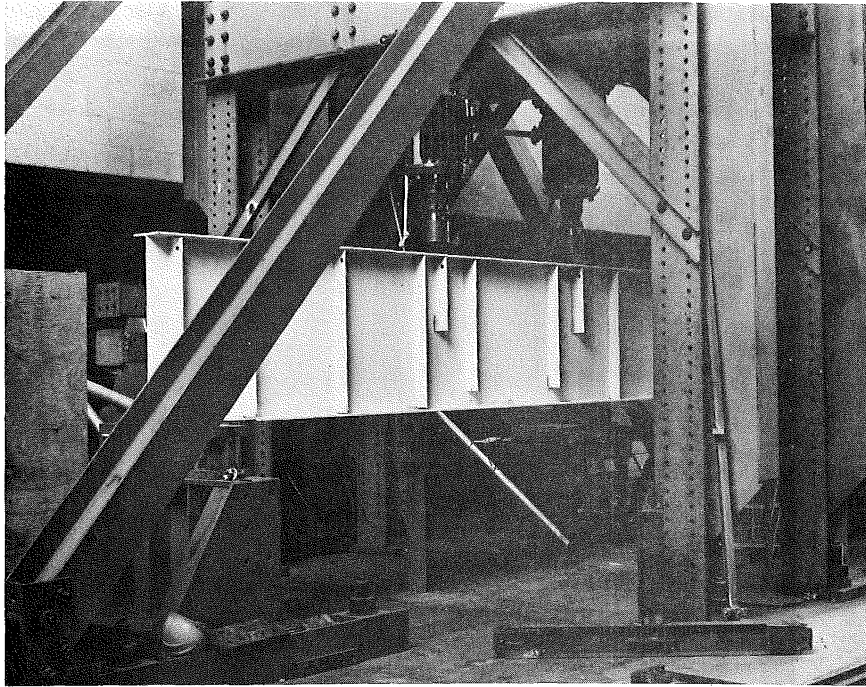


Fig. 4 Test Set-up for SG Girders

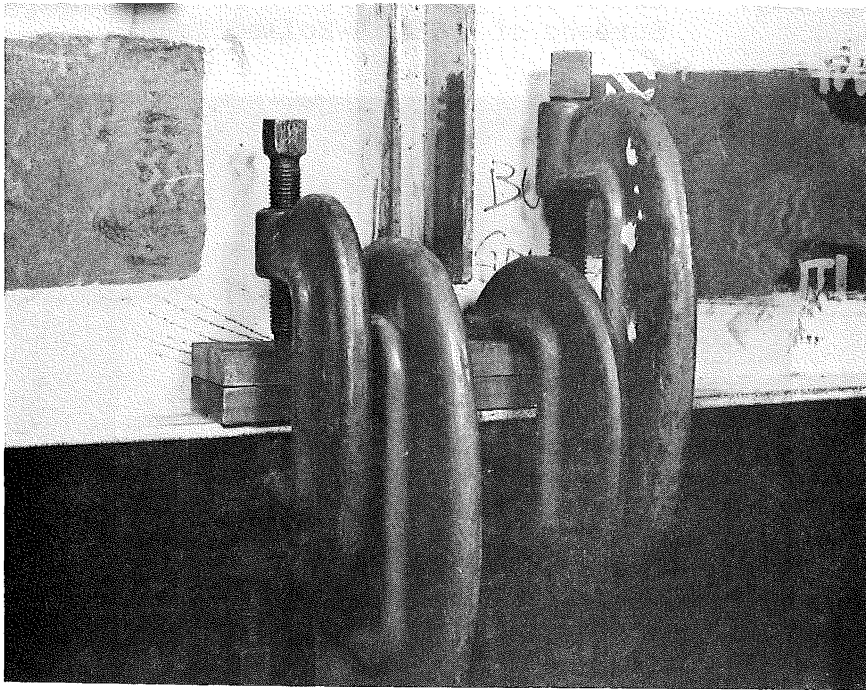


Fig. 6 Tension Flange Splice to Arrest Crack Growth

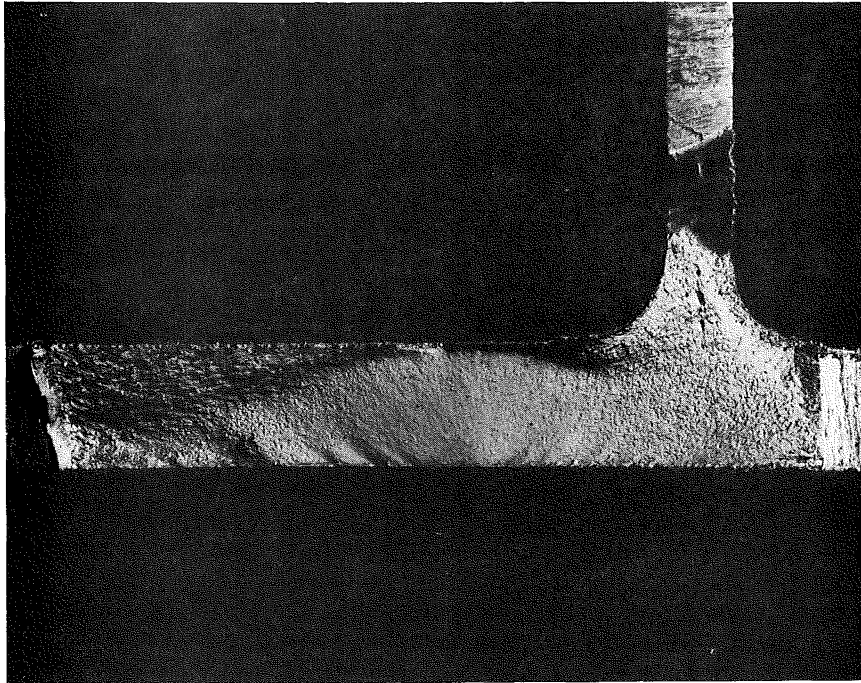


Fig. 7 Crack Initiation from a Flaw in the Rolled Surface of a Plain-Rolled Beam

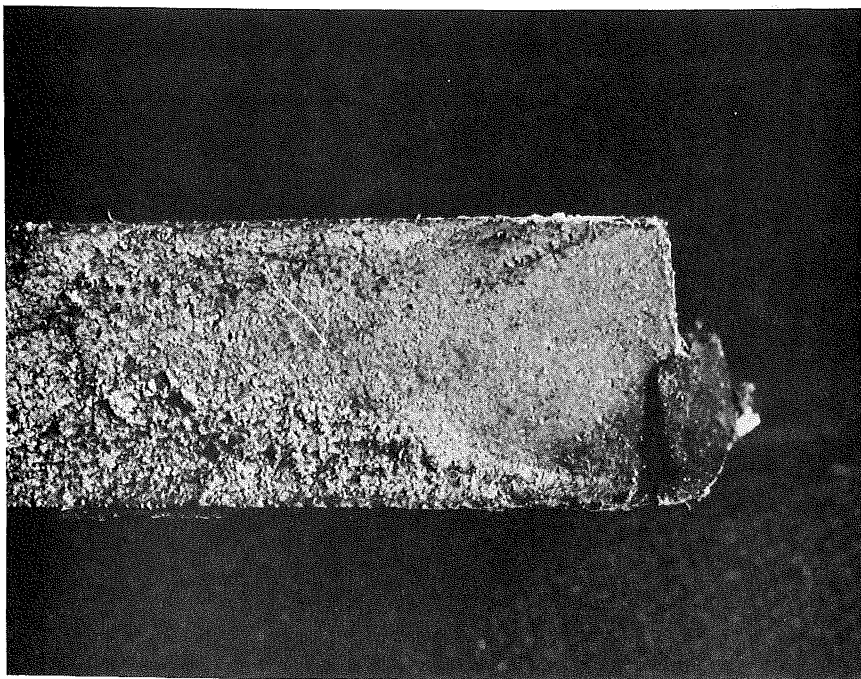


Fig. 8 Example of Crack-Initiation from the Flange-Tip

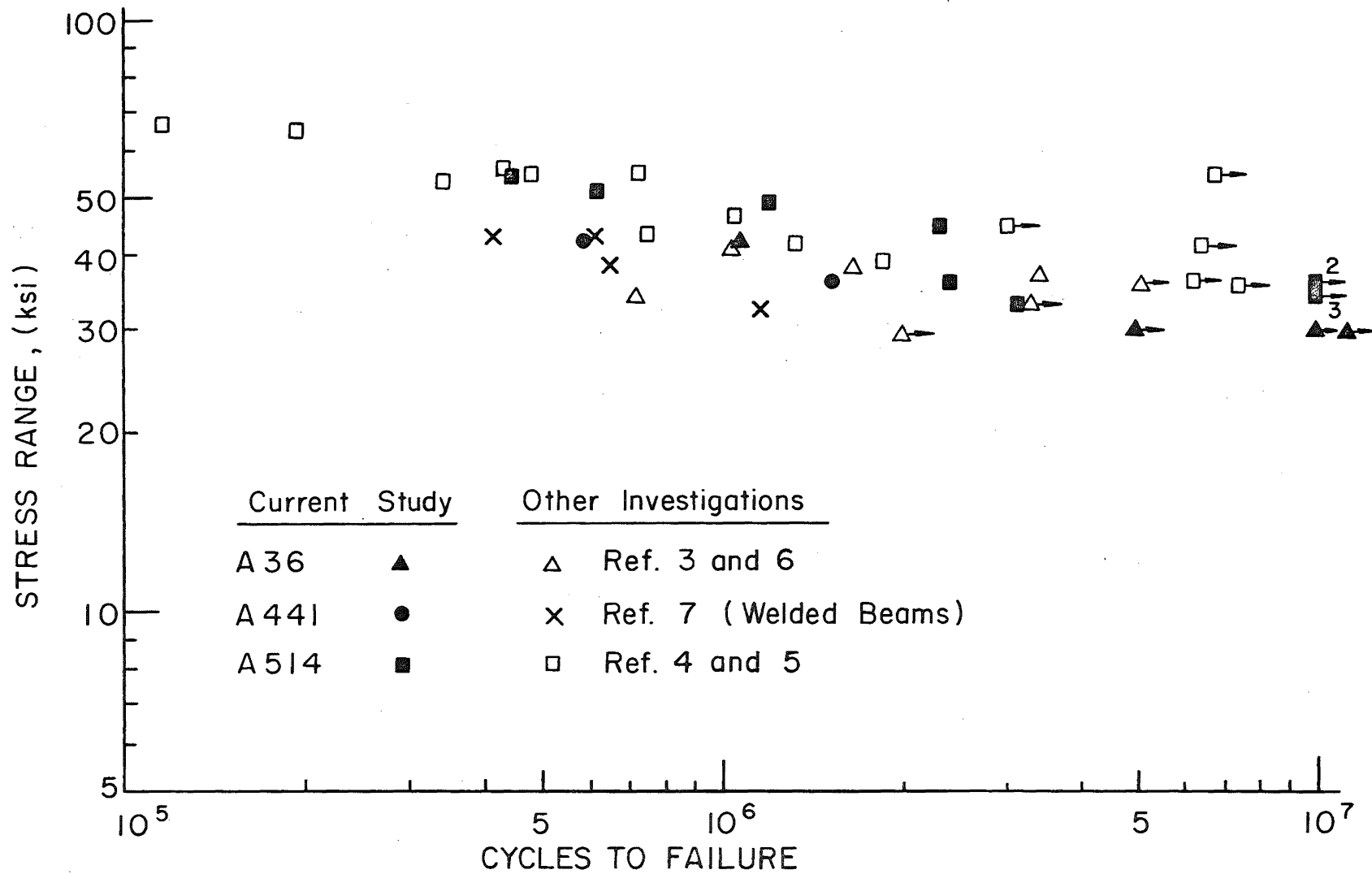


Fig. 9 Comparison of rolled-beam test data with previous results of beams that developed cracks from the rolled surface

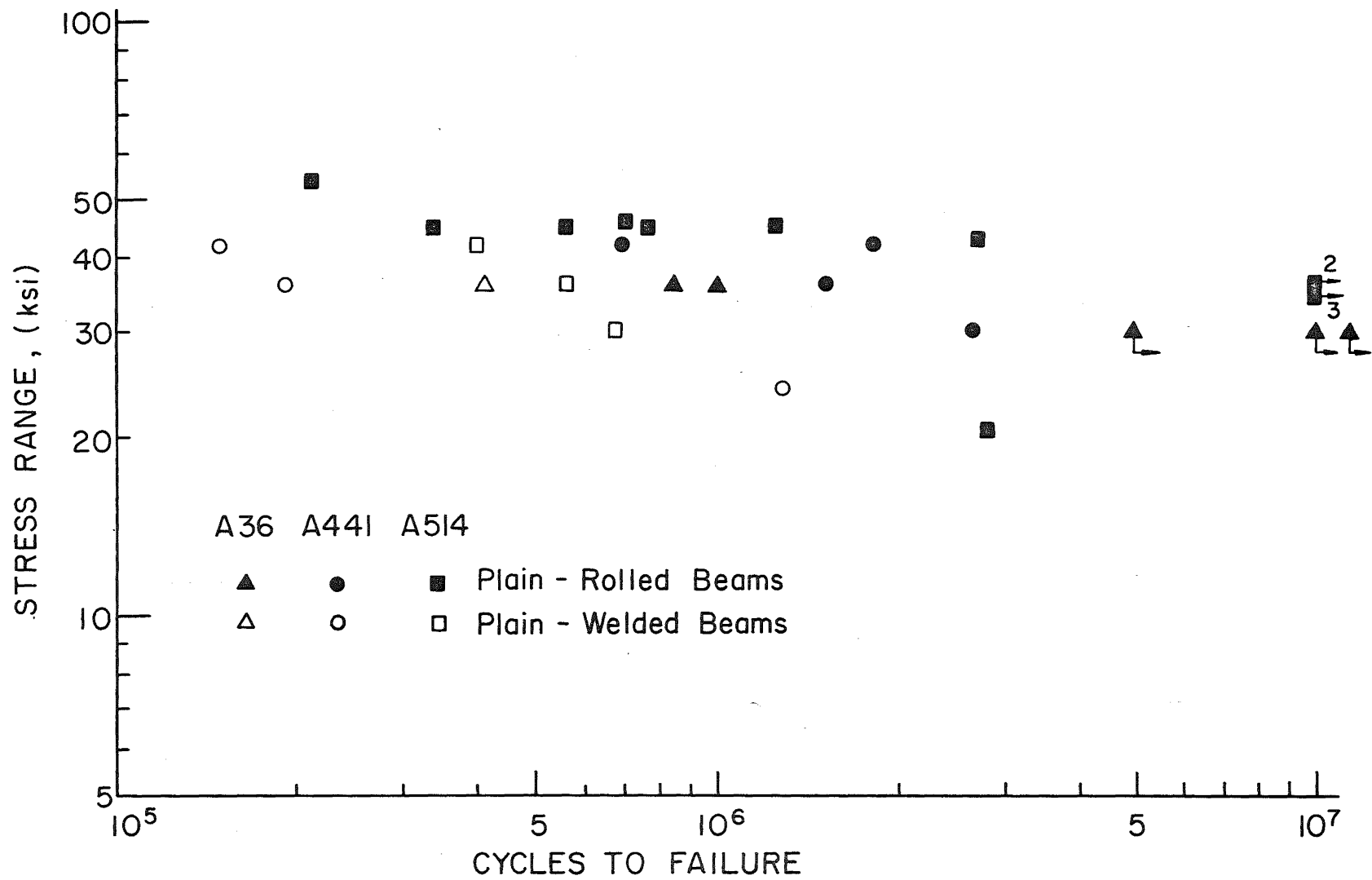


Fig. 10 Comparison of plain-rolled and plain-welded beams with cracks originating at the flange-tip

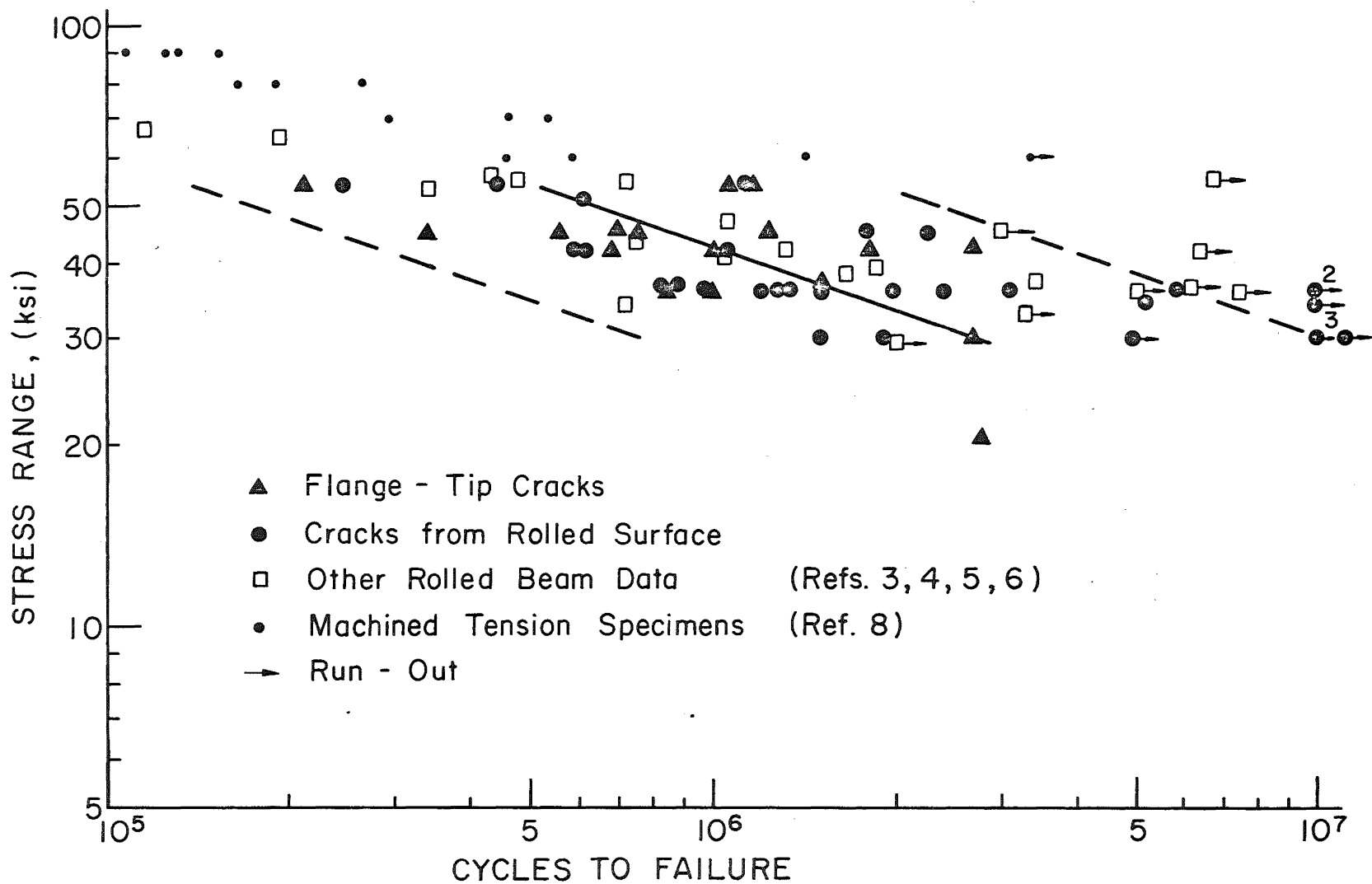


Fig. 11 Summary of rolled-beam data from this study and other investigations

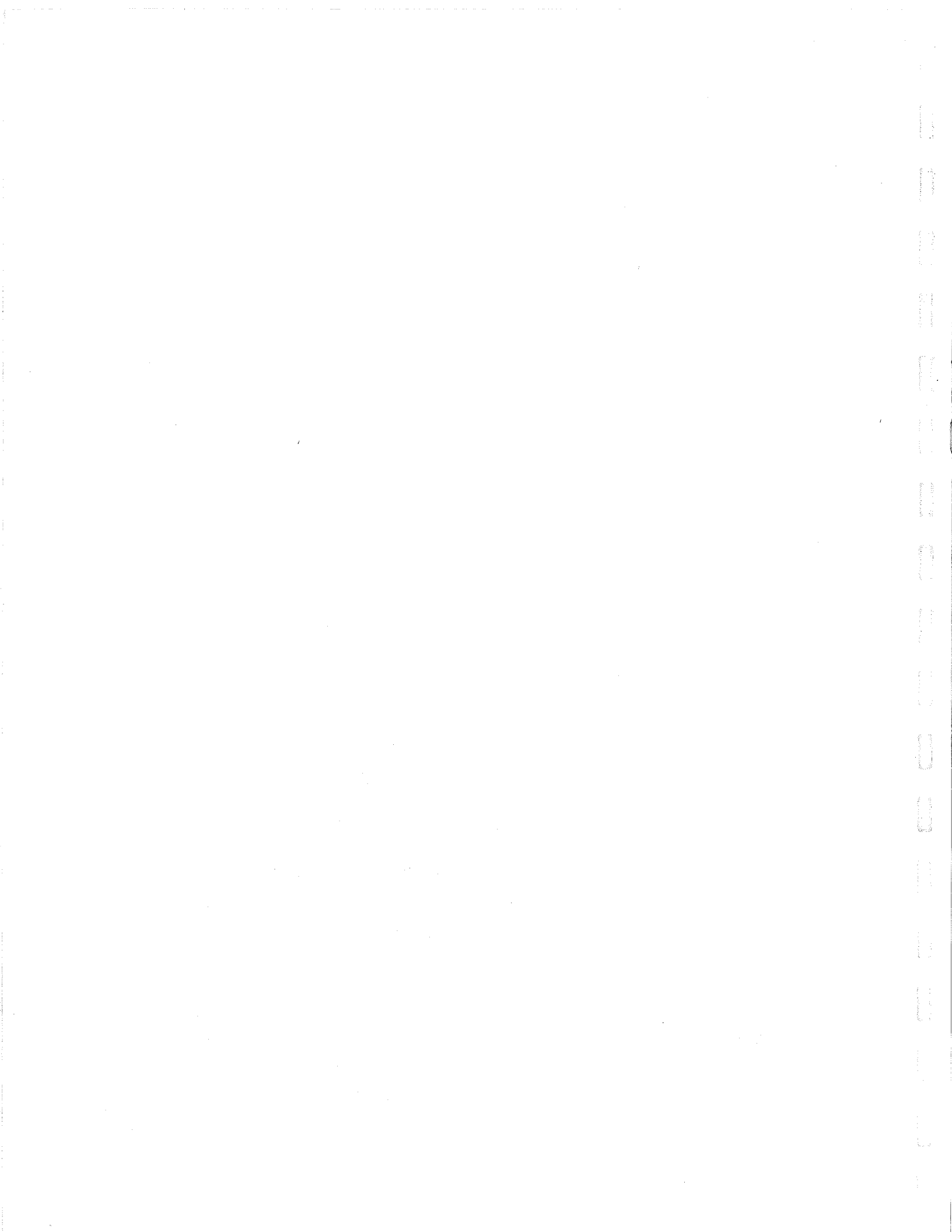




Fig. 12 Typical Failure at
Type 1 Stiffener

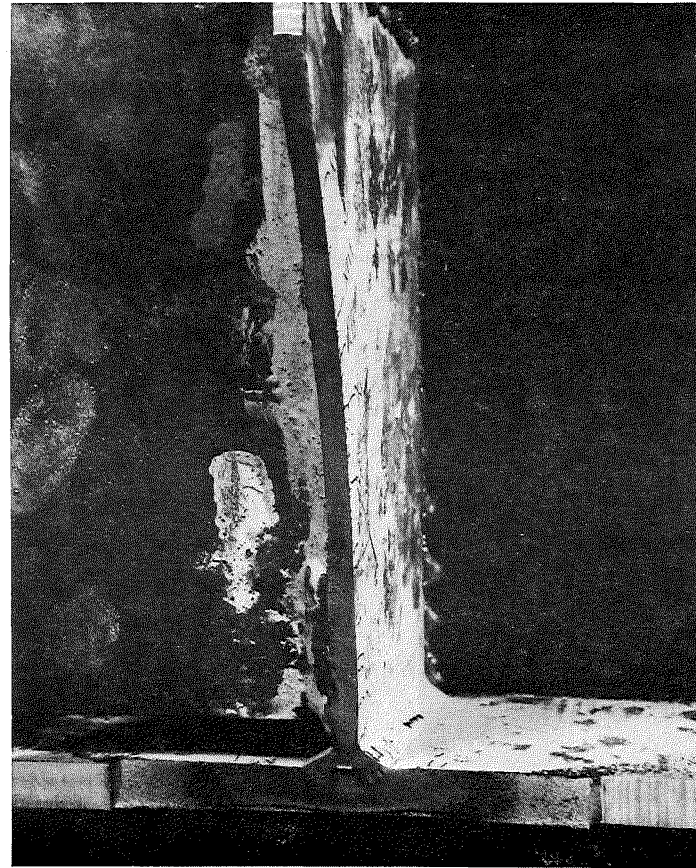
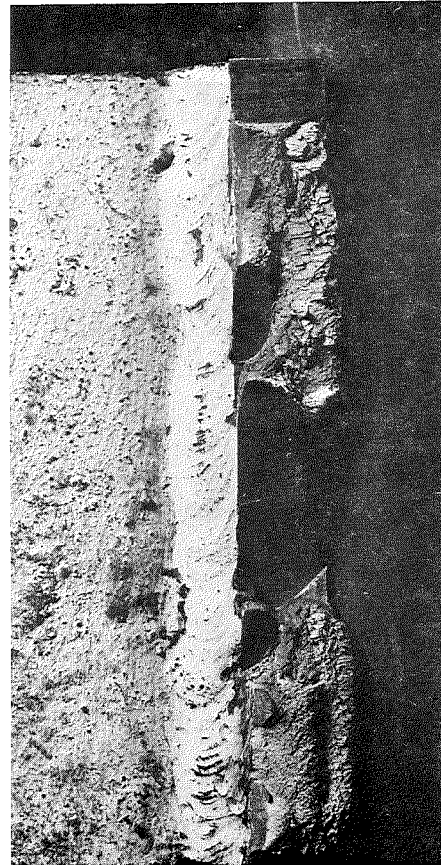


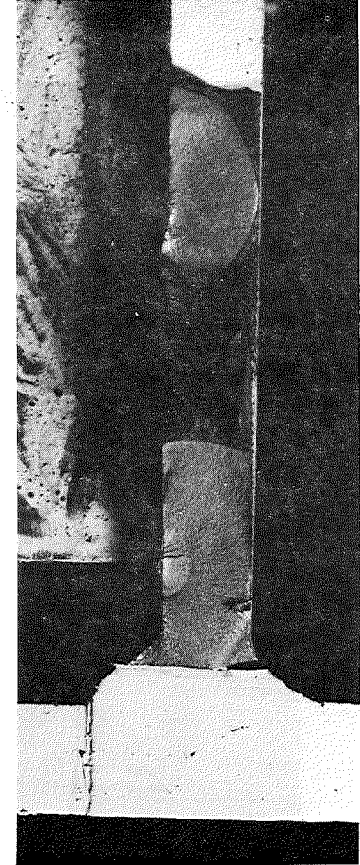
Fig. 13 Typical Fatigue Crack Surface
at Type 1 Stiffener at Failure



(a) 0.035 inch Deep Crack (SCB243)



(b) Multiple Fatigue Cracks



(c) Multiple Fatigue Cracks through the Web

Fig. 14 Fatigue Crack at the Toe of Type 1 Stiffener-to-Web Weld

- Stage 1: Part - Through Crack in Web
- Stage 2: Two - Ended Through Crack in Web
- Stage 3: Three - Ended Crack

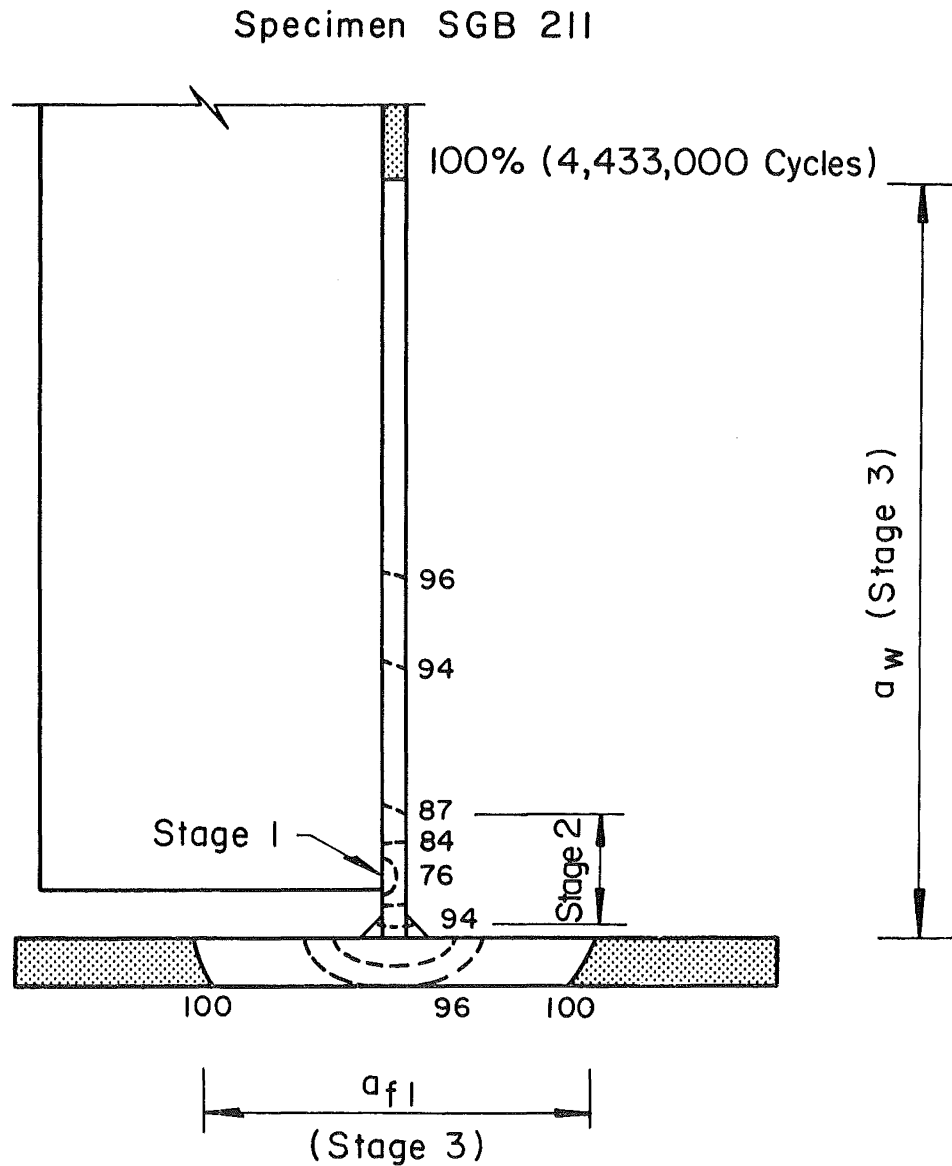


Fig. 15 Stages of crack growth at Type 1 stiffener

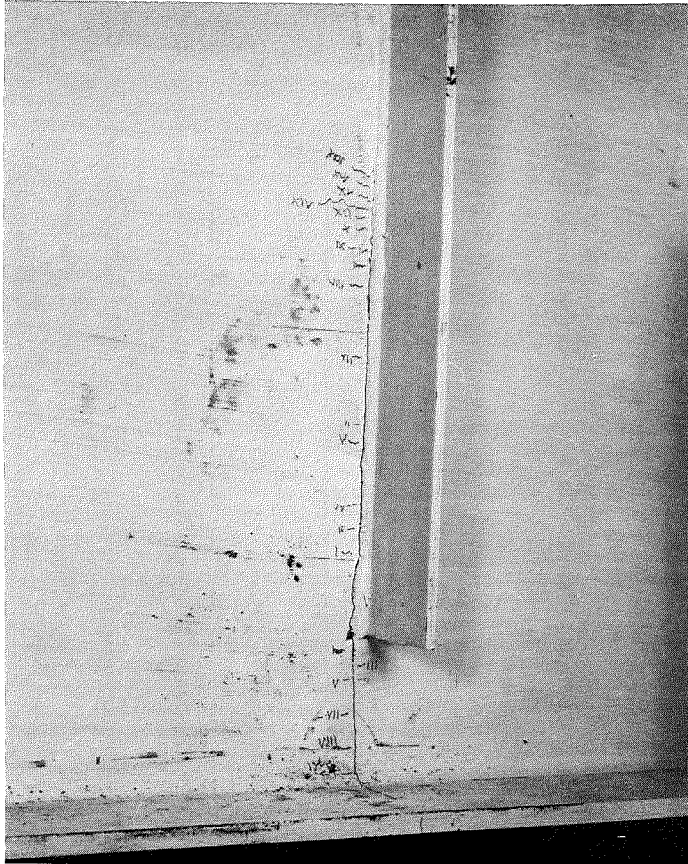


Fig. 16 Typical Failure at
Type 2 Stiffener

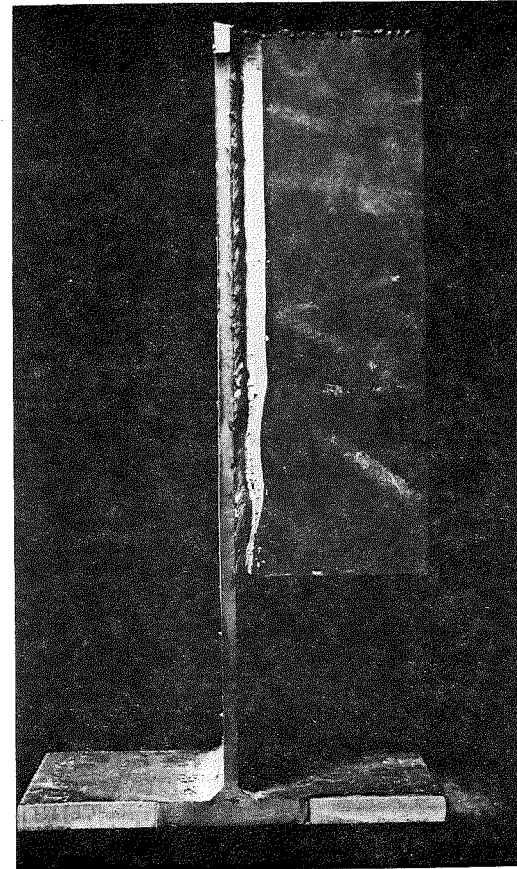


Fig. 17 Typical Fatigue Crack Surface
at Type 2 Stiffener at Failure

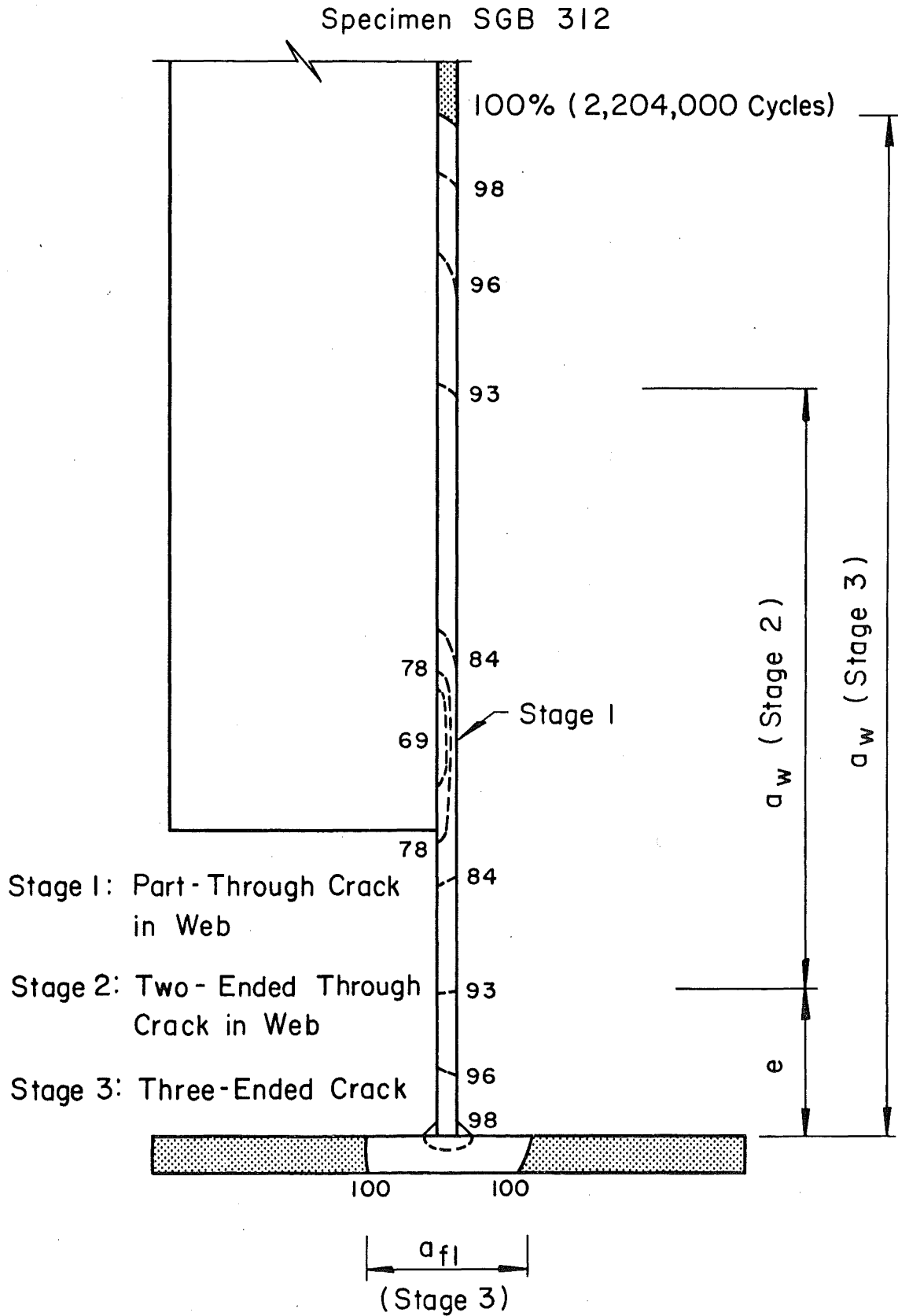
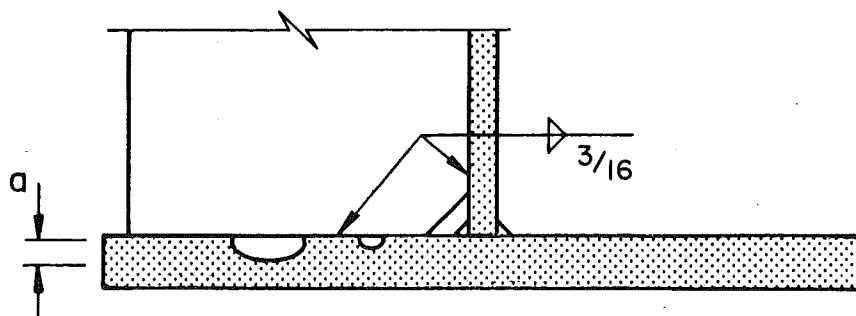
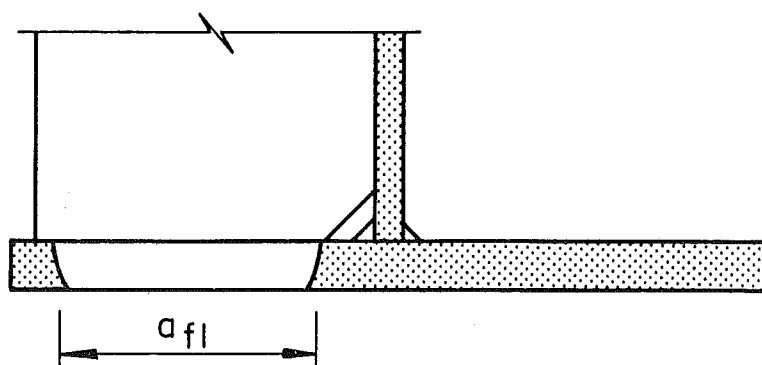


Fig. 18 Stages of crack growth at Type 2 stiffener

Stage 1: Part - Through Crack



Stage 2: Through Crack



Specimen SGB 312

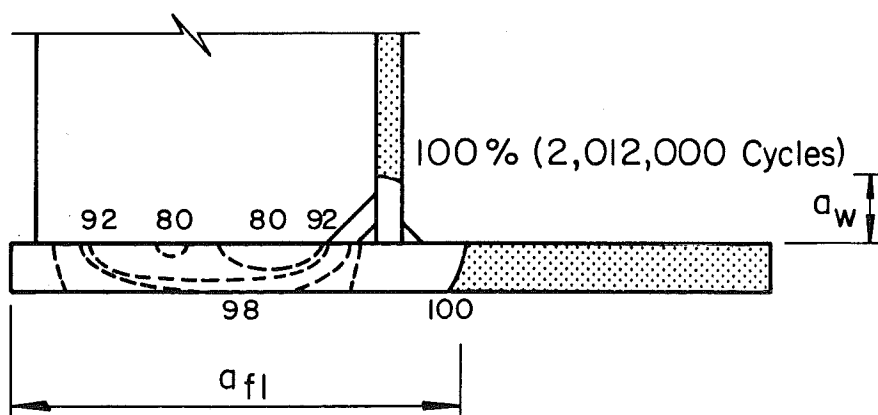


Fig. 20 Stages of crack growth at Type 3 stiffener

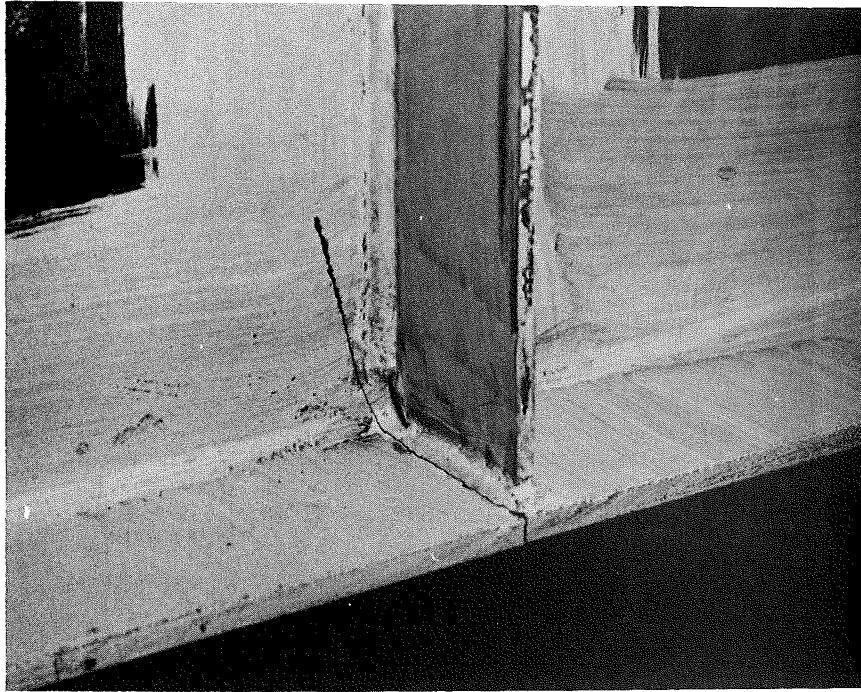


Fig. 19 Typical Failure at Type 3 Stiffener



Fig. 21 0.028 inch Deep Crack at the Toe of Type 3 Stiffener-to-Tension Flange Weld (SGC333)

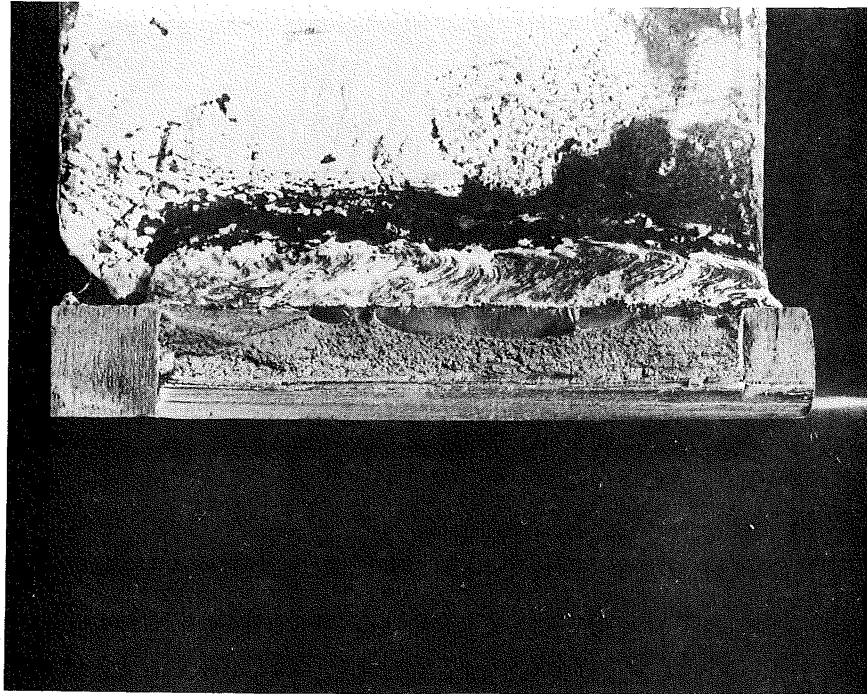


Fig. 22 Multiple Fatigue Crack Growth at the Toe of Type 3 Stiffener-to-Tension Flange Weld

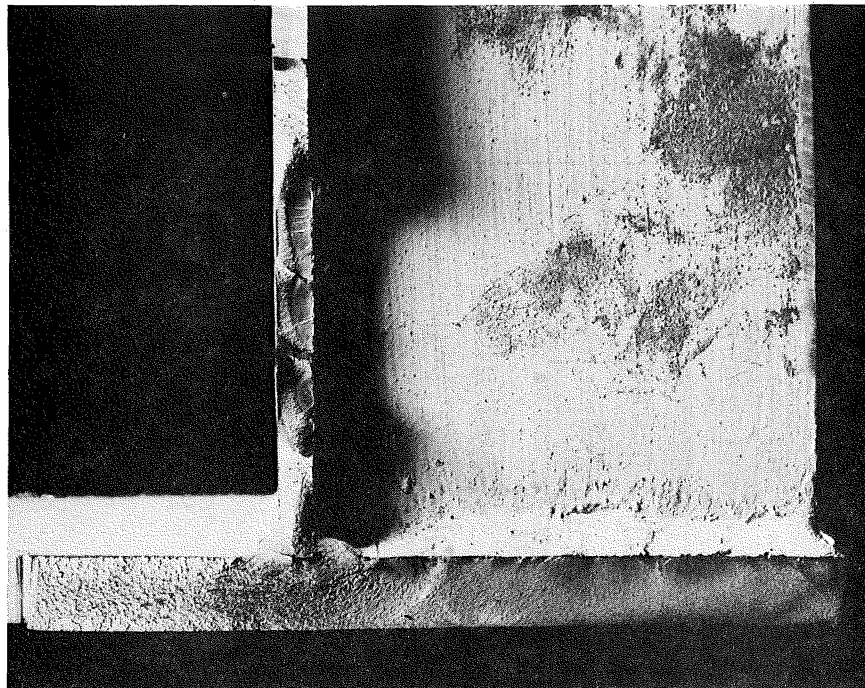


Fig. 23 Typical Fatigue Crack Surface at Type 3 Stiffener at Failure

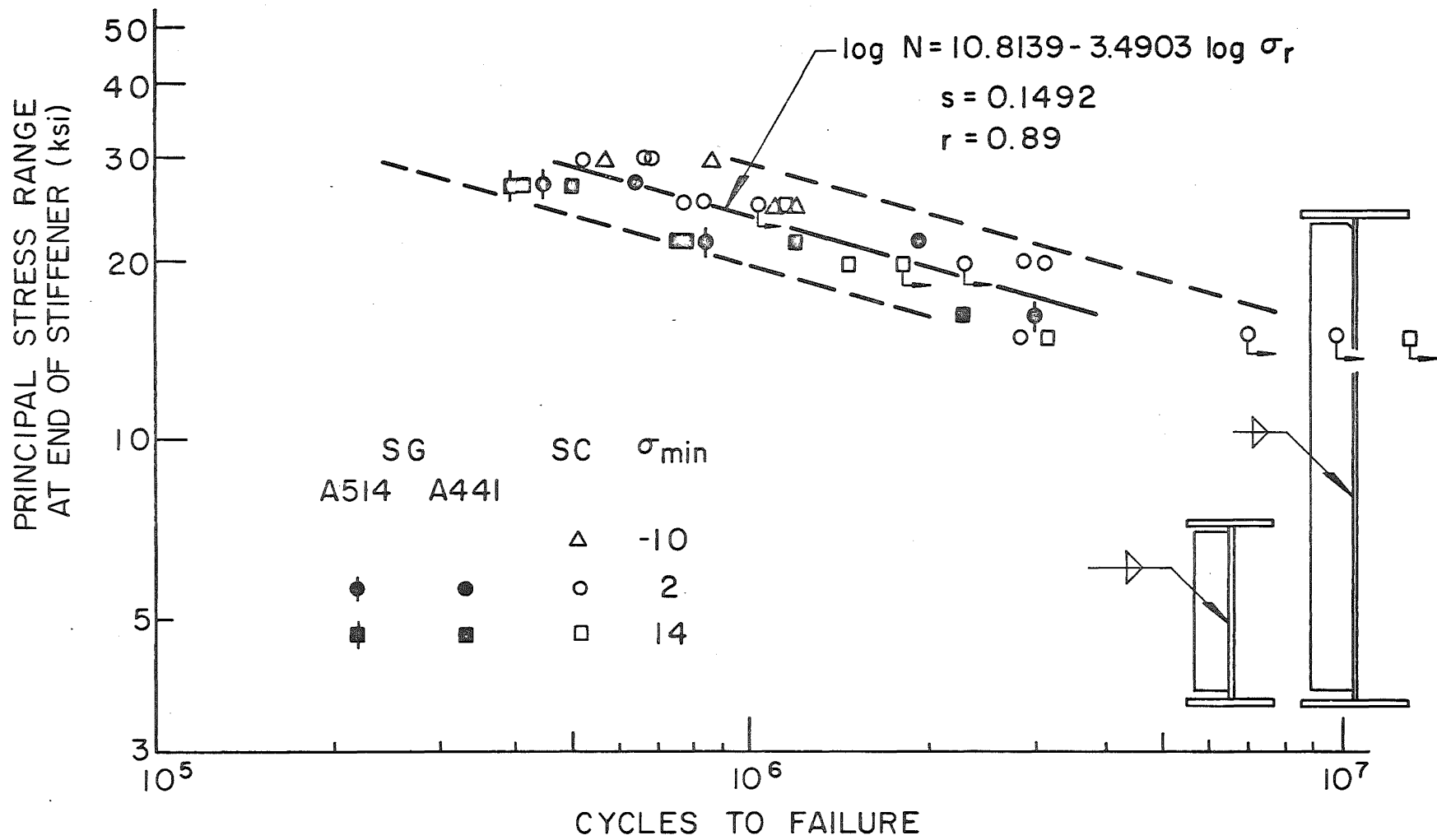


Fig. 24 S-N Plot for Type 1 Stiffeners, SG Girders & SC Beams

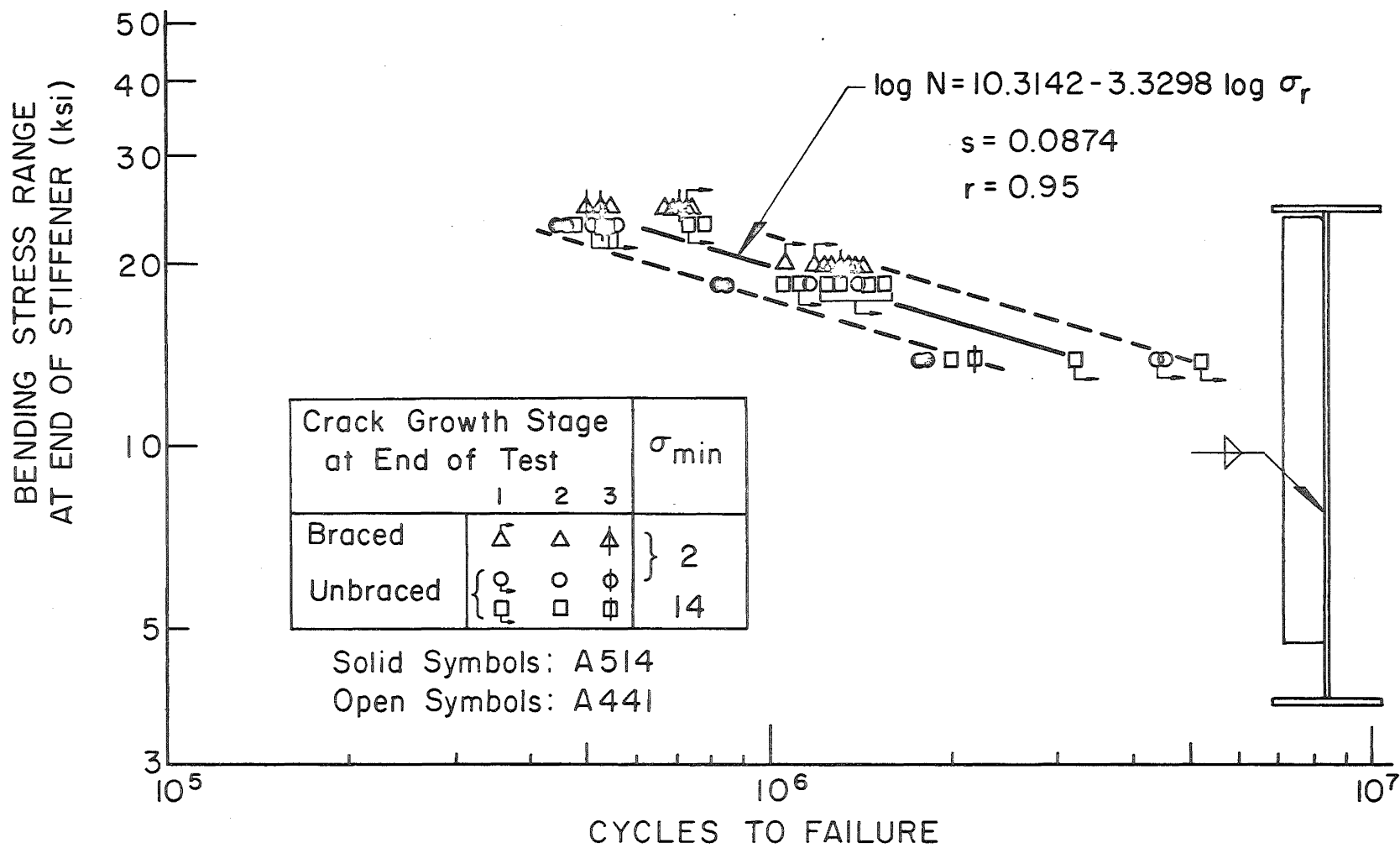


Fig. 25 S-N Plot for Type 2 Stiffeners, SG Girders

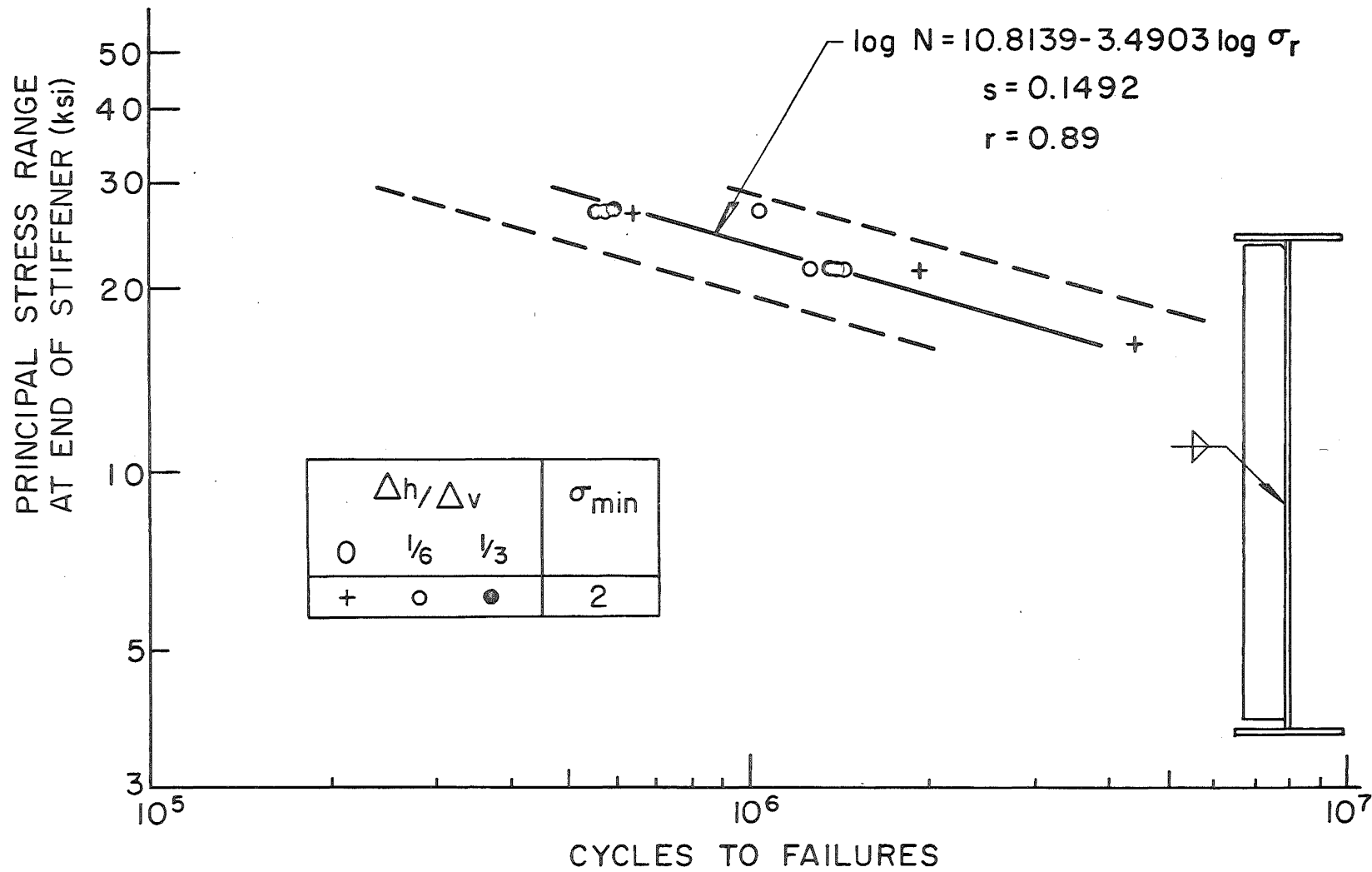


Fig. 26 S-N Plot for Type 1 Stiffeners, SB Girders with Transverse Bracing

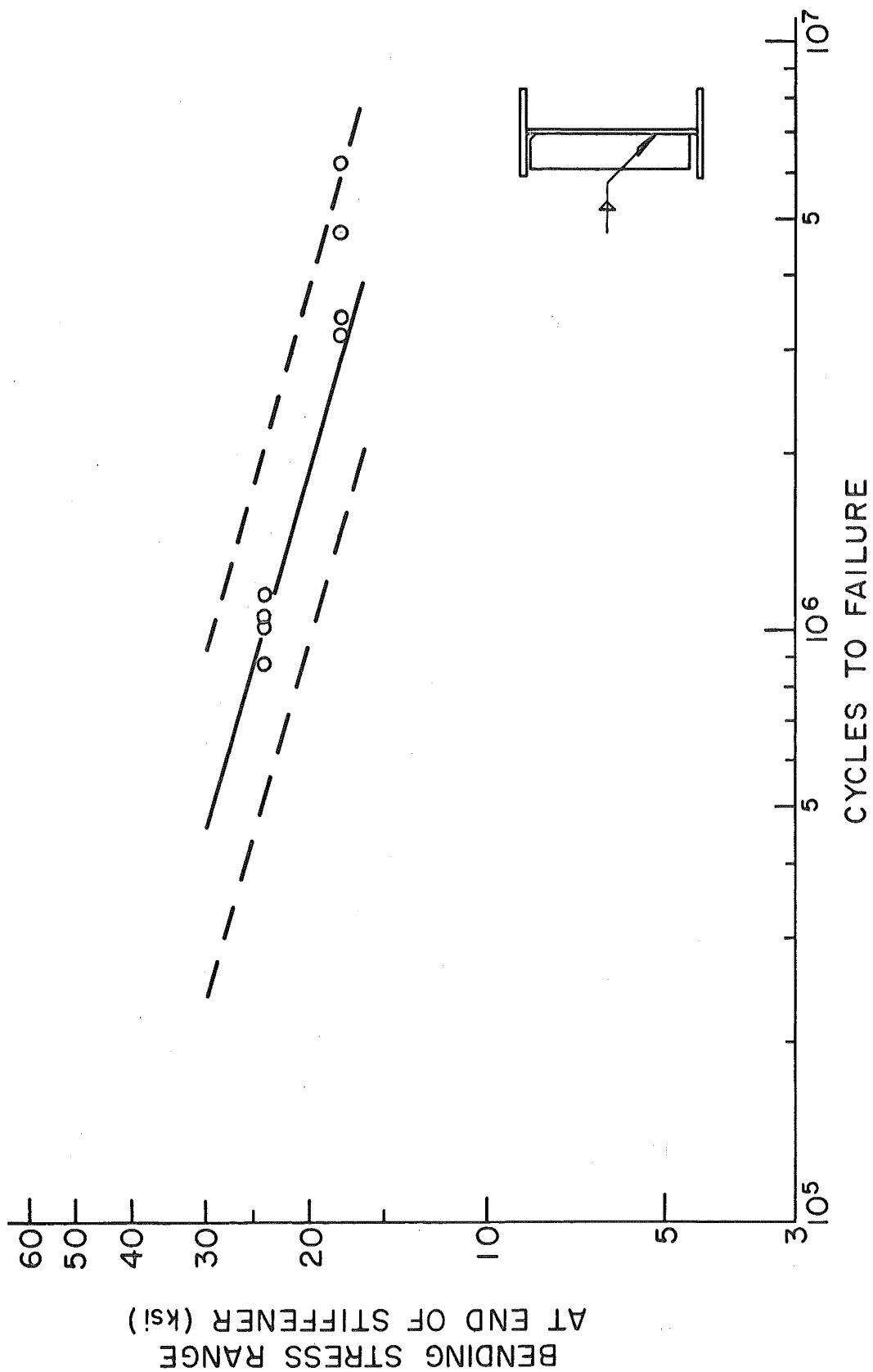


Fig. 27 S-N plot for Type 1 stiffeners
SA beams with alternating shear

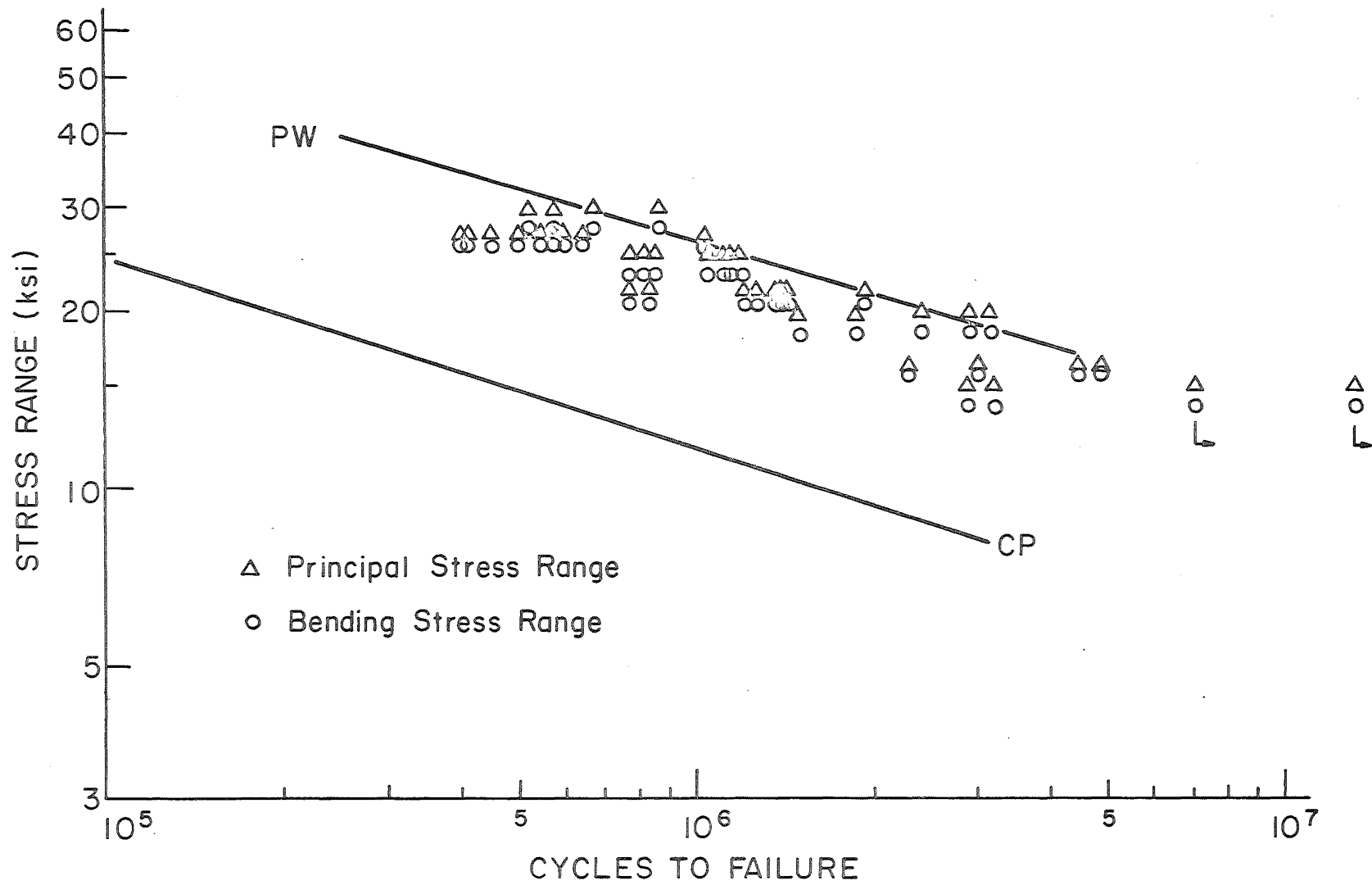


Fig. 28 Effect of bending and principal stress range on the fatigue strength of Type 1 stiffeners

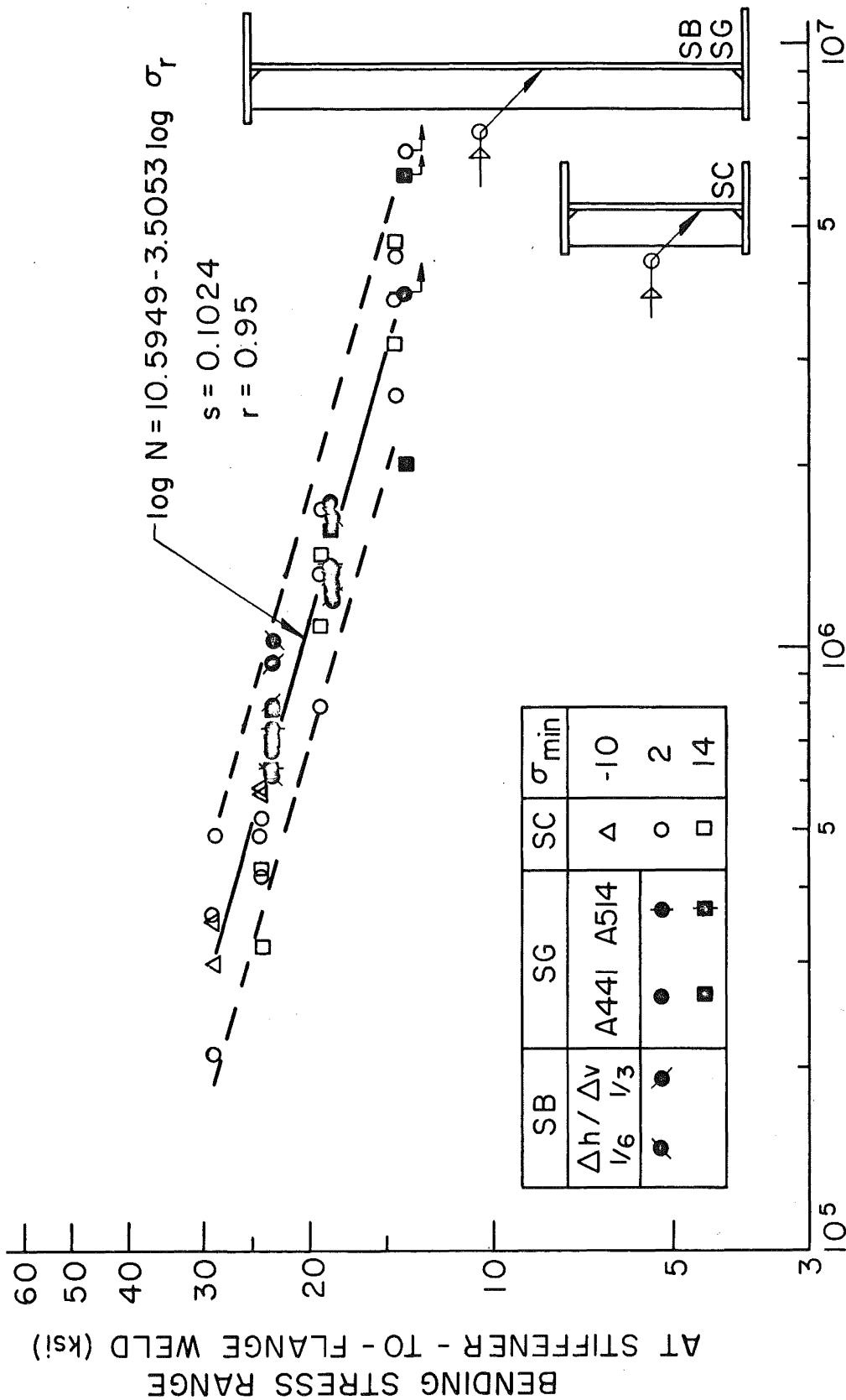


Fig. 29 S-N Plot for Type 3 Stiffeners

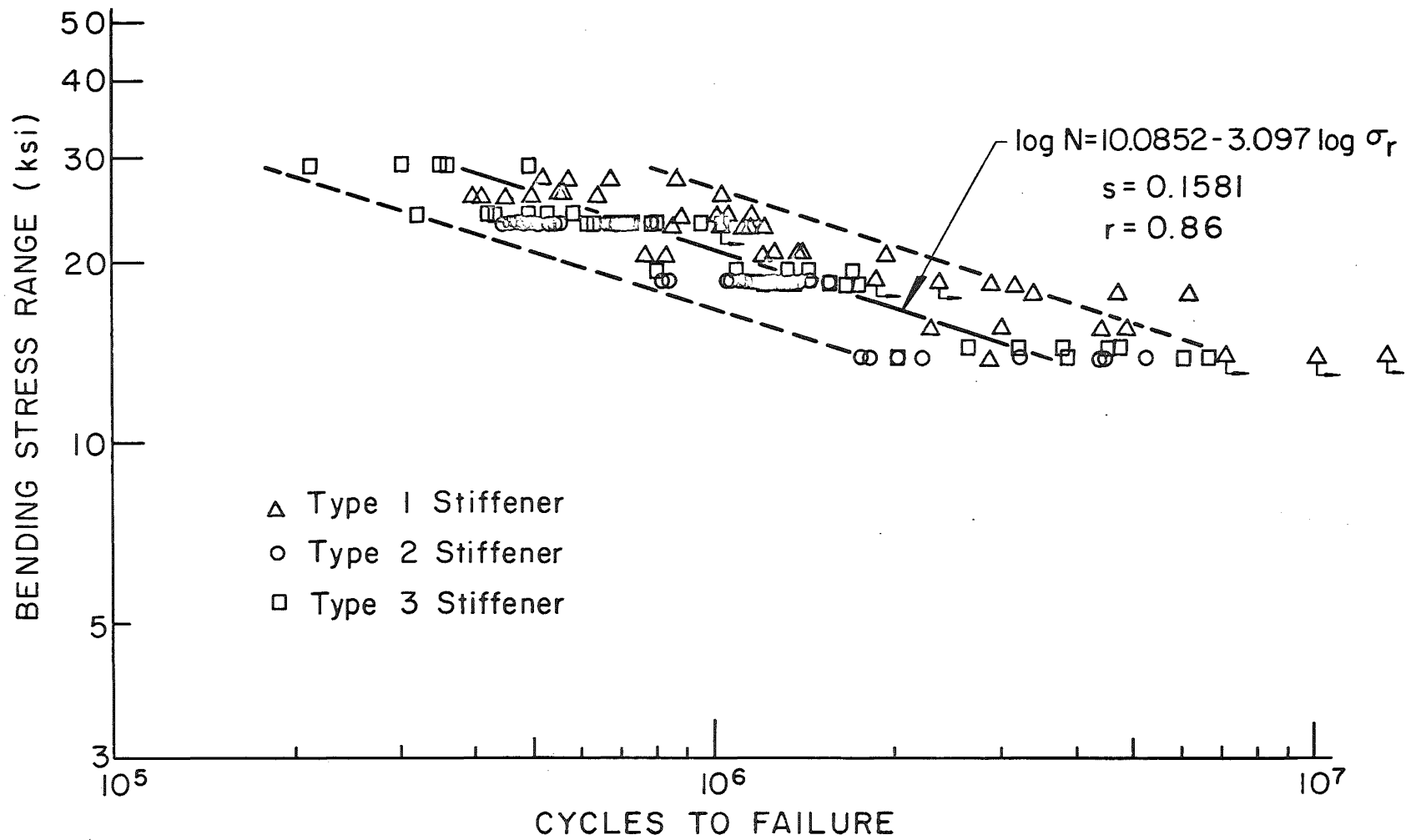


Fig. 30 Summary S-N Plot for Type 1, 2, and 3 Stiffeners

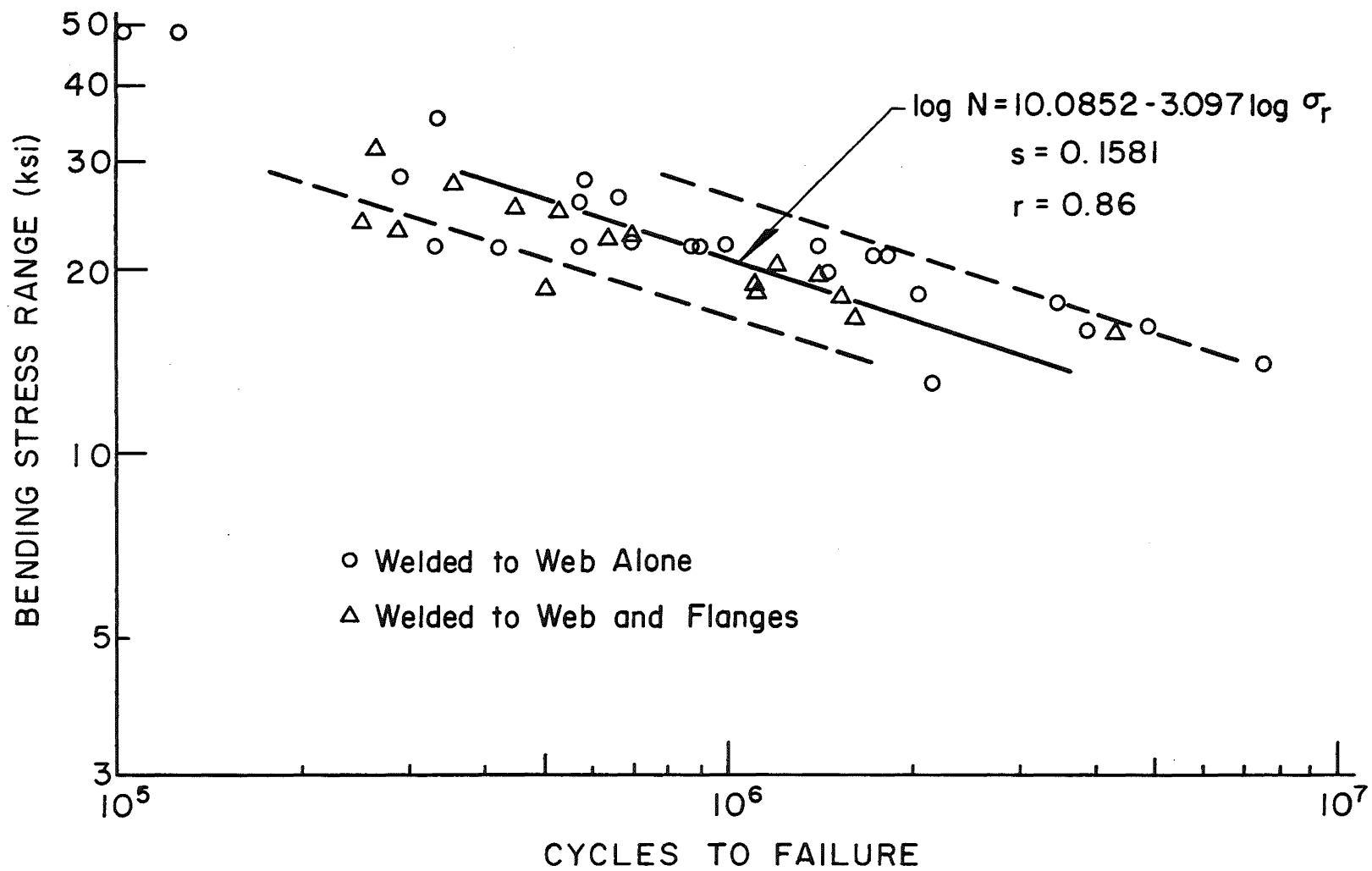


Fig. 31 Comparison of Present Study with Previous Work, All Stiffeners

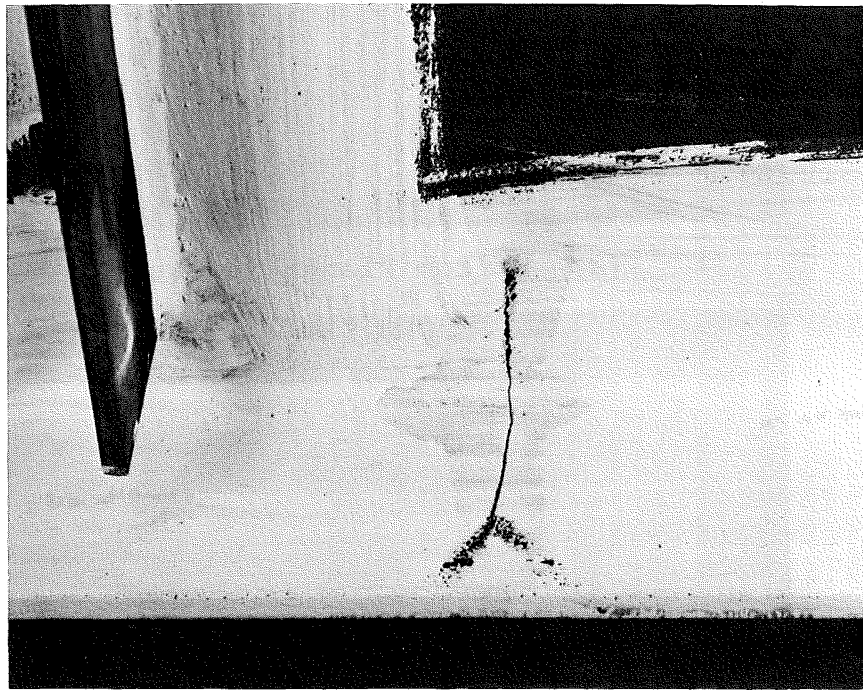
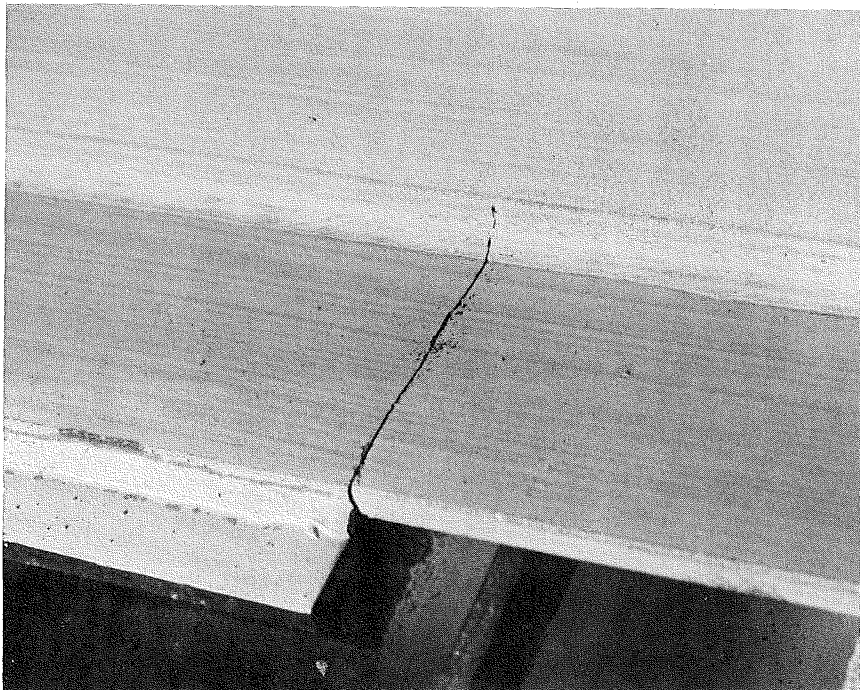


Fig. 32 Typical Plain-Welded Beam Failure

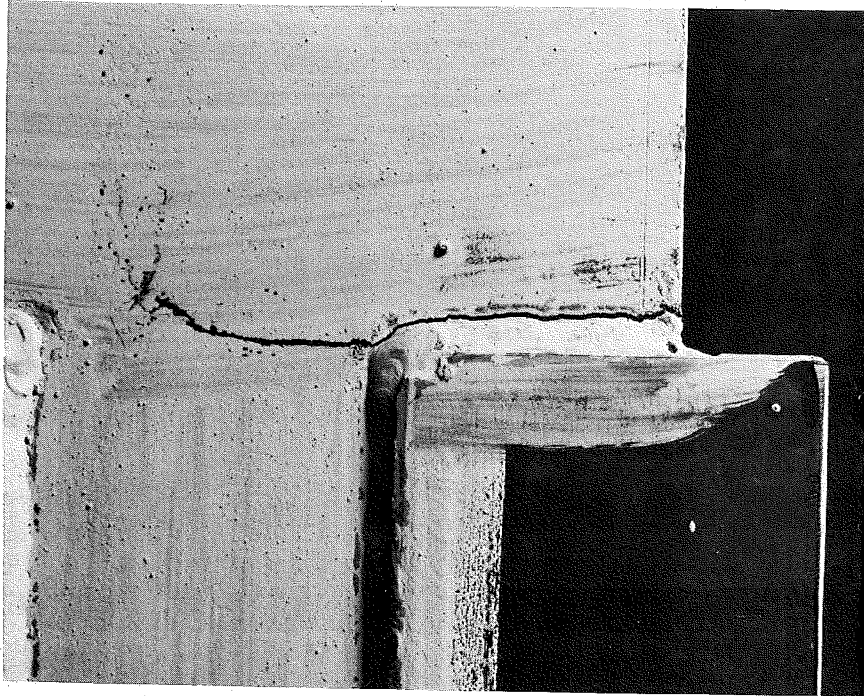


(a) Bottom Flange Surface

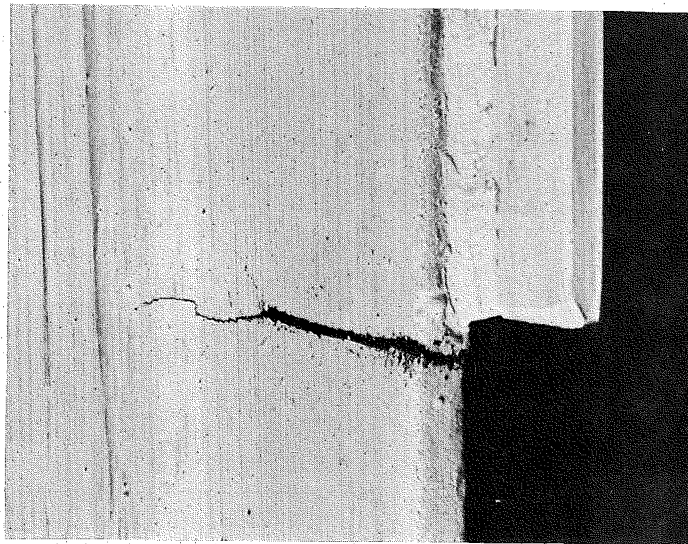


(b) Top of Bottom Flange

Fig. 34 (a)(b) Typical Failure at Flange Attachment with no Transverse Weld



(c) Bottom Flange Surface



(d) Top of Bottom Flange

Fig. 34 (c)(d) Typical Failure at Flange Attachment
with Welds all Around

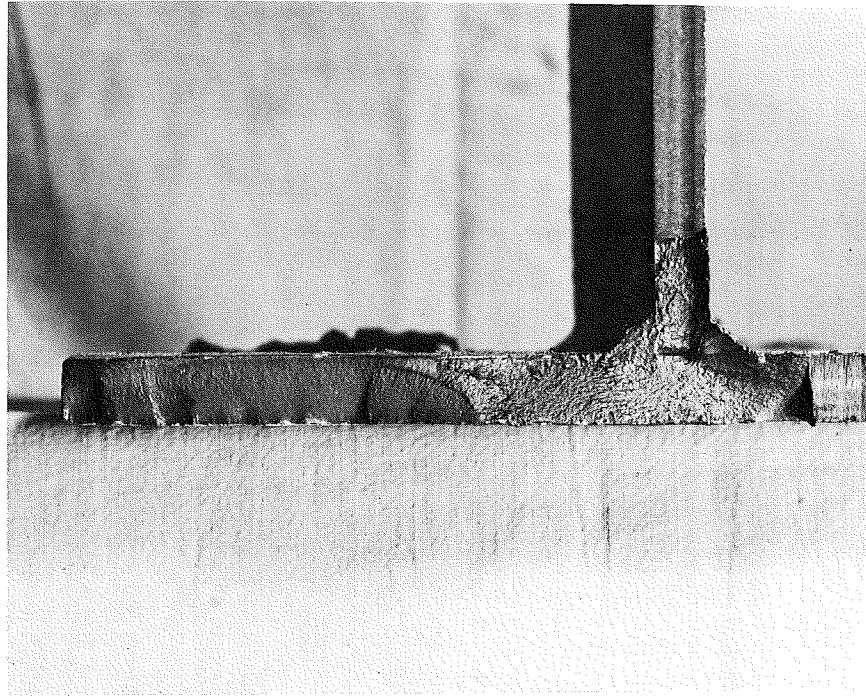


Fig. 35 Typical Fatigue Crack Surface at Flange Attachment with Transverse Weld

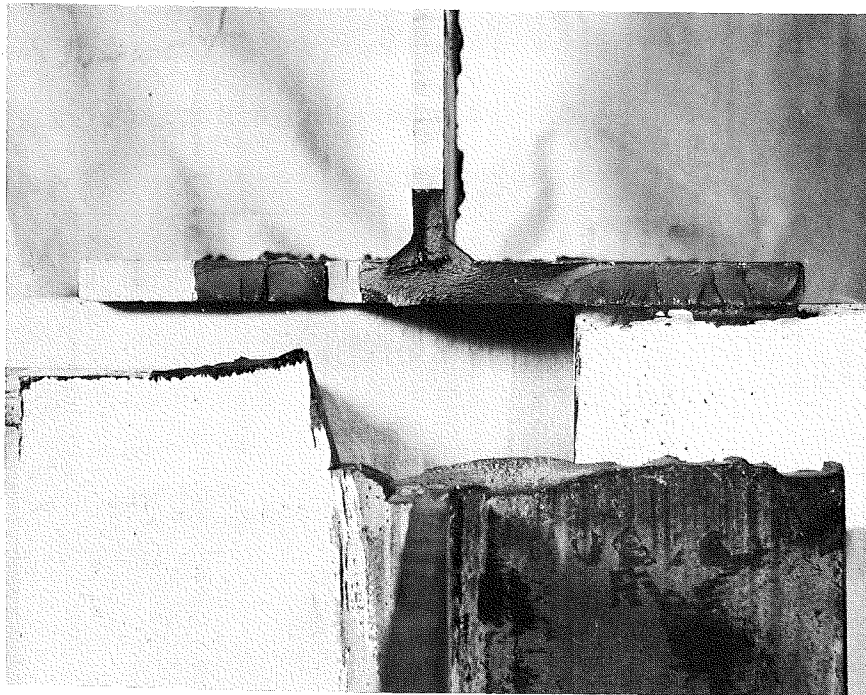


Fig. 36 Fatigue Crack at Short (1/4 in.) Attachment to Flange

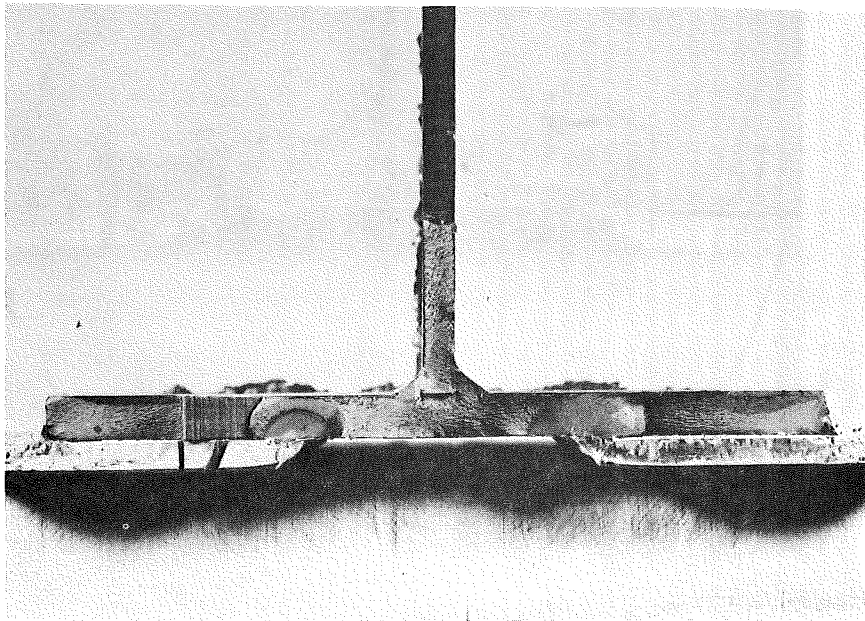
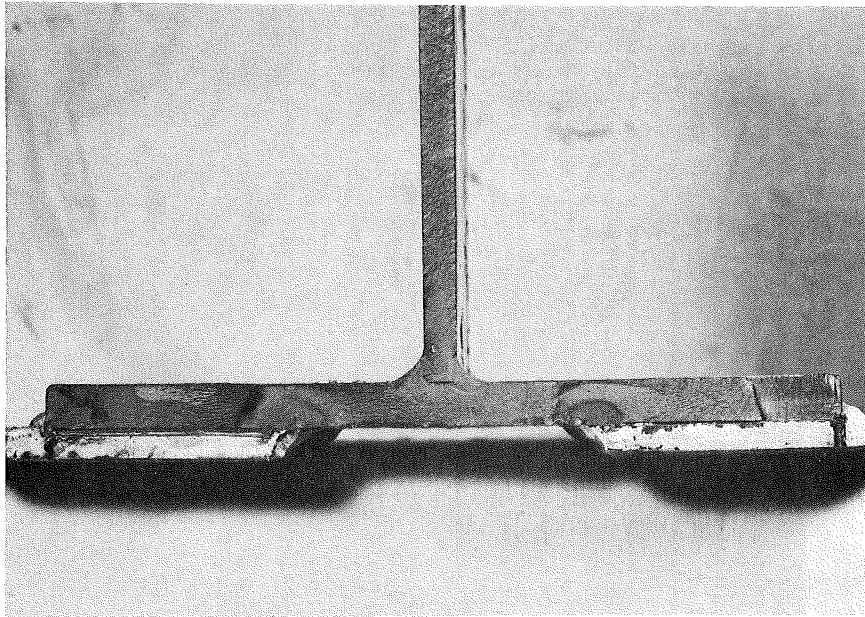


Fig. 37 (a)(b) Typical Fatigue Crack Surface at Flange Attachment with Longitudinal Welds

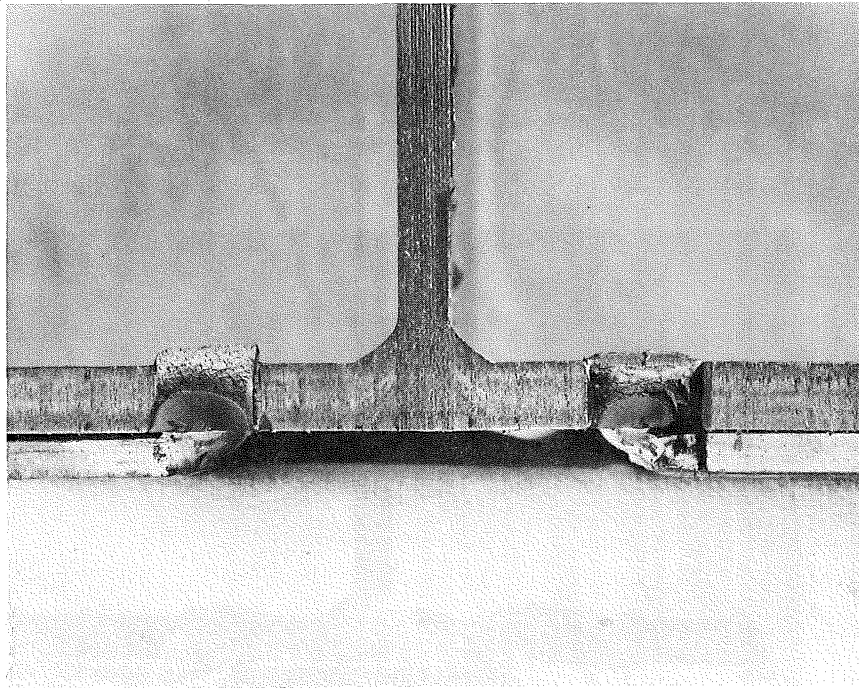


Fig. 38 Simultaneous Crack Growth from Weld Toe Terminations

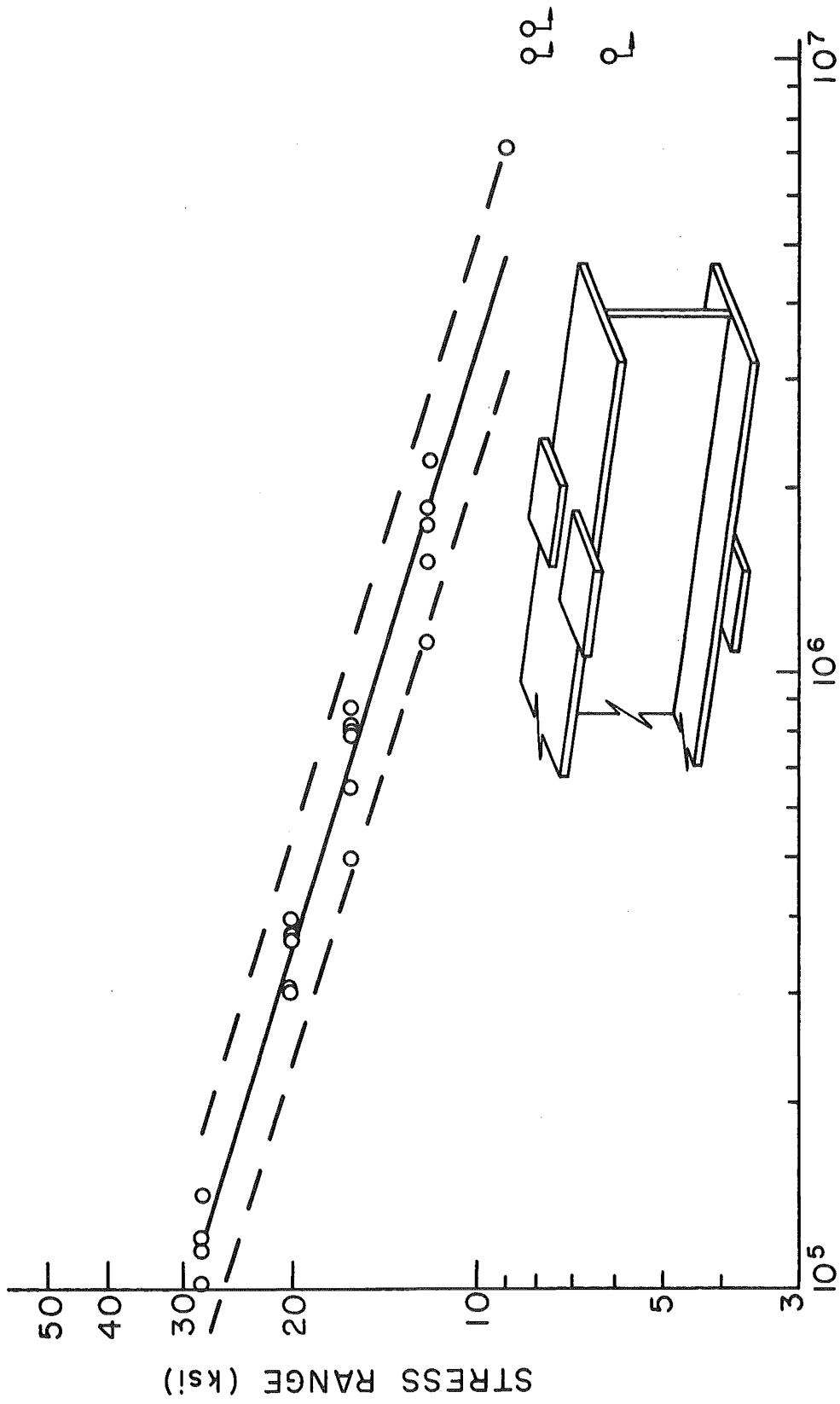


Fig. 39 S-N Plot for 4 in. Attachments Welded All Around

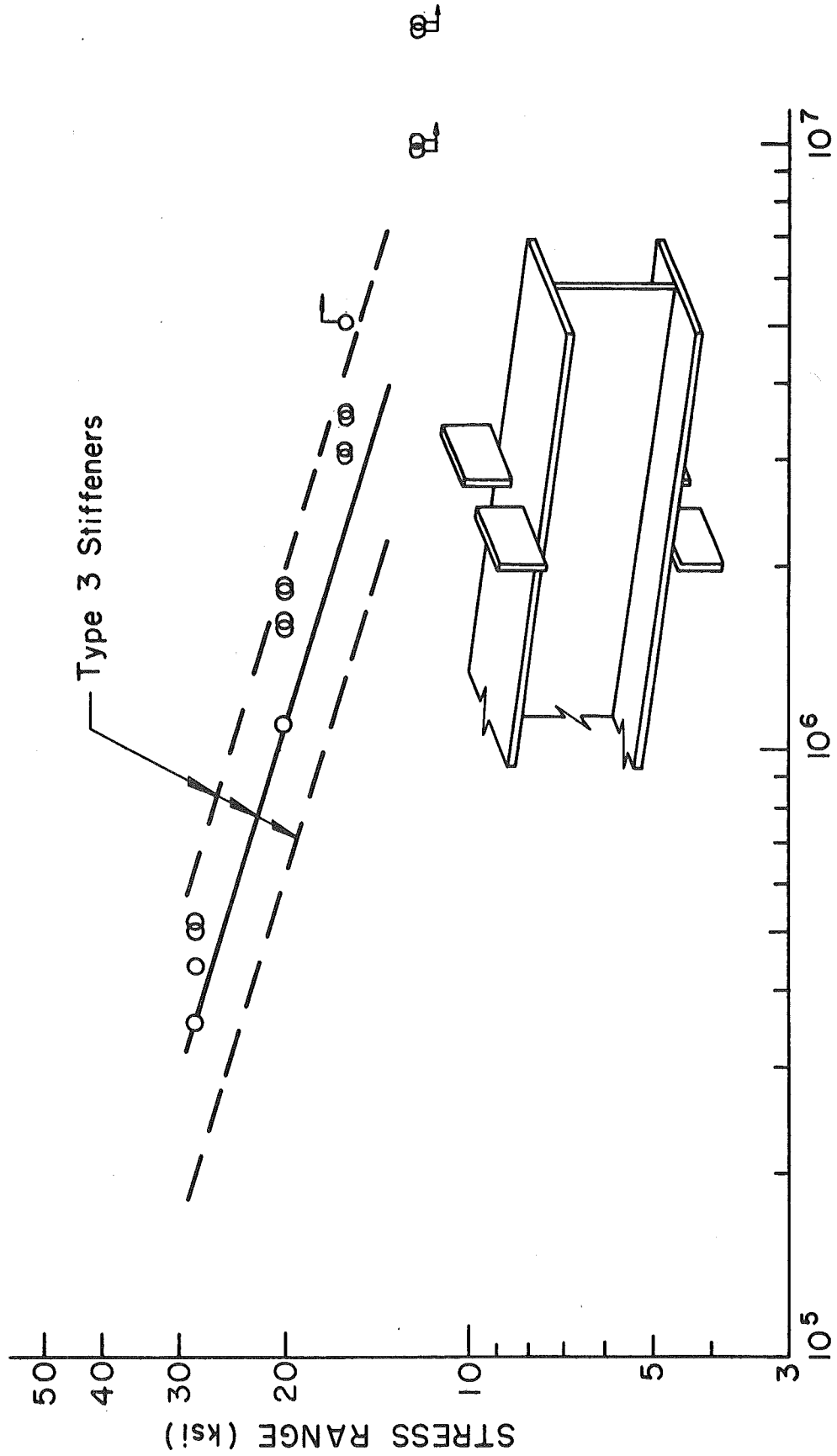


Fig. 40 S-N Plot for 1/4 in. Attachments

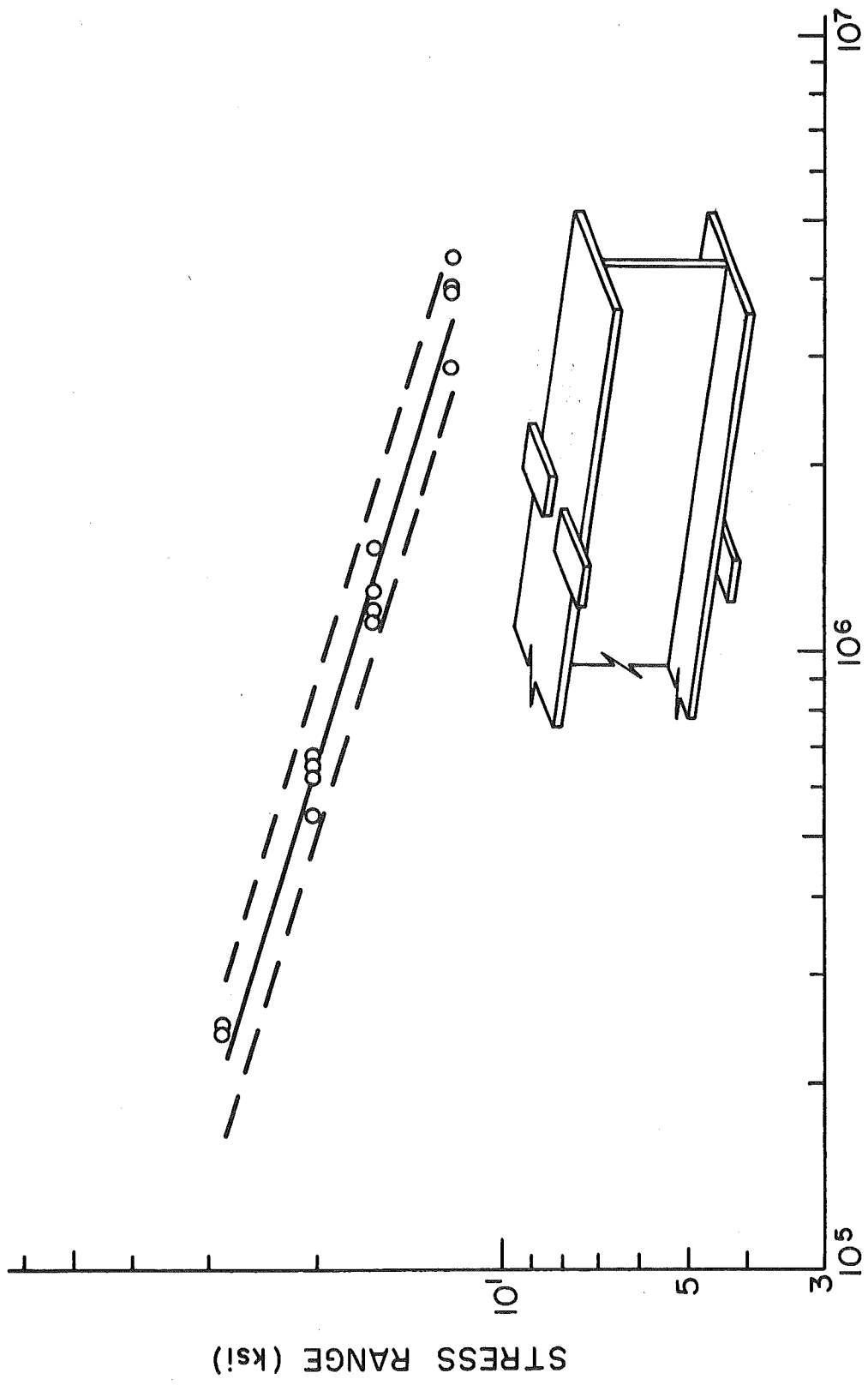


Fig. 41 S-N Plot for 2 in. Attachments

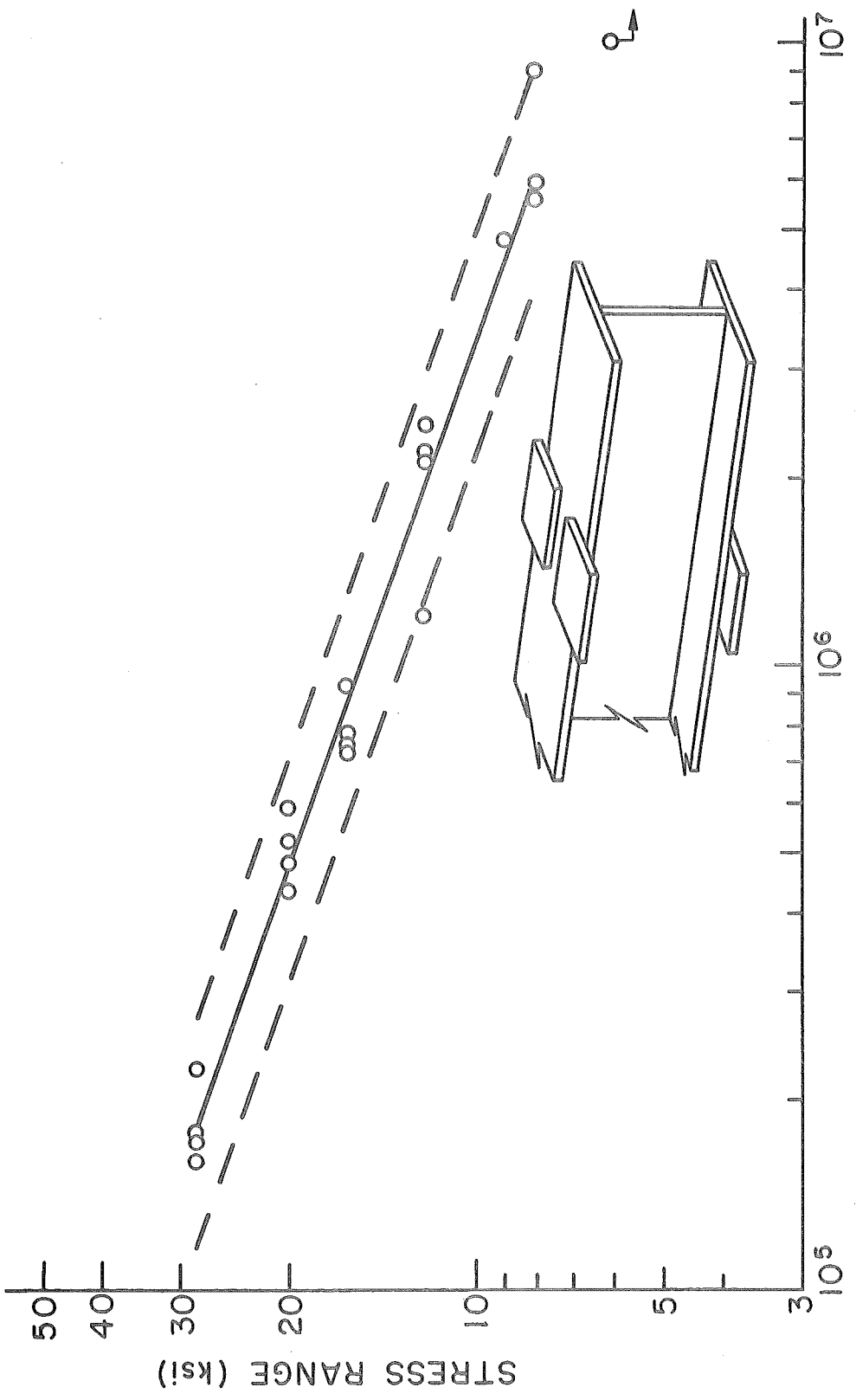


Fig. 42 S-N Plot for 4 in. Attachments Welded Longitudinally

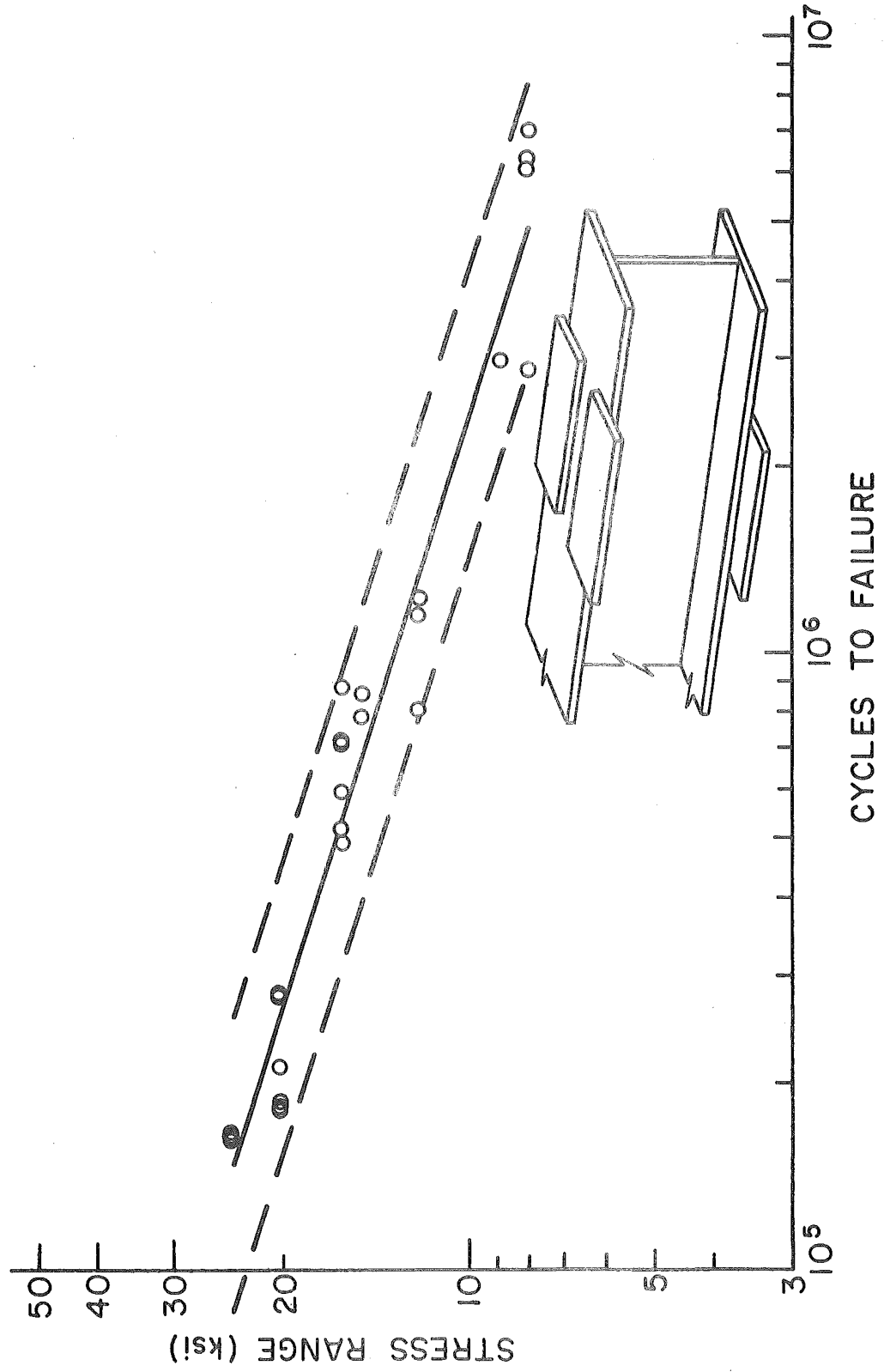


Fig. 43 S-N Plot for 8 in. Attachments

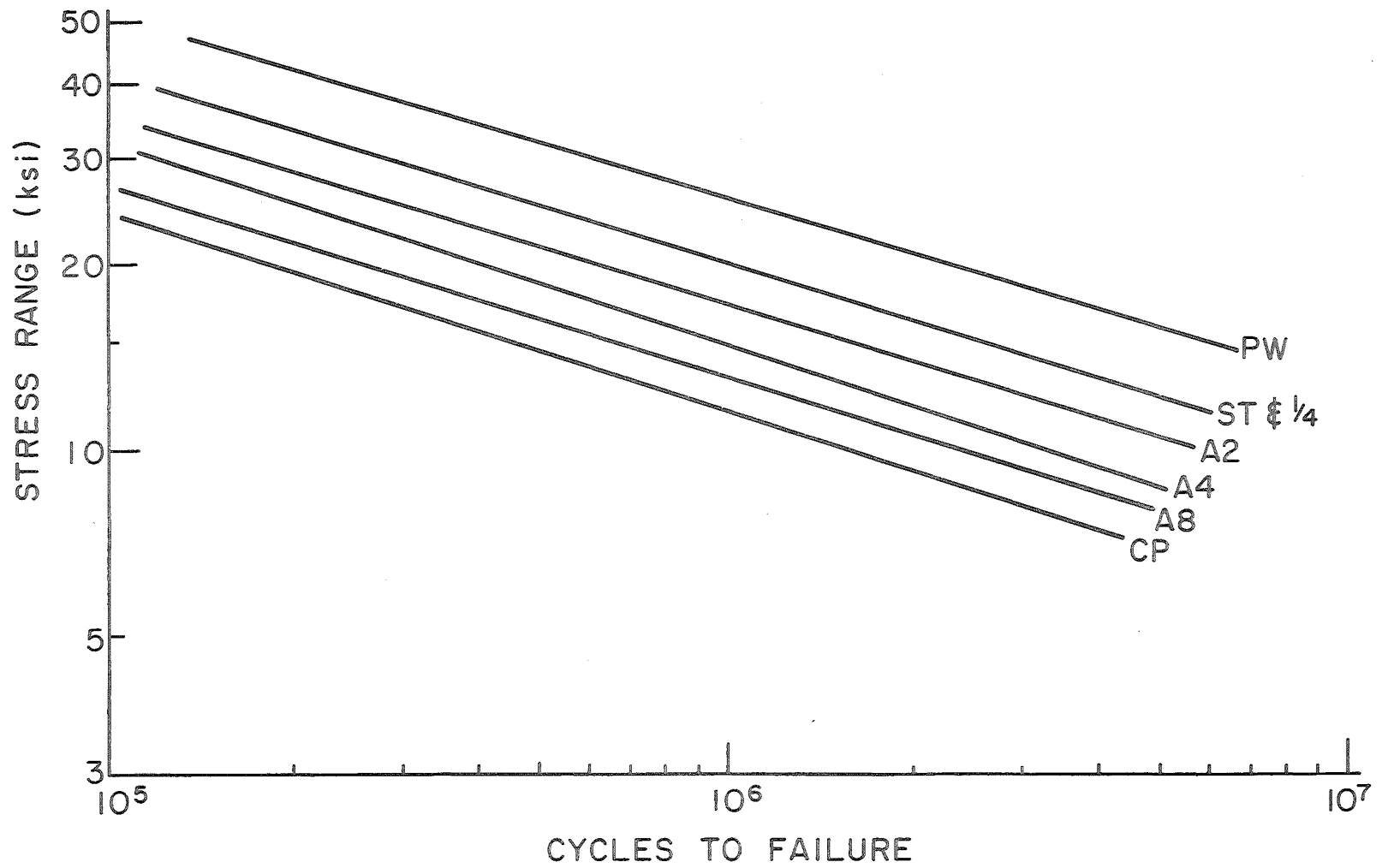


Fig. 44 Summary of S-N Plots for Flange Attachments and Transverse Stiffeners

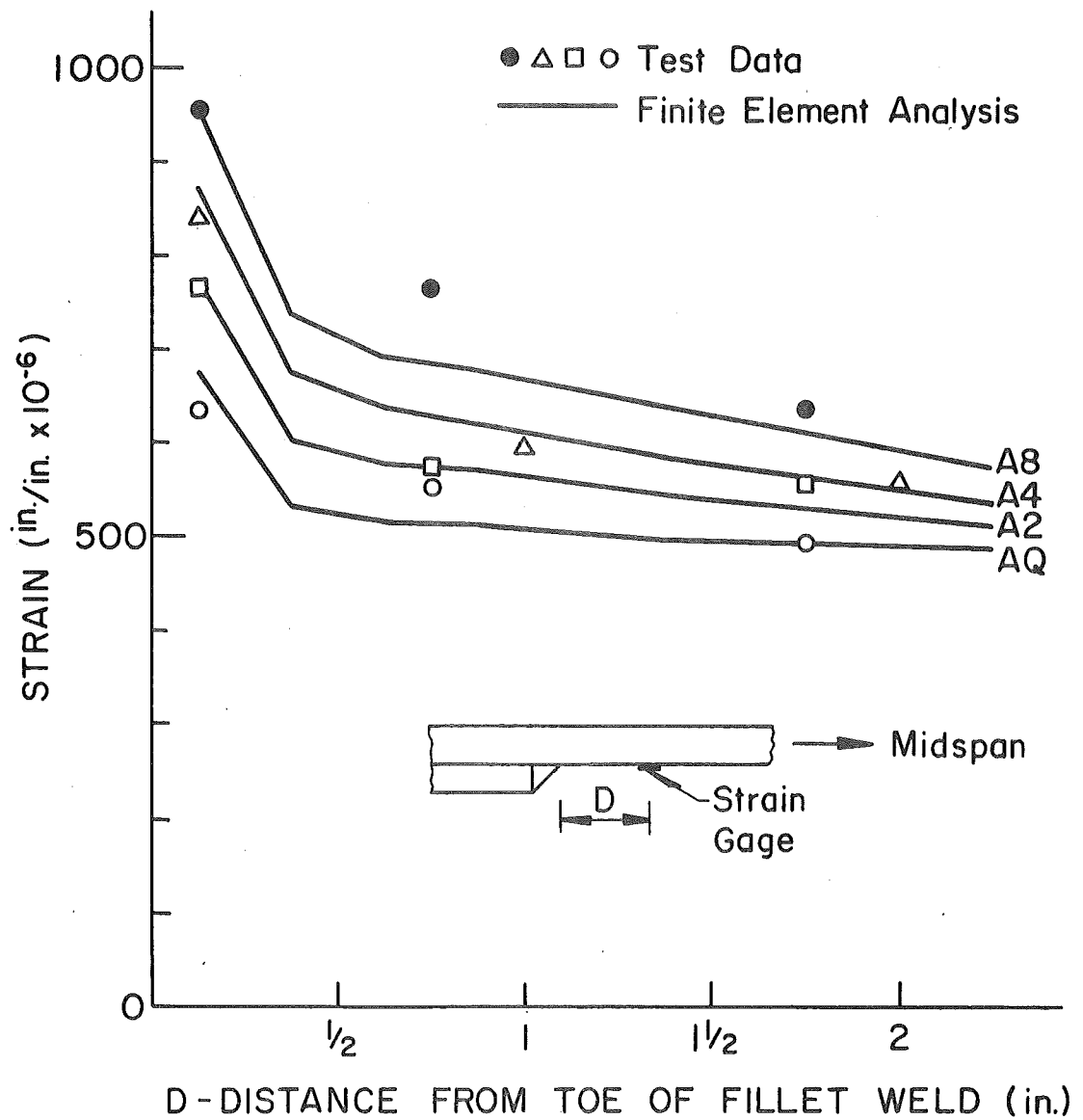


Fig. 45 Strain Distribution in Beam Flange near the Toe of Transverse Weldment of Attachment

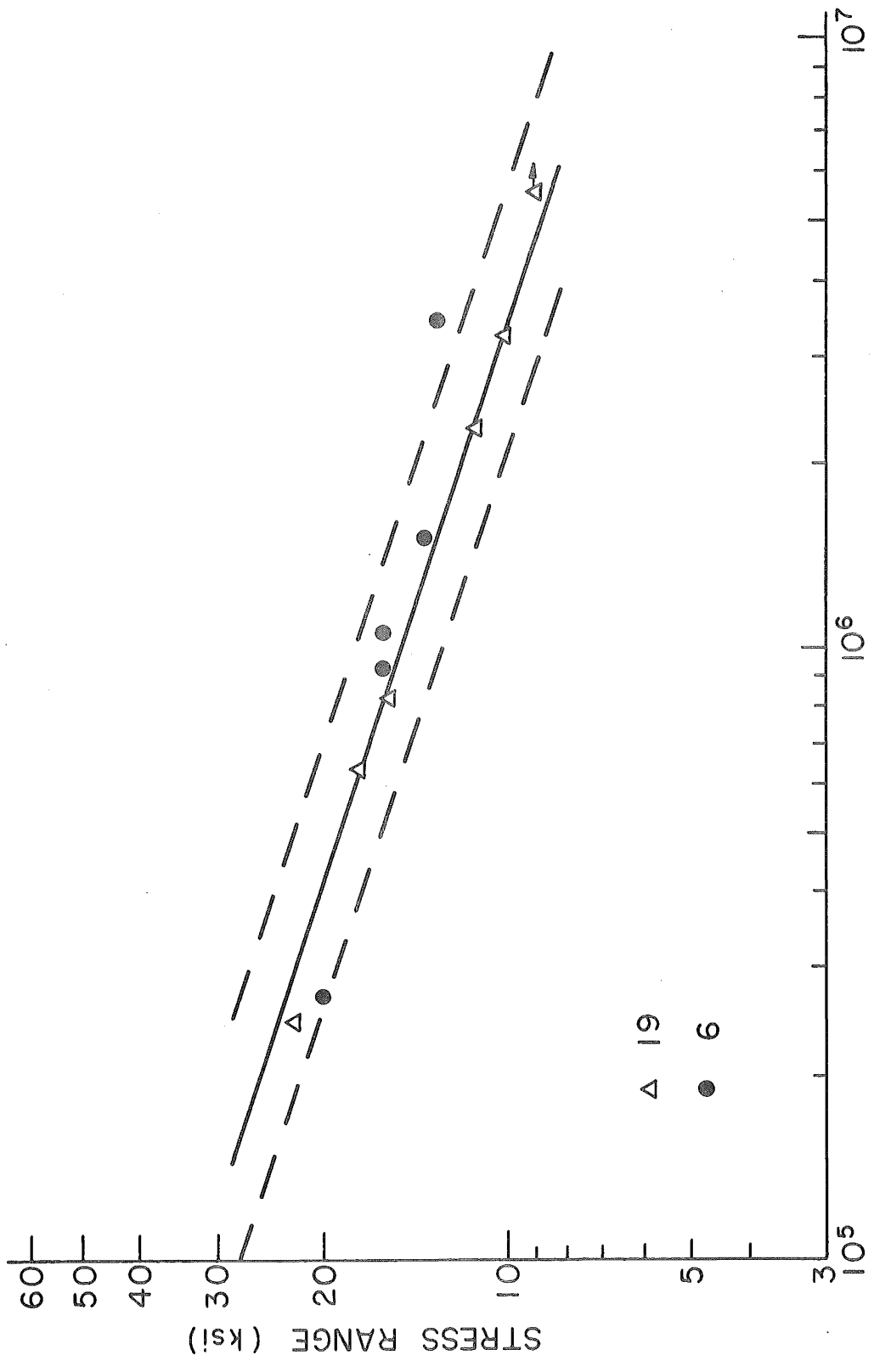


Fig. 46 Comparison of Present Study with Previous Work, 4 in Attachments

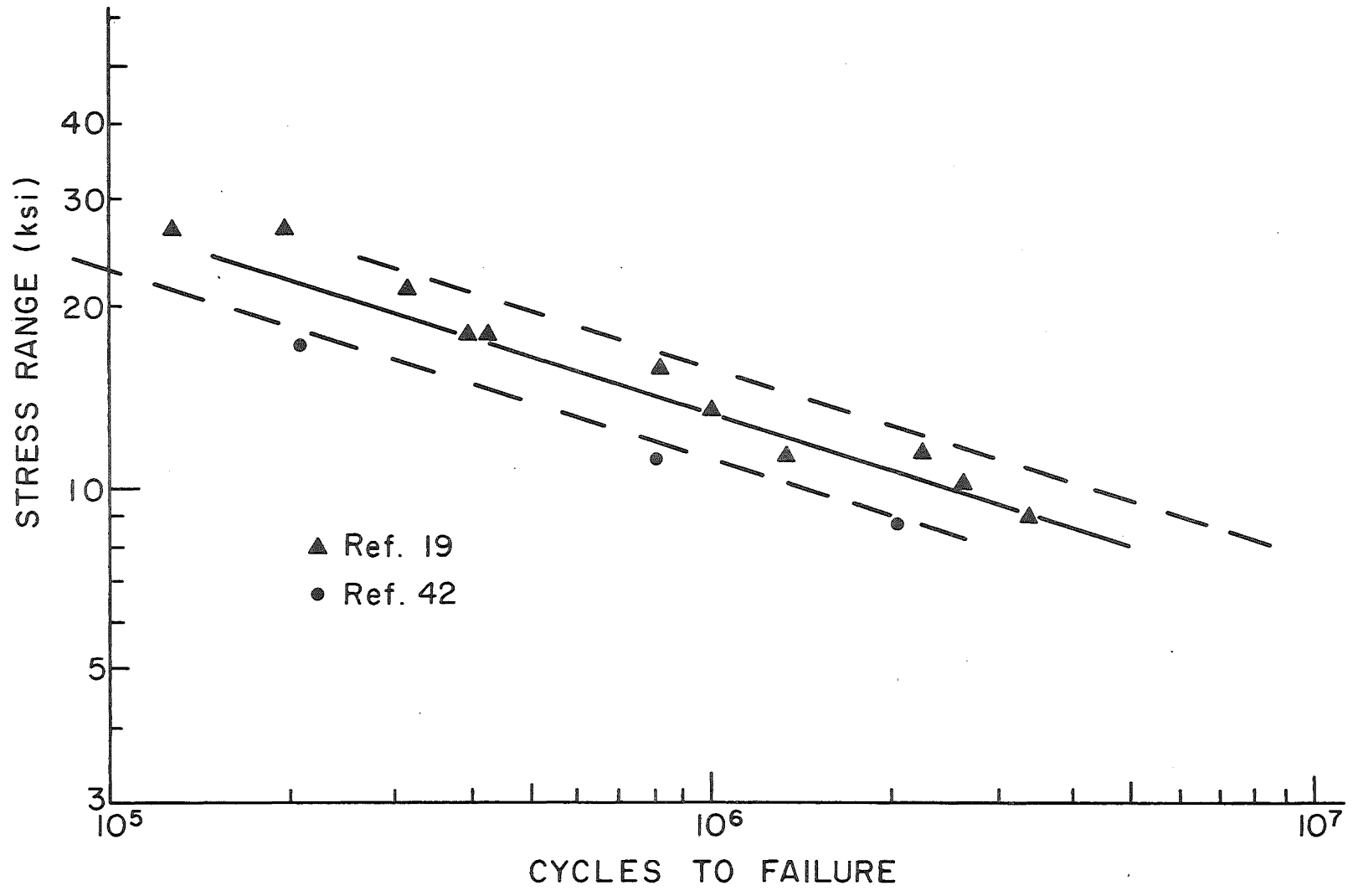


Fig. 47 Comparison of Present Study with Previous Work, 8 in. Attachments

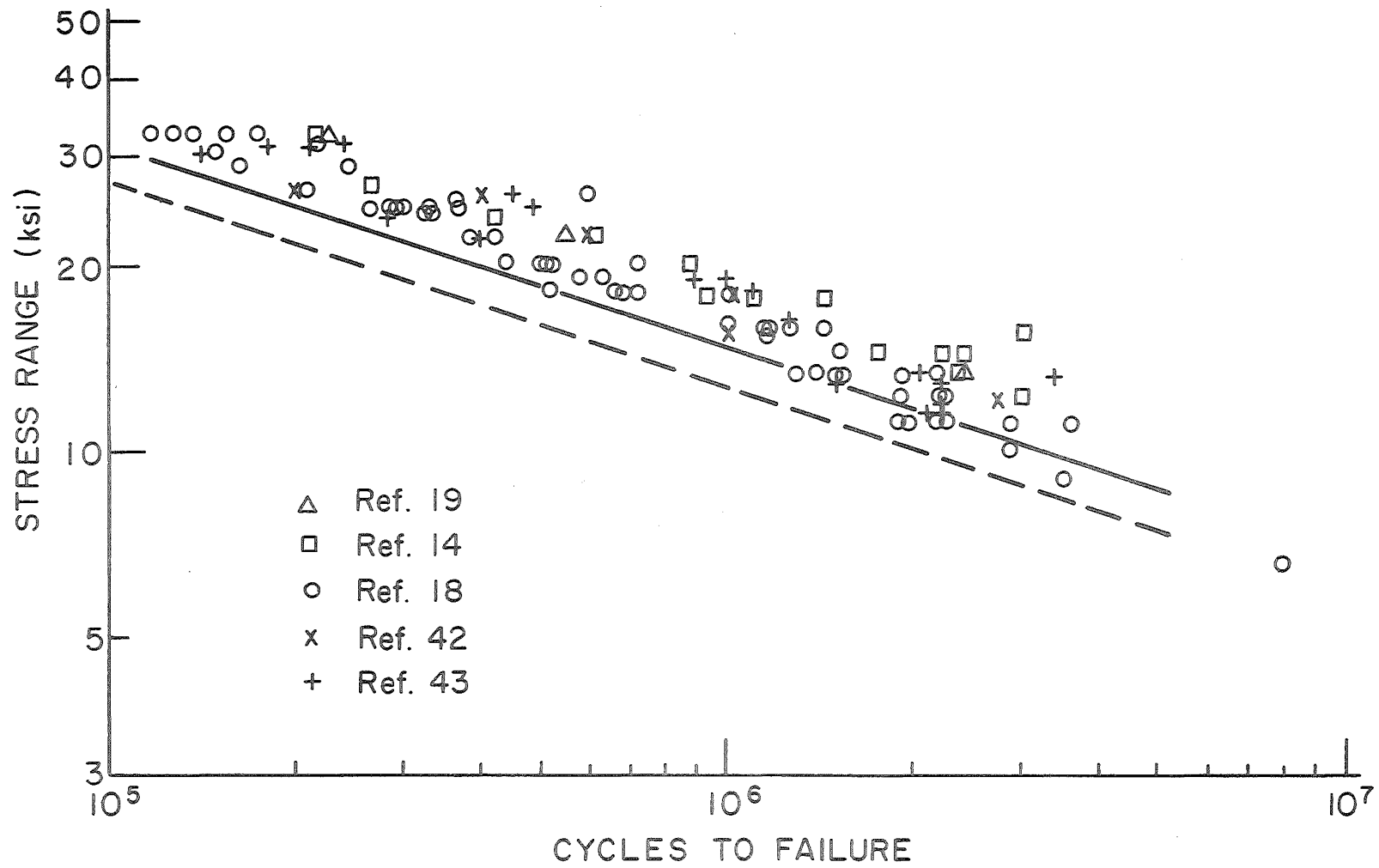


Fig. 48 Comparison of Previous Test Data of 6 in. Attachments with Results of 4 in. Attachments

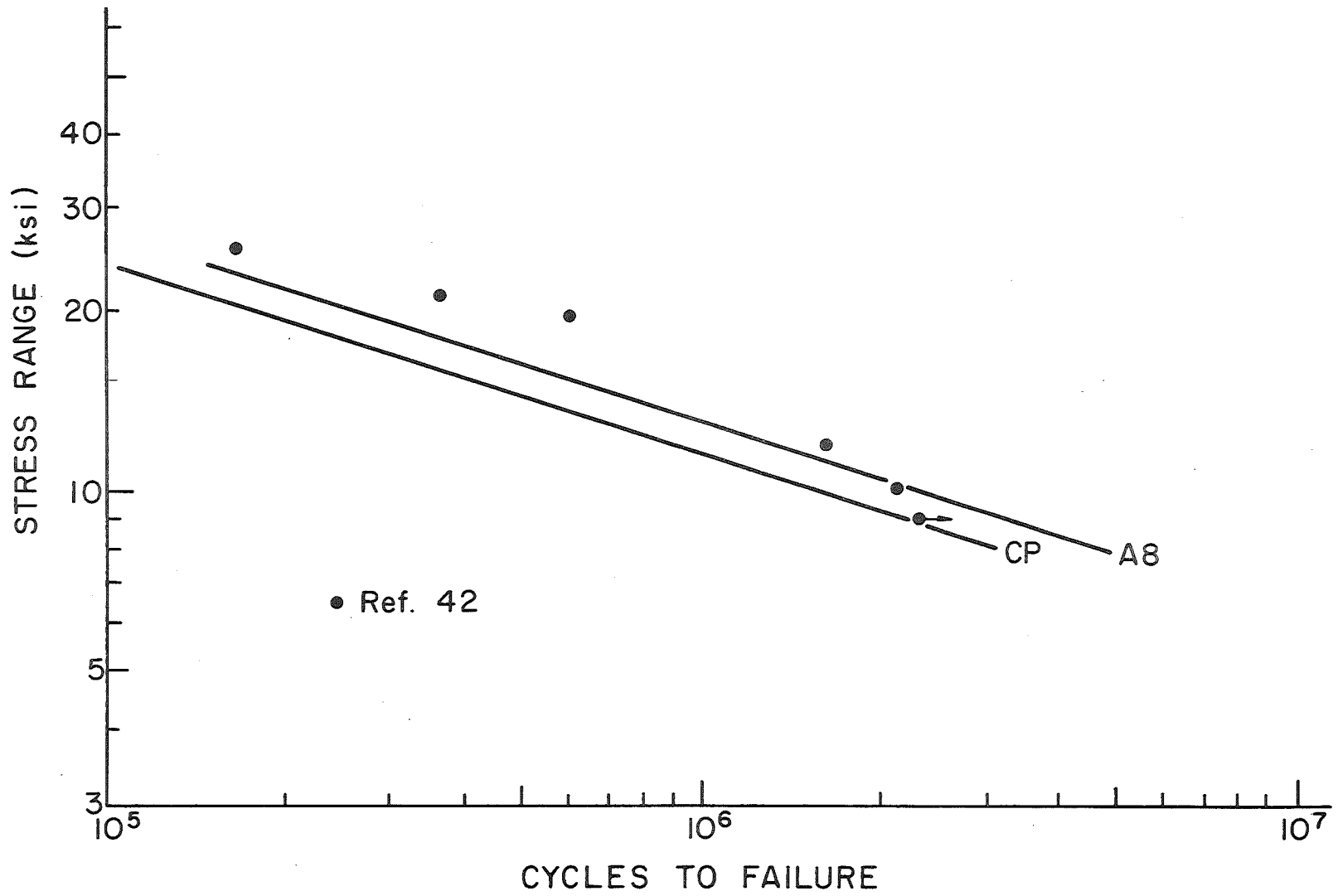


Fig. 49 Comparison of Previous 10 in. Groove-Welded Attachments with 8 in. Attachments and Cover Plated Beams

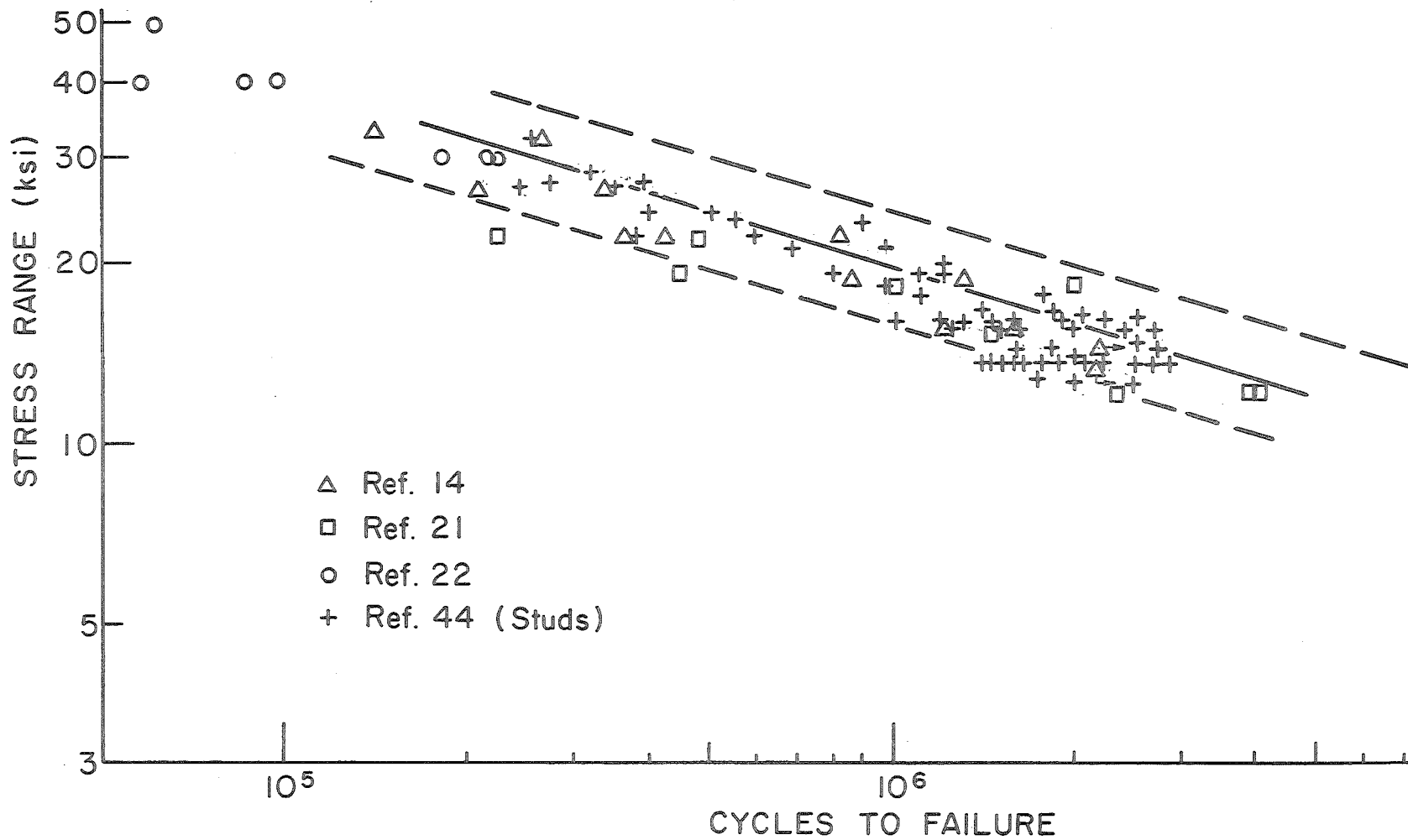


Fig. 50 Comparison of Previous Non-Load Carrying Fillet-Welded Joints with Stiffeners and 1/4 in. Attachments

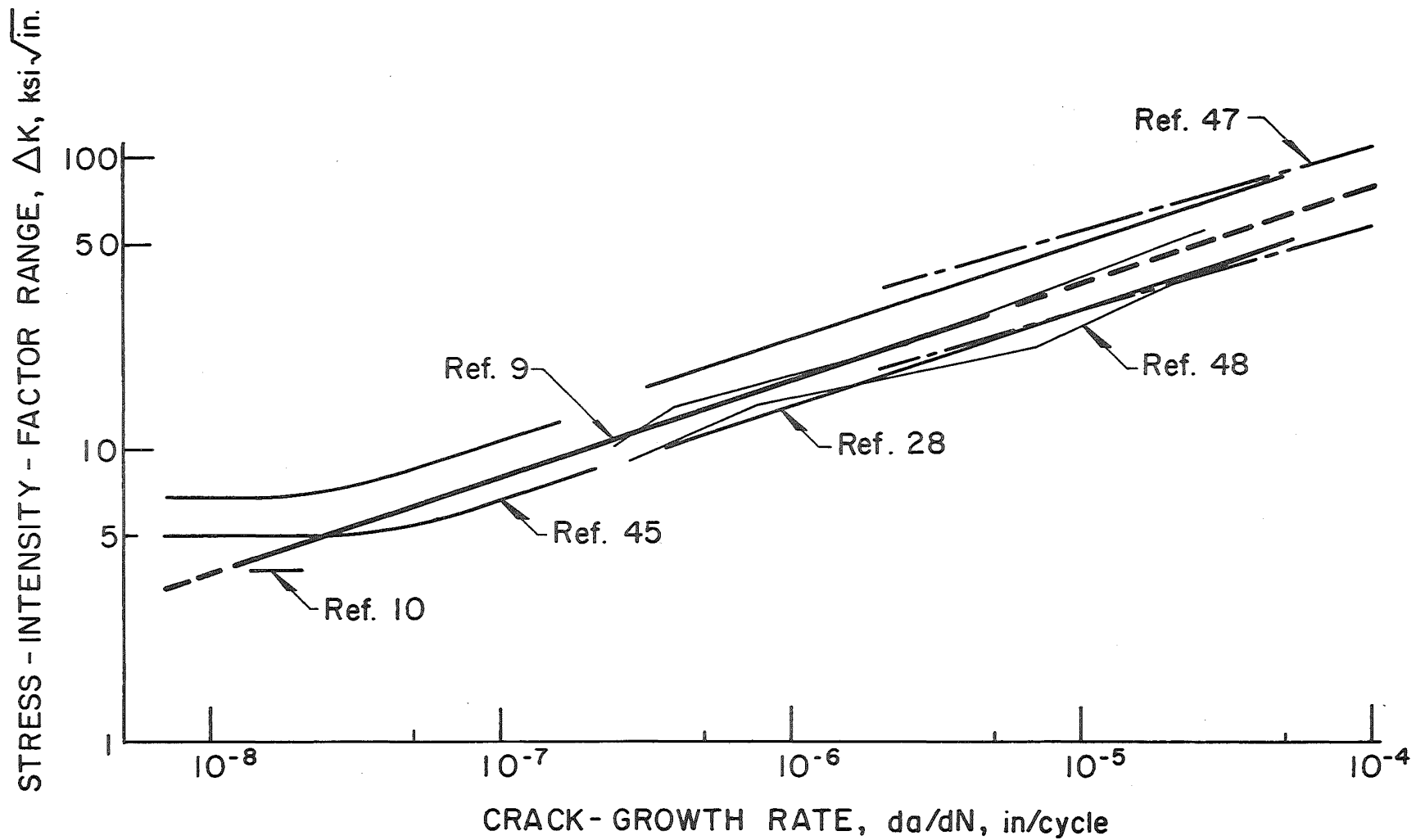


Fig. 51 Crack Growth Rates in Fatigue

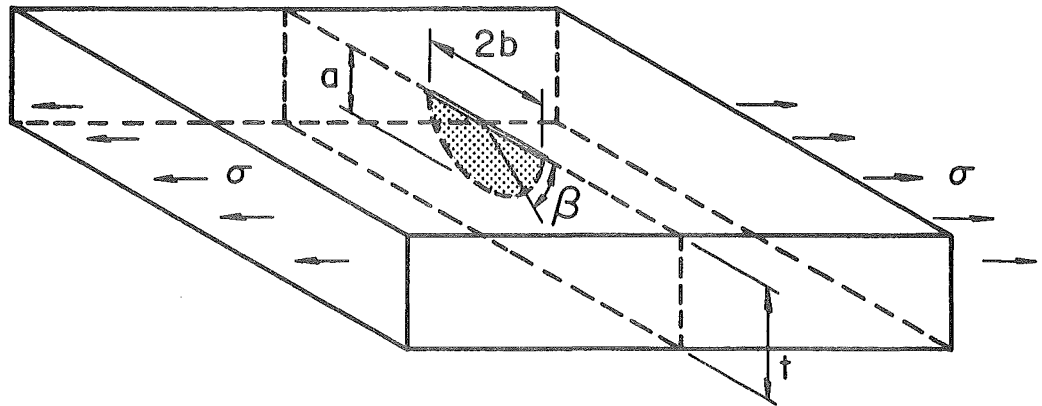


Fig. 52a Part-through crack in a flat plate

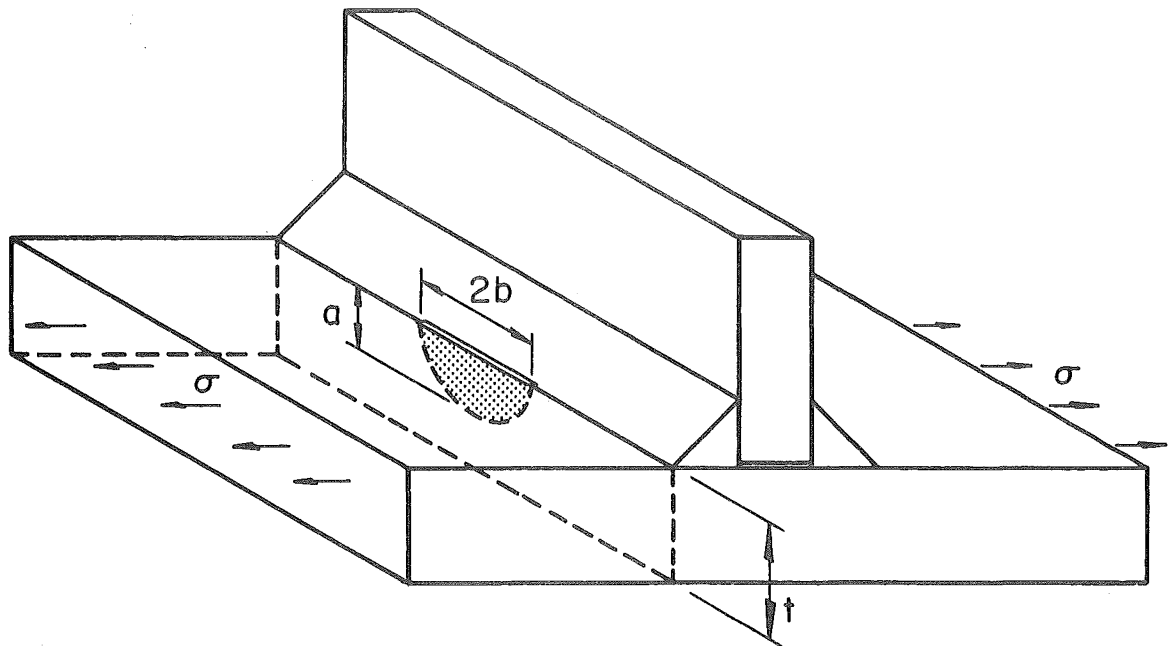


Fig. 52b Part-through crack at the toe of a non-load carrying fillet weld

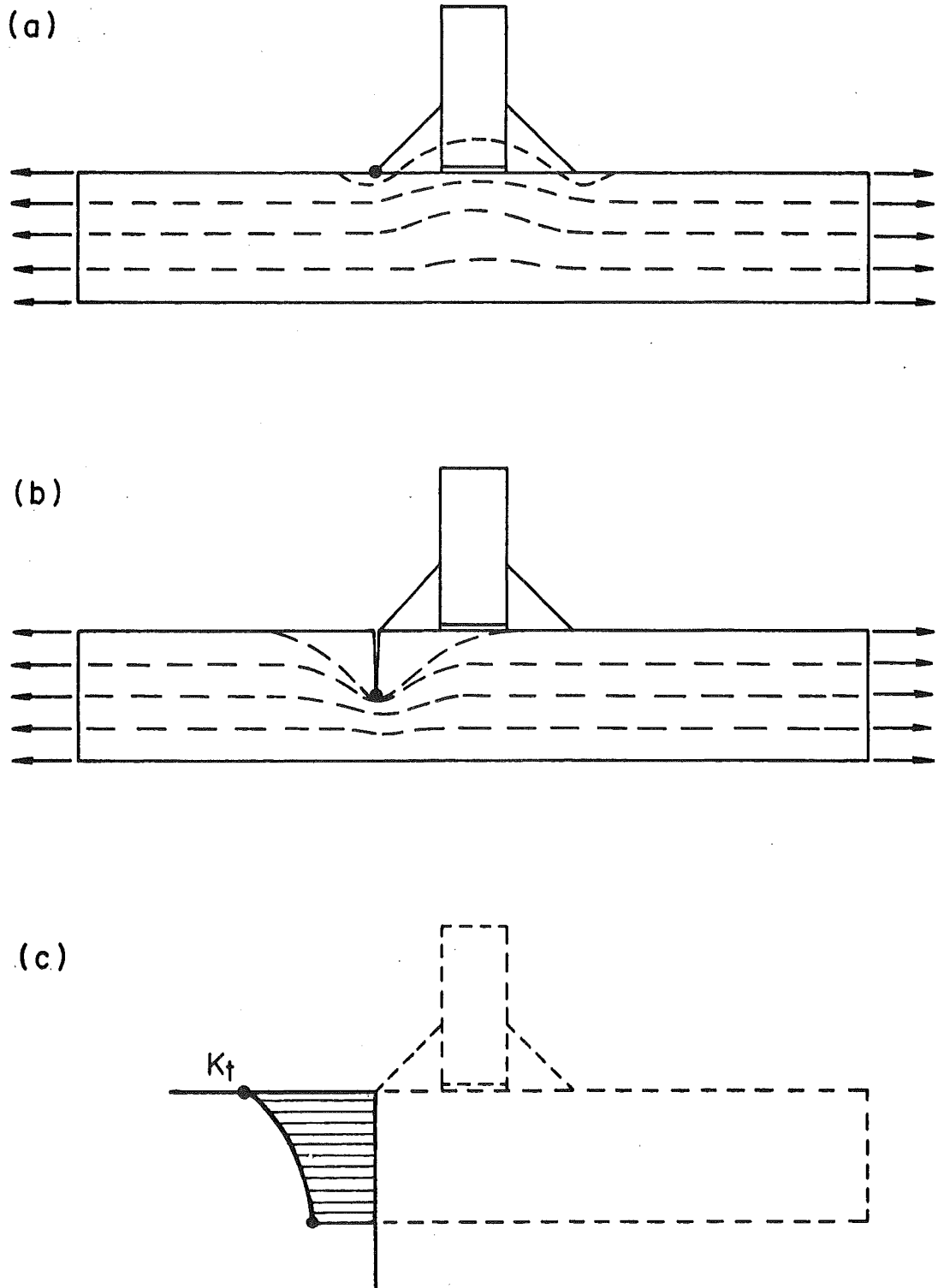


Fig. 53 Correction function for the applied stress field

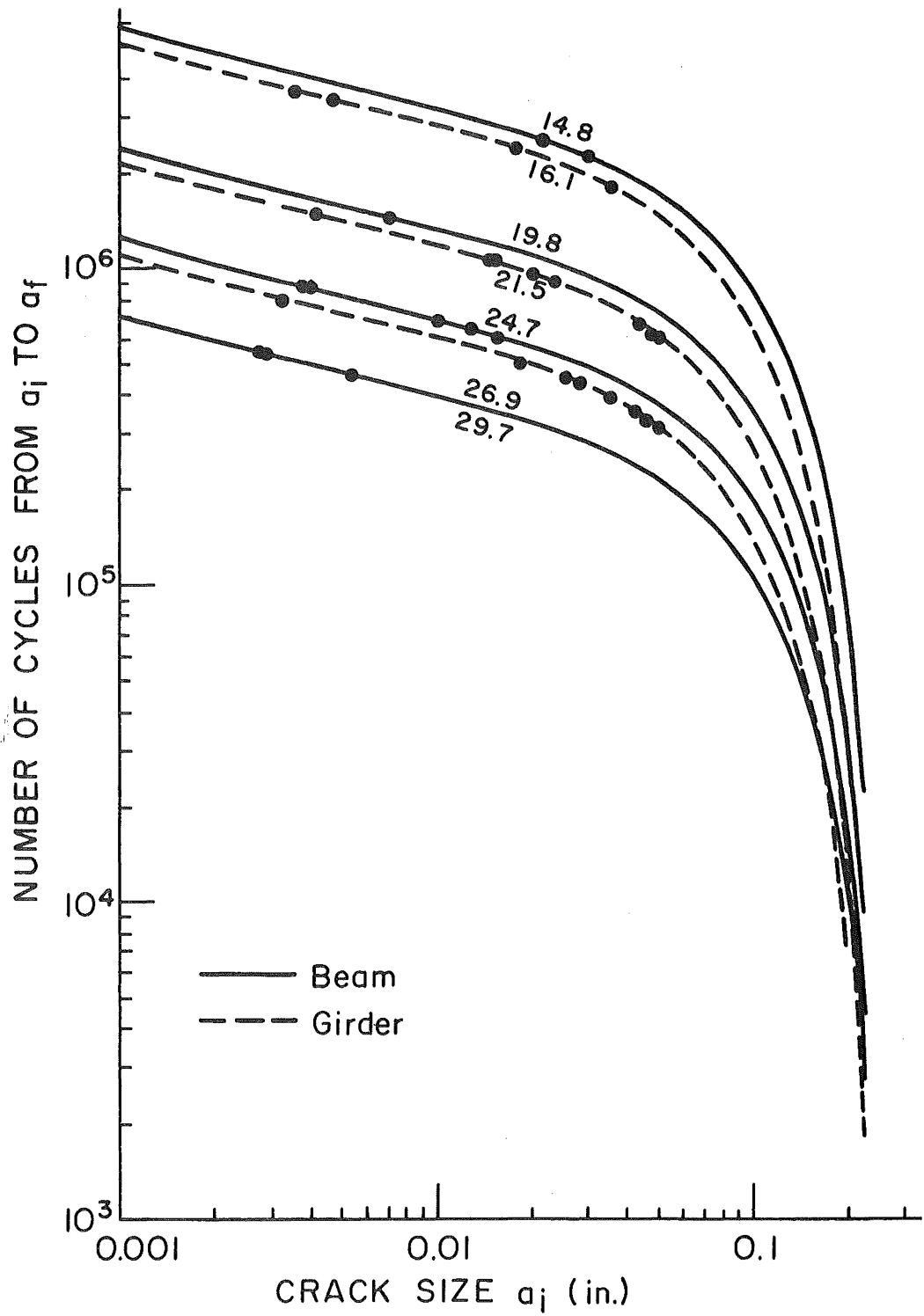


Fig. 54 Propagation of a Part-Through Crack at Type 1 Stiffeners

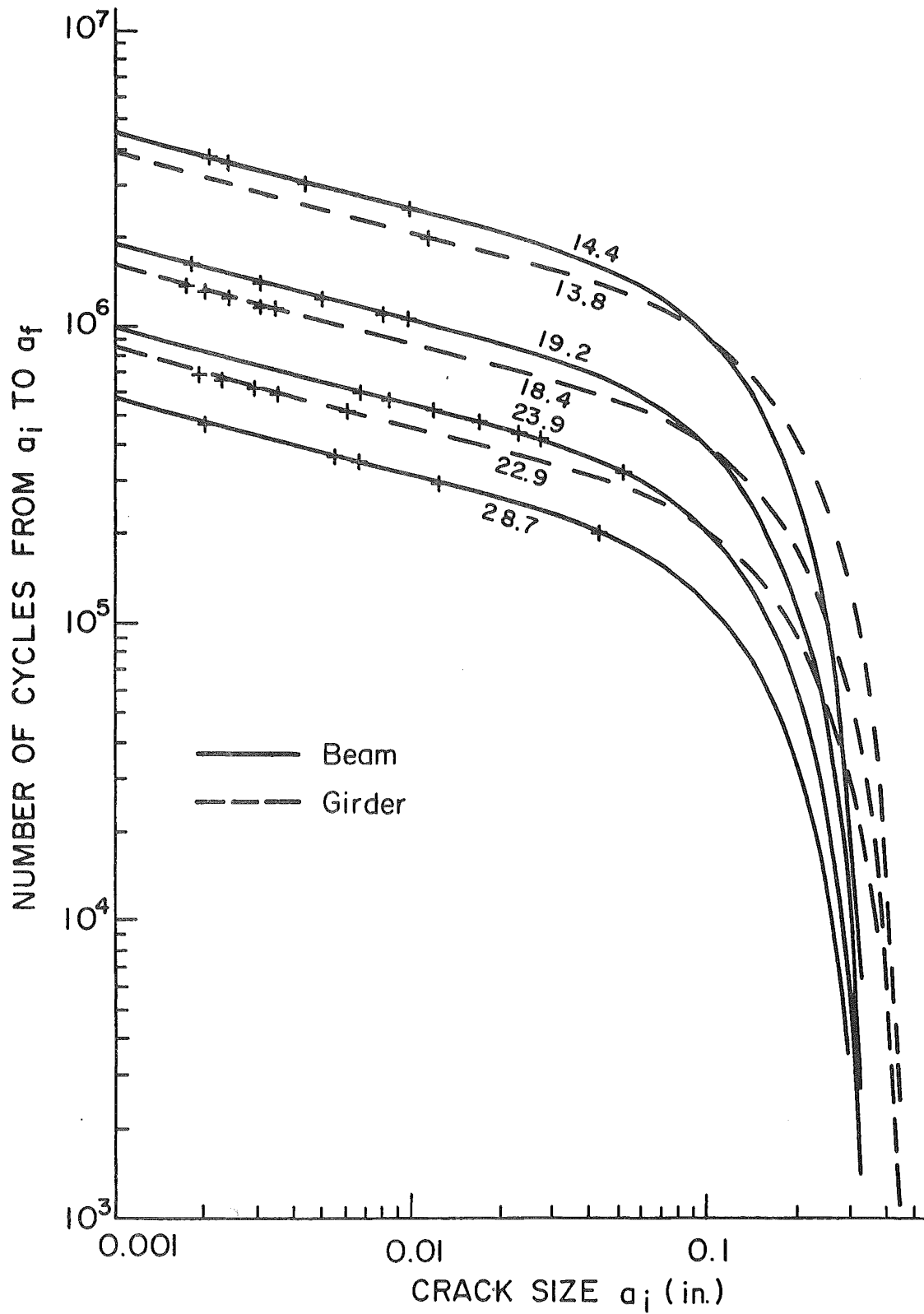


Fig. 55 Propagation of a Part-Through Crack at Type 3 Stiffeners

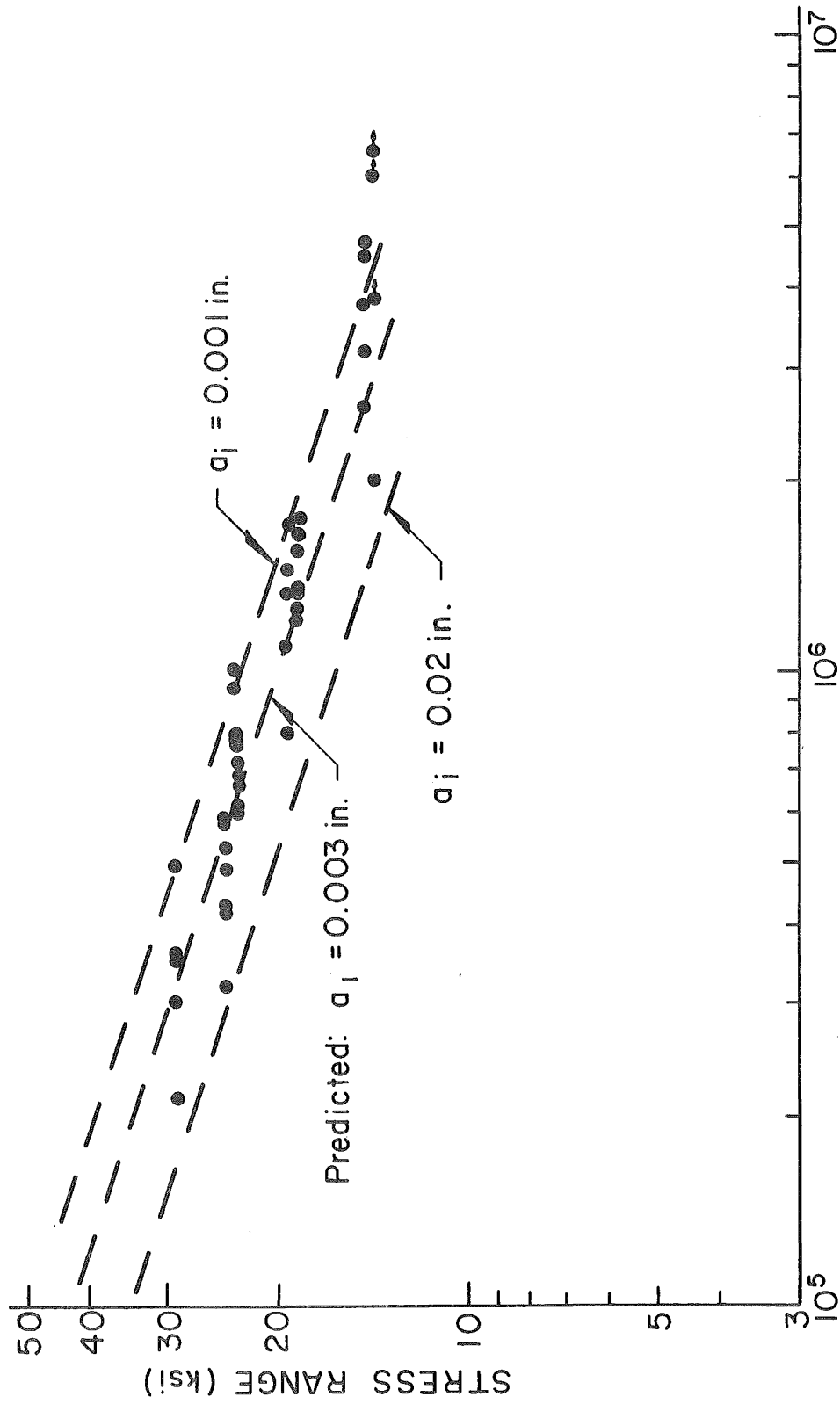


Fig. 56 Comparison of Predicted Fatigue Life with Type 3 Stiffener Test Data

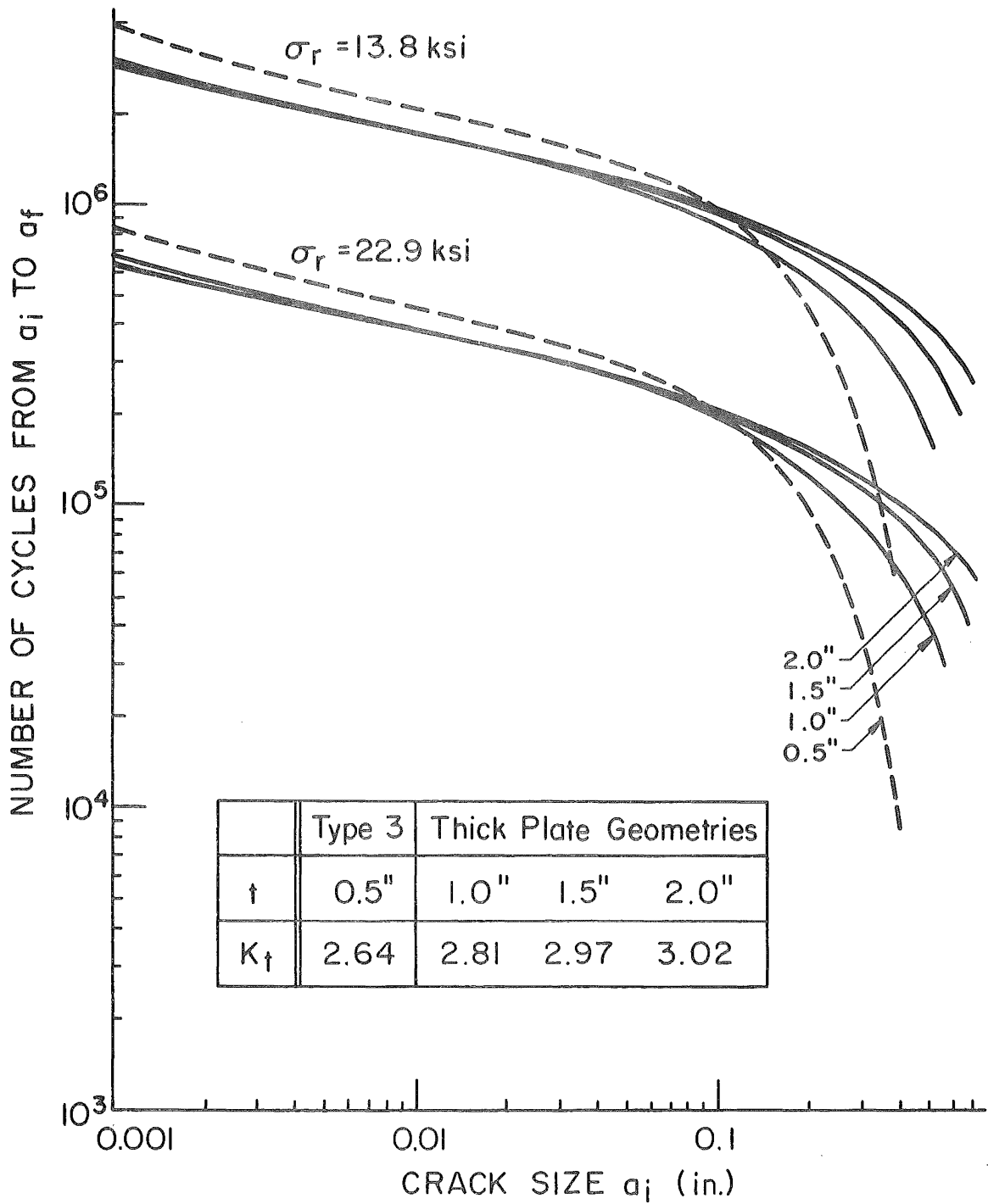


Fig. 57 Effect of Plate Thickness on the Propagation of a Part-Through Crack

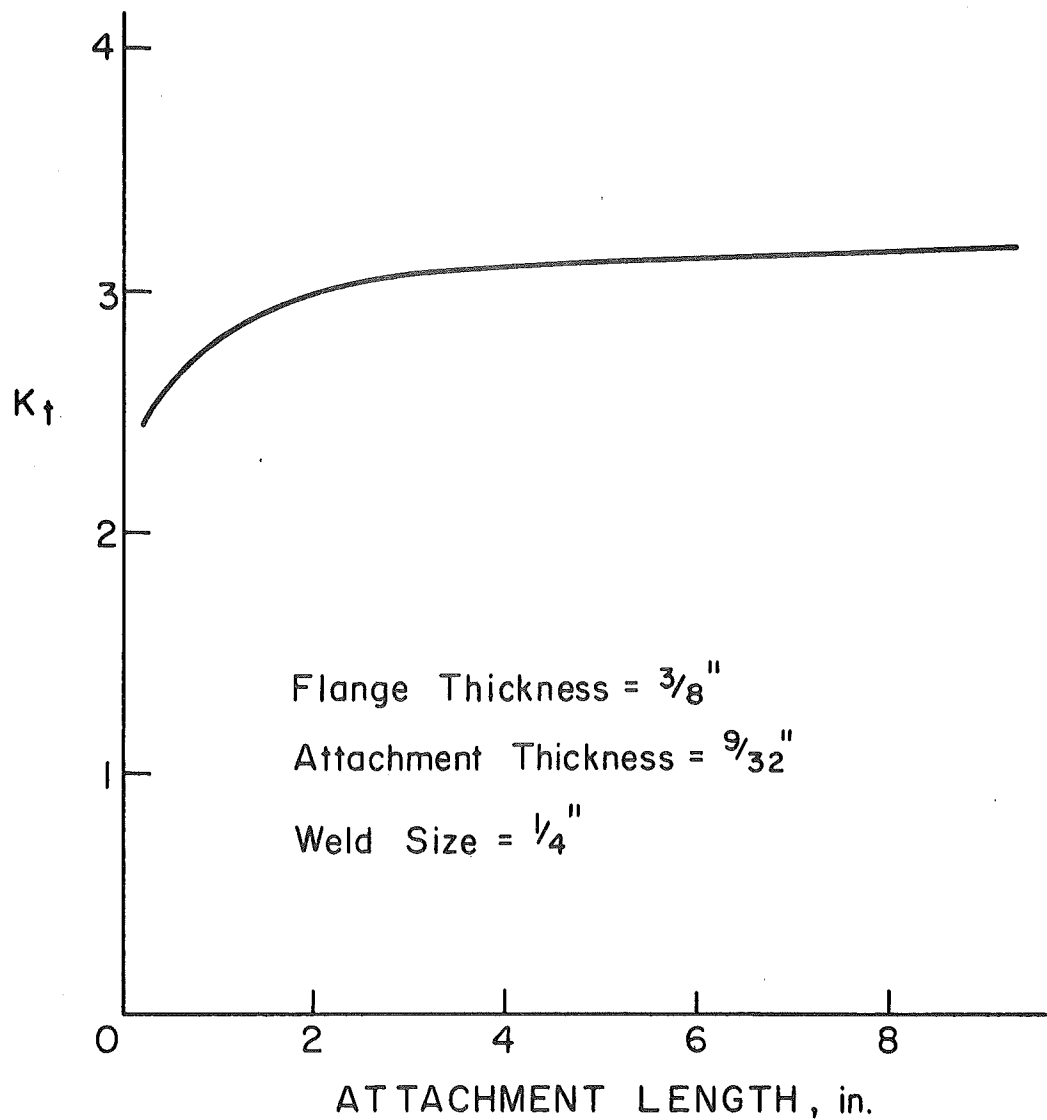


Fig. 58 Effect of Attachment Length on Stress Concentration Factor K_t

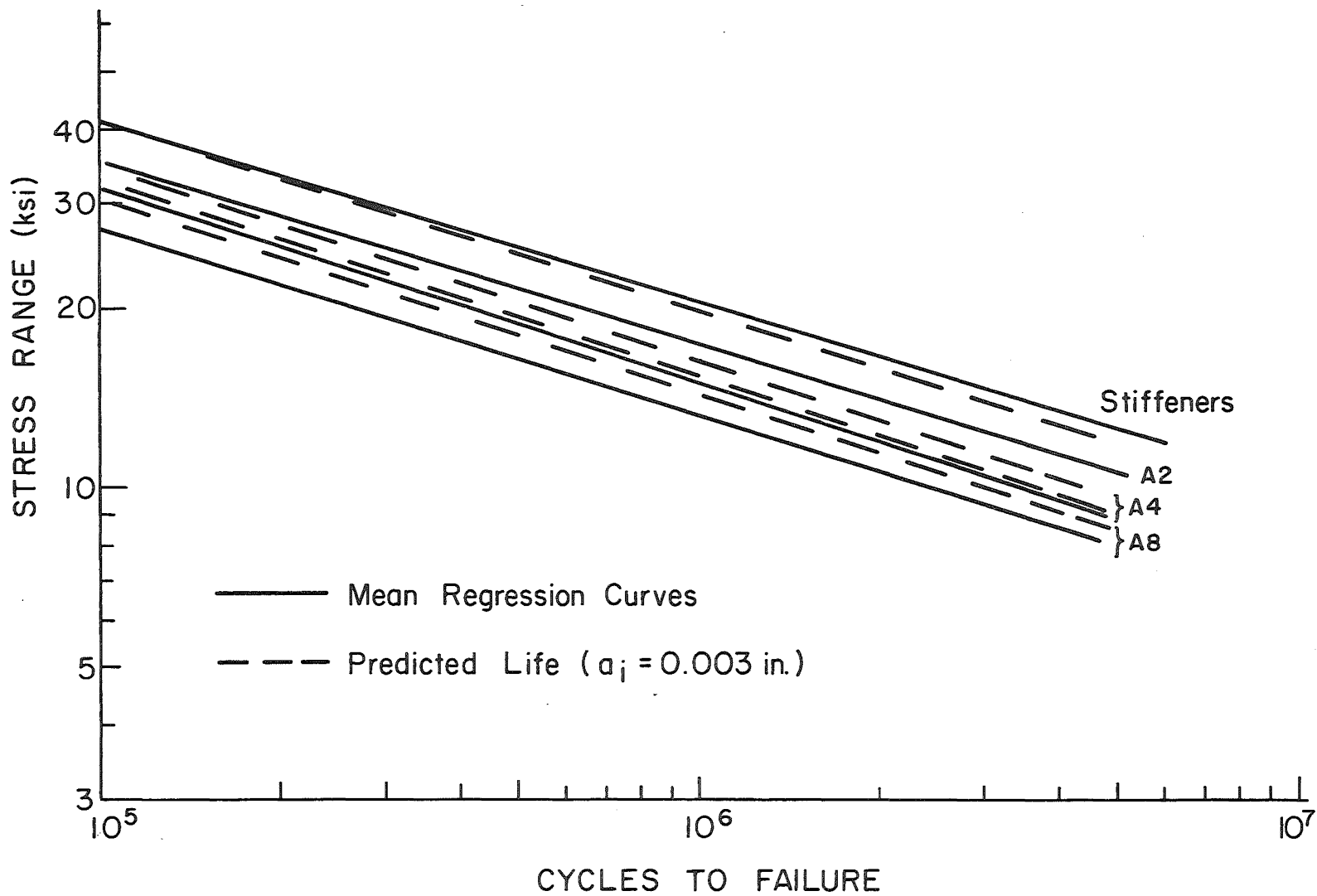
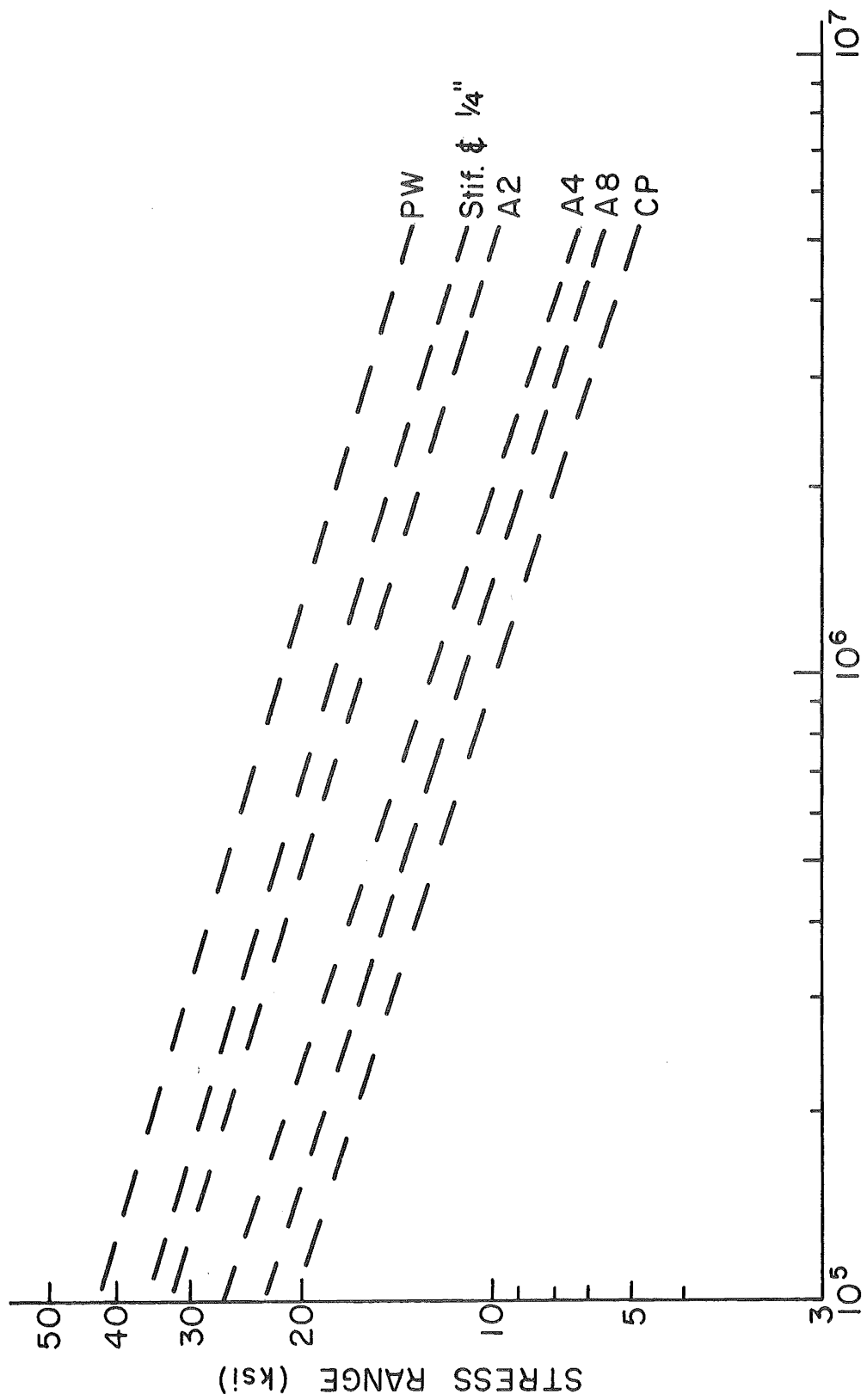


Fig. 59 Predicted Mean Fatigue Strength Compared with Mean Regression Lines, Flange Attachments



CYCLES TO FAILURE

Fig. 60 95% Confidence Limits for 95% Survival

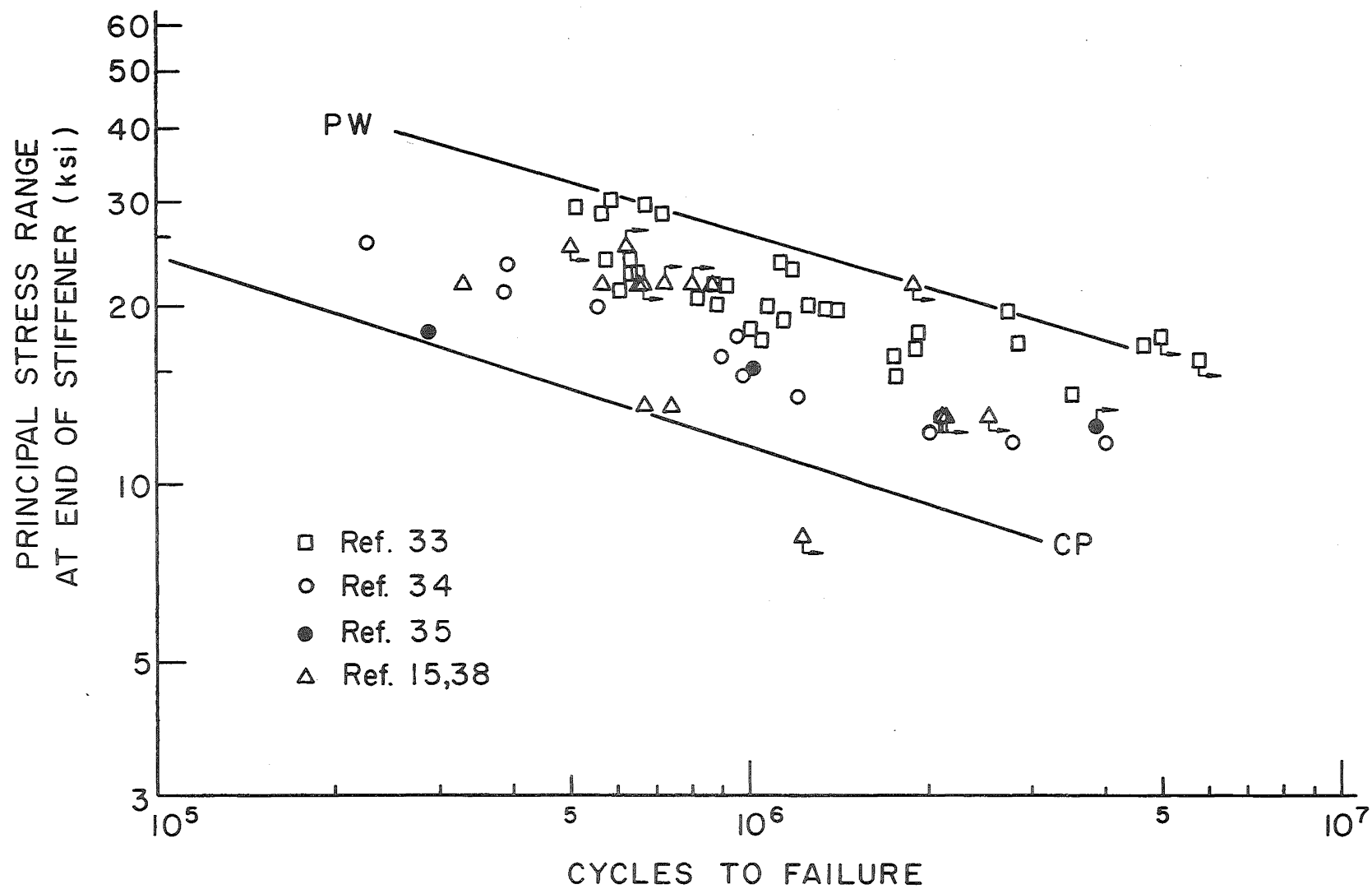


Fig. A1 S-N plot for Type 1 stiffeners welded to the web alone
Summary of previous fatigue test data

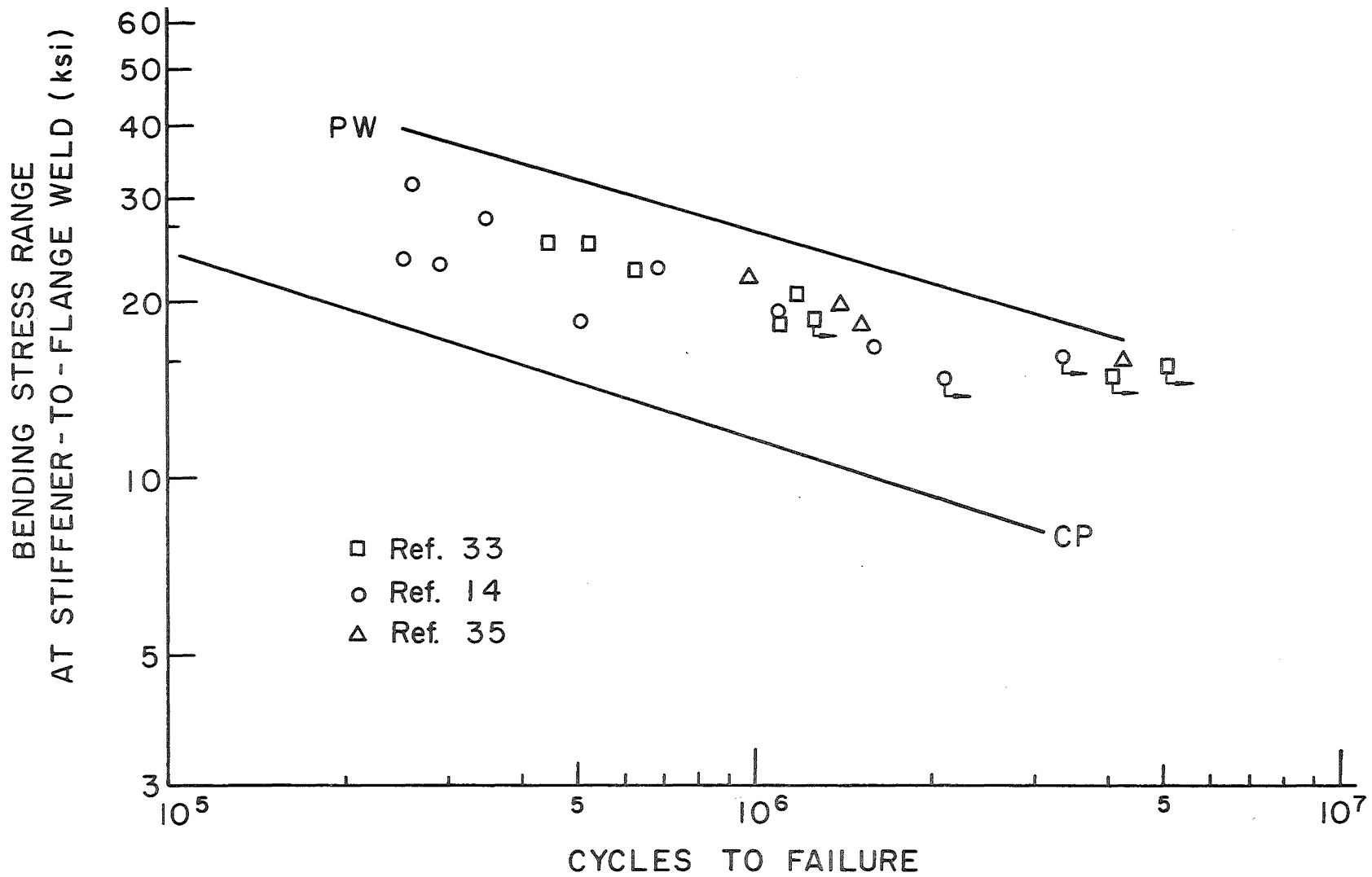


Fig. A3 S-N plot for Type 3 stiffeners welded to the web and flanges
 Summary of previous fatigue test data

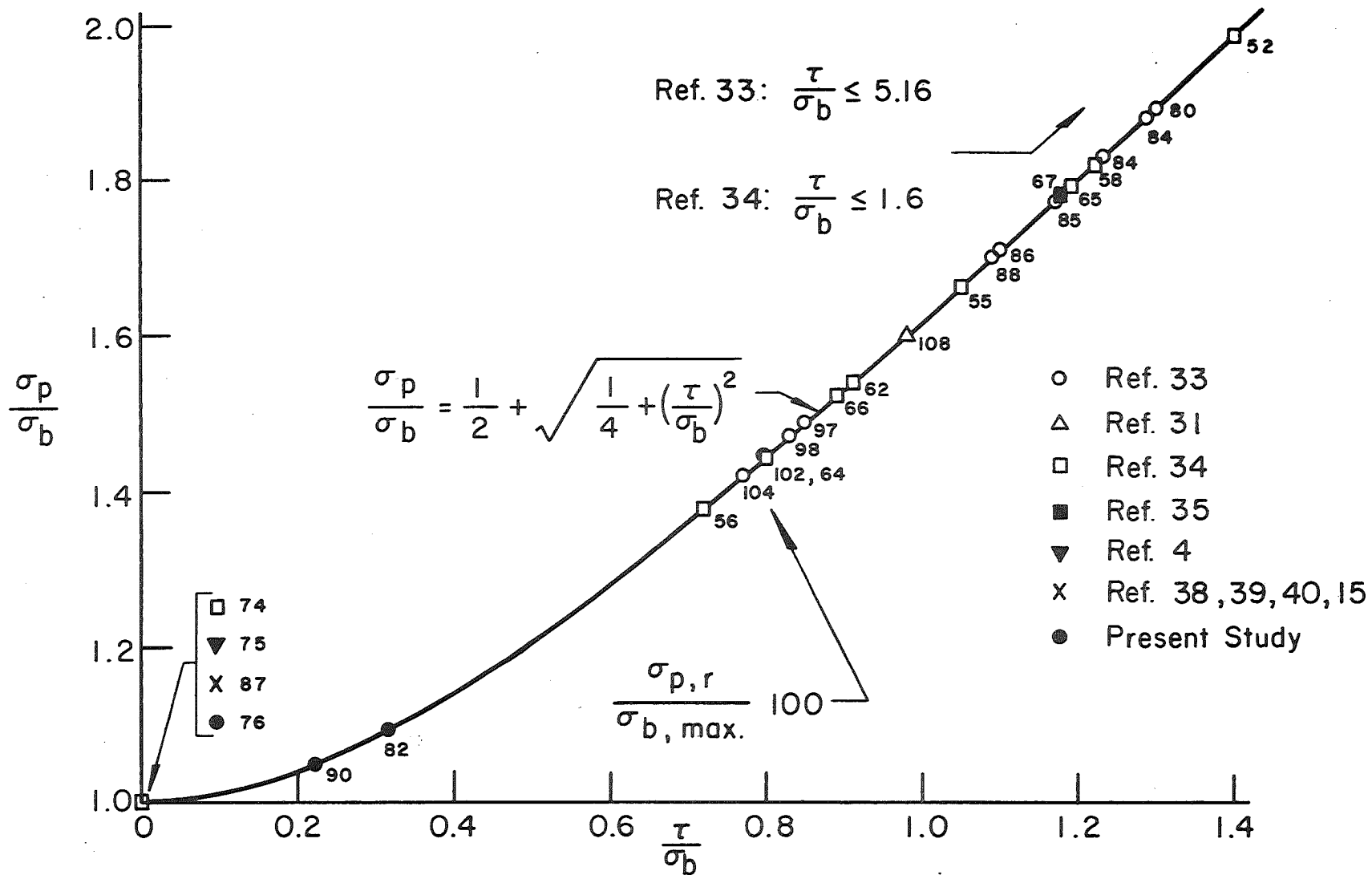
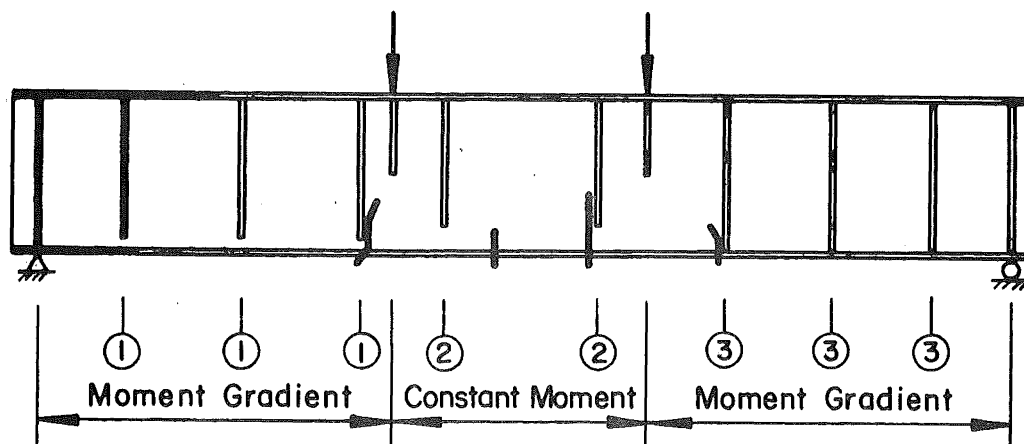


Fig. A4 Ratio of shear-to-bending stresses at the end of Type 1 stiffener-to-web weld



Crack type	At stiff. type	Comment
1	1	Initiated at the toe of the stiffener-to-web weld. Moment gradient region.
2	2	Initiated at the toe of the stiffener-to-web weld. Constant moment region.
3	3	Initiated at the toe of the stiffener-to-flange weld. Moment gradient region.
PW	-	Initiated at tack weld, porosity or repair of web-to-flange fillet weld.

Note

1. Some beams developed Type 1 cracks at the upper (compression) end of the stiffener-to-web weld.
2. Previous investigators reported cracks along the weld toe on the four web panel boundaries in thin-web girders subjected to severe fluctuating out of plane deformations of the web.

Fig. A5 Types of fatigue cracks

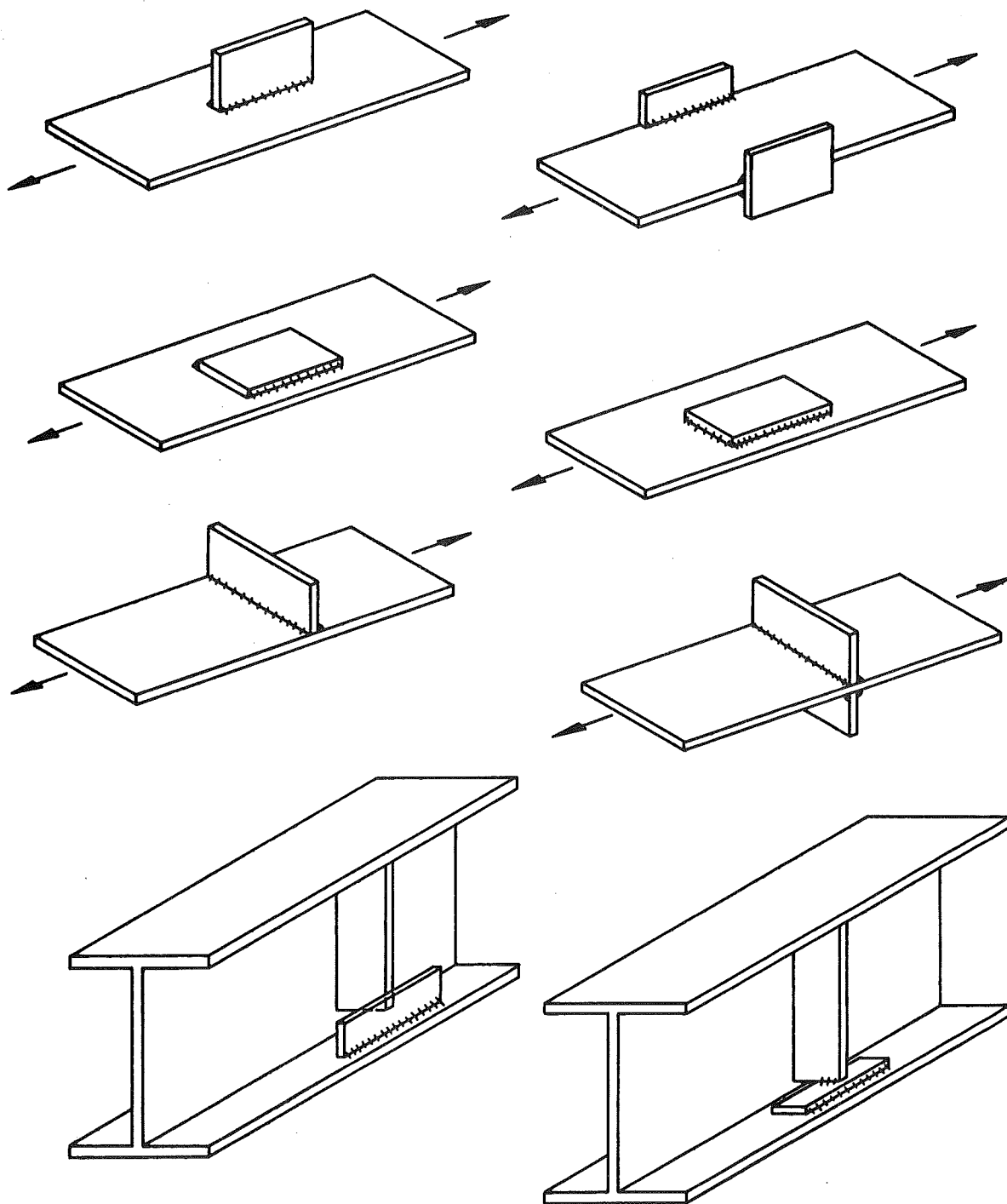


Fig. A6 Flange Attachment Details

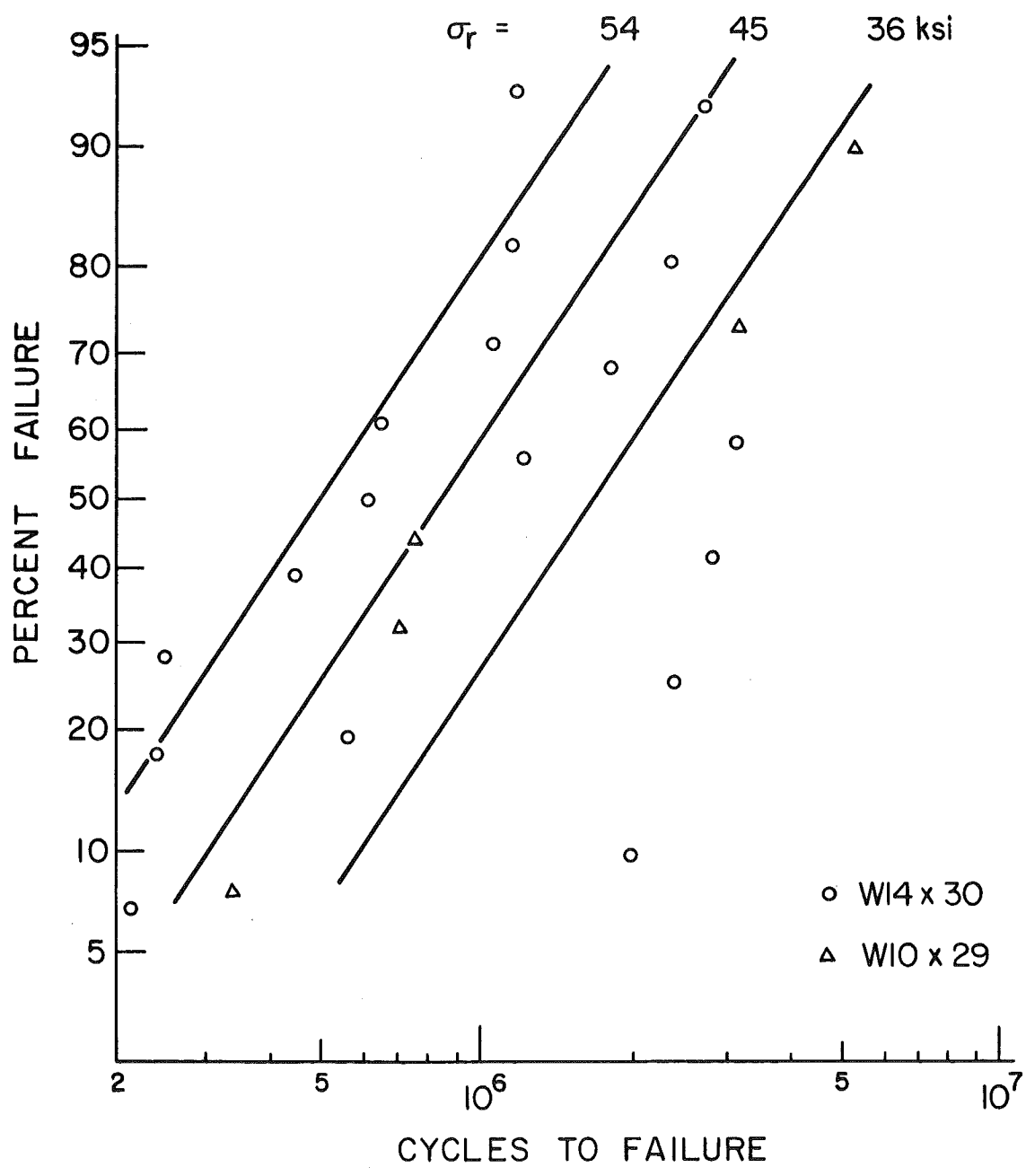
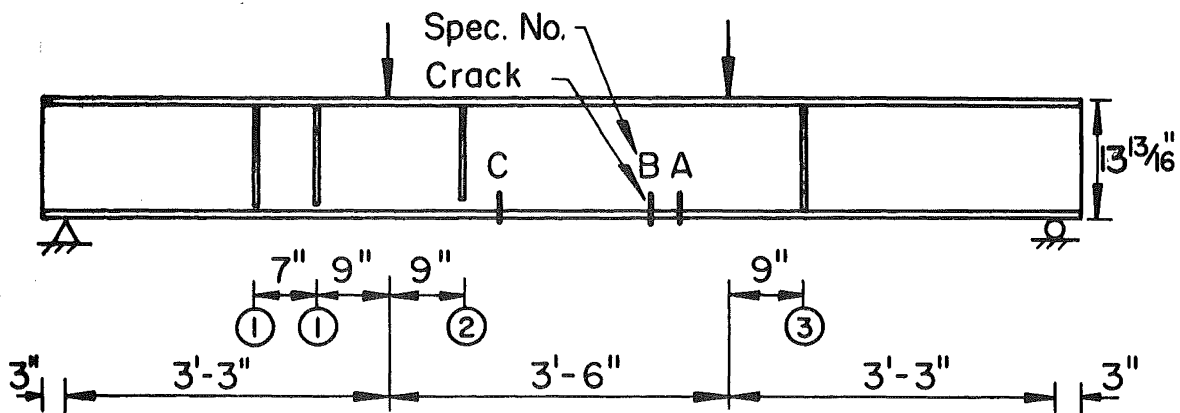


Fig. D1 Cumulative Frequency Distribution for Plain-Rolled A514 Beams

(a) Preliminary Design (3 Specimens)



(b) Additional Pilot Tests (2 Specimens)

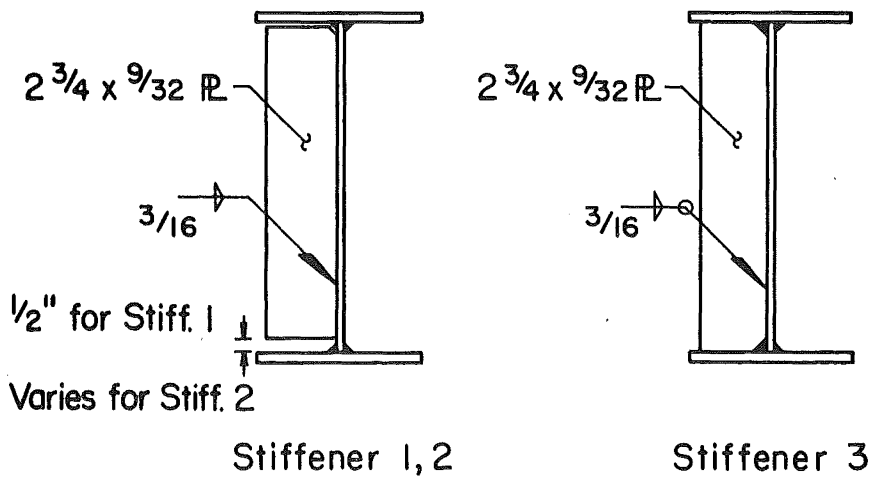
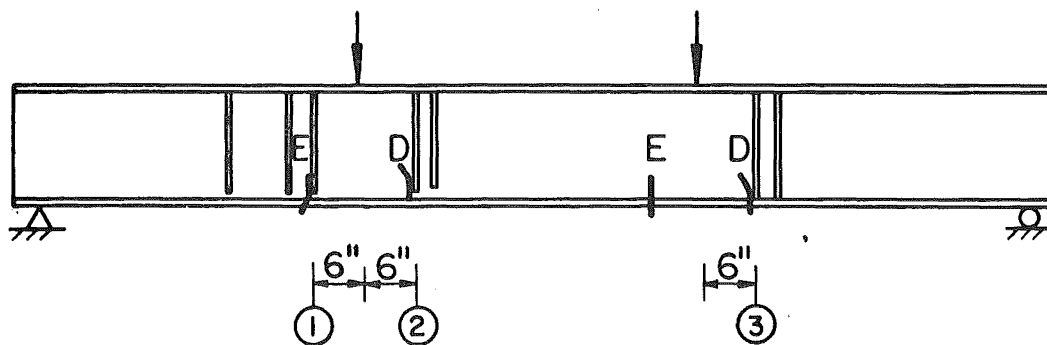
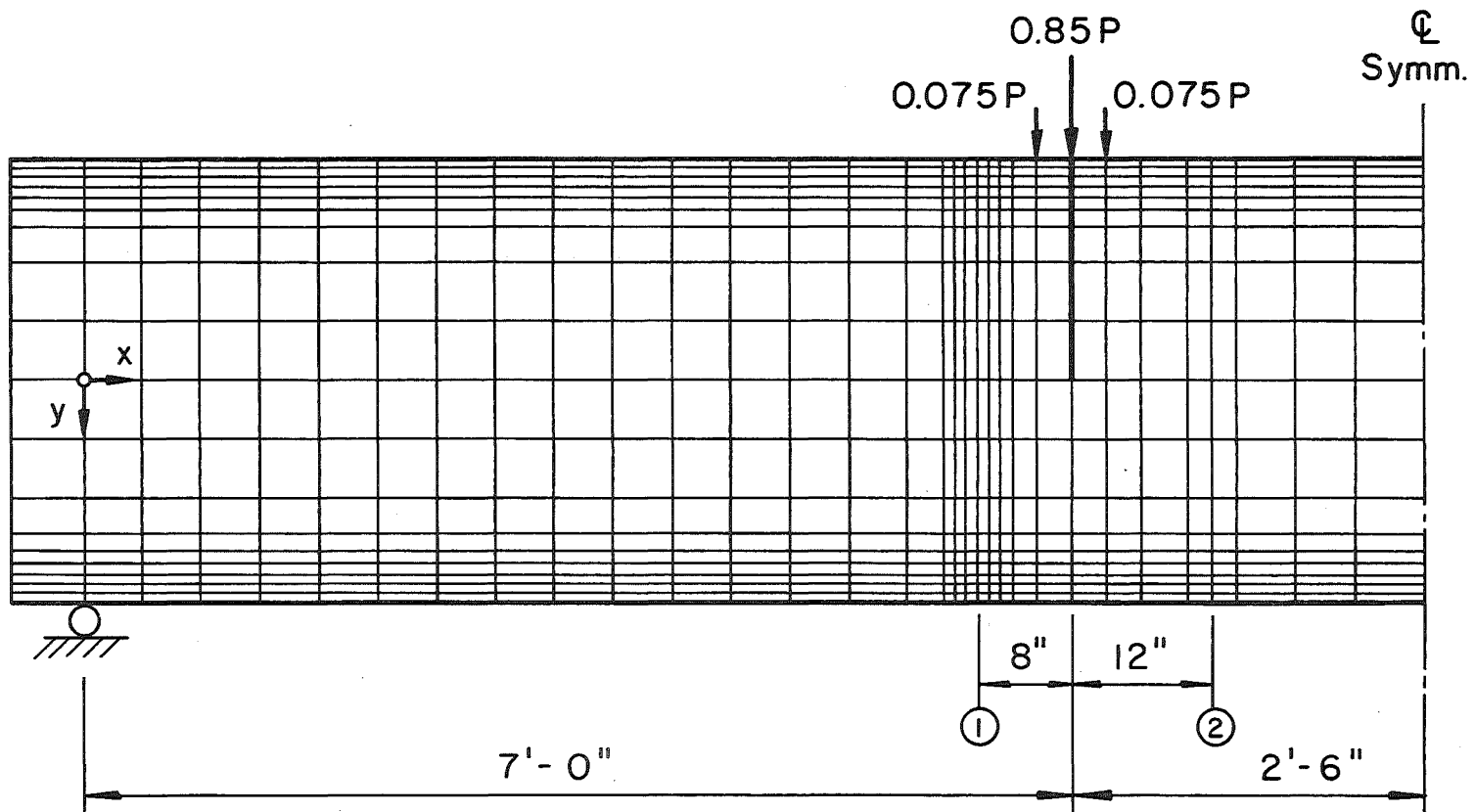


Fig. E1 Details of pilot test beams



Flanges and Load Bearing Stiffener: Bar Elements
Web: Rectangular Elements

Fig. E2 Finite element mesh for stress analysis of 38-inch girder

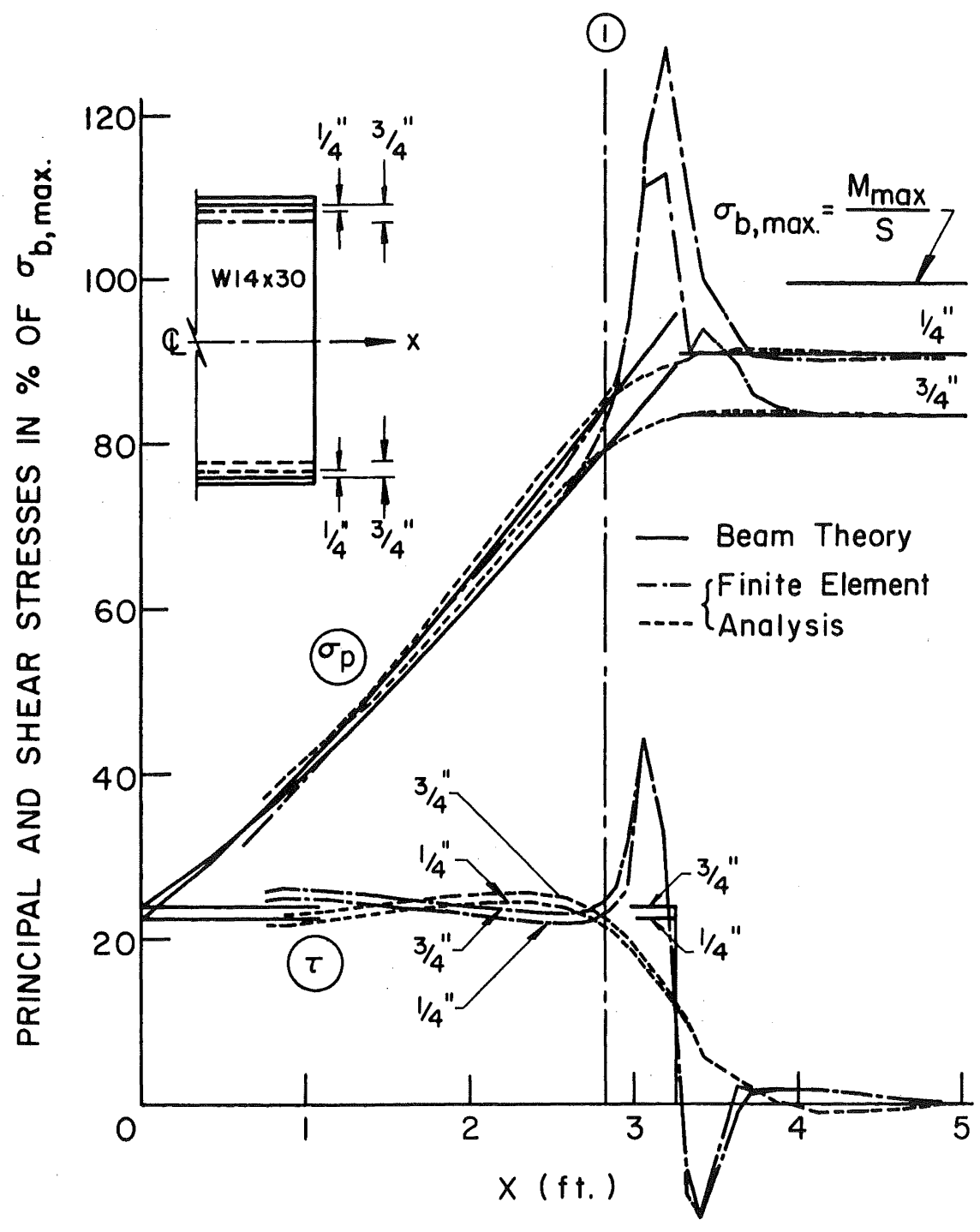


Fig. E3 Stresses in the beam web by beam theory and a finite element analysis

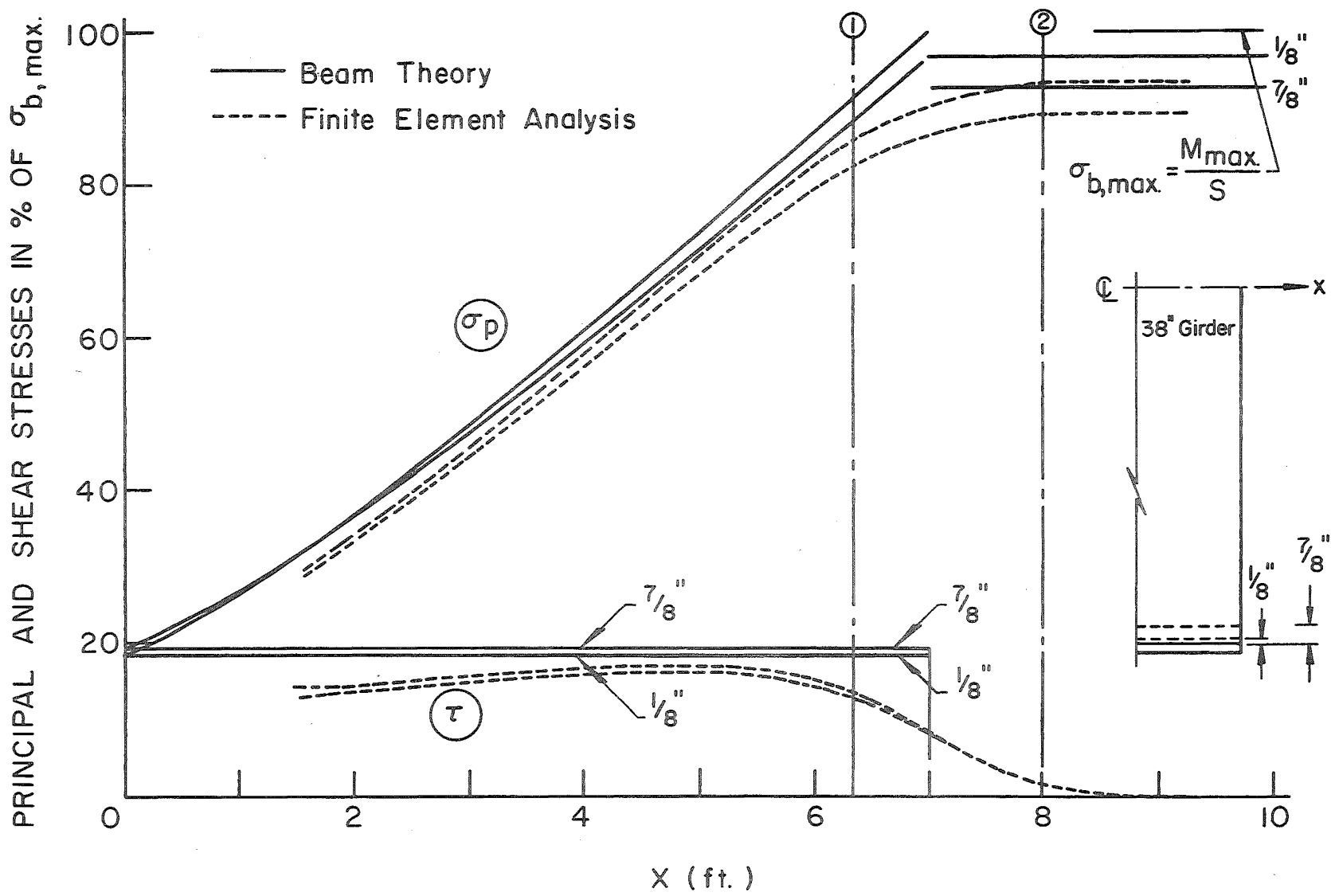


Fig. E4 Stresses in the girder web by beam theory and a finite element analysis

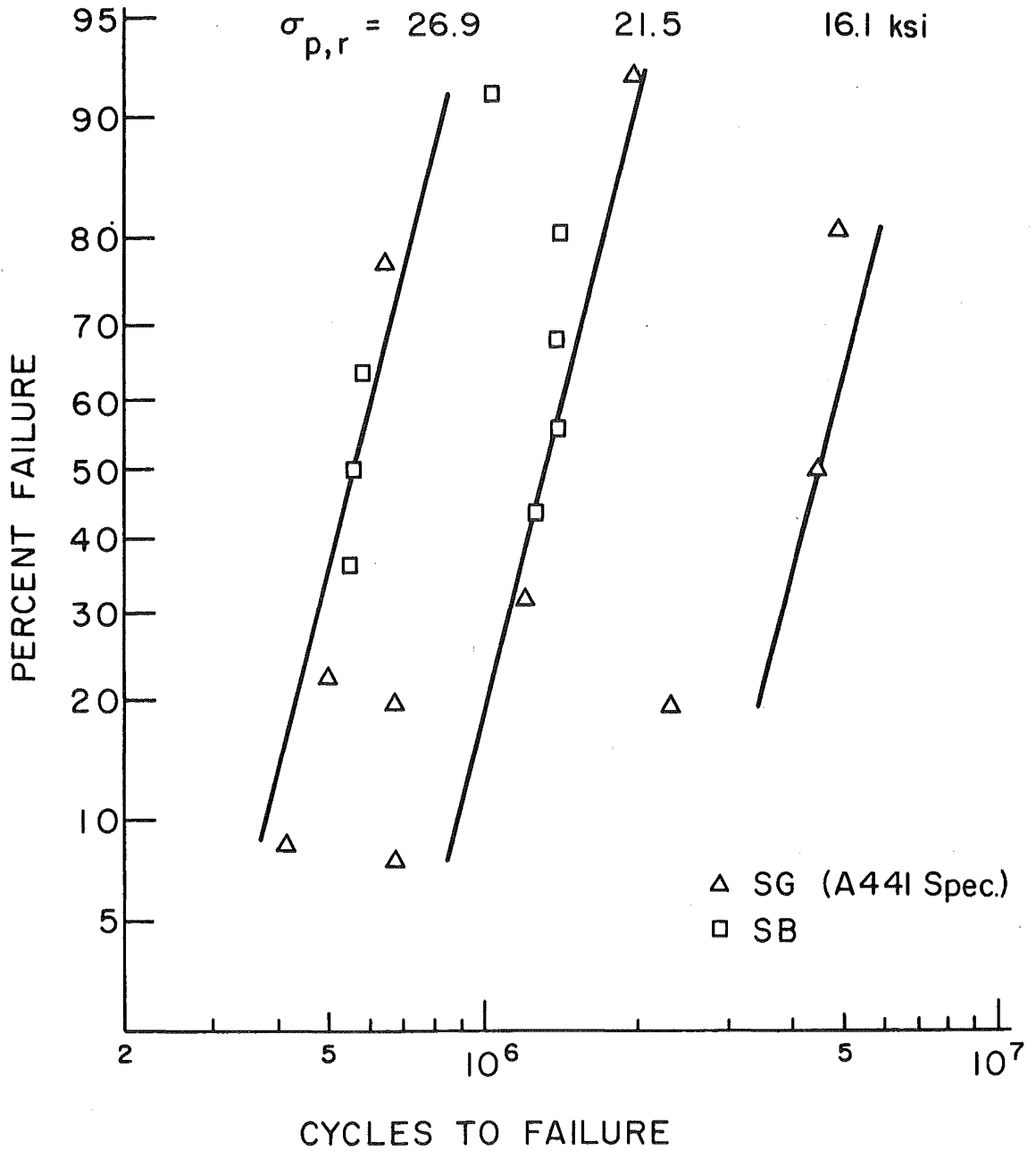


Fig. E5 Cumulative frequency distribution for Type 1 failures

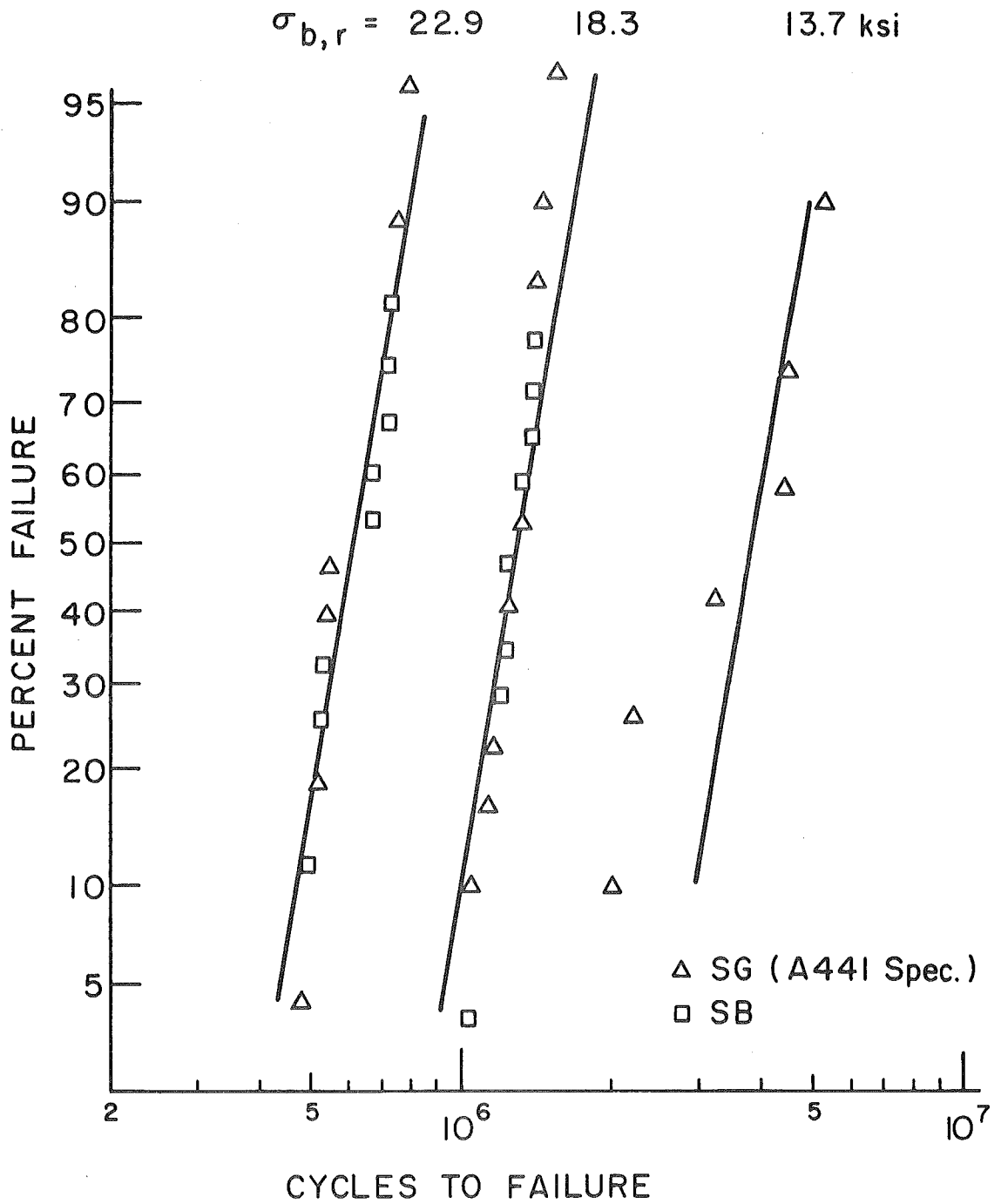


Fig. E6 Cumulative frequency distribution for Type 2 failures

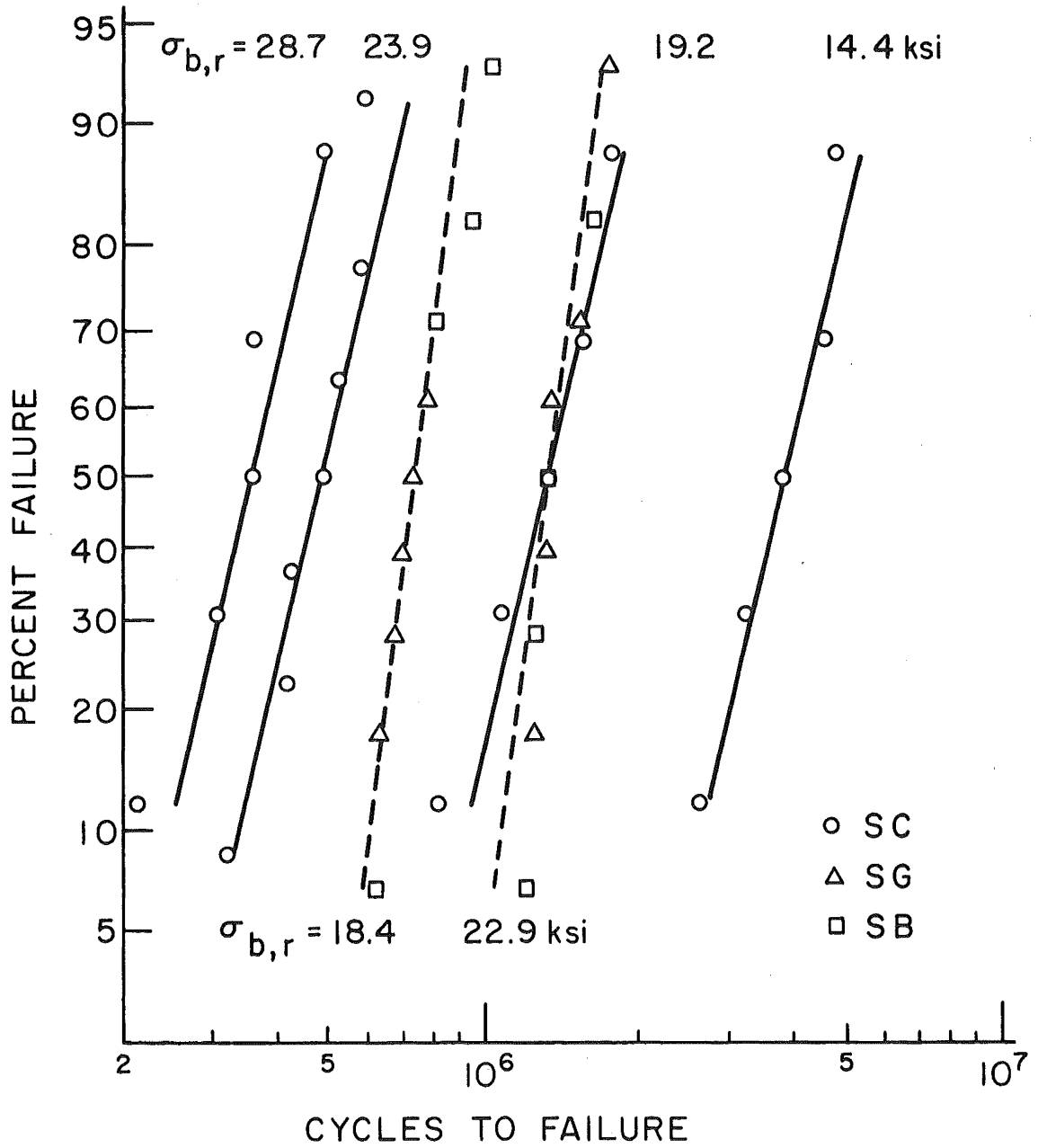
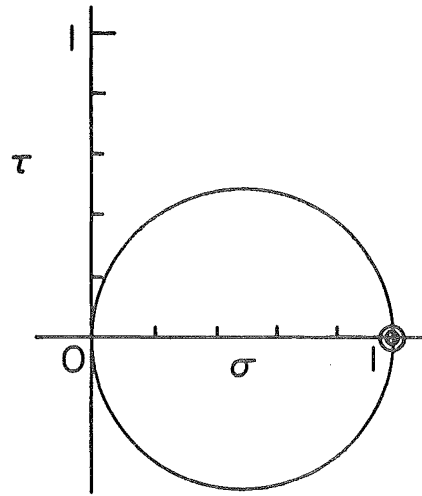
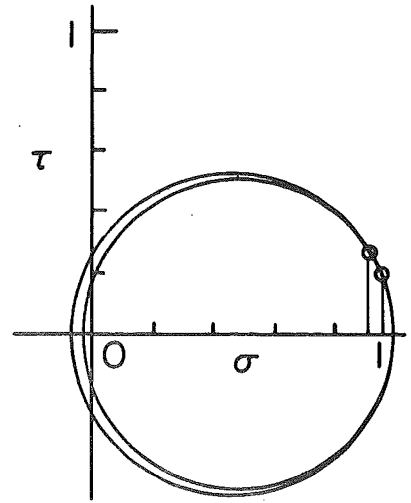


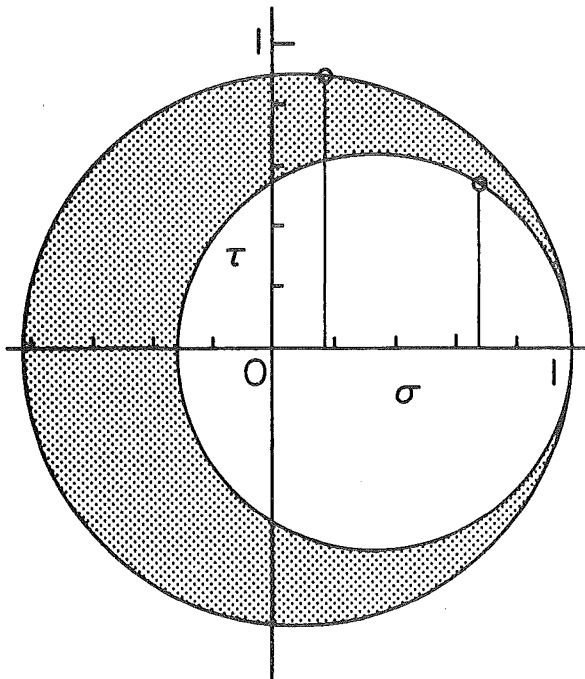
Fig. E7 Cumulative frequency distribution for Type 3 failures



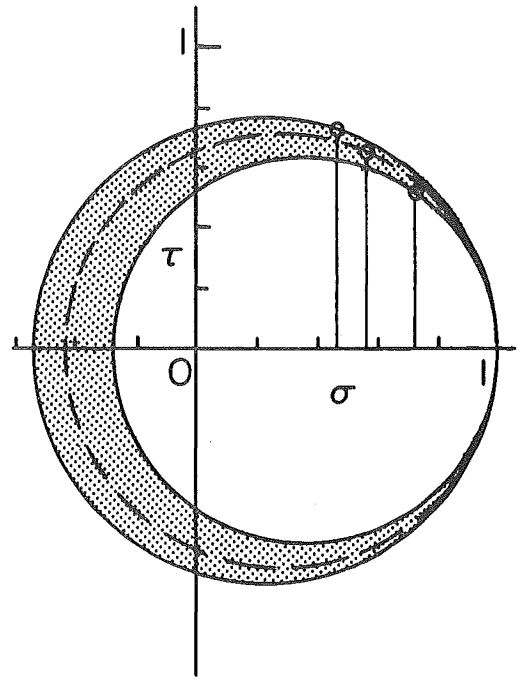
Basic Crack Growth Specimens



Present Study



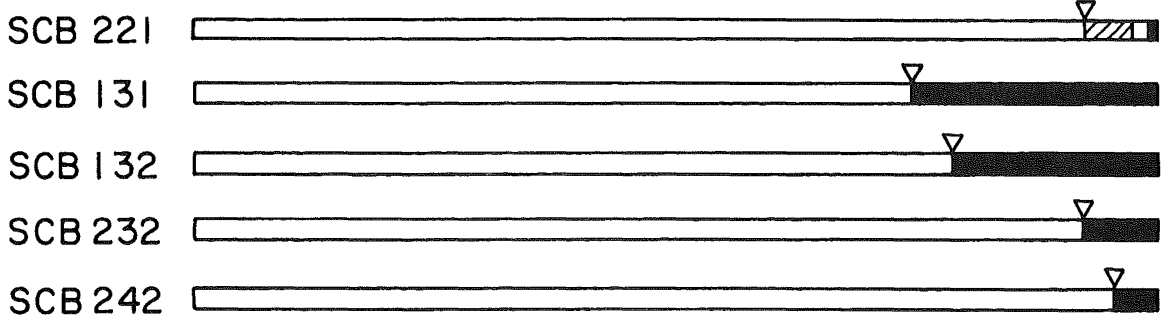
Ref. 33



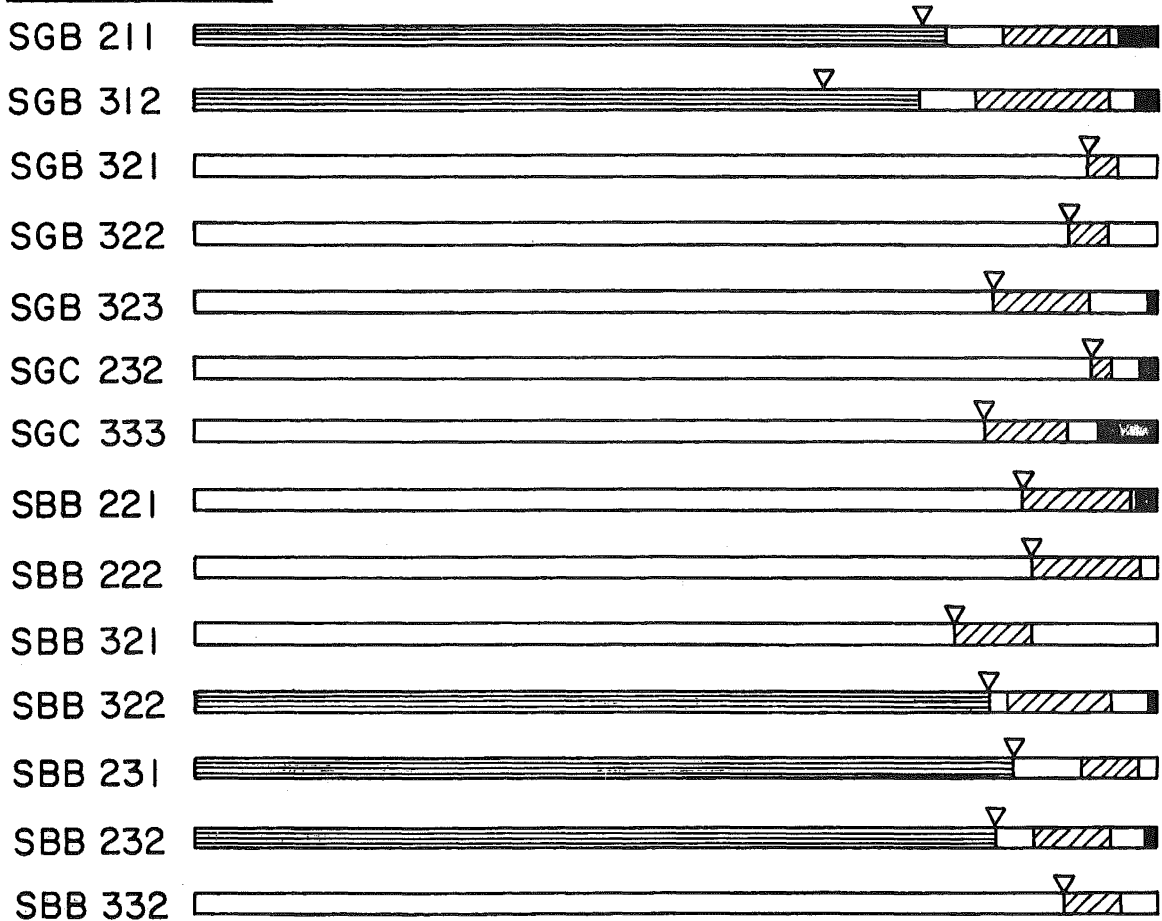
Ref. 34 and 35

Fig. E8 Mohr Circles for Stresses at the End of Stiffener-to-Web Weld

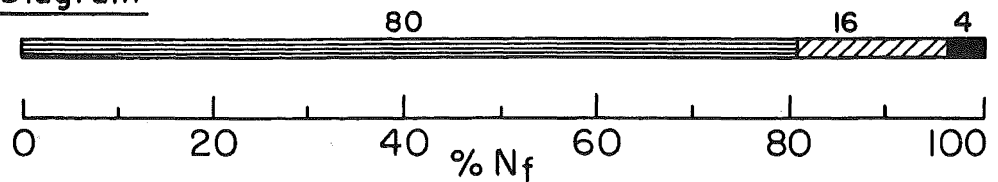
Welded Beams



Welded Girders



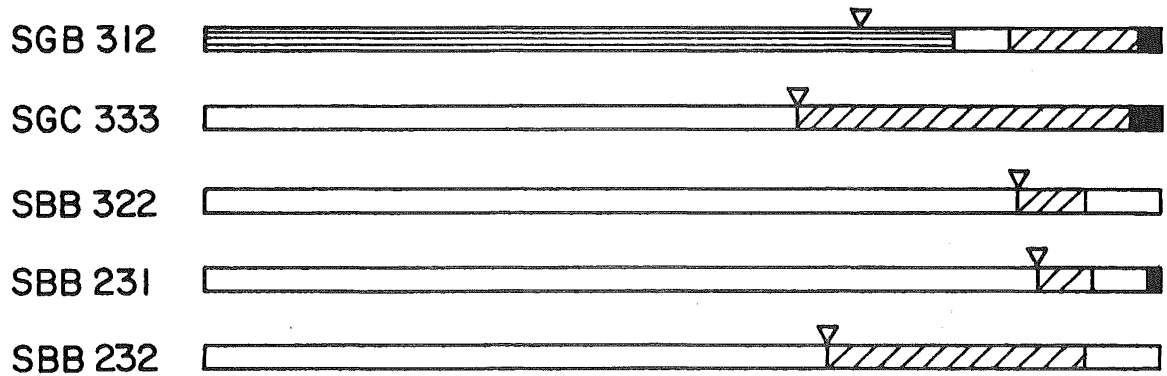
Mean Bar Diagram



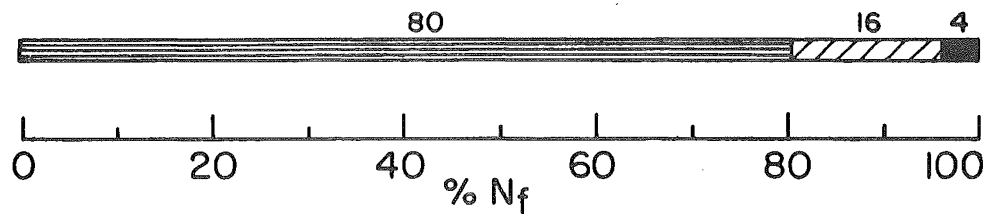
Note: For legend see Fig. E10

Fig. E9 Bar diagram for crack growth at Type 1 stiffeners

W38x50



Mean Bar Diagram








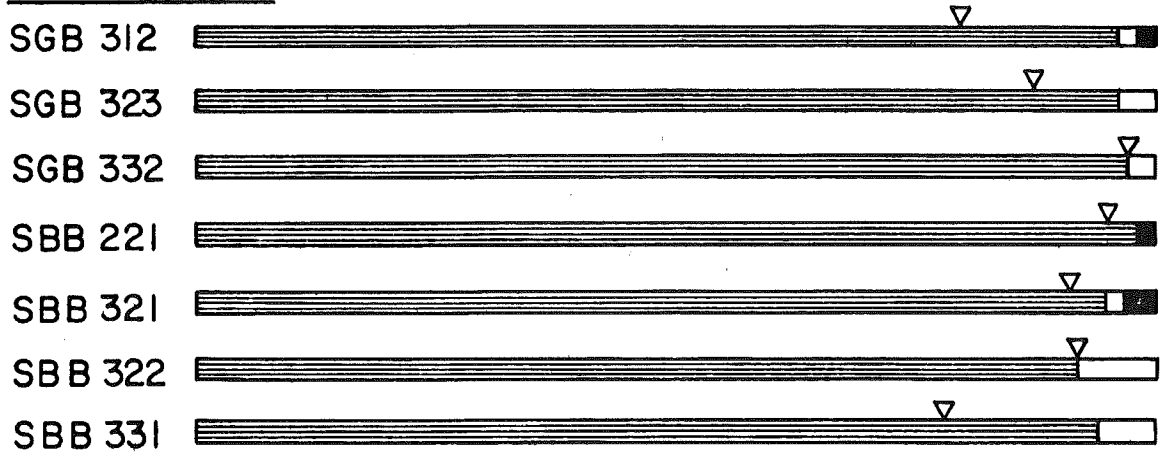
-  Stage 1: Part - Through Crack
-  Stage 2: Two - Ended Through Crack
-  Stage 3: Three - Ended Crack
-  Crack Growth not Observed
-  First Crack Observation

Fig. E10 Bar diagram for crack growth at Type 2 stiffeners

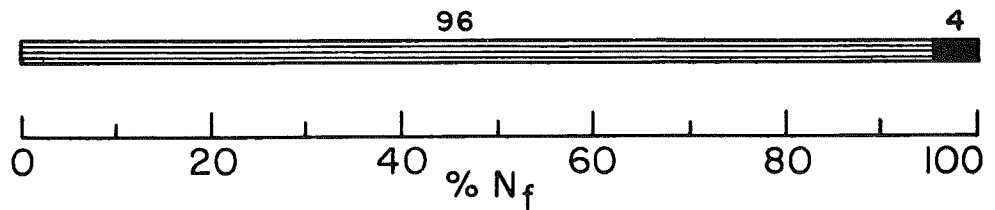
Welded Beams



Welded Girders



Mean Bar Diagram







-  Stage 1: Part - Through Crack
-  Stage 2: Through Crack
-  Crack Growth not Observed
-  First Crack Observation

Fig. E11 Bar diagram for crack growth at Type 3 stiffeners

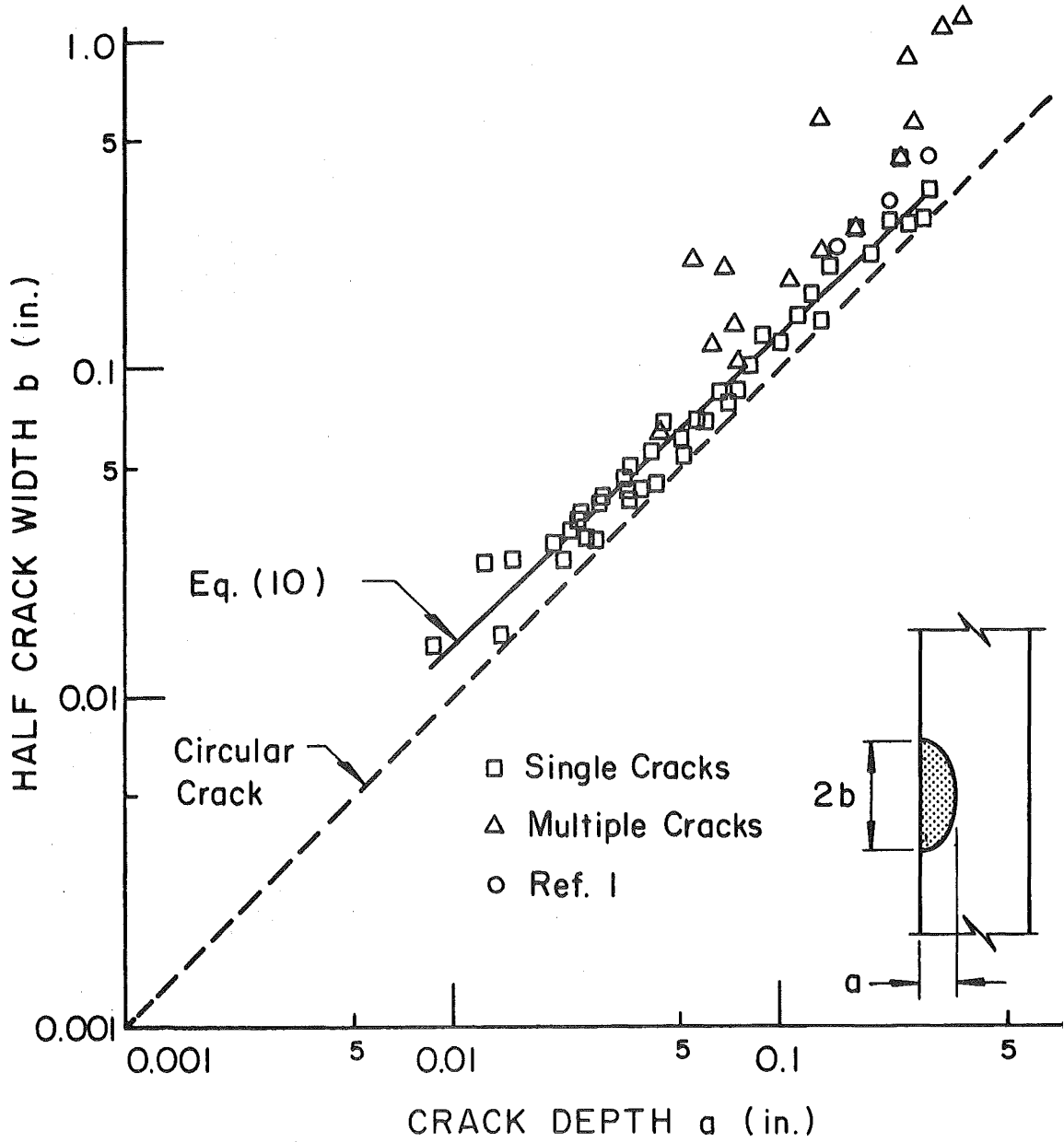


Fig. E12 Size of part-through cracks at fillet weld toes

Type 3 Stiffener
 $\frac{1}{2}$ " Flange, $\frac{1}{4}$ " Stiffener, $\frac{1}{4}$ " Weld

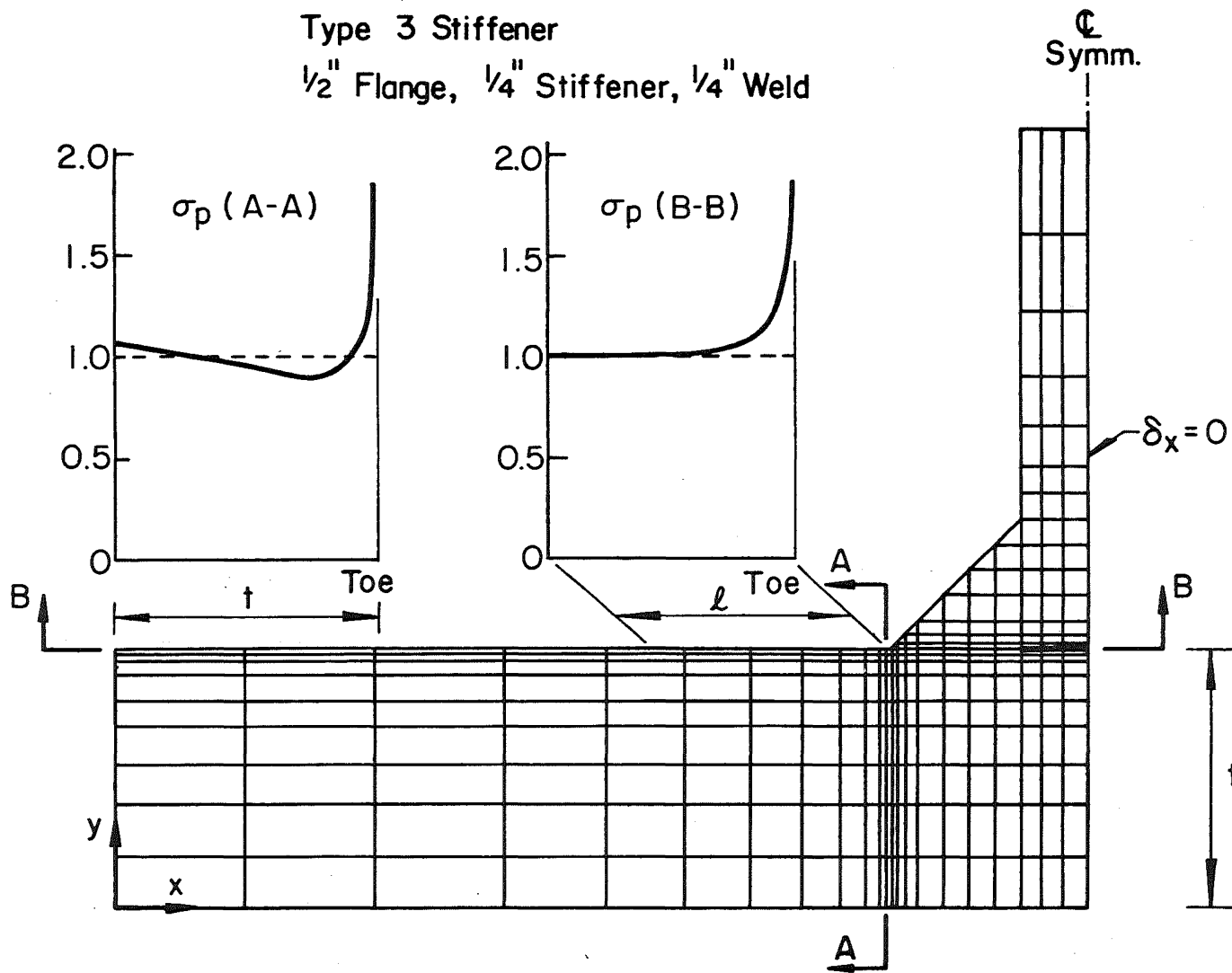


Fig. E13 Typical finite element mesh for the computation of the stress concentration at the weld toe

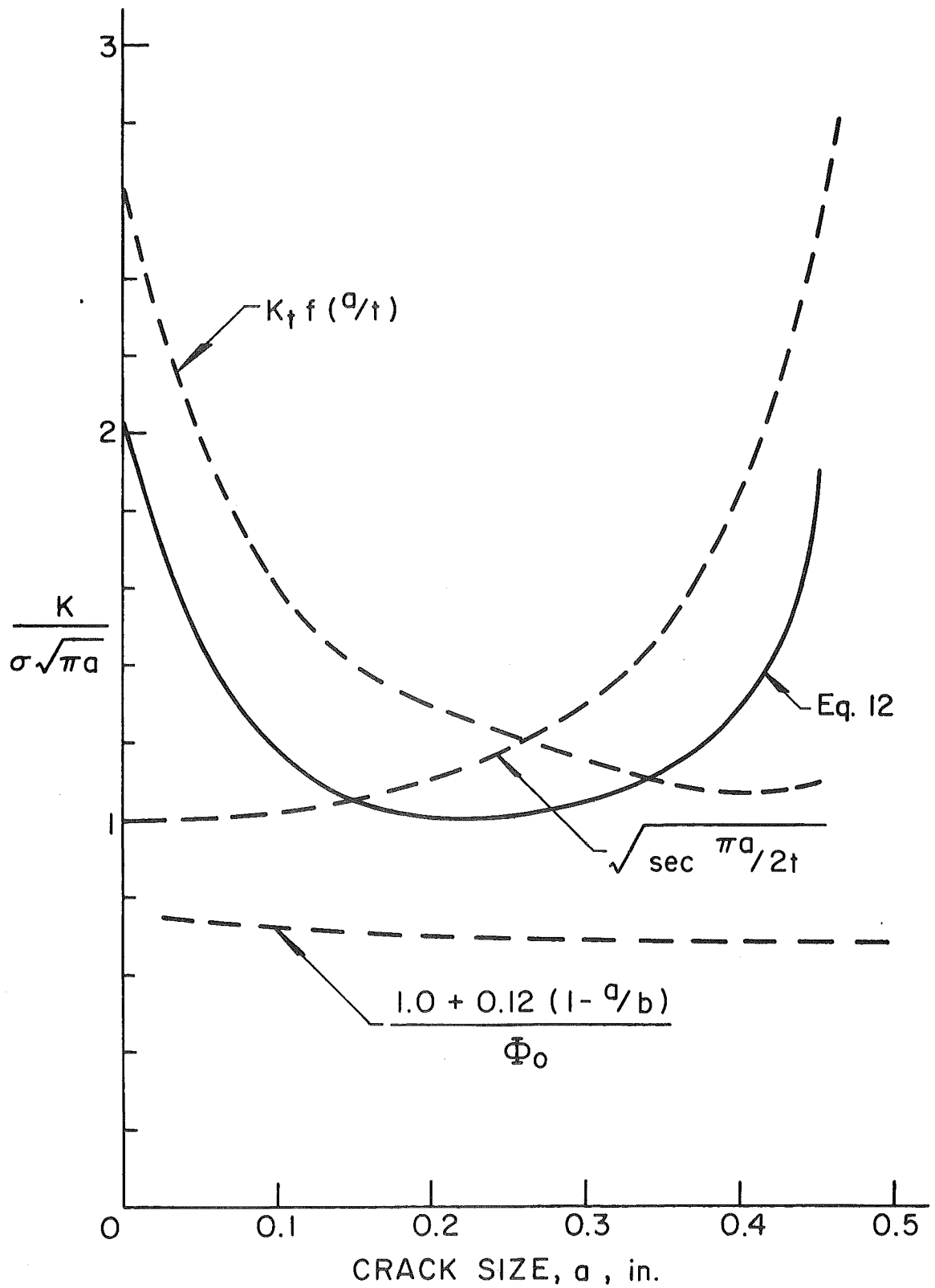


Fig. E14 Stress-Intensity Factor at the Weld Toe of Type 3 Girder Stiffeners

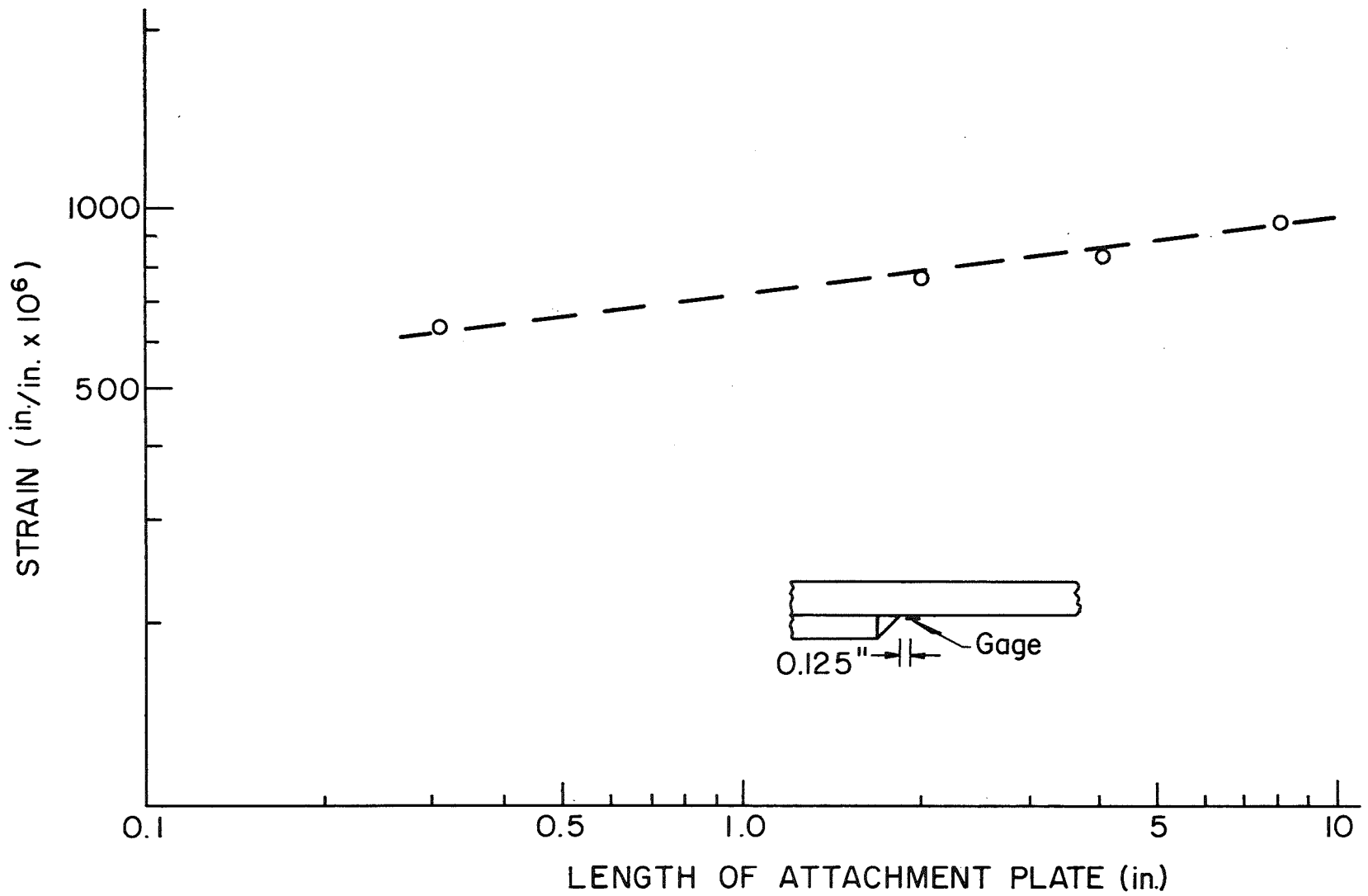


Fig. F1 Measured Strain in Beam Flange at the End of Flange Attachment

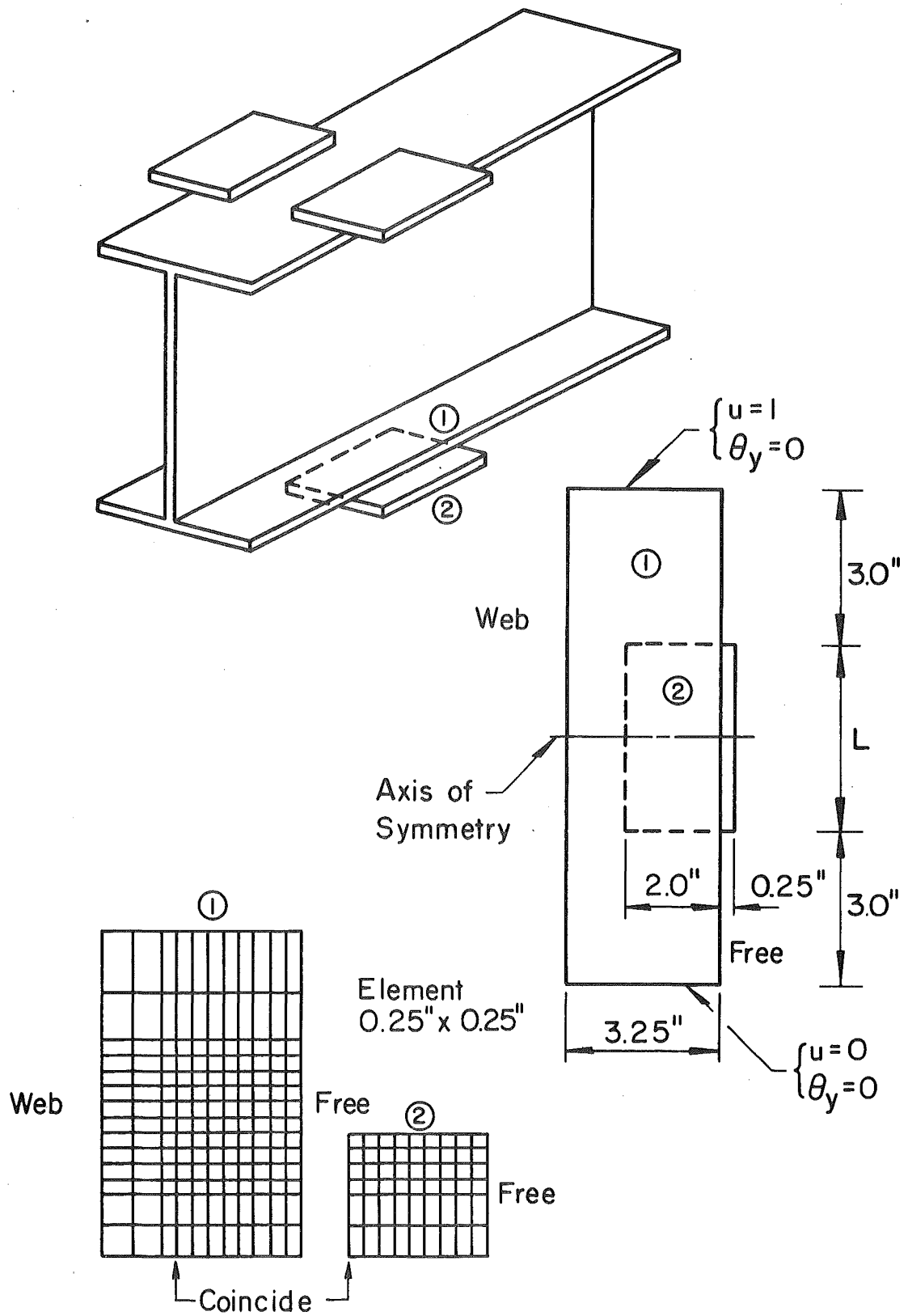


Fig. F2 Finite Element Mesh for the Computation of Stress Distribution at Flange Attachment

REFERENCES

1. Fisher, J. W., Frank, K. H., Hirt, M. A., and McNamee, B. M.
EFFECT OF WELDMENTS ON THE FATIGUE STRENGTH OF STEEL BEAMS, NCHRP Report No. 102, Highway Research Board, National Academy of Sciences - National Research Council, Washington, D. C., 1970.
2. Johnson, K. L. and O'Connor, J. J.
MECHANICS OF FRETTING, Proceedings, The Institution of Mechanical Engineers, Vol. 178, Part 35, 1963-1964, pp. 7-21.
3. Lea, F. C. and Whitman, J. G.
THE FAILURE OF GIRDERS UNDER REPEATED STRESSES, Welding Research Supplement, Vol. 18, No. 1, January 1939.
4. Nee, J. D.
FATIGUE STRENGTH OF USS "T-1" CONSTRUCTIONAL ALLOY STEEL BEAMS WITH AND WITHOUT STIFFENERS, U. S. Steel Corporation, Applied Research Laboratory, Monroeville, Pennsylvania, February 1966.
5. Sherman, D. R. and Stallmeyer, J. E.
FATIGUE OF "T-1" BEAMS, Status Report of the Fatigue Committee - Welding Research Council, University of Illinois, Department of Civil Engineering, Urbana, Illinois, May 1963.
6. Wilson, W. M.
FLEXURAL FATIGUE STRENGTH OF STEEL BEAMS, Engineering Experiment Station Bulletin No. 377, University of Illinois, Vol. 45, No. 33, January 1948.
7. Gurney, T. R.
INVESTIGATION INTO THE FATIGUE STRENGTH OF WELDED BEAMS, PART II: HIGH TENSILE BEAMS WITHOUT STIFFENERS, British Welding Journal, Vol. 9, No. 7, July 1962, pp. 446-454.
8. Jaccard, R. and Fisher, J. W.
FATIGUE STRENGTH OF A514 STEEL MACHINED PLAIN TENSION SPECIMENS, Fritz Laboratory Report 358, Lehigh University, 1972.

9. Hirt, M. A. and Fisher, J. W.
FATIGUE CRACK GROWTH IN WELDED BEAMS, to be published in the Journal of Engineering Fracture Mechanics.
10. Harrison, J. D.
AN ANALYSIS OF DATA ON NON-PROPAGATING FATIGUE CRACKS ON A FRACTURE MECHANICS BASIS, Metal Construction and British Welding Journal, Vol. 2, No. 3, March 1970, pp. 93-98.
11. Signes, E. G., Baker, R. G., Harrison, J. D., and Burdekin, F. M.
FACTORS AFFECTING THE FATIGUE STRENGTH OF WELDED HIGH STRENGTH STEELS, British Welding Journal, February 1967, pp. 108-116.
12. Watkinson, F., Bodger, P. H., and Harrison, J. D.
THE FATIGUE STRENGTH OF WELDED JOINTS IN HIGH STRENGTH STEELS AND METHODS FOR ITS IMPROVEMENT, Proceedings, Fatigue of Welded Structures Conference, The Welding Institute, Brighton, England, July 1970.
13. American Association of State Highway Officials
STANDARD SPECIFICATIONS FOR HIGHWAY BRIDGES, AASHO, Washington, D. C., 1969.
14. Gurney, T. R.
FATIGUE STRENGTH OF BEAMS WITH STIFFENERS WELDED TO THE TENSION FLANGE, British Welding Journal, September 1960, p. 569.
15. Fielding, D. J.
FATIGUE TESTS OF SLENDER-WEB HYBRID PLATE GIRDERS UNDER COMBINED BENDING AND SHEAR, M.S. Thesis, University of Texas, Austin, Texas, June 1968.
16. Ozell, A. M. and Conyers, A. L.
TRANSFER OF STRESSES IN WELDED COVERPLATES, Welding Research Council Bulletin, No. 63, New York, 1960.
17. Struik, J. H.
Documentation Program GENFEMPS', Fritz Engineering Laboratory Report, Lehigh University, (in preparation).
18. Gurney, T. R.
FATIGUE TESTS ON BUTT AND FILLET WELDED JOINTS IN MILD AND HIGH TENSILE STRUCTURAL STEELS, British Welding Journal, Vol. 9, No. 11, 1962, pp. 614-620.

19. Gurney, T. R.
FURTHER FATIGUE TESTS ON MILD STEEL SPECIMENS WITH ARTIFICIALLY INDUCED RESIDUAL STRESSES, British Welding Journal, Vol. 9, No. 11, 1962, pp. 609-613.
20. Gurney, T. R.
THE EFFECT OF PEENING AND GRINDING ON THE FATIGUE STRENGTH OF FILLET WELDED JOINTS IN TWO STEELS, BWRA Report E/12A/67.
21. Weck, R.
RESULTS OF FATIGUE TESTS ON MILD STEEL SPECIMENS WITH WELDED ATTACHMENTS, IIW Doc. XIII-154-58.
22. Frank, K. H.
THE FATIGUE STRENGTH OF FILLET WELDED CONNECTIONS, Ph.D. Dissertation, Lehigh University, Bethlehem, Pennsylvania, October 1971.
23. Maddox, S. J.
CALCULATING THE FATIGUE STRENGTH OF A WELDED JOINT USING FRACTURE MECHANICS, British Welding Journal, August 1970.
24. Gurney, T. R.
FATIGUE OF WELDED STRUCTURES, Cambridge Press, 1968.
25. Paris, P. C., Gomez, M. P., and Anderson, W. E.
A RATIONAL ANALYTICAL THEORY OF FATIGUE, The Trend in Engineering, University of Washington, Vol. 13, No. 1, January 1961.
26. Irwin, G. R.
ANALYSIS OF STRESSES AND STRAINS NEAR THE END OF A CRACK TRAVERSING A PLATE, Transactions, ASME, Series E, Vol. 24, No. 3, September 1957.
27. Irwin, G. R.
CRACK EXTENSION FORCE FOR A PART-THROUGH CRACK IN A PLATE, Transactions, ASME, Series E, Vol. 29, December 1962.
28. Barsom, J. M.
FATIGUE-CRACK PROPAGATION IN STEEL OF VARIOUS YIELD STRENGTHS, U. S. Steel Corp., Applied Research Laboratory, Monroeville, Pennsylvania, 1971.
29. Paris, P. C.
THE FRACTURE MECHANICS APPROACH TO FATIGUE, Proceedings, 10th Sagamore Conference, Syracuse University Press, 1965.

30. AASHO
Interim Specifications 1971, Developed by the AASHO Committee on Bridges and Structures, AASHO, Washington, D. C., 1971.
31. Hall, L. R.
FATIGUE TESTS OF THIN WEB GIRDERS, Status Report to Fatigue Committee - Welding Research Council, University of Illinois, Urbana, Illinois, May 1960.
32. Hall, L. R. and Stallmeyer, J. E.
THIN WEB GIRDER FATIGUE BEHAVIOR AS INFLUENCED BY BOUNDARY RIGIDITY, Structural Research Series No. 278, University of Illinois, Urbana, Illinois, January 1964.
33. Kouba, N. G. and Stallmeyer, J. E.
THE BEHAVIOR OF STIFFENED BEAMS UNDER REPEATED LOADS, Structural Research Series No. 173, University of Illinois, Urbana, Illinois, April 1959.
34. Gurney, T. R. and Woodley, C. C.
INVESTIGATION INTO THE FATIGUE STRENGTH OF WELDED BEAMS, Part III, High Tensile Steel Beams with Stiffeners Welded to the Web, British Welding Journal, September 1962.
35. Braithwaite, A. B. M.
FATIGUE TESTS ON LARGE WELDED PLATE GIRDERS, British Welding Research Association, Report D7/36A/65, May 1965.
36. Goodpasture, D. W. and Stallmeyer, J. E.
FATIGUE BEHAVIOR OF WELDED THIN WEB GIRDERS AS INFLUENCED BY WEB DISTORTION AND BOUNDARY RIGIDITY, Structural Research Series No. 328, University of Illinois, Urbana, Illinois, August 1967.
37. Yen, B. T. and Mueller, J. A.
FATIGUE TESTS OF LARGE-SIZED WELDED PLATE GIRDERS, Fritz Engineering Laboratory Report No. 303.10, Lehigh University, Bethlehem, Pennsylvania, June 1966.
38. Toprac, A. A. and Natarajan, M.
FATIGUE STRENGTH OF HYBRID PLATE GIRDERS, Journal of the Structural Division, ASCE, April 1971.

39. Toprac, A. A. and Fielding, D. J.
FATIGUE TESTS OF A441-A36 HYBRID PLATE GIRDERS, The Structural Engineer, No. 12, Vol. 48, December 1970.
40. Yinh, J. and Toprac, A. A.
STUDY ON FATIGUE OF HYBRID PLATE GIRDERS UNDER CONSTANT MOMENT, Research Report 96-3, University of Texas, Austin, Texas, January 1969.
41. Yen, B. T.
DESIGN RECOMMENDATIONS FOR BRIDGE PLATE GIRDERS, Fritz Engineering Laboratory Report 327.6, June 1969.
42. Gurney, T. R. and Trepka, L. N.
EXPLORATORY TESTS TO DETERMINE THE INFLUENCE OF LOCAL HEATING ON THE FATIGUE BEHAVIOR OF WELDED MILD STEEL SPECIMENS, British Welding Journal, Vol. 7, No. 8, 1960.
43. Gurney, T. R.
INFLUENCE OF RESIDUAL STRESSES ON FATIGUE STRENGTH OF PLATES WITH FILLET WELDED ATTACHMENTS, British Welding Journal, June 1960, p. 415.
44. Gurney, T. R. and Maddox, S. J.
A RE-ANALYSIS OF FATIGUE DATA FOR WELDED JOINTS IN STEEL, BWRA Report E/44/72, January 1972.
45. Paris, P. C.
TESTING FOR VERY SLOW GROWTH OF FATIGUE CRACKS, Closed Loop, MTS System Corp., Vol. 2, No. 5, 1970.
46. Fisher, J. W. and Gurney, T. R.
HIGH CYCLE FATIGUE OF CONNECTIONS AND DETAILS, State-of-Art Report 4, Technical Committee 18, ASCE-IABSE International Conference on Tall Buildings, August 1972, Preprints: Reports Vol. II-18.
47. Crooker, T. W. and Lange, E. A.
HOW YIELD STRENGTH AND FRACTURE TOUGHNESS CONSIDERATIONS CAN INFLUENCE FATIGUE DESIGN PROCEDURES FOR STRUCTURAL STEELS, Welding Research Supplement, Vol. 49, No. 10, October 1970, pp. 488-496.

48. Maddox, S. J.
FATIGUE CRACK PROPAGATION IN WELD METAL AND HEAT AFFECTED ZONE MATERIAL, Members' Report No. E/29/69, The Welding Institute, England, December 1969.
49. Paris, P. C. and Sih, G. C.
STRESS ANALYSIS OF CRACKS, ASTM STP No. 381, 1965.
50. Albrecht, P. A.
FATIGUE STRENGTH OF WELDED BEAMS WITH STIFFENERS, Ph.D. Dissertation, Lehigh University, Bethlehem, Pennsylvania, July 1972.
51. Pearce, S. C.
BIOLOGICAL STATISTICS, McGraw-Hill, 1965, pp. 110-112.
52. Butler, L. J. and Kulak, G. L.
STRENGTH OF FILLET WELDS AS A FUNCTION OF DIRECTION OF LOAD, Welding Journal, Vol. 36, No. 5, May 1971.
53. Munse, W. H. and Stallmeyer, J. E.
INFLUENCE OF WELDED DETAILS ON FATIGUE OF WELDED BEAMS AND GIRDERS, Symposium on Fatigue of Welded Structures, Cambridge University, March-April, 1960.
54. Natrella, M. G.
Experimental Statistics, Handbook 91,
U.S. Department of Commerce, 1963